Modelling Pseudomonas aeruginosa Biofilm Infections in the Lung

Aljalamdeh, Reham

Award date:
2020

Awarding institution:
University of Bath

Modelling *Pseudomonas aeruginosa* Biofilm Infections in the Lung

Reham Saleem Aljalamdeh

A thesis submitted for the degree of Doctor of Philosophy

University of Bath

Department of Pharmacy & Pharmacology

March 2020

Copyright

Table of Contents

List of Figures

List of Tables

List of Abbreviations

ACI Anderson cascade impactor

AHLs Acyl-homo-serine lactones

AML Amiloride

ASM Artificial sputum medium

AMT Amitriptyline

ATP Adenosine triphosphate

BHI Brain heart infusion

BCCM Belgian Coordinated Collection of Microorganisms

CDC Centres for disease control and prevention

CF Cystic fibrosis

CFU Colony forming unit

CFTR Cystic fibrosis transmembrane conductance regulator

CPH Chlorpromazine

COL Colistin

COPD Chronic obstructive pulmonary disease

CV Crystal violet

D_{50} Geometric median diameter

DFM Digital flow meter

DMSO Dimethyl sulfoxide

DNA Deoxyribonucleic acid

DPIs Dry powder inhalers

DSPC Distearoylphosphatidylcholine

DTPA Diethylenetriaminepentaacetic acid

EARSS European antimicrobial resistance surveillance system

EDTA Ethylenediaminetetraacetic acid

EPS Extracellular polymeric substance

ESKAPE Enterococcus *faecium*, *Staphylococcus aureus*, *Klebsiella pneumoniae*, *Acinetobacter baumannii*, *P. aeruginosa*, and *Enterobacter* spp.

E-test Epsilometer test

FIC Fractional inhibitory concentration

FUR Furanone

h Hours

HPMC Hydroxypropyl methylcellulose

HPLC-MS High performance liquid chromatography- mass spectrometry

OD Optical density

OMVs Outer membrane vesicles

LPS Lipopolysaccharides

MDR multi-drug resistant

MFPs Membrane fusion protein

MHB Muller-Hinton broth

MIC Minimum inhibitory concentration

MOC Micro-orifice collector

MOPS 3-(N-Morpholino) propane-sulfonic acid

NGI Next generation impactor

NHS National health service

NIC Niclosamide

PBS Phosphate buffered saline

PQS Pseudomonas quinolones signal

QUE Quercetin

QS Quorum sensing

RH Relative humidity

RNDs Resistance nodulation divisions

rRNA Ribosomal ribonucleic acid

S1-S7 Stage 1 – stage 7

SCVs Small-colony variants

SEM Scanning electron microscopy

SEM Standard error of the mean

Sub-MICs Sub-minimal inhibitory concentrations

t Time

T2SS Type II secretion system

T3SS Type III secretion system

T6SS Type VI secretion system

TSA Tryptic soya agar

TOB Tobramycin

TOBI Tobramycin inhalation powder

WHO World health organization

Dedication

With a heart filled with love, happiness and gratitude,

I would like to dedicate this thesis

To my great father Saleem Aljalamdeh

And

To my amazing mother Jamila Aljalamdeh

who have given me endless support and encouragement

Acknowledgements

First and foremost, I would like to thank God for granting me strength, perseverance and the opportunity to fulfil this research study.

Submission of a PhD thesis is not a simple task and I find myself indebted to a network of people who have kindly supported and contributed to produce this thesis.

At the very outset, I would like to express my sincerest gratitude to my lead supervisor Dr Albert Bolhuis for welcoming me into his lab, giving me the excellent opportunity to do research into the fascinating field of biofilms. At the beginning, working in such research was challenging for me especially that I came from a quite different background of Clinical Pharmacy. However, his continuous support facilitated these difficulties, so I express my deepest gratitude for him for providing me from his precious time to demonstrate lab techniques, to always being approachable for discussions with seemingly limitless patience. I would like also to thank him for all guidance and encouragement, at all stages in my PhD journey, in which I benefited from his scientific advice and his careful editing that contributed enormously to the production of this thesis. It would never have been possible for me to take this work to completion in time without his support.

I would like to extend my gratitude to my co-supervisor Dr Matthew Jones for all his assistance, through sharing his wealth experience in Pharmaceutical Science during every meeting that helped me a lot theoretically and practically in the lab. Many thanks for your important input in editing my thesis writing, and for always being supportive and encouraging. Also, thank goes to my third supervisor Professor Robert Price for giving me the chance to work in his pharmaceutical lab and for his advice about the pharmaceutical instruments. Simply, I appreciate this precious chance to learn Microbiological and Pharmaceutical Sciences under your supervision and thanks for being such great mentors and good people.

I would like also to thank Dr Shaun Reeksting from Chemical Characterization and Analysis Facility for his assistance with the HPLC-MS experiments, for being welcoming all the time and for saving me extra-booking slots in-advance for analysis repetition. Thank you also to Christian Rehbein and Steven Philips for their technical support and all other technical staff in the Department of Pharmacy and Pharmacology for helping me to deal with technical issues. Indeed, special thanks to our Pharmacy librarian Linda Humphreys, and also Thomas Rogers for being welcoming and for their advice regarding referencing issues during writing-up my thesis.

I have spent a wonderful time studying at University and living in Bath, which have offered me the opportunity to meet people and made friends from all over the world, massive thanks to all friends I made here in Bath for their optimism, good humour, lot of trips, dinner parties, and fun times that made these three years most enjoyable.

I gratefully thank Philadelphia University Scholarship Scheme in Jordan which sponsored me and offered me this amazing opportunity to do such exciting research and have a very rewarding experience.

I also express my deepest gratitude to Dr Laila Badran from Jordan for her encouragement, scientific support, for being always listening and offering me the best advice coming deeply from her heart during the 3 years of my PhD journey. Your encouragement was instrumental to the completion of this thesis.

My family deserves special mention and thanks. Father and mother, for your limitless contribution to my life, both before to this academic achievement and throughout every step of the way is profoundly appreciated. Thank you for your unconditional love, for being always supportive, motivating, and having an unwavering belief in me. Many thanks also to my Aunt who took care of me in all her prayers. Also, many thanks to my brothers, sisters, and little nephews who all have offered me support, loving, and happiness throughout this long journey. Their love made me happy all the time and encouraged me to move forward toward graduation.

Declaration

The work presented in this thesis is original work conducted by myself under the supervision of Dr Albert Bolhuis and Dr Matthew Jones. The research was funded by the Philadelphia University of Jordan. All sources of information have been acknowledged by means of references. None of this work has been used in any previous application for a degree at this or any other University or institute of learning.

Abstract

Pseudomonas aeruginosa is the predominant opportunistic bacterium that causes chronic respiratory infections in cystic fibrosis (CF) patients. This bacterium can develop a high level of resistance to multiple classes of antibiotics, and this is partially attributed to the ability of *P. aeruginosa* to grow as a biofilm. Such biofilm offers protection for bacterial cells from the host immune defences and antibiotics. In CF patients, tobramycin is one of the most commonly used antibiotics. However, because of the increasing level of *P. aeruginosa* resistance to tobramycin and other antibiotics, there is a significant challenge in the treatment and eradication of such infections. Therefore, this thesis investigates potential strategies to improve tobramycin efficacy in the eradication of *P. aeruginosa* biofilm. The main aim of this thesis is to evaluate the activity of tobramycin under a clinically relevant condition. Other specific aims are to investigate the influence of dry powder particle size on antibiofilm activity and to evaluate tobramycin combination therapy with non-antibiotic drugs.

The activity of tobramycin against planktonic and biofilms of *P. aeruginosa* was determined using artificial sputum medium (ASM), which is clinically more relevant than standard growth media. It was observed that the susceptibility of strains to tobramycin was reduced by four-fold when ASM was used as compared to the minimal MOPS medium. This highlights the importance of testing antibiotic susceptibility with a physiologically more relevant medium. Beside testing against planktonic cells, the results from biofilms using two different biofilm models indicated that eradication of *P. aeruginosa* biofilms was challenging to achieve with only 40-60% reduction in biofilm biomass or number of viable counts were observed in most strains, which suggest further research and improvement in tobramycin activity against *P. aeruginosa* is required.

Tobramycin dry powder inhaler (TOBI Podhaler®) is widely used in the treatment of *P. aeruginosa* lung infections in CF patients. Currently, the models that are used to test the activity of tobramycin are not representative of lung infections, and better models would provide a significant advantage as these could be used to improve the formulation of dry powder inhalers. For instance, one question that has not been addressed is whether antibiotic particle size influences the antibiofilm activity against *P. aeruginosa*. Therefore, in this thesis, the activity of tobramycin dry powder was investigated in terms of particle size. This was achieved using a Next Generation Impactor (NGI), which was used to fractionate tobramycin powder into different particle sizes. The results described here indicate that the antibiofilm activity of

tobramycin dry powder inhaler can indeed be affected by the size of the powder particles. Against *P. aeruginosa* biofilms of LMG 27643 and LMG 27649 clinical isolates, smaller tobramycin particles (< 2.82 µm) showed better efficacy by ~ 20% as compared to larger tobramycin particles (< 11.7 µm) after 3 hours incubation time. No difference was seen after long incubation times, but these may not be clinically relevant as tobramycin is cleared from the lung in 2-3 hours. This work highlights that particle size of dry powder inhaler can affect antibacterial and antibiofilm activity.

Tobramycin activity in combination with non-antibiotic drugs was also determined, as a limited number of previous studies have investigated this issue against biofilms of *P. aeruginosa*. Moreover, most tobramycin combination studies employed standard growth media, whereas we analyzed this using a more clinically relevant ASM medium. This work was performed firstly by conducting a comprehensive literature review, where several non-antibiotic drugs from different classes that showed antibacterial activity against *P. aeruginosa* were found. These drugs include colistin, amitriptyline, chlorpromazine, niclosamide, furanone, quercetin, and diethylenetriaminepentaacetic acid. Checkerboard assays were used to evaluate tobramycin interactions, and Fractional Inhibitory Concentration (FIC) was used as an index to assess the type of interaction. The results from this work were mixed, with outcomes dependent on bacterial lifestyles (planktonic vs biofilm), type of strains (laboratory vs clinical isolates), and growth medium (ASM vs Mueller-Hinton Broth). For instance, using ASM medium resulted mostly in antagonistic interactions between tobramycin and non-antibiotic drugs against planktonic cells. Although a more clinically relevant ASM medium was used, the *in vivo* significance of our findings remains to be investigated and if it is confirmed, then this suggests careful attention should be considered when other drugs are prescribed simultaneously with tobramycin, particularly as most CF patients regularly use of many non-antibiotic drugs. Apart from antagonistic interactions, some of the non-antibiotic and antibiotic combinations did show synergistic interactions with tobramycin against biofilms of PAO1 but not against all clinical isolates. Such combinations were observed with amitriptyline, niclosamide, and colistin, which resulted in 80% reduction in biofilm biomass as compared to tobramycin alone. These combinations could be used as adjuvants with tobramycin for the treatment of *P. aeruginosa* infections, but further *in vitro* and *in vivo* experiments are warranted to ensure that they are effective.

Chapter 1: Introduction

Pseudomonas aeruginosa Biofilm and the Effect of Tobramycin

1. *Pseudomonas aeruginosa*

1.1 Clinical significance

P. aeruginosa is an opportunistic bacterium, which is the leading cause for several human infections particularly in immunocompromised patients (Kipnis et al., 2006). These involve for example ventilator-associated pneumonia, catheter-related infections, wound infections, and cystic fibrosis (CF) lung infections (Ciofu and Tolker-Nielsen, 2019). For instance, according to the Centres for Disease Control and Prevention (CDC) surveillance, *P. aeruginosa* is the second main causative pathogen of nosocomial pneumonia (14 -16%), the third leading cause of urinary tract infections (7-11%), the fourth most commonly isolated pathogen from surgical site infections (8%), and the major pathogen that caused bloodstream infections (2-6%) (Lister et al., 2009). Moreover, *P. aeruginosa* causes 80% of CF-related lung infections (See Section 1.3) (Hoiby, 2011; Gaspar et al., 2013), which are considered a significant health problem globally and result in high morbidity and mortality rates (Stover et al., 2000; Lenoir et al., 2007; Ashish et al., 2012; Lutz et al., 2013).

Recently, the CDC reported that in the USA, *P. aeruginosa* was responsible for 32,600 infections in hospitalized patients and it was also the causative of an estimated 2,700 deaths (CDC, 2017). Besides this, *P. aeruginosa* is classified as a bacterium that belongs to the ESKAPE pathogens, which also includes *Enterococcus faecium*, *Staphylococcus aureus*, *Klebsiella pneumoniae, Acinetobacter baumannii,* and *Enterobacter* spp. (Askoura et al., 2011; Housseini B Issa et al., 2018; Reza et al., 2019). These bacteria are of significant concern as they cause the majority of nosocomial infections and are increasingly able to escape or resist the action of more than one antibiotic in three or more different antibacterial classes (Magiorakos et al., 2012). Regarding multi drug resistance (MDR) *P. aeruginosa*, a report from the USA found that 13% of severe infections are caused by MDR *P. aeruginosa* isolates (Dreier and Ruggerone, 2015). Similarly, a study from Europe found that between 2005-2013, 14% of *P. aeruginosa* isolates were MDR (Dreier and Ruggerone, 2015). Such MDR *P. aeruginosa* isolates have a significant high level of resistance to multiple classes of antibiotics such as carbapenems, cephalosporins, fluoroquinolones, and aminoglycosides (Dreier and Ruggerone,

2015). This situation has led the World Health Organization (WHO) to consider *P. aeruginosa* a priority for the development of new antibiotics (WHO, 2017). Collectively, MDR bacteria including *P. aeruginosa* are considered a global health hazard, particularly as they are expected to cause 10 million deaths by 2050 (Reza et al., 2019).

1.1.2 General characteristics and natural habitats

P. aeruginosa (Figure 1.1) is a rod-shaped (1-5 µm long), motile, aerobic, Gram-negative bacterium, which has several characteristics that make this organism a versatile pathogen (Diggle and Whiteley, 2019). These include the ability of *P. aeruginosa* to grow in anaerobic environments utilizing nitrite (NO_2^-) and nitrate (NO_3^-) ions as respiratory electron acceptors and utilising of different carbon sources for energy production, the ability to survive under variety of temperatures up to 42°C, and the ability to produce several virulence factors (See Section 1.1.3) that allow for different types of infections (Kung et al., 2010; Ozer et al., 2014; Diggle and Whiteley, 2019).

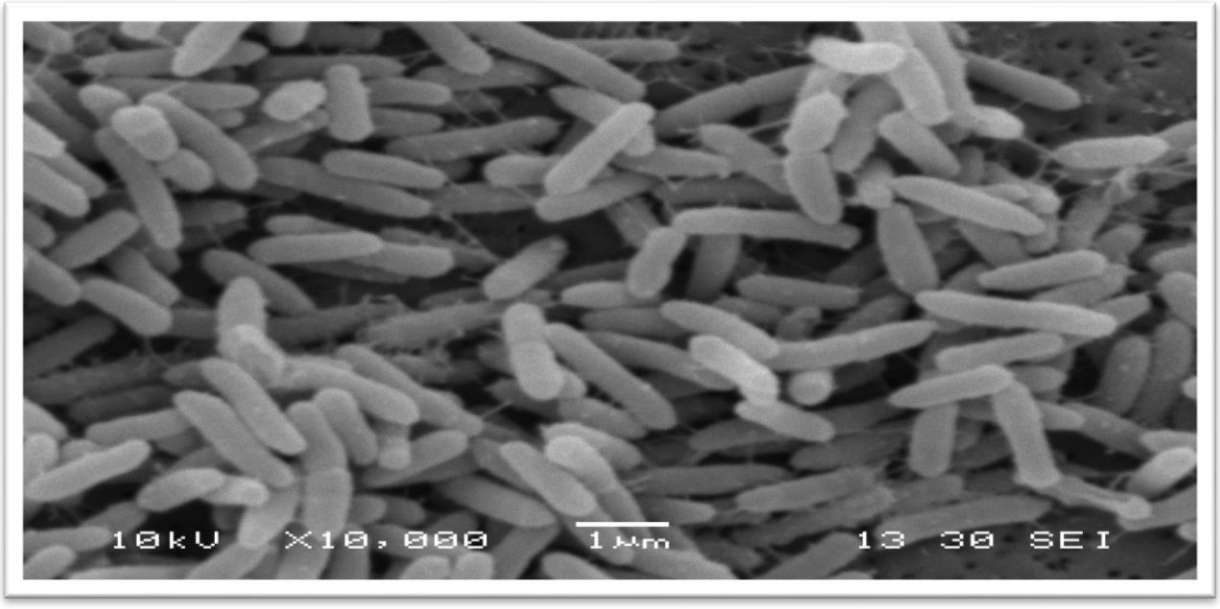

Figure 1.1 Scanning electron micrograph of *P. aeruginosa* (unpublished image)

P. aeruginosa inhabits various types of environment such as soil, water, plants, animals, and humans (Doring et al., 2000; Diggle and Whiteley, 2019). The ability of this bacterium to adapt and grow in such diverse niches is attributed to its genome size, which is relatively large. (Diggle and Whiteley, 2019). *P. aeruginosa* PAO1, which was originally isolated from a wound infection, is now one of the most commonly used strains in research and has a genome size of 6.3 million base pairs (Mbp) that contains 5770 open reading frames (Stover et al., 2000; Kung et al., 2010; Diggle and Whiteley, 2019). This large genome can be classified into core and accessory genomes. The core represents 90% of the genome and is found in all strains of the same species, while the accessory genome represents about 10% and is found only in some strains. This genome codes for many transport proteins, enzymes for metabolism, outer membrane proteins, and virulence factors, which have an important role in causing infections and developing resistance to antibiotics (Rybtke et al., 2011; Ozer et al., 2014).

1.1.3 Virulence factors and pathogenicity

P. aeruginosa uses different types of virulence factors that facilitate its ability to cause infections in humans. Such virulence factors include the proteinaceous surface appendages, which for each cell involves a single flagellum and multiple type IV pili (Gellatly and Hancock, 2013). These are known to have a role in surface adhesion, swimming and twitching motilities. Additionally, they also have a role in starting the inflammatory response in lung infections through binding to epithelial cell receptors called asialo-gangliosides (Gellatly and Hancock, 2013).

Virulence factors that are secreted by *P. aeruginosa* involve five different secretion protein systems, which are named type I to type V (T1SS to T5SS). Among those, the type III secretion system (T3SS) is a major class. This system secretes effector proteins, which are toxic proteins that are released directly into the cytosol of host cells and cause damage to host tissue (Lyczak et al., 2000). These effector proteins include ExoY, ExoS, ExoT, and ExoU. Among those four types, it is known that ExoS and ExoU are major cytotoxins, while ExoT and Exo Y play a minor role in host pathogenesis (Gellatly and Hancock, 2013). Another secretion system is the type II secretion system (T2SS), which secretes several proteins such as elastases, proteases, phospholipase C, and exotoxin A. These are secreted in the extracellular milieu and each one

has a specific function. For example, in lung injury, elastases such as Las A and Las B cause damage to respiratory epithelial tight junctions. Phospholipase C is another secreted protein, which degrades the phospholipids in host cell membranes. Finally, exotoxin A is one of the most toxic virulence factors that can cause apoptosis of host immune cells (Driscoll et al., 2007; Gellatly and Hancock, 2013). In addition to the above-mentioned secretion systems, another type has been characterized and referred to as T6SS (H1-T6SS, H2-T6SS, H3-T6SS) (Filloux et al., 2008; de Bentzmann and Plesiat, 2011; Diggle and Whiteley, 2019). It has been found that H1-T6SS has a role in chronic infections, whereas the function of the other two has not yet been determined (de Bentzmann and Plesiat, 2011). However, T6SS is generally known to support the growth of *P. aeruginosa* by killing the other competing bacterial species and has also been found to have a role in biofilm formation (Chen et al., 2015). Other virulence factors that are also produced by *P. aeruginosa* are siderophores, which include pyoverdine and pyochelin. These have an important role in scavenging iron, which is an essential nutrient necessary for several physiological functions such as energy production and biofilm formation (Banin et al., 2005).

1.2 *P. aeruginosa* and biofilm formation

Biofilms are structured communities of sessile bacterial cells, which are encased within a self-generated extracellular polymeric substances (EPS) matrix that represents 50-90% of the biofilm (Whiteley et al., 2001; Germoni et al., 2016; Whiteley et al., 2017; Roy et al., 2018). The composition of this matrix depends on the type of strain and growth conditions (Ciofu and Tolker-Nielsen, 2019). Generally, the matrix consists of polysaccharides, lipids, DNA, and/or proteins (Hoiby et al., 2010b; Roy et al., 2018). Examples of the polysaccharides that are produced by *P. aeruginosa* and found in the biofilm matrix are Pel, Psl, and alginate. Other lipid components that also play a role in the matrix are rhamnolipids, which are glycolipid virulence factors that have a role in inhibition of phagocytosis, suppression of cilia function, and deactivation of polymorphonucleocytes (Soberón-Chávez et al., 2005). Finally, different types of proteins are also included in the biofilm matrix, examples of which are type IV pili, Cup fimbriae, and adhesins. Collectively, all of these components have an important role in the maintenance and stability of biofilms (Ciofu and Tolker-Nielsen, 2019).

The formation of biofilms by *P. aeruginosa* is controlled by quorum sensing (QS), which is a complex cell- to -cell communication system (Hoiby et al., 2010a; Roy et al., 2018). This is a signalling system that enables bacteria to communicate with each other through signalling molecules called auto-inducers (Schroeder et al., 2017). Three different auto-inducers are produced by *P. aeruginosa*. These include acyl-homo-serine lactones (AHLs), which are in two types. The first AHL is 3-oxo-dodecanoyl homoserine lactone (C12-HSL), which is produced by LasI synthase and binds to a transcriptional activator called LasR, which activates the production of different genes. The second AHL is butyryl homoserine lactone (C4-HSL), which is produced as a part of Rhll synthase and binds to a transcriptional activator termed as RhIR (Masák et al., 2014). Beside AHLs, *Pseudomonas* quinolones signal (PQS) is another type of autoinducer, which is also produced by different pathways described elsewhere (Kipnis et al., 2006; Gellatly and Hancock, 2013; Diggle and Whiteley, 2019). Following production of these autoinducers, they diffuse from the cytoplasm to the extracellular milieu through transporter proteins, and when they reach to critical or threshold concentrations, expression of several genes including those coding for biofilm formation are induced (Hoiby et al., 2010a; Roy et al., 2018).

Biofilm formation in *P. aeruginosa* occurs in different stages (Figure 1.2). These include the initial adhesion of planktonic (freely swimming) bacterial cells to a surface. This attachment is mediated through several components, which involve surface appendages such as flagella, type IV pili, and also other elements such as Psl (mannose-rich polysaccharide) and adhesion proteins termed as Cup-fimbriae (Rybtke et al., 2011). This step is followed by microcolony formation, where cells are downregulating flagella production and also undergoing cycles of cell division. During this stage, bacterial cells start producing constituents of the extracellular matrix that is shown as green areas in Figure 1.2, which offer not the only robust attachment of cells to the surface but also strong links to other cells. Moreover, these matrix components provide cells inside a biofilm with protection from environmental stressors. After microcolony formation, the cells continue to grow leading to the build-up of mature biofilm architecture. Finally, this cycle ends with the biofilm dispersion, which is induced for instance by the restriction of nutrients, and in particular oxygen, iron, and carbon. The biofilm dispersion results in releasing of individual planktonic cells, which start to disseminate to other surfaces and cause further infections (Hoiby et al., 2010a; Taylor et al., 2014; Kang and Kirienko, 2018).

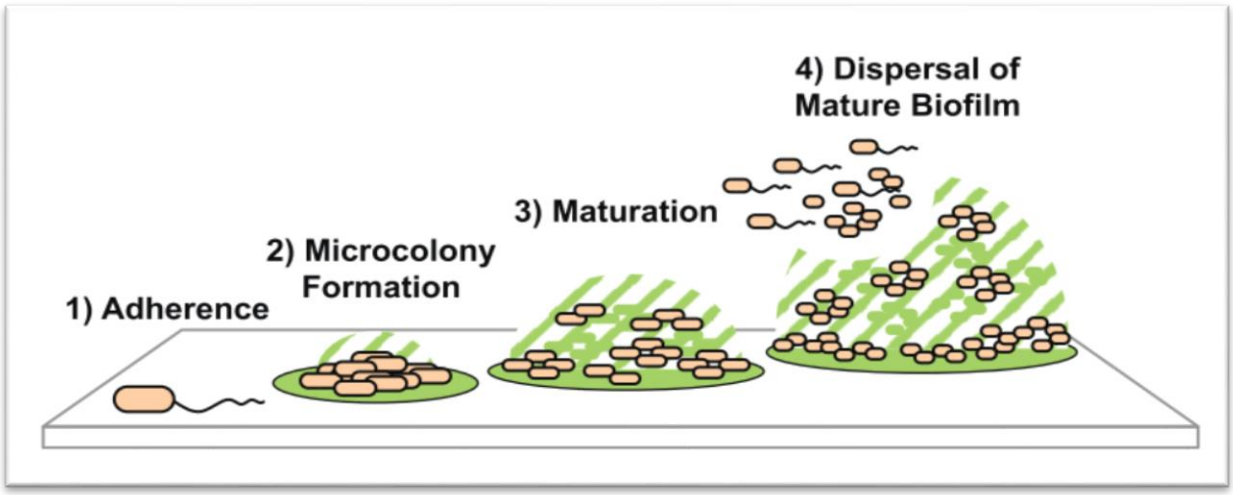

Figure 1.2. Representative stages of biofilm formation. Reproduced from Taylor et al., 2014, with permission. See text for details.

1.3 *P. aeruginosa* and cystic fibrosis

One of the common biofilm-related infections that are caused by *P. aeruginosa* are lung infections in CF patients (Williamson et al., 2012; Ciofu et al., 2015). CF is a genetic disease that affects around 70,000 people worldwide (Moreau-Marquis et al., 2015). This inherited disease results from mutations in a gene that encodes for the cystic fibrosis transmembrane conductance regulator (CFTR) protein (Heijerman et al., 2009). Mutations in the *CFTR* gene lead to a malfunction in chloride channels that are controlled by CFTR. This, in turn, results in an imbalance of electrolytes and water movement across cell membranes. Such impairment leads to alteration in the physical properties of mucus, which becomes highly dehydrated, thick, and viscous (Doring et al., 2000). The abnormal mucus causes a reduction in the effectiveness of mucociliary clearance, which results in the accumulation and formation of mucus plugs in the endobronchial region of the lung. Since mucus accumulates, this offers a fertile environment for the proliferation of several types of bacteria (Heijerman et al., 2009; Moore and Mastoridis, 2017). Bacterial lung colonization in CF patients varies according to age group (Gaspar et al., 2013). For instance, the Cystic Fibrosis Trust national report 2018 (UK CF Registry, 2018) shows that the most commonly isolated bacteria during childhood are *Haemophilus influenzae* and *Staphylococcus aureus* (Figure 1.3), whereas during adulthood *P. aeruginosa* becomes the most dominant bacterium (Figure 1.3).

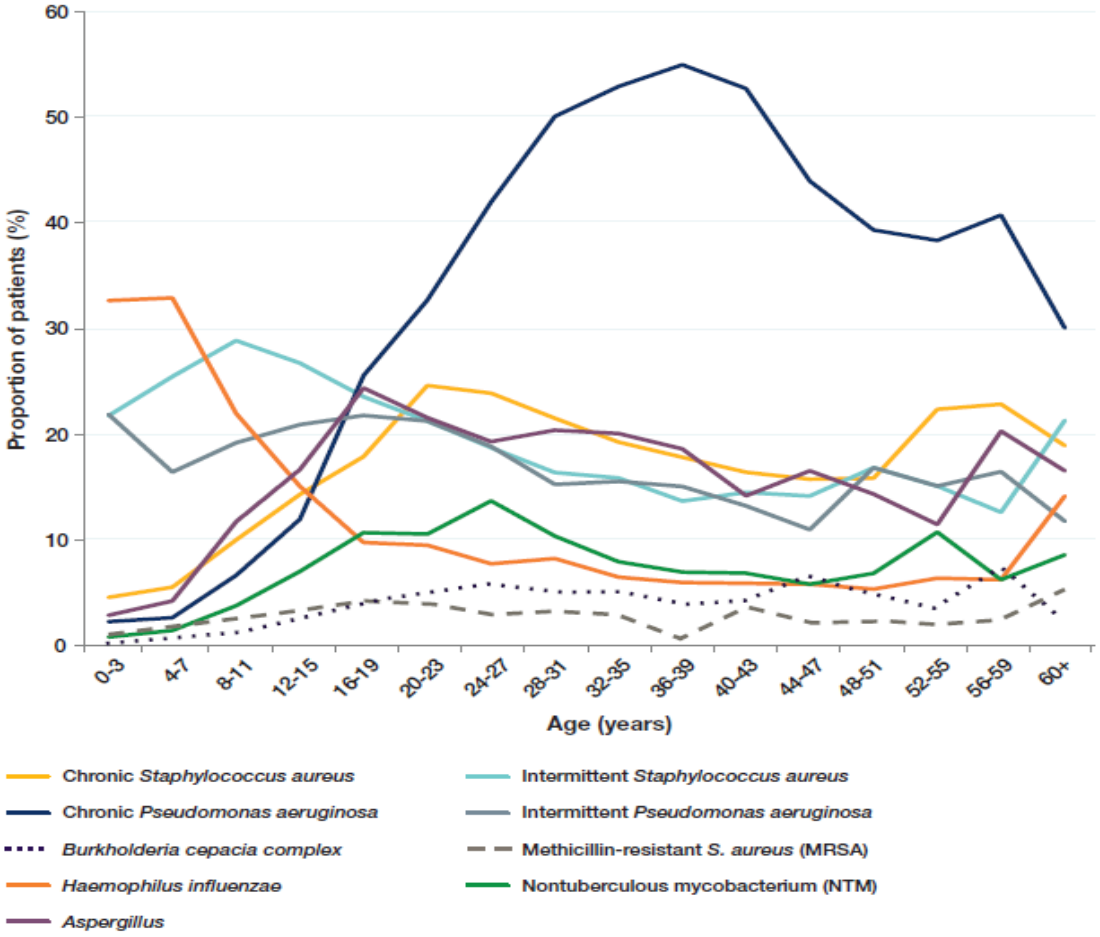

Figure 1.3. Prevalence of respiratory pathogens by age. Reproduced from UK Cystic Fibrosis, 2018 National Data Report (UK CF Registry, 2018) with permission.

CF patients acquire the initial infection with *P. aeruginosa* directly through inhalation from the surrounding environment (Germoni et al., 2016), but it can also be acquired by transmission between patients (Doring et al., 2000; Gaspar et al., 2013). Once *P. aeruginosa* enters the lungs, it binds strongly through flagella and type IV pili to epithelial cell receptors called asialo-gangliosides that are highly expressed in damaged lung tissue (Goldberg and Pier, 2000). During colonization in the lung, *P. aeruginosa* develops different phenotypes. For instance, in early CF lung infections, the colonization is mostly caused by non-mucoid phenotypes (Bjarnsholt et al., 2005), which may be susceptible to antibiotic treatment (Chuchalin et al., 2009; Damron and Goldberg, 2012). However, during long-term infection, *P. aeruginosa* undergoes prominent genetically and phenotypically diversifications, which result in the appearance of different phenotypes with enhanced antibiotic tolerance.

One such phenotype is the small-colony variants (SCVs), which grow as a small colony of 1-3 mm in diameter and emerge after prolonged antibiotic therapy due to high selection pressure. This phenotype is characterised by an enhanced adhesive ability to tissue (Haussler et al., 2003; Malone, 2015). This is attributed to their ability to produce Pel and Psl exopolysaccharides that are important in biofilm formation (Malone, 2015). Additionally, SCV phenotypes are known to be auxotrophic with a slow growth rate and enhanced antimicrobial tolerance (Haussler et al., 2003; Hocquet et al., 2003; Malone, 2015).

Another phenotype that is frequently isolated from CF patients and has considerable attention in medical research is the mucoid variant (Goldberg and Pier, 2000). This mucoid phenotype is triggered by the inflammatory response and oxidative stress environment in the CF lung, which is characterized for instance by the presence of reactive oxygen species such as hydrogen peroxide (H_2O_2) that is released by neutrophils undergoing respiratory burst (Bjarnsholt et al., 2005; Ciofu et al., 2012). Such reactive oxygen species cause mutations in the *mucA* gene (Rybtke et al., 2011), which encodes a transmembrane protein that works as the principal negative controller of the AlgU (also known as the AlgT) protein. AlgU is a sigma factor that is required for the initiation transcription of genes for alginate production through binding to the promoter of a gene called *algD* (Campódonico et al., 2008). This in turns leads to the overproduction of alginate, which is an exopolysaccharide that consists of repeating polymers of mannuronic and glucuronic acid (Kipnis et al., 2006; Hogardt and Heesemann, 2010). Alginate is considered one of the major components of the EPS matrix in biofilms formed by mucoid *P. aeruginosa* strains. In respect of *in vitro* mucoid isolates, it is evident that such phenotypes quickly transform to non-mucoid variant and this is due to mutation suppression (Bergan and Hoiby, 1975; Pritt et al., 2007). Generally, the emergence of mucoid variants in CF lung leads to a poor prognosis because such variants are known to have a significant role in protecting *P. aeruginosa* from phagocytosis and antibiotics (Kipnis et al., 2006; Driscoll et al., 2007). This consequently leads to a high degree of tolerance towards several classes of antibiotics including aminoglycosides such as tobramycin (Hentzer et al., 2001; Ernst et al., 2007; Ciofu et al., 2012; Lamppa and Griswold, 2013; Roy et al., 2018).

1.4 *P. aeruginosa* and antibiotic resistance

P. aeruginosa has an enhanced ability to quickly adapt to changing conditions such as antibiotic exposure, which leads to the development of resistance (Dozzo and Moser, 2010). *P. aeruginosa* antibiotic resistance is growing, and this is also accompanied by the emergence of multi-drug resistant strains, for which treatment options are limited (Dozzo and Moser, 2010; Tunney et al., 2018). For instance, a recent report from the WHO has listed *P. aeruginosa* as a critical pathogen that requires urgent research and development of antibiotics (WHO, 2017). The development of antibiotic therapy requires a better understanding of the mechanisms of such resistance. Several resistance mechanisms have been documented, which involve both acquired and intrinsic resistance, as well as phenotypic tolerance (Khalil et al., 2008; Taylor et al., 2014; Wright, 2016). Acquired resistance has been reviewed elsewhere (Breidenstein et al., 2011; Schroeder et al., 2017), but intrinsic and phenotypic resistance mechanisms are discussed in more detail below.

1.4.1 The outer membrane permeability

Gram-negative bacteria including *P. aeruginosa* are characterized by the presence of an outer membrane in their cellular structure. This outer membrane acts as a barrier and restricts the permeability of both hydrophilic and hydrophobic drugs (Nehme et al., 2018). Generally, the outer membrane comprises of two asymmetric layers, which are the inner core phospholipid and the outer leaflet that contains lipopolysaccharides (LPS) (Nehme et al., 2018). The latter consist of hydrophilic moieties of a core oligosaccharide that is linked to O antigen. These moieties provide a hydration environment. The core oligosaccharide is also covalently bound to lipid A, a hydrophobic moiety that is known to be in a gel-like state with very low fluidity (Delcour, 2009; Muheim et al., 2017). This composition of the outer membrane strongly limits the penetration of hydrophobic drugs (Muheim et al., 2017). For example, the penetration of hydrophobic drugs is limited by 50 to 100-fold in the outer membrane lipopolysaccharides as compared to the inner cytoplasmic phospholipid membrane (Nikaido, 2003). Hydrophilic drugs can cross the outer membrane via protein channels that are embedded within the outer membrane and are termed as β-barrel porins (Delcour, 2009; Muheim et al., 2017). However,

these porin channels are not always functional and also have a low permeation, which is restricted by the charge and the molecular mass of compounds (Nikaido and Vaara, 1985; Nikaido, 2003; Khalil et al., 2008). For instance, only drugs with a molecular mass < 600 g/mol can passively diffuse through these channels. Other charged hydrophilic drugs with a molecular mass > 600 g/mol can penetrate the outer membrane by a different pathway, which is referred to as self-promoting uptake (Nikaido, 2003). This uptake is characterized by the electrostatic interactions between cationic drugs and anionic lipopolysaccharide of the outer membrane. This mechanism was observed to occur mostly with drugs with high molecular mass and positively charged such as polymyxin or aminoglycoside antibiotics (Nehme et al., 2018). Accordingly, it is obvious that *P. aeruginosa* permeability either through porins or self-promoted uptake is restricted by drug properties and the functionality of these barriers, and all of these represent a significant challenge for drug uptake. Importantly, drug penetration in *P. aeruginosa* is reported to be 12 to 100-fold lower than the outer membrane permeability in other Gram-negative bacteria such as *E. coli* (Gellatly and Hancock, 2013; Domalaon et al., 2018). This is related to different characteristics of the outer membrane in *E. coli*, in which there are trimeric porins (e.g. OmpC, OmpF) that allow quick penetration of substances. However, in *P. aeruginosa* there are rather specific and fewer porins (e.g. OprF, OprD), which are also monomeric with a relatively small opening that only permits slow diffusion of substances (Nikaido, 2011; Dreier and Ruggerone, 2015).

1.4.2 Multi-drug efflux pumps

Another mechanism of intrinsic resistance is through multi-drug efflux pumps, which have a major role in *P. aeruginosa* resistance to several antibiotics (Beceiro et al., 2013). These efflux pumps remove drug molecules from the periplasm and cytoplasm, thus significantly lowering intracellular drug concentrations (Kiser et al., 2010; Nikaido and Pagès, 2012). In *P. aeruginosa*, it has been determined that there are twelve efflux pumps belonging to the family of Resistance Nodulation-Cell-division (RND) proteins, four of which have been characterised for their important role in antibiotic resistance (Nikaido, 1996; Nikaido, 2011; Nikaido and Pagès, 2012).

These efflux pumps are MexAB-OprM, MexXY-OprM, MexCD-OprJ, and MexEF-OprN (Table 1.1). Such pumps differ in their substrate affinity and each pump extrudes a wide range or specific classes of antibiotics (Table 1.1). For instance, MexAB is the most commonly expressed efflux pump among the other pumps, and export a wide variety of antibiotic drugs from different families such as fluoroquinolones, cephalosporins, β-lactamase inhibitors, penicillins, and carbapenems (Lister et al., 2009; Housseini B Issa et al., 2018). Other efflux pumps are only expressed under particular conditions and are more specific in the drugs they export (Housseini B Issa et al., 2018). For example, the MexXY pump is known to have a major role in exporting aminoglycosides such as tobramycin (Aeschlimann, 2003; Hocquet et al., 2003; Ratjen et al., 2009; Nikaido and Pagès, 2012).

Table 1.1 Multi-drug efflux pumps with known antibiotic substrate in *P. aeruginosa*.

MexA-MexB- OprM	MexX-MexY-OprM	MexE-MexF-OprN	MexC-MexD-OprJ
Fluoroquinolones [a]	**Aminoglycosides**	**Fluoroquinolones**	**Fluoroquinolones**
Norfloxacin [b]	Tobramycin	Norfloxacin	Trovafloxacin
Levofloxacin	Amikacin	Ciprofloxacin	Norfloxacin
Ciprofloxacin	Gentamycin	Levofloxacin	Ciprofloxacin
Cephalosporins	**Fluoroquinolones**	**β-lactamase inhibitor**	Levofloxacin
Cefuroxime	Ciprofloxacin	Clavulanic acid	**Penicillin**
Ceftazidime	Levofloxacin	Sulbactam	Nafcillin
Cefotaxime	**Cephalosporins**	**Chloramphenicol**	**Macrolides**
β-lactamase inhibitor	Cefepime	**Trimethoprim**	Erythromycin
Sulbactam	Cefotaxime		**Chloramphenicol**
Clavulanic acid	**Macrolides**		**Tetracycline**
Penicillin	Erythromycin		**Cephalosporins**
Nafcillin	**Tetracyclines**		Cefuroxime
Carbenicillin			Cefepime
Piperacillin			
Carbapenem			
Meropenem			
Monobactam			
Aztreonam			
Chloramphenicol			
Trimethoprim			
Tetracyclines			

[a] the name of the antibiotic class, [b] the name of agents in that class.

In order for these pumps to export antibiotics, each pump has tripartite structure (Figure 1.4), with their components acting synergistically in a collaborative manner. Each pump consists of a linker or a membrane fusion protein (MFPs; MexA, MexC, MexE, MexX), a transporter protein belonging to the RND family (MexB, MexD, MexF, MexY), and an outer membrane channel protein (OprM, OprJ, OprN) (Nikaido and Pagès, 2012). Antibiotic or drug can be removed from the cytoplasm, periplasm, and from the cytoplasmic membrane by the RND transporter protein using the proton motive force as a source of energy. MFPs act as a connection between the transporter proteins and the outer membrane proteins, which act in the last step in the process of removing antibiotics (Aeschlimann, 2003; Askoura et al., 2011; Li et al., 2015). Collectively, the abundance of effective efflux pump systems combined with the reduced permeability of the outer membrane all contribute to the intrinsic resistance to antibiotics in *P. aeruginosa* (Delcour, 2009).

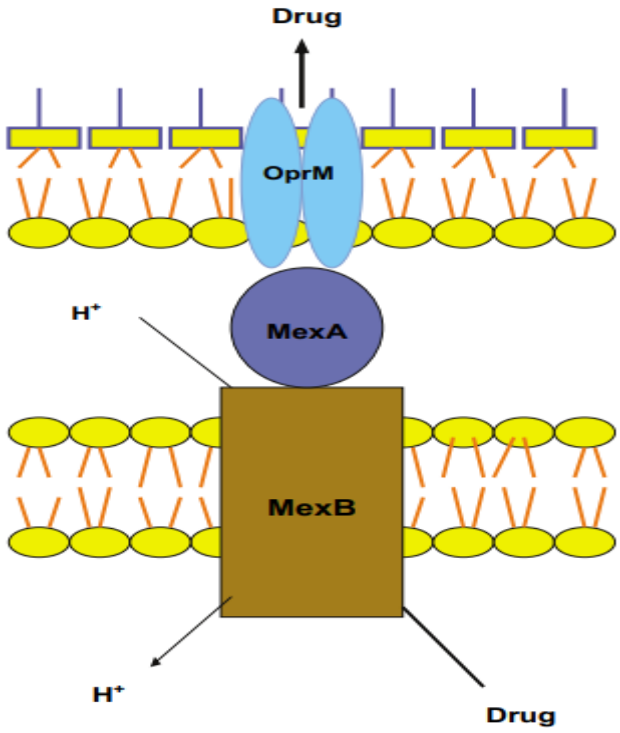

Figure 1.4. Schematic structure of the most commonly expressed efflux pumps (MexAB-OprM) in *P. aeruginosa*. MexB is the transporter protein RND that transports drug using proton motive force as a source of energy. MexA is the linker or membrane fusion protein, and OprM is the outer membrane protein. Reproduced from (Askoura et al., 2011). See details in the text.

1.4.3 Phenotypic or adaptive tolerance

Besides the intrinsic resistance in *P. aeruginosa,* phenotypic or adaptive tolerance also plays an important role. This tolerance is largely associated with environmental conditions, which include for example specific modes of growth such as biofilm formation. It is estimated that more than 80% of human infections are biofilm-related, among them infections caused by *P. aeruginosa* (Song et al., 2016; Meylan et al., 2017). As discussed earlier (Section 1.2), *P. aeruginosa* forms biofilms in several infections including lung infections in CF patients. Such biofilms are difficult to eradicate as these have a tolerance that may be 100-1000 fold increased as compared to their planktonic counterparts (Roberts et al., 2015; Roy et al., 2018).

The tolerance of biofilms is attributed to several structural properties and environment created in the biofilm. For instance, each biofilm is surrounded by an EPS matrix (Roberts et al., 2015). The components of this matrix could bind or adsorb antibiotics, which might result in a reduction of its penetration into a biofilm. As an example, the biofilm matrix of *P. aeruginosa* contains anionic polymers such as extracellular DNA and alginate, which could bind cationic antibiotics such as tobramycin and limit its diffusion (Hoiby et al., 2010a; Rybtke et al., 2011; Ciofu et al., 2015). However, neutral antibiotics such as the fluoroquinolones (e.g. ciprofloxacin) can readily penetrate the biofilm matrix (Ciofu and Tolker-Nielsen, 2019).

Other factors that enhance antimicrobial tolerance are biofilm specific conditions, which affect the characteristics of bacterial cells (Roy et al., 2018). For example, some bacterial cells inside a biofilm are in a (semi-)dormant state, which is due to the reduced availability of nutrients and oxygen. Such cells are known to have a low metabolic rate with a decreased level of gene expression and protein synthesis (Rybtke et al., 2011; Williamson et al., 2012), which results in slow rates of growth and reduced susceptibility to antibiotic treatment. Several antibiotic classes such as tetracycline, fluoroquinolones, and aminoglycosides have a higher killing activity on rapidly dividing cells as compared to slowly growing counterparts, because in the latter the rate of synthesis of proteins and DNA, which are targets for the previously mentioned antibiotics, is at a very low level (Williamson et al., 2012; Ciofu et al., 2015; Ciofu and Tolker-Nielsen, 2019). Polymyxin antibiotics are an exception with colistin being also active against slowly growing cells (Rybtke et al., 2011; Ciofu et al., 2015). This is mainly attributed to the

mechanism of action of colistin, which primarily depends on the disruption of the outer and cytoplasm membranes causing cell lysis (Ciofu and Tolker-Nielsen, 2019).

Besides the role of EPS and dormancy of cells in biofilm tolerance to antibiotics, other factors can also have a role in this. For instance, the microaerobic conditions particularly deep inside a biofilm have been shown to enhance tolerance to some antibiotics such as tobramycin. This is because the uptake of tobramycin (See Section 1.5.1) into bacterial cells is an energy-dependent process and, also, part of the bactericidal activity of tobramycin depends on the production of reactive oxygen species. All of these processes require the presence of oxygen, and an anaerobic environment could therefore significantly impair tobramycin activity (Hoiby et al., 2010a; Roy et al., 2018; Ciofu and Tolker-Nielsen, 2019). Furthermore, due to the dense population of bacterial cells inside a biofilm, fractions of these bacterial cells are exposed to sub-minimal inhibitory concentrations of antibiotics (Hoffman et al., 2005). Such concentrations could also promote antibiotic tolerance, as it has been shown that sub-lethal concentrations of antibiotic agents could induce biofilm formation (Wassermann et al., 2016; Roy et al., 2018). Finally, cells inside a biofilm experience a high level of mutations that could lead to a mucoid conversion , as explained earlier, and resulting in increased the levels of antibiotic resistance (Roy et al., 2018). Indeed, there are significant chances for horizontal gene transfer inside a biofilm, which could also promote antimicrobial resistance (Hoiby et al., 2010b; Beceiro et al., 2013).

1.4.4 Aminoglycoside resistance in *P. aeruginosa*

The resistance of *P. aeruginosa* toward aminoglycoside antibiotics has been well documented (Bassetti et al., 2018). For instance, the European Antimicrobial Resistance Surveillance system (EARSS) has determined resistance in this pathogen around Europe. In several European countries, it has been found that aminoglycoside resistance is high. For example, as determined by the EARSS surveillance in 2018 (Figure 1.5), the percentage of resistance in *P. aeruginosa* clinical isolates was 50.7% in Romania, 37.4% in Slovakia, 26.5% in Greece, and 26% in Poland. In the UK, the resistance is low 4.5% (EARS-NET, 2018), however, it should be noted that this was increased from only 1.9% in 2010 (EARS-NET, 2010).

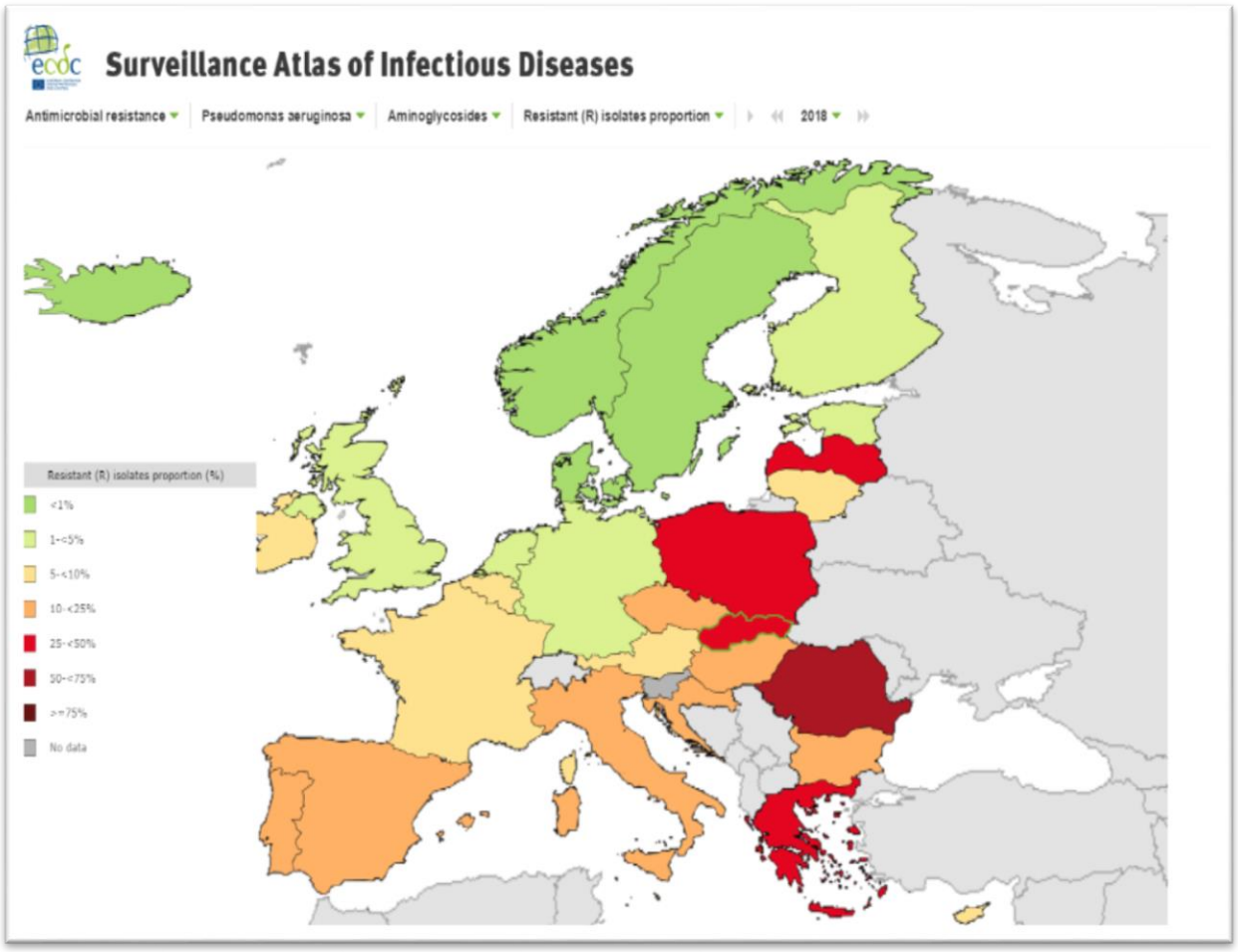

Figure 1.5. Distribution of aminoglycoside resistance in *P. aeruginosa* in EARS-Net countries in 2018 (EARS-NET, 2018).

P. aeruginosa resistance to aminoglycosides including tobramycin is related to the outer membrane permeability and efflux pumps as discussed above (Gaspar et al., 2013). For instance, the permeability of these porin channels to aminoglycosides such as tobramycin is relatively low because of the small porin size of < 600 Da, and other studies suggested that such porin limits the penetration of any molecules larger than 200 Da. As the molecular weight of tobramycin (467.5 Da) is relatively large, this can strongly restrict tobramycin penetration (Zgurskaya et al., 2015). Besides this, aminoglycosides are considered a substrate for MexXY efflux pumps, which can extrude antibiotics from cells before reaching their cellular target (Nikaido and Pagès, 2012). Additionally, other mechanisms of resistance also have an important role (Avent et al., 2011). Firstly, there may be acquired resistance that occurs through the expression of aminoglycoside modifying enzymes (Avent et al., 2011; Halfon et al., 2019). These enzymes include aminoglycoside acetyltransferases that target the antibiotic at NH_2-

groups, and aminoglycoside phosphotransferases that target antibiotic at OH- groups. Such alterations to the aminoglycoside molecule can impair the binding affinity to their target, resulting in loss of antibacterial activity. Another resistance mechanism is through target site modifications, which include for instance methylation of the ribosomal 16S rRNA subunit, which decreases the binding affinity of drug molecules to the target site (Ramirez and Tolmasky, 2010).

1.5 Antibiotic treatment for *P. aeruginosa* lung biofilm infections

Antibiotics are the standard drugs for the treatment of *P. aeruginosa* lung infections (Greally et al., 2012). Several antibiotic classes have been used, these include β-lactams such as extended-spectrum penicillin (e.g. piperacillin-tazobactam), monobactam (e.g. aztreonam), carbapenems (e.g. meropenem), and cephalosporins (e.g. ceftazidime, cefepime). Other antibiotic classes are fluoroquinolones (e.g. ciprofloxacin), polymyxins (e.g. colistin or polymyxin E), macrolides (e.g. azithromycin), and aminoglycosides (e.g. tobramycin) (Rybtke et al., 2011; Ashish et al., 2012; Ciofu et al., 2012; Bassetti et al., 2018). Aminoglycosides and particularly tobramycin are the most widely used therapy in the treatment of *P. aeruginosa* infections in CF patients (Konstan et al., 2011; Gaspar et al., 2013). Therefore, this thesis focuses mainly on the role of tobramycin (Figure 1.6) on eradication *P. aeruginosa* biofilms.

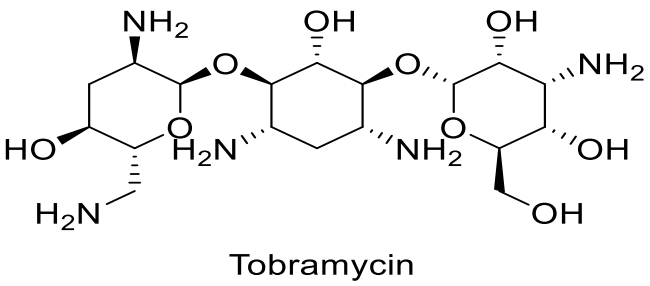

Figure 1.6. Chemical structure of tobramycin

1.5.1 Tobramycin mechanism of action

As discussed earlier, tobramycin belongs to the class of aminoglycoside antibiotics, which exert their activity by inhibiting protein synthesis. Tobramycin suppresses protein production by irreversible binding to the 30S subunit of the bacterial ribosome, thereby enhancing mistranslations and errors in protein synthesis (Doring et al., 2000; Heijerman et al., 2009; Avent et al., 2011; Krause et al., 2016). To achieve this, tobramycin needs to be taken up by bacterial cells. The uptake of tobramycin into bacterial cells takes place through two steps, which are all concentration-dependent but differ in their energy requirements.

The first step is the energy-independent uptake, which includes an electrostatic interaction between the cationic tobramycin and anionic lipopolysaccharides in the outer membrane (Avent et al., 2011). Such interaction can result in the displacement of cations (Mg^{+2}, Ca^{+2}), which have an important role in maintaining the stability and the integrity of the outer membrane. Therefore, elimination of these cations from their binding sites disrupts the outer membrane and enhances the permeation of tobramycin directly into the periplasm of bacteria (Avent et al., 2011; Domalaon et al., 2018).

The second step is an energy-dependent transport process that requires ATP, which is produced by ATP-synthetase (Ramirez and Tolmasky, 2010). This step includes two phases, which are the slow phase (I) and the rapid phase (II) (Nikaido, 2003; Avent et al., 2011). During phase I, tobramycin adsorbs to the cytoplasmic membrane and enters in low concentrations. These small amounts of tobramycin lead to the interruption of protein synthesis, which results in the production of impaired membrane proteins. The latter create non-specific channels or pores when inserted into the cytoplasmic membrane, which induces further uptake of tobramycin via the rapid phase II (Ramirez and Tolmasky, 2010; Krause et al., 2016). During phase II, the uptake of tobramycin is accelerated leading to more inhibition of protein production and finally cell death. Through this mechanism tobramycin has a bactericidal action against several aerobic Gram-positive and -negative pathogens (Ramirez and Tolmasky, 2010). Among the Gram-negative bacteria, tobramycin for instance inhibits the growth of *Klebsiella pneumonia*, *Escherichia coli*, and *P. aeruginosa* (Heijerman et al., 2009; Krause et al., 2016).

1.5.2 Tobramycin administration

Several routes of administration for tobramycin have been used in the treatment of *P. aeruginosa* CF lung infections. Unfortunately, oral delivery of tobramycin is not feasible because of the low bioavailability following oral administration (Ramirez and Tolmasky, 2010; Krause et al., 2016). This is attributed to the hydrophilic properties of tobramycin, which result in the efflux of tobramycin by P-glycoprotein pumps in the brush border of the small intestine and prevent its absorption from the gut (Banerjee et al., 2000). Tobramycin is bioavailable via the intravenous route, but this requires high doses to get an effective concentration in the respiratory epithelial tissue and bronchial secretions (Lenoir et al., 2007; Gaspar et al., 2013). Such high plasma levels are associated with severe side effects such as nephrotoxicity and ototoxicity (Lenoir et al., 2007; Ramirez and Tolmasky, 2010; Avent et al., 2011; Becker, 2013). Therefore, to avoid the concerns that are associated with poor oral bioavailability and the side effects of parenteral administration, the pulmonary administration of tobramycin by inhalation is the most widely used route in the treatment of CF lung infections (Lenoir et al., 2007).

1.5.3 Inhaled tobramycin

Inhaled tobramycin is considered as the frontline treatment for chronic CF lung infections with *P. aeruginosa* (Chuchalin et al., 2009; Konstan et al., 2011; Krause et al., 2016; Moore and Mastoridis, 2017; Jung et al., 2018; Moller et al., 2019). This is due to the local action of inhaled tobramycin directly at the site of infection and also has the advantage that higher concentrations can be achieved as compared to parenteral administration (Tiddens, 2004; Geller et al., 2011). Importantly, the occurrence of systemic organ toxicity is lower in comparison with an intravenous administration (Tiddens, 2004; Lenoir et al., 2007; Chuchalin et al., 2009; Heijerman et al., 2009; Bos et al., 2015; Krause et al., 2016). Moreover, delivering tobramycin by inhalation can reduce the emergence of antibiotic resistance due to the diminished exposure of the normal bacterial flora (Labiris and Dolovich, 2003; Chuchalin et al., 2009; Jung et al., 2018). With regards to patient outcomes, inhaled tobramycin results in better lung function, reduces hospitalisation duration time, and decreases the usage of intravenous antibiotics (Chuchalin et al., 2009). Therefore, inhaled tobramycin has been

recommended as the maintenance therapy in chronic CF patients by the European Consensus guidelines (Chuchalin et al., 2009). Two types of tobramycin inhalation formulation are available, which are tobramycin nebulizer solutions and inhalation powder (Tiddens, 2004; Tiddens et al., 2014).

1.5.3.1 Tobramycin nebulization

Nebulization of tobramycin in solution is frequently used in CF patients and has been shown to promote lung function, but this formulation has some drawbacks (Konstan et al., 2011). These include long treatment time for at least 20 min (Gaspar et al., 2013). Moreover, the drug is delivered using nebulizers, which are bulky devices that also require regular cleaning and disinfection (Geller et al., 2011; Konstan et al., 2011). Besides this, drug delivery from these devices results in a poor lung (5-11%) deposition (Pilcer et al., 2013; Hamed et al., 2017). Additionally, the drug in solution form is unstable at room temperature and requires specific storage conditions (VanDevanter and Geller, 2011). Collectively, these factors negatively affect the adherence of patients, especially considering that CF patients regularly use several other medications including inhaled drugs such as bronchodilators and mucolytics (Hamed et al., 2017). Therefore, a more appropriate delivery system has been developed using a dry tobramycin inhalation powder.

1.5.3.2 Tobramycin inhalation powder

The inhaled dry powder formulation of tobramycin overcomes the shortcomings of the nebulized solutions. For instance, tobramycin dry powder formulation is administered via a simple portable device (Figure 1.7) that only requires ~5 min administration time. Moreover, tobramycin dry powder formulation has better lung deposition of about 50% as compared to the inhaled solution. Also, no specific storage conditions or regular disinfections are required (Gaspar et al., 2013). Therefore, this leads to a decrease in the burden of treatment and better patient adherence, thereby improving treatment success (Geller et al., 2011; Woods and Rahman, 2018). The *in vitro* and *in vivo* efficacy as well as safety of tobramycin dry powder formulation have been documented, which have shown improvement in lung functions and

reduction in bacterial density (Konstan et al., 2011). The FDA approved tobramycin dry powder inhaler for CF patients is TOBI Podhaler® (Figure 1.7), which is made up of tobramycin as an active drug and other excipients. Tobramycin powder from 28 mg capsule is aerosolized using Podhaler device (Figure 1.7) by the energy of the patient's own inspiration (Konstan et al., 2011). This means the particles in the powder are separated from each other and carried in the airstream down to the lungs where they deposited (See details below). Similar to TOBI Podhaler®, another FDA-approved dry powder inhaler antibiotic for CF patients is Colobreath®, which contains colistin as an active ingredient (Woods and Rahman, 2018). Beside the abovementioned approved dry powder inhalers, there are number of antibiotics that are currently in the process of development as a dry powder formulation, these include levofloxacin, ciprofloxacin, and clarithromycin (Tiddens et al., 2014).

Figure 1.7. TOBI Podhaler® 28 mg (unpublished image).

Antibiotic from dry powder formulation is delivered via inhalation, in which after dry powder antibiotic is inhaled, the particles deposit into different compartments of the lung. Briefly, the lung consists of two regions (Figure 1.8), which are the conducting and the respiratory zones. The conducting zone includes trachea, bronchi, bronchioles, and terminal bronchioles, whereas the respiratory zone comprises of the respiratory bronchioles, alveolar ducts, and alveolar sacs (Hoiby, 2011). With regards to *P. aeruginosa* colonization, it has been found by a study from the Cystic Fibrosis Centre in the Copenhagen that non-mucoid strains are mostly present in the conducting zone, while mucoid variants distribute in both the conducting and respiratory zones. The reason for this could be because the mucoid variants are protected from immune defence

mechanisms such as polymorphonucleocytes in the conducting zone or alveolar macrophages in the respiratory zone (Bjarnsholt et al., 2009; Gaspar et al., 2013).

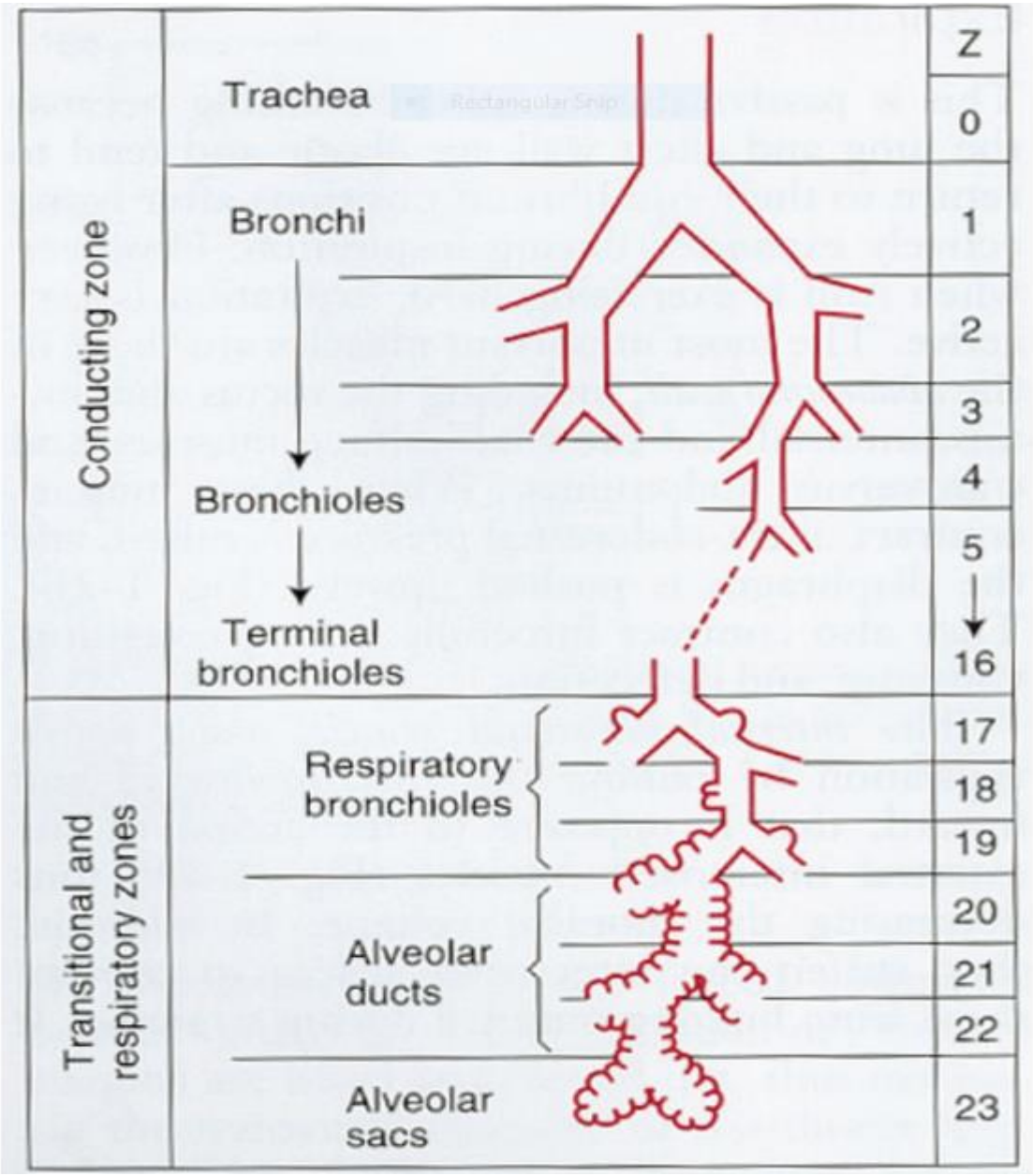

Figure 1.8. The conductive and respiratory zones (Z) of the lung. Conducting region that distributes through the 1st to the 16th airway generations or divisions, while respiratory zone represents the generations from 17th through 23rd. Reproduced from (Hoiby, 2011).

Following inhalation, these different zones in the lung receive inhaled drug particles, and the deposition of drug particles in such zones depends on several factors such as patient-associated factors and inhaled powder formulation properties (Tiddens et al., 2014). These characteristics involve particle shape, density, and size (Figure 1.9). Our particular interest was in powder

particle size and its impact on the pharmacological activity of the inhaled drugs. For instance, inhaled drug powder is known to be polydisperse in nature (Figure 1.9), with particles in the range of 3 - 10 µm mostly depositing in the conducting zone, whereas smaller drug particles in a range of 1-3 µm mainly deposit in the respiratory zone (Verbanck et al., 2006; Geller et al., 2011; Nafee et al., 2014). From a clinical efficacy point of view, for such differently sized particles to exert their pharmacological activity, they must dissolve in the first instance and this depends on the size of these particles, which in turn can influence drug efficacy (Nafee et al., 2014). For instance, it is unknown how these different particle sizes could influence the activity of dry powder inhalers antibiotics such as colistin or tobramycin against *P. aeruginosa* biofilms.

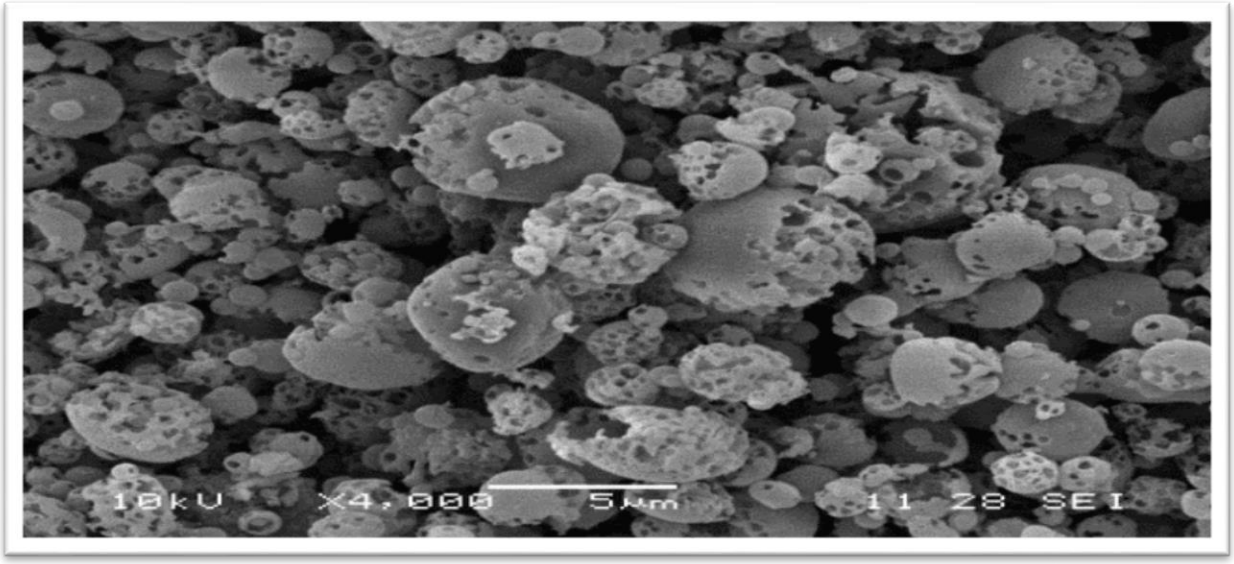

Figure 1.9. Scanning electron micrograph of tobramycin inhalation powder with different particle sizes (unpublished image).

The effect of particle size has, however, been studied for other drugs. For instance, nebulised solution of dornase alfa (a mucolytic agent that is used by CF patients), showed a trend of a better lung function when this drug was administered as small particles of 3.42 µm as compared to large particles of 6.87 µm (Shah et al., 1997; Heijerman et al., 2009). The authors explained this by the ability of small particles to penetrate into peripheral airways, while the penetration of larger particles is disrupted due to the pathologic conditions in the lung, which include structural changes and narrowing of the airways due to the mucus plugging, inflammation, and infection (Shah et al., 1997; Heijerman et al., 2009). Similarly, a study with inhaled beclomethasone nebulised solution that is used in asthmatic patients, also showed improvement

in lung functions when it was administered as extra fine particles of 1.1 µm compared to fine particles of 4 µm (Vanden Burgt et al., 2000; Van Schayck and Donnell, 2004; Leach et al., 2009). In the same way, other studies have reported that reduction in drug particle size is an efficient method to improve dissolution rate and absorption of orally administered drugs (Jinno et al., 2006; Liu et al., 2015). For example, a study with cilostazol, an oral anti-platelet and vasodilator drug, has shown better dissolution rate and solubility when it was delivered in small particle size of 2.4 µm as compared to the large particle size of 13 µm (Jinno et al., 2006). Therefore, a deep understanding of the impact of antibiotic particle size on its activity against *P. aeruginosa* biofilms could offer important data for the improvement and development of dry powder inhaler antibiotics.

1.6 Tobramycin combination therapy

To date, despite the improvement in antibiotic therapy for the management of *P. aeruginosa* infections, these are still difficult and challenging to eradicate (Silver, 2016; Wright, 2016; Momin et al., 2018; Miró-Canturri et al., 2019). The Infectious Disease Society of America has considered *P. aeruginosa* as one of top-threatening multi-drug resistant pathogens, for which considerable efforts should focus on the discovery and development of antibiotic therapies (Kung et al., 2010). Therefore, finding new strategies for treating such infections is warranted and recommend (Doern, 2014; Wright, 2016; Umerska et al., 2018).

Such strategies may involve combination antibiotic therapy. For example, several studies have reported that the use of aminoglycosides as monotherapy is one of the possible reasons for the inefficient treatment of *P. aeruginosa* infections (Driscoll et al., 2007; Bjarnsholt et al., 2018). Therefore, using two or more antibiotics in combination could potentially improve the activity of the currently available antibiotics (Balke et al., 2006; Imperi et al., 2013; Otto et al., 2019). Such an approach restores antibacterial activity and reduces antibiotic resistance because targeting bacterial pathogens through different inhibition mechanisms simultaneously renders bacteria unable to tolerate antibiotic treatment, making it harder to evolve resistance (Sader et al., 2003; Wright, 2016).

Currently, investigating tobramycin combinations with non-antibiotic drugs has attracted considerable interest as compared to traditional combinations with antibiotic agents (Wright, 2016; Laudy et al., 2017; Liu et al., 2017; Otto et al., 2019). This is mainly because of the current situation of antibiotic resistance and decreasing pipeline production of new antibiotics, in which using non-antibiotic drugs can be advantageous in different ways. For instance, these drugs do not affect bacterial growth, which can result in decreasing antibiotic selection pressure for resistance. Moreover, the development and improvement of these drugs are easier and quicker than producing new antibiotics, particularly because these non-antibiotics drugs are already FDA-approved. Additionally, the information on the pharmacokinetics and pharmacodynamics of these drugs is known and established. Therefore, the number of pre-clinical and clinical studies needed to evaluate its efficacy for another indication are much less (Rampioni et al., 2017b; Maiden et al., 2018; Miró-Canturri et al., 2019).

Recently, several non-antibiotic drugs have been found to possess anti-bacterial activity against biochemical processes without affecting bacterial growth (Imperi et al., 2013; Nehme et al., 2018; Miró-Canturri et al., 2019). Examples of these are anti-depressants such as amitriptyline and sertraline, which showed activity against Gram-negative pathogens including *P. aeruginosa.* Such activity was found to be due to the inhibitory effect on efflux pumps (Kaatz et al., 2003; Mandal et al., 2010; Ayaz et al., 2015). Niclosamide and albendazole are anti-helminthic drugs that have shown activity against *P. aeruginosa* through inhibition of QS (Imperi et al., 2013; Chen et al., 2018; Singh and Bhatia, 2018; Domalaon et al., 2019). Anti-hypertensives are also another classe that has been shown activity against bacterial pathogens. This activity is associated with their ability to decrease concentrations of cations such as sodium and potassium, which can counteract the action of some antibiotics such as tobramycin. Examples of drugs in this class are amlodipine and amiloride (Middleton et al., 2005). The other group that has shown activity are flavonoids such as quercetin, whose antibacterial action is related to the suppression of QS (Pawlikowska-Pawlęga et al., 2007; Siriwong et al., 2016; Roy et al., 2018). Another class of non-antibiotic drugs with antibacterial activity are anti-psychotics such as chlorpromazine and thioridazine. The activity of these is related to the disruption of the bacterial cytoplasmic membrane (Amaral et al., 2001; Dastidar et al., 2013; Nehme et al., 2018). Chelating agents such as diethylenetriaminepentaacetic acid also have antibacterial action by sequestering cations in the outer membrane (Banin et al., 2006; Finnegan and Percival, 2015). Finally, furanone is a natural compound that has antibacterial action

through QS suppression (Hentzer et al., 2002; Maeda et al., 2012; Rampioni et al., 2017b; Miró-Canturri et al., 2019). In summary, investigating the role of non-antibiotic drugs as an adjuvant with tobramycin could be a promising strategy to improve the antibacterial activity of tobramycin particularly in the current situation of global hazard concern about antibiotic resistance and the decreasing development of new antibiotics.

1.7 Hypothesis and aims

The introduction above has described *P. aeruginosa* lung infections and the effect of inhaled tobramycin in the treatment of biofilms formed by this bacterium. Currently, most studies that evaluate the *in vitro* activity of tobramycin rely on testing its efficacy against *P. aeruginosa* biofilms as an aqueous solution. However, as discussed earlier, in lung infections, tobramycin is usually delivered as a dry powder formulation. This tobramycin powder formulation has characteristics that could have an effect on the antibiofilm activity. Importantly, such characteristics are missing in the currently used in *vitro* models. Our hypothesis is that the particle size of tobramycin dry powder inhaler influences the activity against *P. aeruginosa* biofilms. The manipulation of particle size would therefore offer a new mechanism to improve the activity of inhaled tobramycin. However, the effects of particle size on antibacterial activity have not been previously documented. To test our hypothesis, tobramycin powder was fractionated into different sizes using pharmaceutical techniques, and these fractions were then used to challenge *P. aeruginosa* biofilms. In addition, we aimed to investigate the synergy of non-antibiotic drugs in combination with tobramycin, as this could be a second route through which tobramycin formulations could be improved.

The specific aims of the thesis were:

- To evaluate the activity of tobramycin against a number of *P. aeruginosa* isolates using a clinically relevant medium and two different *in vitro* biofilm models.

- To develop and optimize *in vitro* models that allow the study and characterisation of tobramycin dry powder inhalations. These require the use of a pharmaceutical size

analyser to separate tobramycin powder into different particle size categories, and chemical analysis to quantify the mass of tobramycin powder.

- To investigate the influence of these differently sized particles against *P. aeruginosa* isolates in a model that possibly simulates lung infections.

- To investigate the influence of tobramycin combinations therapy with non-antibiotic drugs against *P. aeruginosa* biofilms using a clinically relevant medium, and to compare this with a standard growth medium.

Chapter 2: Materials and Methods

Part A- Microbiological techniques

2.1 Chemicals and bacterial culture media

All chemicals and culture media were purchased from Sigma-Aldrich or Fisher Scientific, unless stated otherwise. TOBI Podhaler ® was purchased from Novartis.

2.2 Bacterial strains

All bacterial strains used in this research are listed in Table 2.1. Strains were preserved as glycerol stocks at – 80 °C in sterile cryogenic vials. *P. aeruginosa* glycerol stocks were prepared by mixing the bacterial cells with 70% (w/v) glycerol to a final concentration of 20 % (v/v) glycerol. Overnight cultures were prepared in either Mueller-Hinton broth (MHB) or MOPS minimal medium and incubated 16-18 h at 37°C.

Table 2.1 Bacterial strains used in this study.

Strain	Details	Source	Reference
***P. aeruginosa* lab strains**			
PAO1			(Stover et al., 2000)
NCTC 6750			
***P. aeruginosa* clinical CF isolates "Belgian Coordinated Collection of Microorganisms (BCCM)"**			
LMG 27648	Large genome, converted to mucoid; produces LPS which lacks O-side chains; lacks motility	Boston, MA, chronic CF patient	(Mathee et al., 2008)
LMG 27643	Paediatric CF patient (mucoid) form hospital de Santa Maria, Lisbon	Libson Portugal, CF patient	(Leitão et al., 1996)
LMG 27649	Stable CF sputum mucoid isolate; alginate hyperproducer; has functional QS system.	Denmark CF patient	(Hoffmann et al., 2005)

2.3 Alginate detection assays

2.3.1 Congo red agar

This experiment was performed to differentiate between two different *P. aeruginosa* phenotypes, mucoid and non-mucoid. This was carried out using Congo red agar described elsewhere (Mishra et al., 2015). Briefly, the medium was composed of brain heart infusion (BHI; 37 g/L), sucrose (50 g/L), agar (10 g/L) and Congo red stain (0.8 g/L). Sucrose solution was prepared separately, and filter sterilized to avoid its degradation by heat, and Congo red was prepared as a concentrated aqueous solution and autoclaved at 121°C for 15 min. After this, Congo red and sucrose were added to the BHI agar medium after it was cooled down to 55°C. Finally, mucoid and non-mucoid isolates were cultivated on prepared BHI agar plates and were incubated at 37°C for 24 h. Alginate producing strains are indicated by black colonies, whereas non-producing strains are indicated by red colonies.

2.3.2 MacConkey agar

The MacConkey agar assay was used also to detect slime-producing strains as described elsewhere (Evans and Linker, 1973). Briefly, MacConkey agar was prepared according to the manufacturer's instructions. MacConkey agar was supplemented with 5% glycerol as a good source for alginate or biofilm production. Bacterial suspensions were streaked out onto the surface of MacConkey agar. Afterward, plates were incubated for 48 h either at 37°C or at room temperature 25°C, as it was reported that slime production is better at room temperature (Evans and Linker, 1973). The appearance of slimy colonies was considered a positive indication for the presence of alginate producing cells.

2.4 Bacterial growth media

2.4.1 Mueller-Hinton Broth (MHB)

MHB is a nutrient-rich medium and it consists of beef infusion solid 2 g/L, casein hydrolysate 17.5 g/L, and starch 1.5 g/L. MHB was prepared according to the manufacturer's instructions and sterilized by autoclaving at 121°C for 20 min.

2.4.2 Minimal MOPS Medium (MOPS)

MOPS (3-(N-Morpholino) Propane-Sulfonic Acid) is a chemically defined minimal medium. MOPS medium was prepared as described elsewhere (LaBauve and Wargo, 2012) and was filter sterilized using a Nalgene vacuum filtration system® (Thermo Scientific; 0.22 µm; 75 mm filter).

2.4.3 Artificial Sputum Medium (ASM)

ASM was prepared following the protocol previously described by Kirchner et al (2012) with components that are, as closely as possible, similar to CF sputum. It contains a highly glycosylated protein, mucin, essential and non-essential amino acids, salts, and DNA. Briefly, 5 g mucin from porcine stomach type II, which has a long chain of O-linkages, was slowly dissolved overnight in 250 ml sterile Milli-Q water at 4°C. Similarly, 4 g deoxyribonucleic acid DNA from salmon sperm was slowly dissolved overnight in 250 ml sterile Milli-Q water at room temperature. Then 5.9 mg of a chelating agent, diethylenetriaminepentaacetic acid (DTPA), 5 g NaCl, and 2.2 g of KCl; were dissolved in 100 ml Milli-Q sterile water. After which, mucin, DNA, and DTPA, NaCl, KCl were all combined with the addition of 5 g casamino acids (Bacto). The volume was brought to 1 L with sterile Milli-Q water. The pH was adjusted to 6.9 by adding 1.81 g Tris-base to mimic CF sputum pH, which varies from 6.5 to 7.1 (Kirchner et al., 2012). Then the solution was autoclaved at 121°C for 15 min (Ghani

and Soothill, 1997; Aristoteli and Willcox, 2003). Afterward, a 5 ml of egg yolk emulsion was added. The prepared ASM was stored at 4°C.

2.5 Antibiotic sensitivity

2.5.1 Minimum inhibitory concentration (MIC)

The MIC tests were performed as described elsewhere (Andrews, 2001) using the macro-dilution protocol. The MIC is defined as the lowest concentration of an antibiotic agent that results in an inhibition visible growth of a microorganism after overnight incubation.

2.6 Biofilm assays

2.6.1 96-well plate assay

Biofilm formation was performed using a 96-well plate assay as described elsewhere (Merritt et al., 2005; Coffey and Anderson, 2014), which was used to investigate the activity of tobramycin against *P. aeruginosa* biofilms. Briefly, overnight cultures were adjusted to an optical density (OD_{600}) of 0.05 with MHB, MOPS medium, or ASM and then 100 µl aliquots were added to 96-well microtiter plates (Costar). Next, the microtiter plates were incubated at 37°C for 24 h on a 3D plate rotator at 20 rpm. Afterward, planktonic bacteria were removed, and biofilms were gently washed three times with phosphate-buffered saline (PBS). Then the biofilms were treated by adding 100 µl fresh medium per well containing various concentrations of tobramycin and incubated for a further 24 h. This was followed by removing planktonic cells, washing biofilms three times with PBS, and drying plates for 1 h at 60°C. Following this, the biofilms were stained with 125 µl of 0.1% (v/v) crystal violet solution (CV; Prolab Diagnostics) for 15 min. Excess crystal violet stain was removed by washing plates in trays filled with lukewarm tap water three times. After this, the bound crystal violet was

solubilized by adding 150 µl of 30% (v/v) acetic acid. The absorbance was measured at a wavelength of 595 nm.

2.6.2 Colony biofilm assay

This assay was performed as described elsewhere (Merritt et al., 2005) and used to analyse tobramycin or colistin activity against *P. aeruginosa* biofilms. Briefly, two sterile semipermeable polycarbonate membranes (Whatman; 0.2 µm pore size, 25 mm) were placed on the surface of MH (Oxoid) agar plates (Figure 2.1). Then an aliquot of 50 µl of overnight culture, adjusted to an OD at 600 nm of 0.05, was spotted on each membrane. After that, the inoculated membranes were incubated for 48 h at 37°C to permit biofilm formation. The polycarbonate membranes were moved to fresh agar plates with sterile forceps on a daily basis. On the third day, 30 µg tobramycin or 50 µg colistin discs (Oxoid) were placed on the biofilms using sterile forceps and then incubated for a further 24 h as above. After this, biofilms were harvested by resuspension in 900 µl of sterile PBS, vortexed vigorously, and serially diluted. Serial dilutions from 10^{-1} to 10^{-7} were performed in sterile PBS for the suspended cells and 10 µl of the 10^{-5}, 10^{-6}, and 10^{-7} dilutions were spotted as three drops for each dilution on MH agar plates and incubated for 24 h at 37°C. On the following day, the number of colonies was counted, and the Colony Forming Unit (CFU)/ml was determined using the Miles and Misra equation.

Colony Forming Unit (CFU/ml) = ((number of colonies * dilution factor) / volume of culture plated)

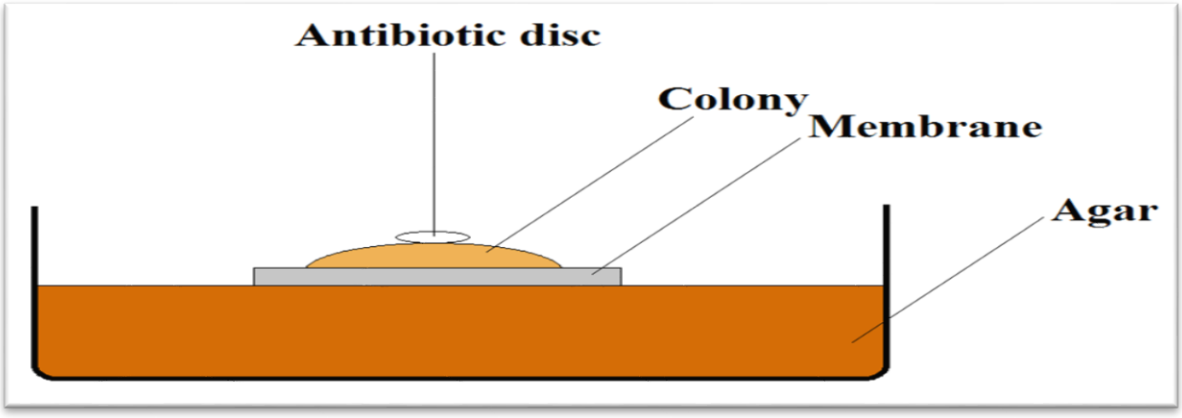

Figure 2.1 Colony biofilm assay. Schematic depiction of a colony biofilm assay.

2.7 The *in vitro* tobramycin drugs combination assay

Tobramycin and drugs/compounds combination interactions against *P. aeruginosa* were investigated using a checkerboard technique. Drugs used in the combination study are listed in Table 2.2.

Table 2.2 The drugs/compounds used in combination study with tobramycin.

Drugs/Compounds name	Property	Reference
Colistin	Polymyxin antibiotic	(Herrmann et al., 2010)
Amitriptyline hydrochloride	Anti-depressant	(Miró-Canturri et al., 2019)
Niclosamide	Anti-helminthic	(Imperi et al., 2013; Domalaon et al., 2019)
Amiloride	Diuretic	(Giunta et al., 1984; Treerat et al., 2008)
Quercetin	Plant flavonoid	(Gopu et al., 2015)
Chlorpromazine hydrochloride	Anti-psychotic	(Miró-Canturri et al., 2019)
Diethylenetriamine pentaacetic acid	Chelating agent	(Miró-Canturri et al., 2019)
4-hydroxy-2,5-dimethyl-3(2H) furanone	Strawberry furanone	(Vestby et al., 2010)

2.7.1 Checkerboard assay

A checkerboard microdilution assay was conducted to examine interactions of tobramycin according to a previously published technique (Domalaon et al., 2019). This was performed using 96-well microtiter plates (Figure 2.2). Firstly, stock and diluted solutions of these drugs were prepared on the same day of experiment either in sterile Milli-Q water or dimethyl sulfoxide (DMSO), which was used at a final concentration of 0.2%. Bacterial cultures grown overnight were diluted 1:100 in MHB and allowed to grow to exponential phase for 3-4 h. After this, they were further diluted in ASM to achieve CFU/ml= $2.9*10^9$.

Tobramycin concentrations (µg/ml)										**Negative control**	**Positive control**
	32	2/32	4/32	8/32	16/32	32/32	64/32	128/32	256/32	512/32	
	16	2/16	4/16	8/16	16/16	32/16	64/16	128/16	256/16	512/16	
	8	2/8	4/8	8/8	16/8	32/8	64/8	128/8	256/8	512/8	
	4	2/4	4/4	8/4	16/4	32/4	64/4	128/4	256/4	512/4	
	2	2/2	4/2	8/2	16/2	32/2	64/2	128/2	256/2	512/2	
	1	2/1	4/1	8/1	16/1	32/1	64/1	128/1	256/1	512/1	
	0.5	2/.5	4/0.5	8/0.5	16/0.5	32/0.5	64/0.5	128/0.5	256/0.5	512/0.5	
	0	2	4	8	16	32	64	128	256	512	
	Second drug/compound concentrations (µg/ml)										

Figure 2.2. The illustration above shows how tobramycin and second drug/compound were distributed in checkerboard assay using 96-well plate. The controls are indicated by the green color, the wells where each combination are intersecting are indicated by pink colors. Vertical gray wells represent tobramycin concentrations alone, whereas the horizontal gray wells represent second drug/compound concentrations alone. The numbers displayed in the figure represent tobramycin/second drug final concentrations in µg/ml.

In brief, in each well of 96-well plate, the final volume was brought up to 150 µl as the following, firstly the 96-well plate was inoculated with 50 µl of diluted bacterial culture, then

100 µl of different concentrations of tobramycin (Figure 2.2) dissolved in ASM was individually dispensed in the columns of each respective concentration. Similarly, for the second compound, 100 µl of different concentrations dissolved in ASM was dispensed in the rows of each respective concentration (Figure 2.2). Then for the drug combinations, 50 µl from tobramycin and 50 µl from the second compound of each individual concentrations were distributed in a cross-fashion into 96-well plate as shown in Figure 2.2. Next, two controls were included in each plate, the positive control (medium with *Pseudomonas* strain) and the negative or sterility control (medium only). After this, the plates were incubated overnight at 37°C for 16-18 h on a 3D- rotator at 20 rpm.

Following incubation, the absorbance of each well was measured using a microplate reader at a wavelength of 595 nm. The MIC of separate or combined drugs wells was considered to be the wells without growth, where MICs were calculated and defined as described elsewhere (Meletiadis et al., 2010). Briefly, we firstly subtracted the blank from each well. Secondly, we considered that those wells that are close to zero as no growth, in which close to zero was defined as any well with < 10% of the highest absorbance value that we had. Finally, the checkerboard data were analysed by calculating fractional inhibitory concentrations (FICs) and the average of the FICs index from three checkerboard repeats was used to classify results (synergy, antagonist, indifference) using the following formula previously described (Ghorbani et al., 2017).

FIC = FIC drug A + FIC drug B

$$= MIC_{AB}/MIC_{A} + MIC_{BA}/MIC_{B}$$

FIC of drug A = MIC of drug A in combination with drug B/ MIC of antibiotic A alone

FIC of drug B = MIC of drug B in combination with antibiotic A/ MIC of drug B alone.

The FIC index data were interpreted according to the following criteria described before (Sopirala et al., 2010). Synergy was defined as an FIC index of ≤ 0.5, additive was defined as an FIC index >0.5 and ≤ 1, indifferent was defined as an FIC index > 1 and ≤ 4, and antagonistic was defined as an FIC index > 4.

2.7.2 Evaluation of tobramycin and drugs/compounds combinations against biofilm

To investigate the activity of tobramycin drug combinations against *P. aeruginosa* biofilm, the 96-well plate assay was used as described earlier (Section 2.6.1). Briefly, overnight cultures were adjusted to an OD_{600}= 0.05 with MHB and then further diluted 1:100 in ASM. An aliquot of 100 µl was added to 96-well microtiter plates. Next, microtiter plates were incubated at 37°C for 24 h on a 3D plate rotator at 20 rpm. Afterward, planktonic bacteria were removed, and biofilms were treated by adding 100 µl fresh ASM per well containing different concentrations of either tobramycin alone/compound alone or a combination of both tobramycin and drug/compound. The plates were incubated for a further 24 h. Then the biofilms were quantified as described in section 2.6.1.

Part B - Pharmaceutical techniques

2.8 TOBI Podhaler® and Next Generation Impactor (NGI) measurement methodologies

2.8.1 TOBI Podhaler ®

TOBI Podhaler® 28 mg (Novartis, UK) is a dry powder inhalation formulation of tobramycin (Figure 2.3), and it is approved as maintenance therapy for chronic *P. aeruginosa* infections in cystic fibrosis patients aged 6 years and older (McKeage, 2013). Tobramycin from TOBI Podhaler ® was analyzed in terms of particle size distribution using an instrument called a Next Generation Pharmaceutical Impactor (NGI; Copley Scientific, Nottingham-UK). The NGI consists of several parts, and more details about the NGI components will be in chapter 4 (Section 4.1).

Figure 2.3. TOBI Podhaler® 28 mg (unpublished image).

2.8.2 Tobramycin particle size analysis

2.8.2.1 Scanning Electron Microscopy (SEM)

Tobramycin particles from all the NGI stages were collected separately on glass fibre filters using the method that will be described below (Section 2.8.5). These particles were analyzed using SEM by applying conditions stated elsewhere (Li et al., 2014). Tobramycin samples were fixed into aluminum stubs (Agar Scientific) using double-sided adhesive carbon tabs (Agar Scientific). Then, the samples were coated with a thin film of gold using a sputter coater (Edwards Sputter Coater S 150B). The coating process was operated at 1 kV of voltage for 3 min. The images were captured using Jeol SEM (Jeol Jsm-6480LV Scanning Electron Microscope), and several magnifications levels were used. The captured images were further analyzed for size determination using the software package ImageJ (University of Wisconsin-Madison, Broad Institute of MIT and Harvard, and Max Planck Institute of Molecular Cell Biology and Genetics). For every ImageJ analysis, manual particle size measurements were performed, and for every measurement fix criteria were used as following, all particles in the given image were measured even the small particles that were on top of large particles, specific

number of particles were selected randomly, the same magnification was used for all images, and the diameters of all particles were measured in the vertical direction.

2.8.3 Quantification of tobramycin mass deposited in the NGI

2.8.3.1 High Performance Liquid Chromatography-Mass Spectrometry (HPLC-MS) quantification

An HPLC-MS method for the determination of tobramycin deposited on the NGI stages was developed and validated. The chromatographic system that was used consists of a pentafluoro phenyl F5 column (Phenomenex; 2.6 µM, 2.1 x 100 mm) as the stationary phase, which was used with a flow rate of 0.3 mL/min at 25°C and an injection volume of 10 µL of each sample was injected in triplicate. The mobile phase involved utilizing two solvents, which were 100% water with 0.1% (v/v) formic acid as solvent A and 100% methanol with 0.1% (v/v) formic acid as solvent B. The proportion of these solvents in the mobile phase was controlled during the analysis by the UHPLC instrument. Elution was carried out with 0% mobile phase B for 3 min followed by a linear gradient to 100% B for 7 min. Mass spectrometer (Bruker Daltonik GmbH, Bremen, Germany) was operated in electrospray time of flight (ESI) positive-ion MS mode, and the following conditions were used during the MS analysis. The capillary voltage was set to 4500 V, nebulizing gas at 4 bar, and drying gas at 12 L/min at 220°C. The tobramycin concentration in injected samples (and thus the mass of deposited tobramycin on NGI compartments) was determined by constructing a calibration curve using kanamycin as an internal standard. A tobramycin sulphate stock solution for the calibration curve was prepared in Milli-Q water at a concentration of 500 µg/ml, which then was diluted in Milli-Q water to provide desired working concentrations (5-20) µg/ml. Kanamycin stock solution was prepared in Milli-Q water at a concentration of 400 µg/ml, then kanamycin was added to achieve a final concentration of 4 µg/ml in every calibration and unknown sample. Following the addition of kanamycin, samples were vigorously vortexed prior to HPLC-MS analysis. All stock solutions were prepared on the same day of the experiment, and HPLC-MS analysis was performed with 24 h.

2.8.4 Tobramycin capsule filling and humidity control

Hydroxypropyl methylcellulose capsules (HPMC; transparent; size #3; Capsugel®; UK) were used in this study for tobramycin filling. Before each experiment, capsules were filled manually with the tobramycin powder from the TOBI Podhaler® and weighed using a four-place analytical balance (Sartorius, Balance Technology, UK). They were then stored for 24 h in a sealed desiccator under a controlled temperature of 25°C and relative humidity (RH) of 43%. This RH was produced using a saturated salt solution of potassium carbonate (K_2CO_3) (Miller et al., 2017). Temperature and relative humidity were monitored using a thermohygrometer that was placed inside the desiccator. In the following day, these capsules were fired through the NGI as described below (Section 2.8.5).

2.8.5 Determination tobramycin particle size distribution following aerosolization from the TOBI Podhaler®

The NGI was used to analyse the tobramycin particle size distribution following aerosolization from TOBI Podhaler®. The test was performed as described in the British Pharmacopeia for dry powder inhalers (DPIs). Before testing, the NGI stages were coated with a solution of 1% v/v glycerol in methanol (VWR chemicals) to minimize particle bounce. The solution was left to dry for around five minutes during which the methanol evaporated leaving behind a thin layer of glycerol.

A tobramycin capsule was placed within the TOBI Podhaler® device, then the capsule was pierced by pressing the blue button on the inhaler device (Figure 2.4; 1). After this, the closed Podhaler® device was tightly connected to ensure a good seal with a mouthpiece adaptor (Figure 2.4; 2) joined to the induction port (Figure 2.4; 3). The pre-separator (Figure 2.4;4) was filled with 15 ml Milli-Q water. After that, the NGI parts were joined together and closed. A critical flow controller (Figure 2.4; 6, Copley Scientific, Nottingham-UK) was used to adjust the flow rate of the air. This flow controller was connected to a vacuum air pump (Figure 2.4;7, Copley Scientific, Nottingham-UK), which was used to produce airflow through the NGI. The flow rate was determined using a digital flow meter (See Figure 2.8 below, DFM 2000, Copley

Scientific, Nottingham-UK). Flow rates of either 30 L/min and 60 L/min were consistently maintained throughout all the investigations. These two flow rates were selected because they are representative of the flow rates in CF patients (Tiddens et al., 2014), and the diameters for particles collected on each stage of the NGI are known for these flow rates (Marple et al., 2003). The vacuum pump was switched on and allowed to stabilise, before the value of the critical flow controller was opened for 10 seconds to draw air through the NGI and aerosolise the tobramycin powder into the NGI compartments.

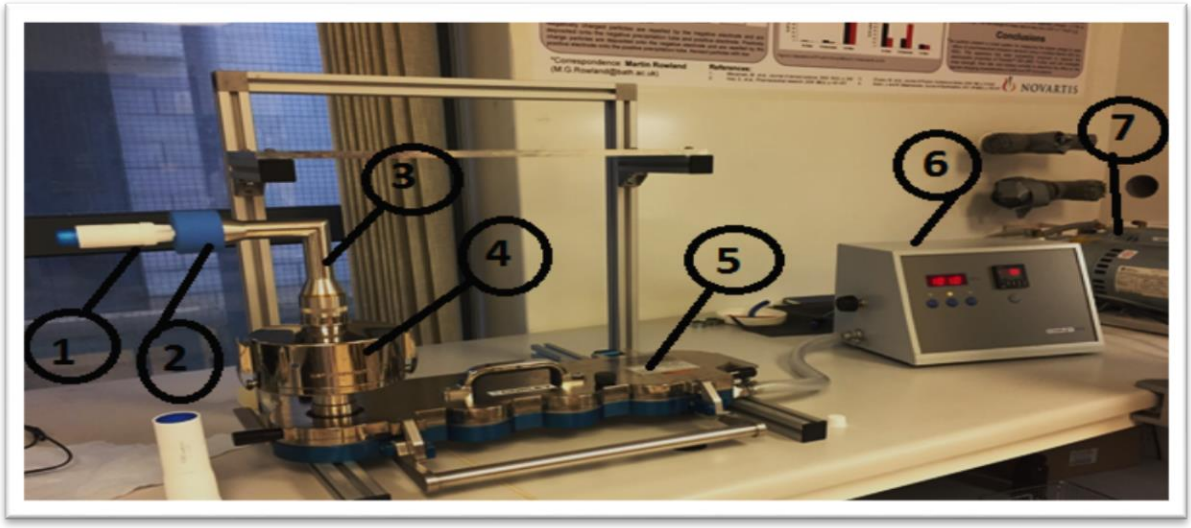

Figure 2.4 Complete closed NGI setup system. Inhaler device (1), mouthpiece adaptor (2), induction port (3), pre-separator (4), NGI (5), critical flow controller (6), vacuum air pump (7). (unpublished image)

After the dispersion of tobramycin powder (Figure 2.5), the NGI was disassembled and each individual component including the capsule, mouthpiece adaptor with induction port was washed with known volumes of Milli-Q water into separated volumetric flasks to recover tobramycin (Figure 2.5). Similarly, the pre-separator, each collection stage S1-S7, and MOC were also washed with known volumes of Milli-Q water. Then each collection stage was placed on a magnetic stirrer for 10 min to ensure complete dissolution and recovery of tobramycin. Then, the extracted samples were collected in glass autosampler vials for analysis after appropriate sample dilutions were made. The mass of tobramycin deposited on each collection stage, mouthpiece, induction port, and pre-separator was determined by HPLC-MS as discussed in section 2.8.3.

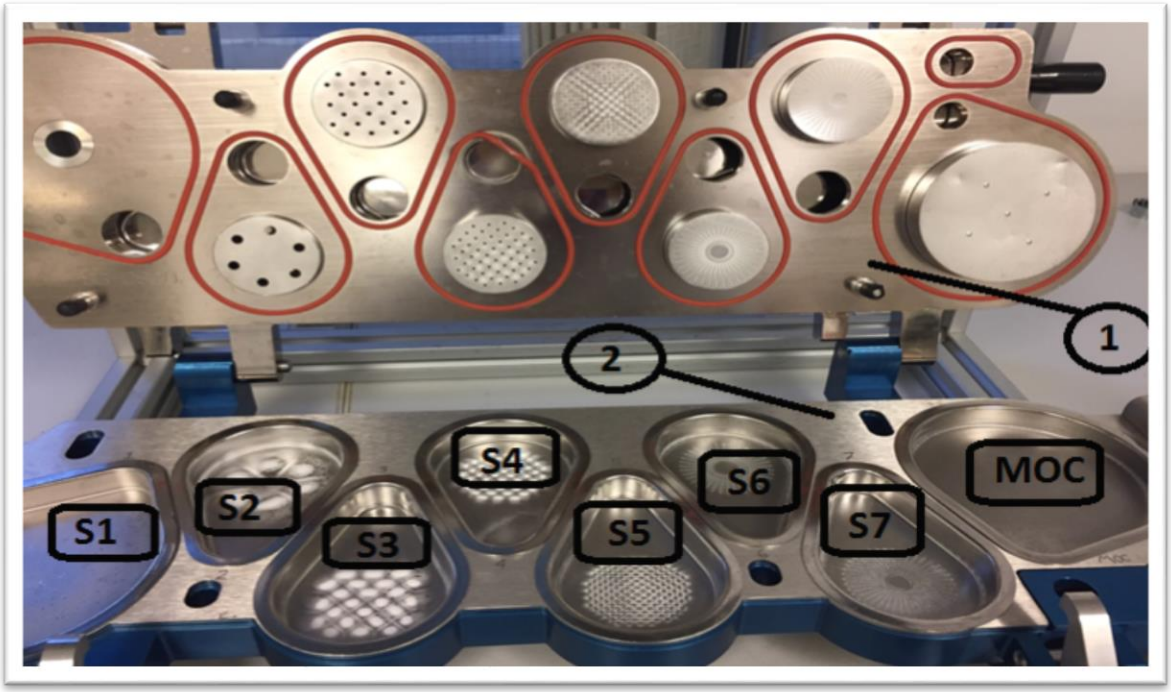

Figure 2.5. NGI in an open position. A nozzle plate with several nozzles diameters (1), a stage plate (2) with seven collection stages (S1-S7) and MOC: micro-orifice collector to collect the incoming powder from the above nozzles. (unpublished image)

2.8.6 Determination of the mass of tobramycin deposited on the aerosol collection apparatus attached to different NGI stages

The aerosol collection apparatus with a glass fibre filter is an instrument that was introduced to the main NGI compartments to collect tobramycin particles (more details in chapter 4, section 4.1). The glass fibre filter (Figure 2.6) was replaced for each repeat of the experiment and the flow rate was adjusted for each experiment after placing the filter in the aerosol collection system.

Two types of aerosol collection apparatuses were used, either a single (Figure 2.7) or double aerosol collection apparatus (Figure 2.8). The aerosol collection apparatus parts were assembled together and mounted either on either stage 2 or stage 4. The experimental set up with aerosols collection apparatus was performed as mentioned before (Section 2.8.5) with some modifications as follows. First, a rubber stopper (Figure 2.7; 1) was placed in the air

outlet from stage 2 or stage 4 to disrupt airflow and ensure the collection of all tobramycin particles. Second, the aerosol collection apparatus with a glass fibre filter (Copley®, 25 mm diameter, 1 µm pore size) was mounted either at stage 2 or stage 4 to collect tobramycin particles. Finally, every part of the NGI was washed as described above (Section 2.8.5), with the addition to the filter washing. Accordingly, the filter was rinsed with known volumes of Milli-Q water and sonicated for 10 min in an ultrasonic water bath to ensure complete dissolution of tobramycin powder.

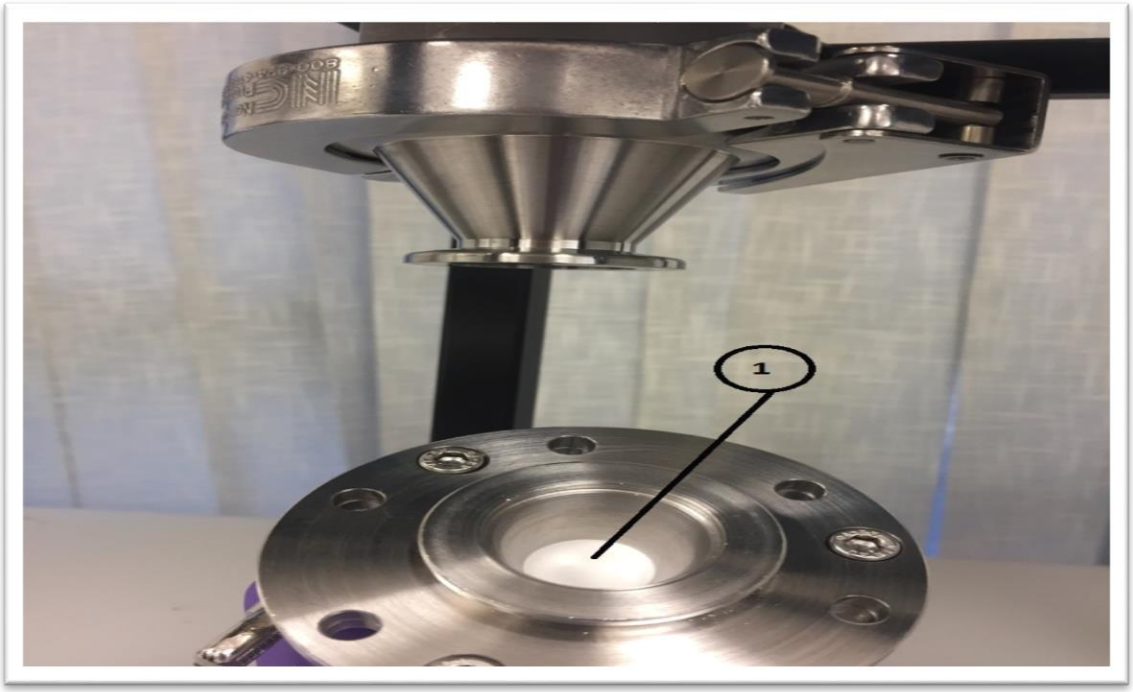

Figure 2.6. Aerosol collection apparatus with glass fibre filter inserted (1) to collect tobramycin particles. (unpublished image)

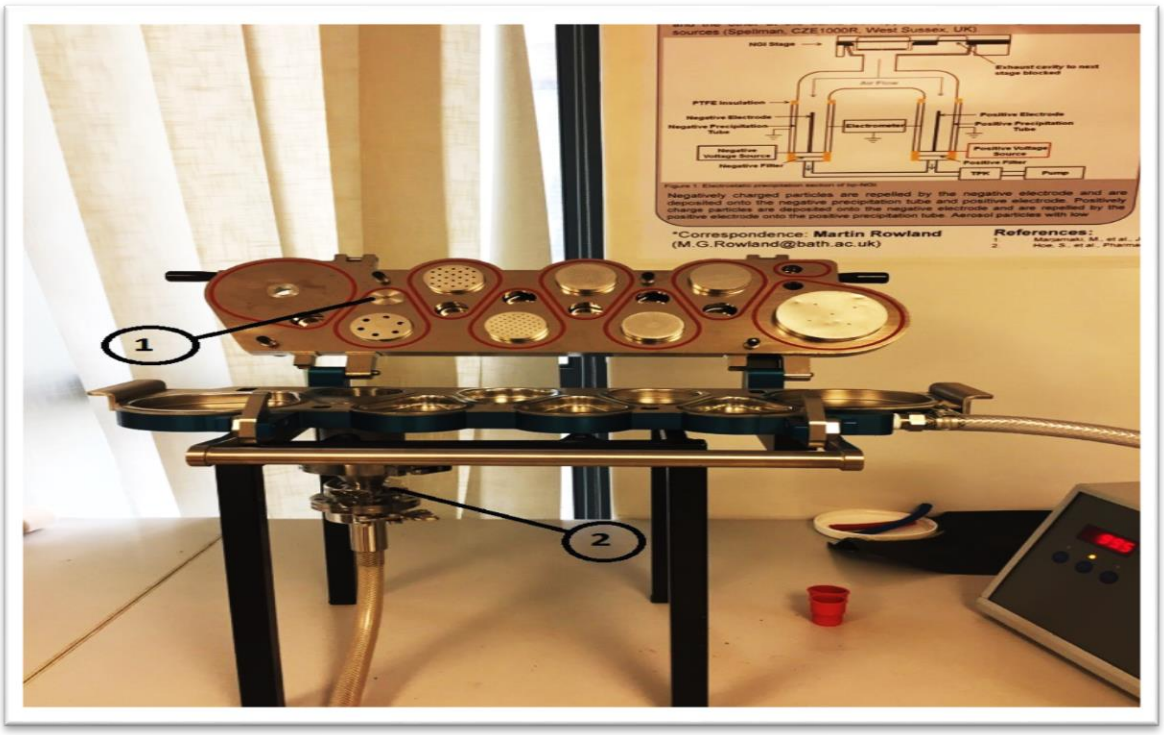

Figure 2.7. NGI with a rubber stopper (1) and a single aerosol collection apparatus (2) down the NGI. (unpublished image)

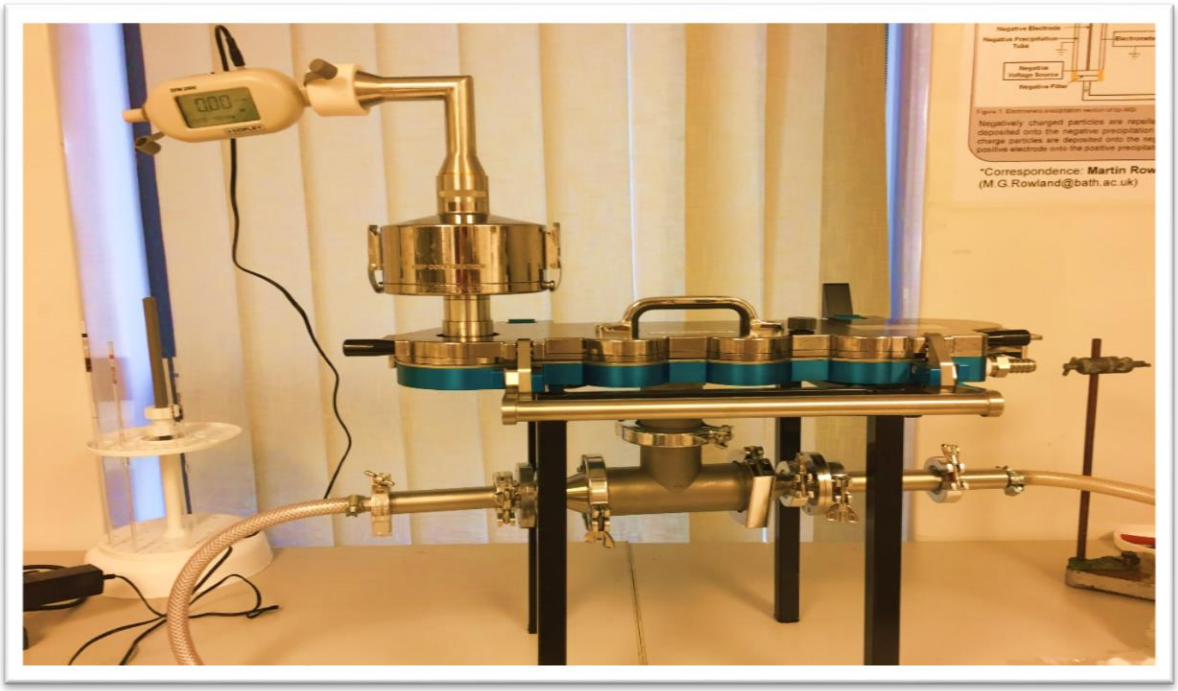

Figure 2.8 NGI incorporated with a digital flow meter at the top of the NGI, and a double aerosol collection apparatus with two collection sites down the NGI. (unpublished image)

2.9 Applying different tobramycin particle sizes to *P. aeruginosa* biofilms

After quantifying and equalizing the mass of tobramycin particles collected on the glass fibre filters at different NGI stages and flow rates using the methods outlined in the above (Section 2.8.5 and 2.8.6), this experiment here was performed to examine the effect of different sized tobramycin particles on the eradication of *P. aeruginosa* biofilms. Briefly, colony biofilms were grown as outlined above (Section 2.6.2). Then the biofilms were treated with equal doses and different sized tobramycin particles (more detailed in chapter 4). This was performed by applying the glass fibre filters that hold tobramycin particles with direct physical contact on the top of the biofilms, controls were covered with a filter without tobramycin. Then, the biofilms with and without the treatment were incubated for 1.5, 3, 5, 6, 8 and 24 h at 37°C. Afterward, the CFU was determined as presented before (Section 2.6.2).

2.10 Statistical analysis

Data were presented as the mean ± standard error of the mean (SEM) of $n \geq 3$ independent biological repeats. Results were analysed using GraphPad Prism 7 by applying either one-way or two-way ANOVA, followed by multiple comparisons using Tukey or Dunnett tests. Additionally, the Student *t*-test was also used. Values of $p < 0.05$ were considered statistically significant. In figures where the data are normalised and shown as a percentage of the control, statistical analysis was carried out on raw, non-normalised data values.

Chapter 3: Results Section I

Evaluation of the Activity of Tobramycin Against *P. aeruginosa* Biofilms

3.1 Introduction

Pseudomonas aeruginosa is an opportunistic Gram-negative bacterium that causes serious and life-threatening infections in immunocompromised individuals such as in cystic fibrosis (CF) patients. In CF lung infections, *P. aeruginosa* is the predominant pathogen that has a major role in increased morbidity and mortality rates among those patients. This is attributed to the ability of this bacterium to resist the action of several antibiotic classes. Such resistance involves the limited permeability of the outer membrane, the abundance of efflux pumps, and phenotypic features including biofilm formation (Nikaido and Pagès, 2012; Ciofu et al., 2015; Muheim et al., 2017).

Biofilms are highly organized communities of cells that are attached to each other and/or to surfaces and are embedded within a self-synthesized extracellular polymeric substance (EPS) matrix, mainly containing extracellular DNA, polysaccharides, and/or proteins (Furiga et al., 2015). These biofilms are characterized by a high tolerance rate for both immune defensive mechanisms and for most of the available antibiotic therapies. For instance, it is assumed that cells inside biofilms are 10-1000 times less susceptible to anti-microbial therapies than planktonic free-floating cells (Patton et al., 2010; Marshall et al., 2016; She et al., 2018). This is attributed to, for example, a low metabolic rate for cells inside the biofilms as this can impair the activity of some antibiotics. Another factor is related to the effect of the EPS matrix, which may act as a barrier and impede the penetration of antibiotics into biofilms (Schneider-Futschik et al., 2018).

Generally, *P. aeruginosa* biofilms in CF patients are treated with different classes of antibiotics, which are one of the cornerstone therapies for chronic lung infections (Greally et al., 2012). Aminoglycosides are one of the most commonly used antibiotic classes for the treatment of such infections in CF patients (Tre-Hardy et al., 2010). Aminoglycosides consist of several agents; however, tobramycin is the most prevailing used aminoglycoside in those patients (Olivares et al., 2017). Tobramycin has a well-known and established efficacy against *P. aeruginosa* in patients with CF. The bactericidal activity of tobramycin is related to its ability to inhibit protein synthesis through binding to the 30 S ribosomal subunit that leads to

disruption of protein production and finally cell death (Babić et al., 2010; Tre-Hardy et al., 2010; Olivares et al., 2017). Currently, *P. aeruginosa* resistance to tobramycin is growing and many factors have been reported to enhance tobramycin resistance in *P. aeruginosa*. Firstly, there is a general belief that using antibiotics at sub-inhibitory doses can modulate several processes in bacteria such as gene expression, virulence activities, quorum sensing (QS), and biofilm formation (Cummins et al., 2009; Andersson and Hughes, 2014; Sato et al., 2018). Studies demonstrated that tobramycin at sub-lethal concentrations can act as a signalling molecule and can alter the expression of several genes (Hoffman et al., 2005; Tahrioui et al., 2019). These changes can result in inducing the formation of robust biofilms and accelerating antimicrobial tolerance towards tobramycin (Babić et al., 2010). Therefore, more studies are needed to clearly understand the effects of tobramycin at sub-MICs level, particularly that there is a relatively small number of studies available on the effects of tobramycin at sub-MICs in clinical CF isolates.

Iron also plays a role in promoting tobramycin tolerance through enhanced formation of biofilms by *P. aeruginosa* (Cai et al., 2009). Iron is an essential element required by *P. aeruginosa* for several physiological processes including energy production, oxygen transport, gene expression, and biofilm formation (Moreau-Marquis et al., 2009). During chronic CF lung infections, iron homeostasis is imbalanced and elevated from normal very low level of 10^{-18} M to a high concentration of 63 µM. Indeed, others have reported that the elevated iron level can reach up to 130 µM or sometimes above 200 µM, which results in the exacerbation of lung damage (Schaible and Kaufmann, 2004; Berlutti et al., 2005; Kreamer et al., 2015; Ezraty and Barras, 2016; Tunney et al., 2018). This elevated level of iron is attributed to the lung injury, inflammation, and decreasing activity of lactoferrin, an iron-binding protein, as a result of degradation by bacterial proteases (Berlutti et al., 2005; Tunney et al., 2018). Such a high iron concentration can therefore serve as a stimulus factor to enhance biofilm formation in CF lung infections (Marshall et al., 2016). Accordingly, this would enhance the tolerance of *P. aeruginosa* to antimicrobial treatment such as tobramycin (Oglesby-Sherrouse et al., 2014).

The host environment in CF lung infections can also affect the activity of tobramycin (Sherrard et al., 2014). For instance, in a CF lung, *P. aeruginosa* grows in a viscous dehydrated mucus (Moore and Mastoridis, 2017). This mucus consists of several components including DNA,

mucin glycoproteins, and others (Lai et al., 2009). Currently, there is growing evidence that these mucus constituents could interact with tobramycin and dramatically inhibit its activity (Schneider-Futschik et al., 2018). Accordingly, a clinically relevant medium called artificial sputum medium (ASM) has been developed, which is a culture medium consisting of CF sputum-like components including, mucins, DNA, salts, and amino acids (Kirchner et al., 2012). Recently, few studies have used such medium to evaluate the impact of mucus components on the *in vitro* activity of tobramycin against *P. aeruginosa*. Therefore, it is essential to consider testing tobramycin susceptibility by using growth media that reflect pathologic conditions at the site of infection.

Besides the role of tobramycin in the management of *P. aeruginosa* lung infections, colistin is also used in the treatment of CF patients. Colistin (polymyxin E) is a cyclic polypeptide antibiotic, which has a documented efficacy against Gram-negative bacteria (Pamp et al., 2008). Colistin exerts antibacterial action through an extracellular mechanism, which depends on self-promoting uptake (porin channels independent) via direct interaction with the outer membrane components (Chiang et al., 2012). Such binding takes place by binding colistin to negatively charged phosphate groups within the surface molecule lipid A in the lipopolysaccharide of the bacterial outer membrane. This interaction results in the displacement of divalent cations, disruption of the outer membrane, and finally leakage of cell contents (Pamp et al., 2008). Resistance to colistin has evolved in many *P. aeruginosa* isolates (Fong et al., 2018). This resistance includes the ability of *P. aeruginosa* to create some the modifications in the colistin target site. Such modifications are mediated by expressing genes that are responsible for modification of the lipopolysaccharide layer, in which these called lipopolysaccharide modification genes *pmr* (Rybtke et al., 2011). Expression of such genes results in decreasing the net negative charge of the lipopolysaccharides in the outer membrane, and this is by the addition of a functional amino arabinose group instead of phosphate negative group in lipid A (Hamad et al., 2012). This functional group leads to reduced colistin binding affinity and consequently strengthens the outer membrane (Delcour, 2009). Additionally, it has been found that outer membrane vesicles (OMVs), which are released from the outer membrane by Gram-negative bacteria including *P. aeruginosa*, play a role in colistin resistance (Beceiro et al., 2013). These small spherical vessels are enriched with several constituents such as outer membrane proteins, lipopolysaccharides, phospholipid, virulence factors, quorum sensing signalling molecules, and nucleic acid such as DNA and RNA (Jan, 2017). These

components enable suppression of host immune defence and enhanced biofilm formation, which consequently leads to enhancing antibiotic tolerance (Jan, 2017). Finally, other studies have determined that colistin tolerance is also associated with the biofilm mode of growth. For instance, some bacterial cells inside a biofilm are with high metabolic activity and these are known to be less susceptible to colistin treatment than other slowly multiplying cells because the former cells can alter the outer membrane lipopolysaccharide layer through up-regulation *pmr* and *mexAB-oprM* genes (Haagensen et al., 2007; Pamp et al., 2008; Herrmann et al., 2010).

This chapter aimed to evaluate the activity of tobramycin against biofilms of *P. aeruginosa* PAO1 and clinical CF isolates into several aspect. Firstly, to study the anti-biofilm activity of tobramycin using two different biofilm models. Secondly, to evaluate factors that can affect antibiofilm activity of tobramycin. These include studying the following, the impact of tobramycin at sub-MICs on the formation of biofilms, the influence of iron concentrations on anti-bacterial and anti-biofilm activity of tobramycin. Moreover, to evaluate the use of a clinically relevant ASM medium on the activity of tobramycin. Finally, to assess the activity of another anti-pseudomonas antibiotic, colistin, against *P. aeruginosa* clinical CF isolates.

3.2 Results

3.2.1 Alginate producing strains

To verify the mucoid state of *P. aeruginosa* CF clinical isolates, MacConkey agar and Congo Red agar were used to achieve this. However, the difference between mucoid and non-mucoid clinical CF isolates was not so obvious, with minimal differences in colours on these agar plates. Nevertheless, two clinical isolates had a different appearance when they were grown as a colony biofilm with a slimier appearance. These strains are LMG 27648 and LMG 27649, which were isolated from CF patients, and both are described as alginate producer (See Materials and Methods Chapter, Section 2.2). Therefore, the mucoid appearance that was observed indicates that they are phenotypically different. This was likely associated with the presence of alginate.

3.2.2 The *in vitro* activity of tobramycin against planktonic *P. aeruginosa*

Tobramycin is the mainstay therapy for the treatment of *P. aeruginosa* lung infections in CF patients (Babić et al., 2010). Therefore, our aim was to investigate its activity against a group of clinical CF isolates of *P. aeruginosa*. The minimum inhibitory concentrations (MICs) for planktonic lab strains and clinical CF isolates of *P. aeruginosa* were determined in MOPS medium using a macro-dilution protocol. MOPS medium was used in our studies in a way to mimic nutrient conditions in the lung, where bacteria grow under restricted nutrient conditions (Maeda et al., 2012; Charrier et al., 2014). As shown in Table 3.1, PAO1 and all of the clinical isolates were found to be susceptible to tobramycin with MICs ≤ 1µg/ml with the exception for NCTC 6750, the MIC of which was just over 1 µg/ml, but it is still within the susceptible range.

Table 3.1. The MICs of tobramycin against lab strains and clinical CF isolates *P. aeruginosa* determined in triplicate by macro-dilution method in MOPS medium.

Lab strains/clinical CF isolates of *P. aeruginosa*	MICs (µg/ml) of tobramycin in MOPS medium
PAO1	0.5
NCTC 6750	1.6
LMG 27648	0.5
LMG 27643	0.25
LMG 27649	1

3.2.3 The *in vitro* activity of tobramycin against biofilms of *P. aeruginosa* using different biofilm models

3.2.3.1 The *in vitro* activity of tobramycin determined using 96-well microtiter plate biofilm assay

In the earlier section, the activity of tobramycin was determined against the planktonic form of *P. aeruginosa*, but it was also essential to explore its activity against the biofilm counterparts using a 96-well plate assay. Accordingly, the strains were grown in MOPS medium for 24 h and then challenged with range of tobramycin concentrations. Since the objective of studying tobramycin activity is to predict what might occur *in vivo*, we selected clinically achievable tobramycin concentrations (16-204 µg/ml), which were measured in the CF lung after tobramycin inhalation (Bahamondez-Canas et al., 2018). Our results showed that the response of the tested strains for tobramycin was different. For instance, tobramycin resulted in a strong reduction in biofilm biomass by around 80-90% in LMG 27649 and NCTC 6750 (Figure 3.1 C and E). However, for the other tested strains LMG 27643 and PAO1 (Figure 3.1 A and D)

the amount of biofilm biomass was reduced to only 50-60%. The least reduction in biofilm biomass was observed in LMG 27648 (Figure 3.1 B) by just 40% at the concentrations from 30-200 µg/ml. The different response that was observed in this strain could be attributed to its mucoid nature, as mucoid strains presumably are known to be more tolerant to tobramycin than non-mucoid counterparts, which could be due to alginate polysaccharide (Ciofu et al., 2012; Moller et al., 2019).

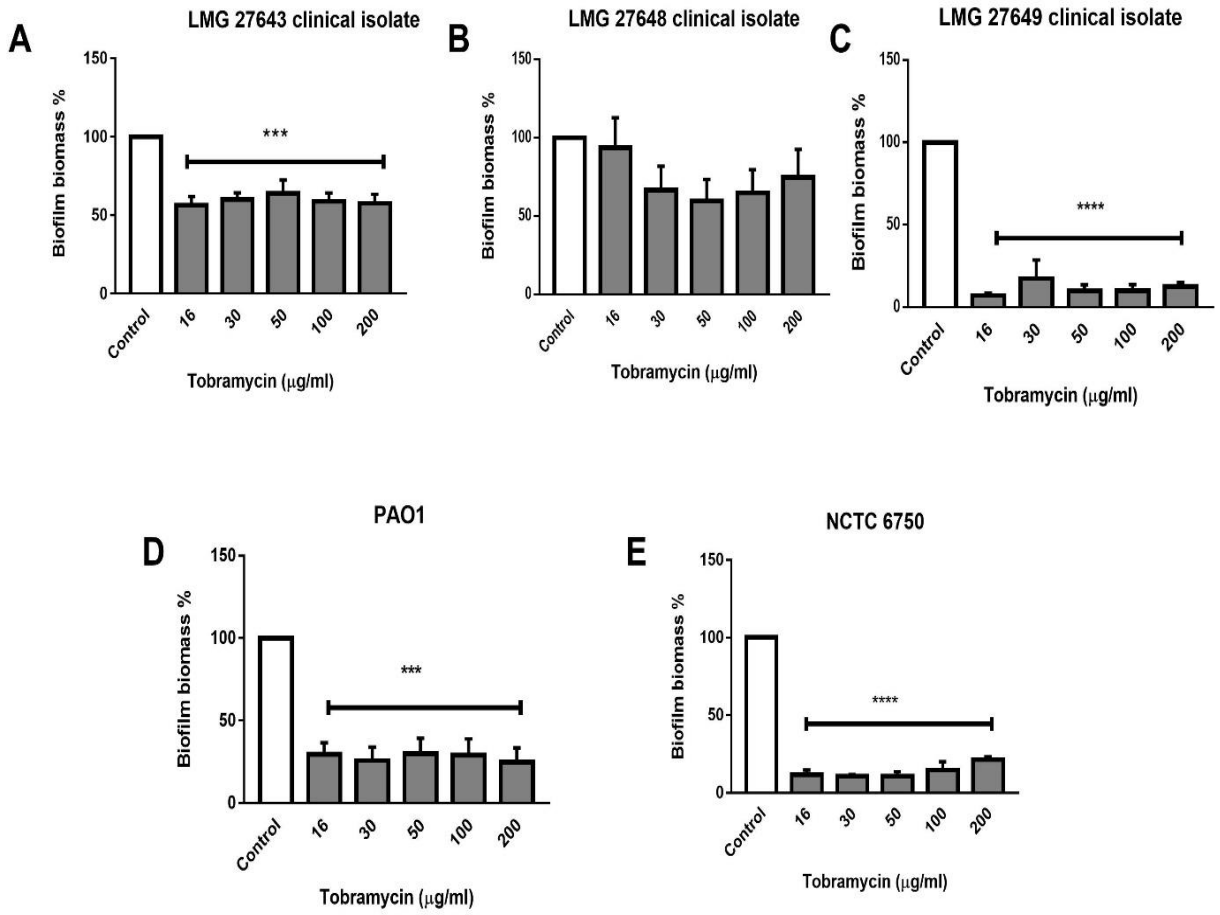

Figure 3.1. The *in vitro* activity of tobramycin against *P. aeruginosa* biofilms determined using the 96-well plate assay. (A – C) show clinical CF isolates and (D-E) indicate lab strains. Wells in a 96-well plate contained different concentrations of tobramycin (dissolved in MOPS medium) with an inoculum were incubated for 24 h at 37°C. The control represents biofilms without tobramycin. Error bars represent the standard error of the mean from five independent experiments with at least six technical replicate wells. Statistical significance was analysed using one-way analysis of variance (ANOVA) followed by Dunnett's multiple comparison test. Statistically significance differences between treated biofilms (***, $p<0.001$; ****, $p<0.0001$) and the control are indicated. Full details of the statistical analysis are shown in appendix 1 and 2.

3.2.3.2 The *in vitro* activity of tobramycin determined using colony biofilm assay

In the previous section, the anti-biofilm activity of tobramycin was measured using the 96-well plate model. Here, it was of interest to test this activity using a different model, the colony biofilm assay, which is possibly a better representative of biofilms in the lung, as unlike the 96-well plates, it has an air interface. To that purpose, all *P. aeruginosa* clinical isolates (LMG27643, LMG27648, and LMG27649) and lab strains (PAO1 and NCTC 6750) were inoculated on polycarbonate membranes that were placed on MH agar plates and allowed to develop biofilms for 48 h and then challenged with 30 µg tobramycin discs for 24 h at 37°C. The results showed (Figure 3.2 A; B; C; D; and E), in all tested strains, tobramycin moderately reduced the amount of viable count by approximately 60%.

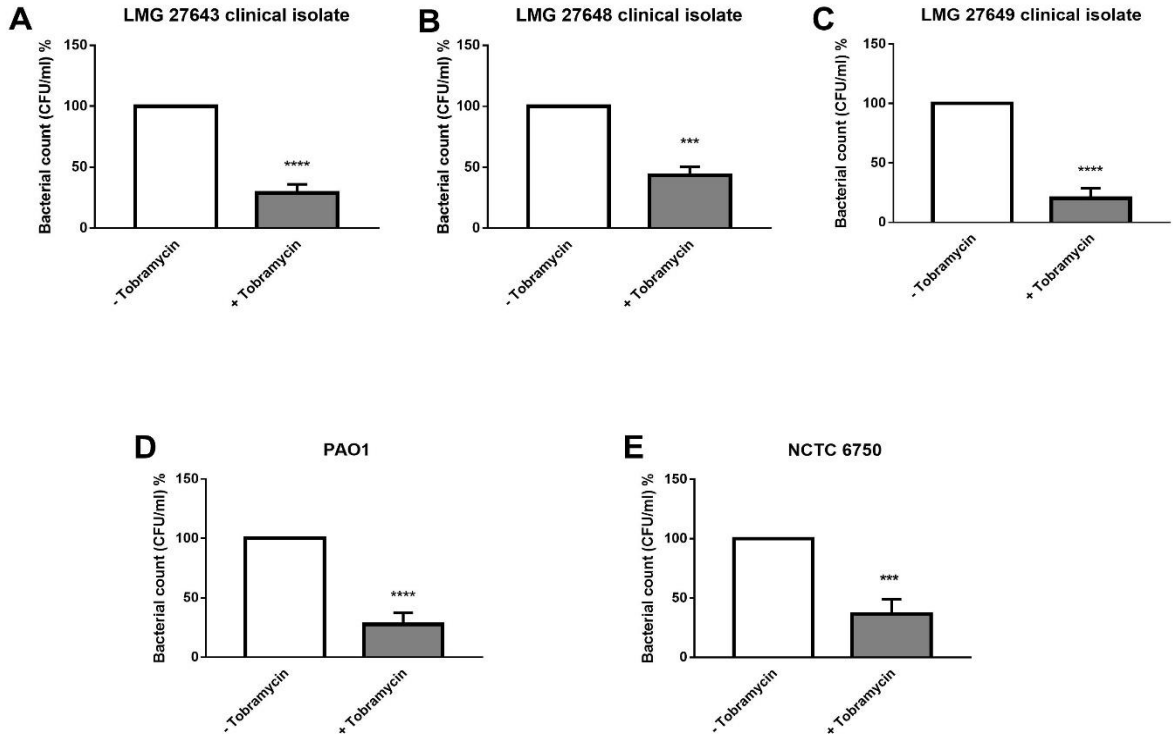

Figure 3.2. The *in vitro* activity of tobramycin against *P. aeruginosa* using the colony biofilm assay. (A – C) show clinical CF isolates and (D-E) indicate lab strains. All *P. aeruginosa* biofilms were grown for 48 h in MOPS medium, treated with 30 µg/disc tobramycin, and incubated for 24 h at 37°C. The controls represent biofilms without tobramycin. The data shown represent the standard error of the mean from three biological repeats and each biological repeat consisted of at least two technical repeats. Statistics were analysed using unpaired 2-tailed *t* test. Statistical significance differences between treated biofilms (***, $p<0.001$; ****, $p<0.0001$) and the control are indicated. Full details of the statistical analysis are shown in appendix 1.

3.2.3 The *in vitro* influence of sub-MIC tobramycin against biofilms of *P. aeruginosa*

After studying the effect of therapeutic concentrations of tobramycin in the earlier sections, our aim here was to examine the influence of sub-MICs of tobramycin against *P. aeruginosa* biofilms. In CF lung infections, bacterial cells grow inside a biofilm and such biofilm might act as a barrier that can decrease the penetration of antibiotics. This could result in exposing bacterial cells to sub-inhibitory concentrations of antibiotics (Hoffman et al., 2005; Linares et al., 2006).

Several studies found that antibiotics at sub-therapeutic concentrations could enhance various functions in bacteria such as the expression of virulence genes, motility, and biofilm formation (Cummins et al., 2009; Ratjen et al., 2009; Morita et al., 2014; Tahrioui et al., 2019). We were particularly interested in the latter and therefore, to address this effect, a range of sub-minimal inhibitory concentrations of tobramycin were used to challenge biofilms of *P. aeruginosa* using the previously described 96-well plate assay. All strains were tested with the MIC value as the highest concentration. Generally, under the tested conditions the results showed that there was a trend toward enhancing biofilm formation at sub-MICs of tobramycin albeit this trend was not reached to the statistical significance level, and it was not obvious in all cases. For instance, in LMG 27643 (Figure 3.3; A) there was a slight increase, in a dose-dependent manner, with biofilm biomass increased by approximately up to 50% as compared with that in the absence of tobramycin. Similarly, in the lab strain PAO1 (Figure 3.3; B), there was a moderate increase in biofilm formation in a dose-dependent pattern with an exception at 0.03 and 0.1 µg/ml. However, in the other strains (LMG 27648 and LMG27649) these trends were not observed (Figure 3.3, C and D). Noteworthy to mention is that in all tested strains, even at the MIC values (indicated in green bars), biofilm formation was observed. Taken together, these results suggest that tobramycin at doses below or at the MIC has a little effect on biofilm formation and, depending on the strain, could even promote biofilm formation in *P. aeruginosa*.

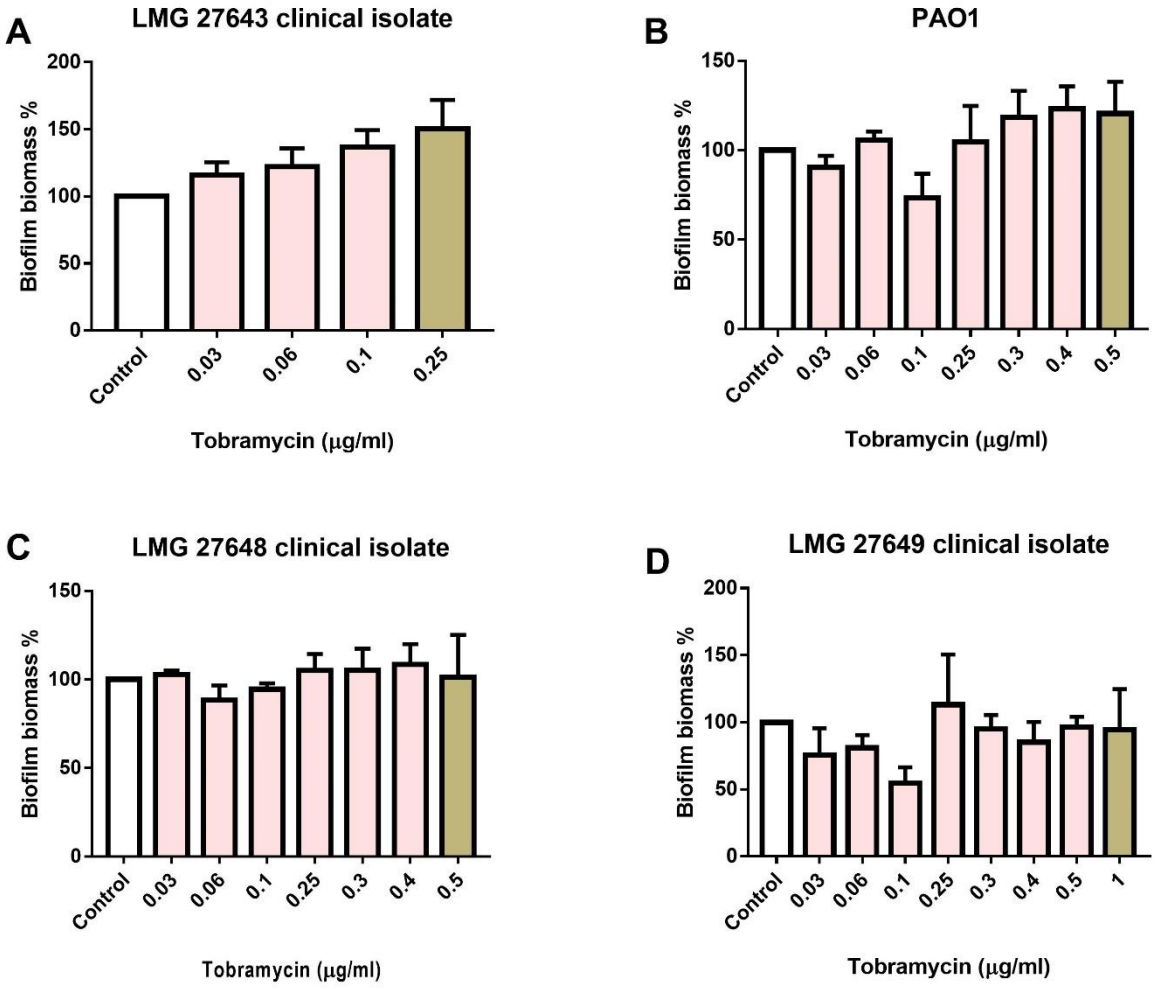

Figure 3.3. The effect of sub-MICs of tobramycin on biofilm formation in *P. aeruginosa.* (A, C, D) show clinical CF isolates and (B) indicates a lab strain. The 96-well plate assay was used as described in materials and methods. Wells in a 96-well plate contained MOPS medium supplemented with an inoculum were incubated for 24 h at 37°C. This was followed by treatment with a range of sub-MIC tobramycin concentrations and incubated in the same conditions described above. The controls represent the *P. aeruginosa* biofilms without tobramycin treatment. The data shown presented the standard error of the mean from three biological repeats with at least six technical repeats. Statistical significance was analysed using one-way analysis of variance (ANOVA) followed by Dunnett's multiple comparison test. White bars: controls, *Pseudomonas* without tobramycin; pink bars: *Pseudomonas* exposed to sub-MICs tobramycin; green bars: *Pseudomonas* exposed to MICs of tobramycin. Full details of the statistical analysis are shown in appendix 1 and 2.

A previous study has shown that the composition of the growth medium can have a significant effect on biofilm formation (Haney et al., 2018). Therefore, it was of interest to determine if MOPS medium that we used would have an effect on the obtained results. Therefore, the experiments were also performed using MHB (rich medium) instead of MOPS medium. The

results (Figure A-D) showed that by using MHB there was no effect of tobramycin at sub-MIC on enhancing biofilm formation.

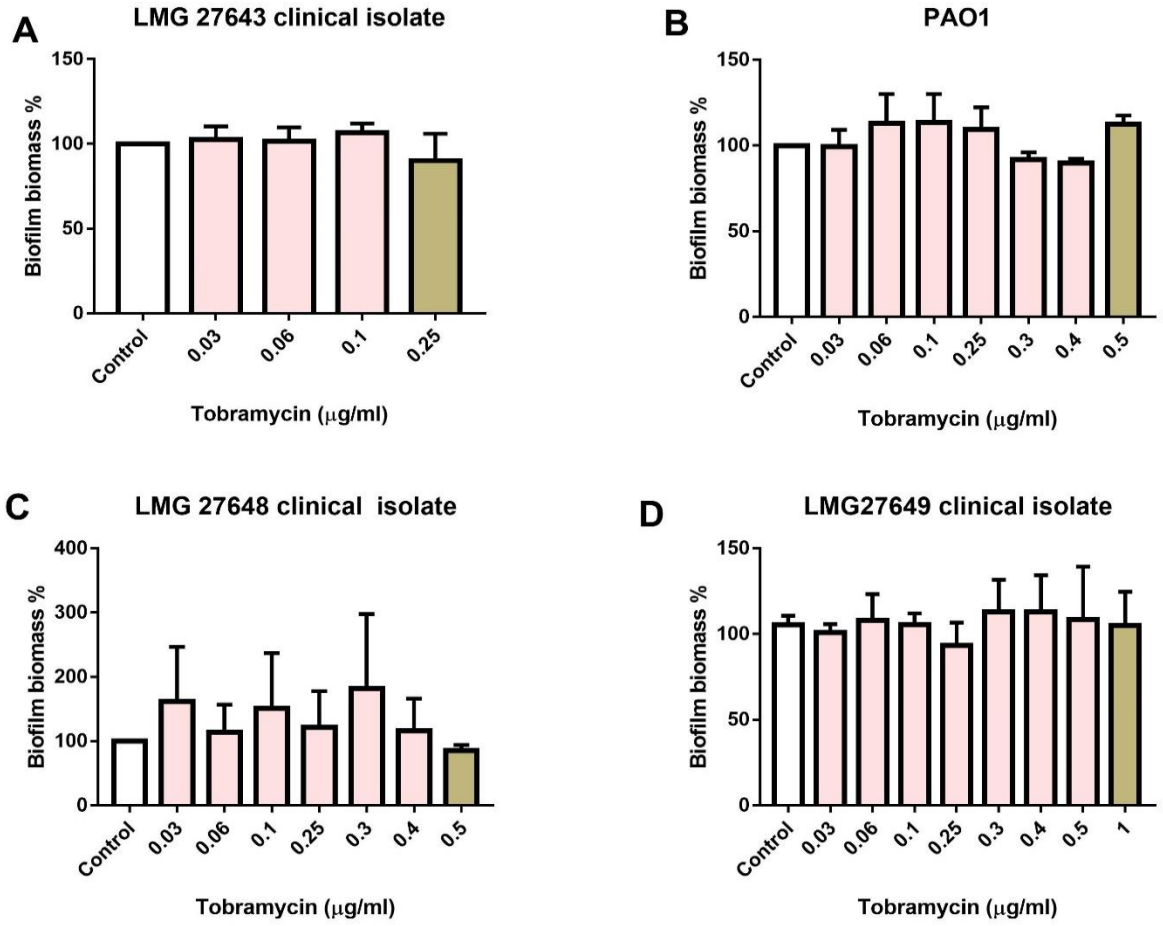

Figure 3.4. The effect of sub-MICs of tobramycin on biofilm formation of *P. aeruginosa.* (A, C, D) show clinical CF isolates and (B) indicates a lab strain. The 96-well plate assay was used as described in materials and methods. Wells in a 96-well plate contained MHB medium supplemented with an inoculum were incubated for 24 h at 37°C. This was followed by treatment with a range of sub-MIC tobramycin concentrations and incubated in the same conditions described above. The controls represent the *P. aeruginosa* biofilms without tobramycin treatment. The data shown presented the standard error of the mean from three biological repeats with at least 6 technical repeats. Statistical significance was analysed using one-way analysis of variance (ANOVA) followed by Dunnett's multiple comparison test. White bars: controls, *Pseudomonas* without tobramycin; pink bars: *Pseudomonas* exposed to sub-MICs tobramycin; green bars: *Pseudomonas* exposed to MICs of tobramycin. Full details of the statistical analysis are shown in appendix 1 and 2.

3.2.4 The *in vitro* influence of iron on *P. aeruginosa*

In the section discussed before, the biofilm formation as the result of using sub-MIC tobramycin was evaluated. Here, our aim was to explore more about the role of other factors in enhancing biofilm formation. Recently, the influence of iron on enhancing biofilm formation and resistance to tobramycin in *P. aeruginosa* has received considerable attention in research (Oglesby-Sherrouse et al., 2014). For instance, it was previously established that the *in vivo* iron levels in CF lung infections play a major role in the recalcitrance of *P. aeruginosa* to tobramycin (Oglesby-Sherrouse et al., 2014). Therefore, the role of iron was investigated against *P. aeruginosa* planktonic growth rate, biofilm formation, and tobramycin susceptibility.

3.2.4.1 The *in vitro* influence of iron on planktonic growth rate

This experiment was performed to assess the impact of iron on the growth rate of planktonic *P. aeruginosa.* Overnight cultures were prepared and diluted 1:100 into MOPS medium supplemented with different ammonium iron citrate $(NH_4)_5[Fe(C_6H_4O_7)_2]$ concentrations, followed by incubation at 37°C. The growth rates were monitored hourly over six hours. Data revealed (Figure 3.5, A-D) that iron concentration had no effect on the growth rates of planktonic *P. aeruginosa* clinical isolates and PAO1. This means under the tested conditions, iron is not a limiting factor for *P. aeruginosa* growth. It was also noted that a small difference in growth rate under high iron level was observed only at 4 h in two clinical isolates LMG 27643 and LMG 27649 (Figure 3.5 B and C). This time point more or less corresponds to the end of the exponential growth phase, indicating that at low iron concentrations the bacteria may enter the stationary phase slightly earlier. However, it should be noted that this experiment has only performed once, and it needs to be demonstrated that results are reproducible. The same experiment was also performed but without adding any iron to MOPS medium. The results (data not shown) suggested that MOPS medium without iron did not support the growth of LMG 27649 clinical isolate, but other clinical isolates and PAO1 were able to grow, indicating that there is a low concentration of iron present as contaminate that can support the growth of other strains. The addition of 0.01 µM iron to the medium was however sufficient also for LMG

27649 growth, and this concentration was therefore used in all subsequent experiments as the low iron condition.

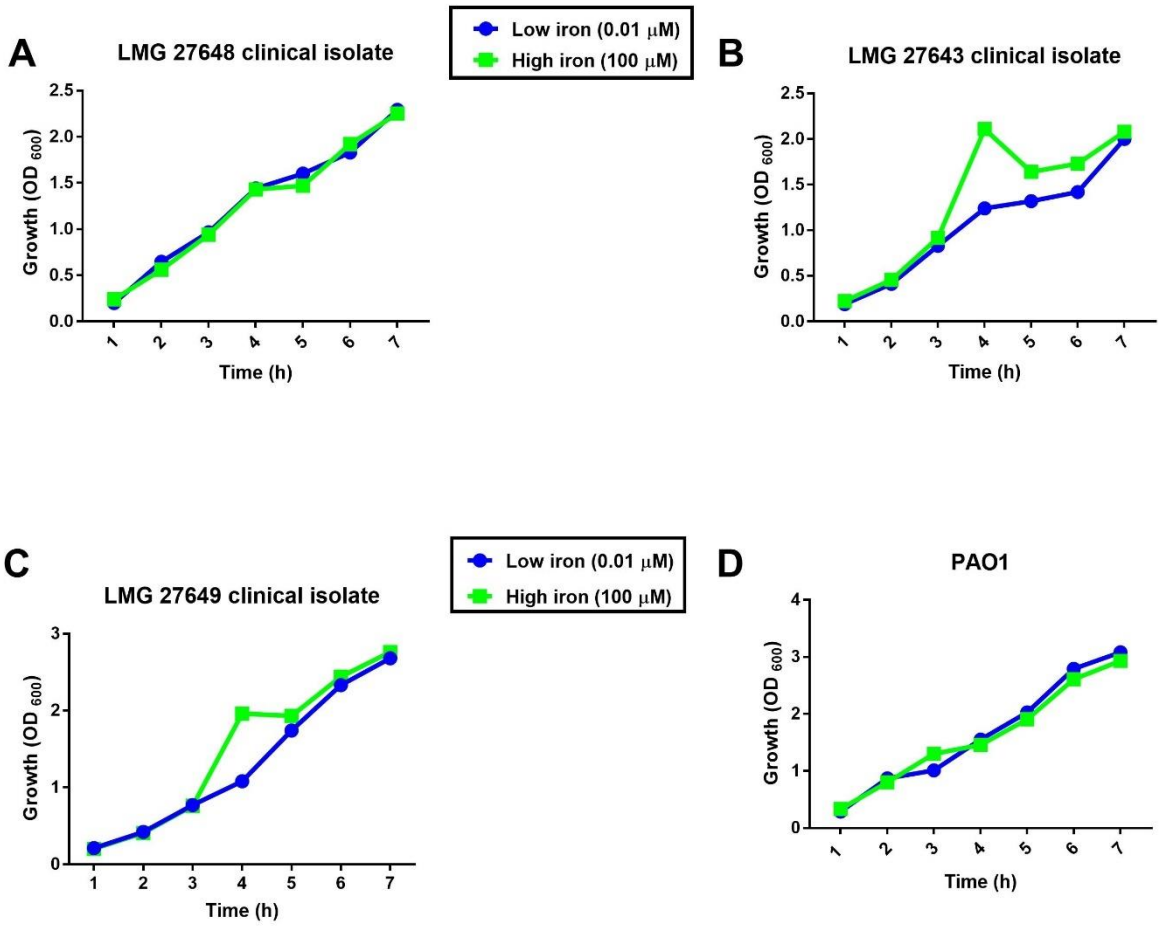

Figure 3.5. The effect of different iron levels on the growth rate of planktonic *P. aeruginosa*. (A-C) indicate clinical CF isolates and (D) shows a lab strain PAO1. Bacterial cells were grown at 37°C in MOPS medium supplemented with either 0.01 µM or 100 µM of iron. Growth measurements were taken every hour. The data shown one biological repeat (n = 1).

3.2.4.2 The *in vitro* influence of iron on planktonic susceptibilities to tobramycin (MICs)

As the above section described the effect of iron on the growth rate of *P. aeruginosa*, this section was to understand whether different ammonium iron citrate $(NH_4)_5[Fe(C_6H_4O_7)_2]$ availability can affect *P. aeruginosa* susceptibility towards tobramycin. A recent study has examined the effect of iron on MICs of tobramycin against *P. aeruginosa* and the results

showed that different iron availability has no effect on MIC values (Musk et al., 2005). To replicate this, the MICs for tobramycin in MOPS medium supplemented with either low iron (0.01 µm) or high iron (100 µm) was measured using macro-dilution assay. The MIC data are presented in Table 3.2. Our results suggested that the MICs for tobramycin were similar under different iron availabilities for all tested clinical CF isolates and lab strain and the results were in accordance with the above-mentioned study.

Table 3.2. The MICs of tobramycin in low iron and rich iron MOPS medium against lab strain PAO1 and clinical CF isolates *P. aeruginosa* were determined in triplicate by macro-dilution assay.

Lab strain/clinical CF isolates of *P. aeruginosa*	**MICs (µg/ml) in low iron (0.01 µm)**	**MICs (µg/ml) in high iron (100 µm)**
PAO1	0.5	0.5
LMG 27648	0.5	0.5
LMG 27643	0.25	0.25
LMG 27649	1	1

3.2.4.3 The *in vitro* influence of iron on biofilm formation in *P. aeruginosa* and boosting resistance of tobramycin

After we illustrated the effect of iron on planktonic *P. aeruginosa* susceptibilities towards tobramycin in the previous section, it was interesting to know how the biofilm susceptibility to tobramycin is affected by different iron concentrations. Therefore, to address this issue, clinical CF isolates and lab strains *P. aeruginosa* were inoculated in the 96-well plates containing MOPS medium supplemented with different concentrations of ammonium iron citrate $(NH_4)_5[Fe(C_6H_4O_7)_2]$. The concentrations included were 8, 63, and 100 µm iron; these represent the standard iron concentration in MOPS medium, and the elevated concentrations found in CF lungs respectively (Berlutti et al., 2005; LaBauve and Wargo, 2012; Ezraty and

Barras, 2016). Then the biofilms were incubated for 24 h at 37°C, after this they were challenged with 50 µg/ml tobramycin and incubated for a further 24 h. The results (Figure 3.6 A-D) showed that there was no significant difference between various iron concentrations on biofilm biomass and tobramycin resistance.

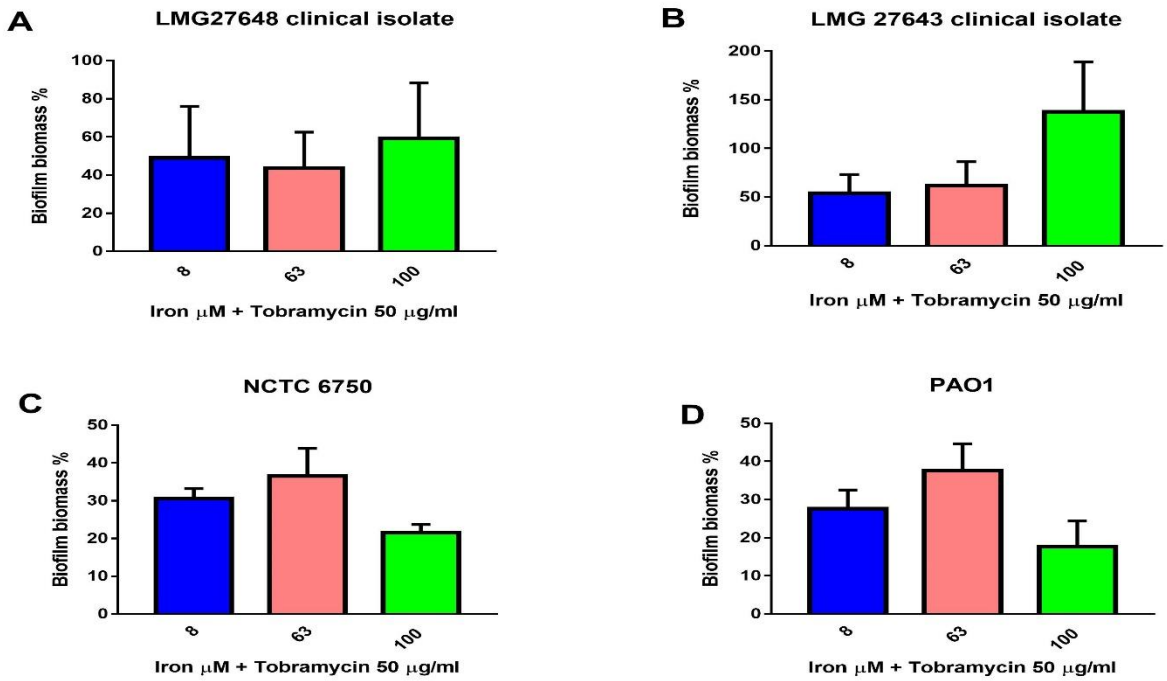

Figure 3.6. The influence of different iron availability on biofilm formation and tobramycin resistance of *P. aeruginosa*. (A- B) show clinical CF isolates and (C-D) indicate lab strains. The 96-well plate assay was used as described in materials and methods. Wells in a 96-well plate contained different concentrations of iron in MOPS medium supplemented with an inoculum, and then the plate was incubated for 24 h at 37°C. This was followed by treatment with 50 µg/ml tobramycin concentrations dissolved in various iron concentrations. Blue bars: 8 µM iron, pink bars: 63 µM iron, and green bars: 100 µM iron. The data shown are presented as standard error of the mean from three independent experiments with at least six technical replicates. Statistical significance was analysed using one-way analysis of variance (ANOVA) followed by Tukey multiple comparison test. Full details of the statistical analysis are shown in appendix 1.

In the previous pre-liminary iron experiment on biofilm formation, the effect of different iron availability on biofilm formation was tested. Here, we sought to test the effect of low iron levels of 0.01 µM as probably represent restricted iron concentration in healthy lung and compare it to the high iron level of 100 µM that represents the concentration in CF lung. This was evaluated on a range of tobramycin concentration. Results obtained for LMG 27648, LMG 27643, and PAO1 (Figure 3.7; A, B, and D) showed that at 100 µM iron, there was a trend of

enhancing tobramycin tolerance as compared to 0.01 µM iron, albeit this was not statistically significant. Conversely, for the other strain, NCTC 6750 (Figure 3.7, C), we found that trend for low iron concentration, while this was not the case for the high iron concentration again this was statistically not significant. This may be because at low iron concentrations, *P. aeruginosa* enhances expression of *mexA-mexB -oprM* gene operon. This leads to the synthesis of the MexA-MexB-OprM efflux pump, in which it is considered one of the highly characterized pumps of resistance nodulation division (RND) family. It is well-known that MexAB-OprM provides an intrinsic resistance for *P. aeruginosa* against several antibiotics including tobramycin (Ezraty and Barras, 2016; Rampioni et al., 2017a; Diggle and Whiteley, 2019). However, it is unclear why this happened only with NCTC 6750 strain.

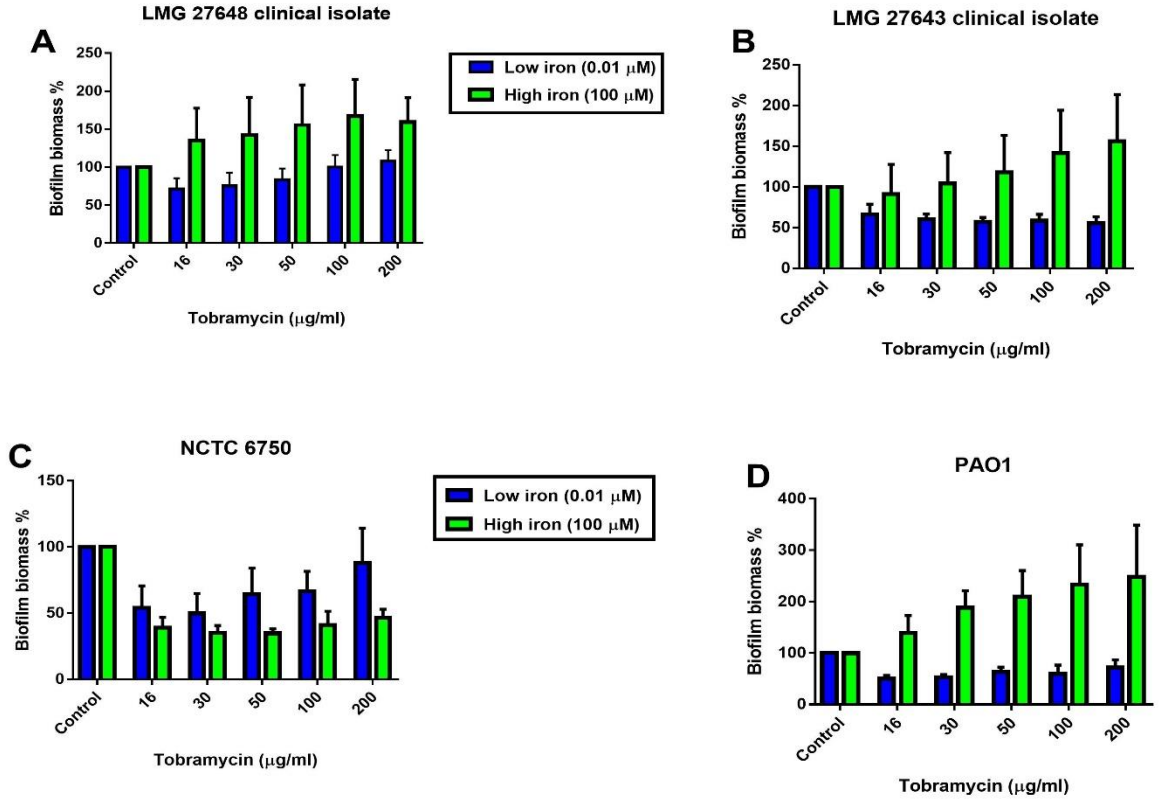

Figure 3.7. The influence of different iron availability on biofilm formation and tobramycin resistance of *P. aeruginosa.* (A-B) show clinical CF isolates and (D) indicate a lab strain. The 96-well plate assay was used as described in materials and methods. Wells in a 96-well plate contained different concentrations of iron in MOPS medium supplemented with an inoculum, and then the plates were incubated for 24 h at 37°C. This was followed by treatment with tobramycin dissolved in various iron concentrations. Green bars: 100 µM iron, blue bars: 0.01 µM iron, the controls represent biofilms without tobramycin. The data shown are presented as the standard error of the mean from three independent experiments with at least six technical replicates. Statistical significance was analysed using two-way analysis of variance (ANOVA) followed by Tukey multiple comparison test. Full details of statistical analysis are shown in appendix1.

3.2.5 The *in vitro* activity of tobramycin using artificial sputum medium (ASM)

In all of the above sections, the activity of tobramycin was analysed using MOPS medium. Currently, a study has importantly recommended the use of a more clinically relevant medium to test the activity of antibiotics against *P. aeruginosa* (Kirchner et al., 2012). Accordingly, in this section, we aimed to get further insights on exploring tobramycin activity under a condition that is as close as possible simulate the chemical environment of the CF lung. To achieve this, ASM was developed and optimized as outlined in the Materials and Method chapter. This ASM contains mucin, DNA, amino acids, and salts. The highly glycosylated proteins (mucin) and DNA are the main macromolecular components of the CF sputum (Yang et al., 2010; Huang et al., 2015). Amino acids are also found in a high concentrations in CF sputum in a range between 3.77 – 6.77 mg/L (Barth and Pitt, 1996), where this is attributed to the infection and inflammation. This is because neutrophils and pathogens release proteases that degrade proteins, resulting in the release of peptides and amino acids (Thomas et al., 2000; Yang et al., 2010). This medium was used to examine the activity of tobramycin against planktonic and biofilms of *P. aeruginosa*.

3.2.5.1 The *in vitro* activity of tobramycin against planktonic *P. aeruginosa* in ASM

The antibacterial activity of tobramycin (MICs) was determined against planktonic lab strain and clinical isolates of *P. aeruginosa* in ASM medium using the macro-dilution assay. As shown in Table 3.3, PAO1 and all of the clinical isolates were found to be susceptible to tobramycin with MICs 4 µg/ml. However, there was a four-fold increase in the MICs as compared to the earlier reported MICs in MOPS medium (Section 3.2.2).

Table 3.3. The MICs of tobramycin against PAO1 and clinical CF isolates *P. aeruginosa* determined in triplicate by macro-dilution method in ASM medium.

Lab strain/clinical CF isolates of *P. aeruginosa*	**MICs (µg/ml) of tobramycin in ASM medium**
PAO1	4
LMG 27648	4
LMG 27643	4
LMG 27649	4

3.2.5.2 The *in vitro* activity of tobramycin against biofilms of *P. aeruginosa* in ASM

As the previous section showed that ASM had an effect on the activity of tobramycin against planktonic *P. aeruginosa*, this encouraged us to study its effect on the biofilm phenotypes. Therefore, all *P. aeruginosa* clinical isolates and PAO1 were inoculated on polycarbonate membranes that were placed on MH agar plates and allowed to develop biofilms using ASM for 48 h and then challenged with 30 µg tobramycin discs for 24 h at 37°C. Unexpectedly to what is already known about the role of ASM components, where they bind tobramycin and reduce its activity and also in comparison to the results outlined earlier in MOPS medium (Section 3.2.3.2), tobramycin retained its activity against ASM grown biofilms where it displayed a significant reduction in the viable count by 60% against LMG 27649, LMG 27643 and PAO1 (Figure 3.8 B; C; and D). Likewise, the remaining clinical isolate LMG 27648 (Figure 3.8 A), behaved similarly as other isolates, where there was a reduction in the viable count by 40% as compared to control, but it was statistically not significant.

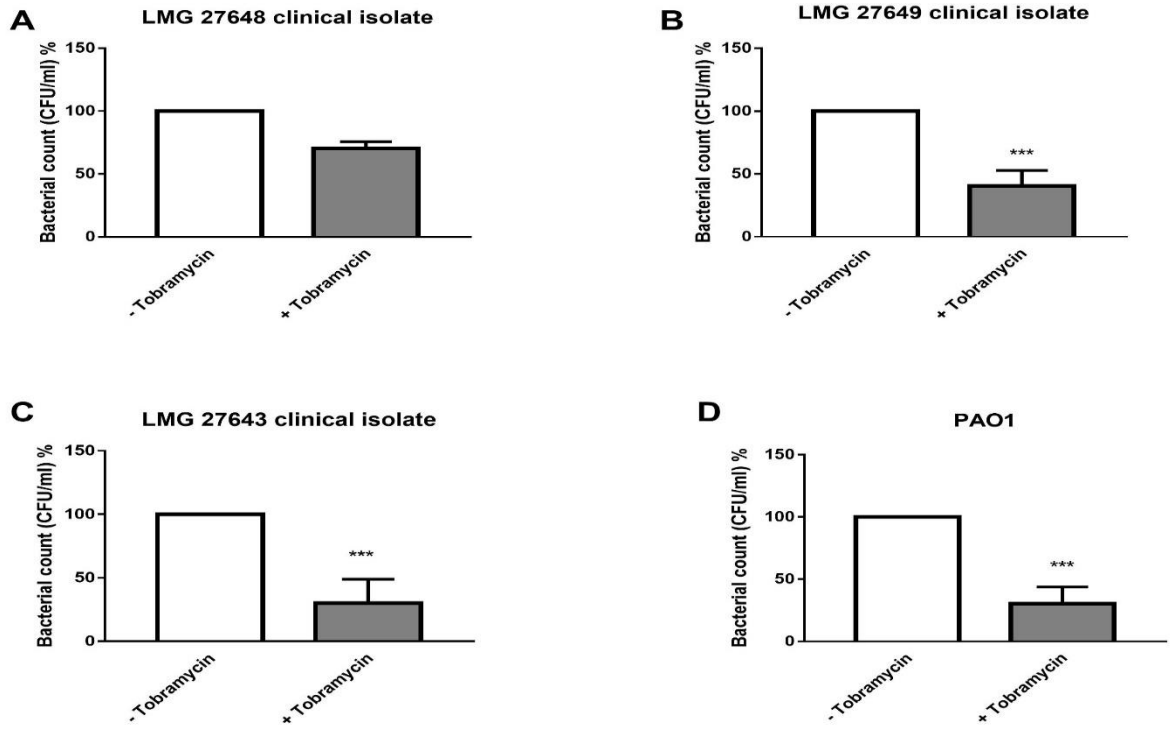

Figure 3.8. The *in vitro* activity of tobramycin in ASM against *P. aeruginosa* determined using the colony biofilm assay. (A – C) show clinical CF isolates and (D) indicates a lab strain. All the clinical isolates or a lab strain were grown in ASM for 48 h and then treated with 30 µg/disc tobramycin and incubated for 24 h at 37°C. The controls represent the biofilms without tobramycin. The data shown represent the standard error of the mean from three independent experiments with at least two technical replicates. Statistical significance was analysed using unpaired 2-tailed *t* test. Statistical significance differences between treated biofilms (***, $p<0.001$) and the control are indicted. Full details of the statistical analysis are shown in appendix 1.

3.2.6 The *in vitro* activity of colistin against planktonic and biofilms of *P. aeruginosa*

Earlier, the activity of tobramycin was determined against *P. aeruginosa.* Here, we aimed to evaluate the activity of colistin, which is another antipseudomonal antibiotic that has been introduced for the treatment *P. aeruginosa* lung infections due to the emergence of multidrug resistance pathogens (Gutu et al., 2013). Accordingly, the following sections will investigate the activity of colistin against planktonic and biofilms phenotypes of *P. aeruginosa* using ASM.

3.2.6.1 The *in vitro* activity of colistin against planktonic *P. aeruginosa* in MOPS and ASM media

To investigate the antibacterial activity of colistin against planktonic *P. aeruginosa*, MICs were established against a lab strain PAO1 and clinical isolates of *P. aeruginosa* in MOPS medium and compared to the MICs in ASM using macro-dilution protocol. As shown in Table 3.4, in MOPS medium, PAO1 and all of the clinical isolates were found to be susceptible to colistin with MICs ≤ 1 µg/ml. Similarly, in ASM all the strains were susceptible but with a slight increase in the MICs by a two-fold in PAO1 and in two clinical isolates, (LMG 27648 and LMG 27649), whereas the MIC for the other clinical isolate LMG 27643 was not changed with ASM.

Table 3.4. The MICs of colistin against PAO1 and clinical CF isolates *P. aeruginosa* determined in triplicate by macro-dilution method in MOPS and ASM media.

Lab strain/clinical CF isolates of *P. aeruginosa*	**MICs (µg/ml) of colistin in MOPS**	**MICs (µg/ml) of colistin in ASM**
PAO1	0.25	0.5
LMG 27648	1	2
LMG 27643	1	1
LMG 27649	0.5	1

3.2.6.2 The *in vitro* activity of colistin against biofilms of *P. aeruginosa* determined in ASM medium

In the above section the activity of colistin was investigated against planktonic *P. aeruginosa*. In the current section, it was important to determine the *in vitro* activity of colistin against biofilms of *P. aeruginosa* clinical CF isolates (LMG27648, LMG27649, and LMG27643 and lab strain PAO1). Therefore, the strains were inoculated on polycarbonate membranes that were placed on MH agar plates and allowed to develop biofilms using ASM for 48 h, then these challenged with 50 µg colistin discs for 24 h at 37°C. The results (Figure 3.9 A and B) for LMG 27648 and LMG 27649 clinical isolates showed that colistin caused a 40% reduction in the viable count but this was statistically not significant ($p > 0.05$). In comparison with other strains, LMG 27643 and PAO1 (Figure 3.9 C and D), a significant ($p < 0.05$) reduction in the viable count by 60% was observed.

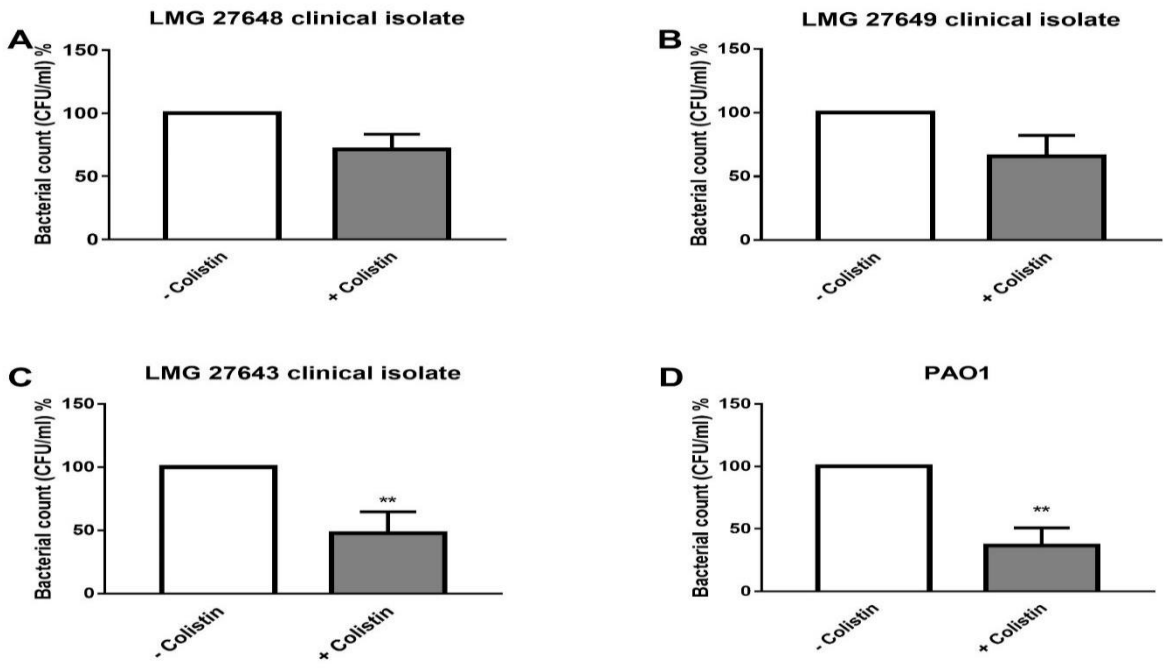

Figure 3.9. The *in vitro* activity of colistin against *P. aeruginosa* biofilms determined using the colony biofilm assay. (A – C) show clinical CF isolates and (D) indicates a lab strain. All clinical isolates and a lab strain were grown in ASM for 48 h and then treated with 50 µg/disc colistin, and incubated for 24 h at 37°C. The controls represent biofilms without colistin. The data shown represent the standard error of the mean from three independent experiments with at least two technical replicates. Statistical significance was analysed using unpaired 2-tailed *t*-test. Statistically significant differences between treated biofilms (**, $p<0.01$) and the control. Full details of the statistical analysis are shown in appendix 1.

3.3 Discussion

In this chapter, we investigated the activity of tobramycin against planktonic cultures and biofilms of *P. aeruginosa* clinical CF isolates and lab strains. Also, we determined the effects of several factors on the antibiofilm activity of tobramycin including, the influences of tobramycin at sub-MICs and the effect of various iron availability. Indeed, the effect of growth media MOPS and ASM on tobramycin activity was determined. Finally, we also examined the activity of colistin against planktonic and biofilms of *P. aeruginosa*.

Tobramycin is one of the most commonly used antibiotics in the treatment of *P. aeruginosa* infections in CF patients (Kaushik et al., 2016). Therefore, in this study, tobramycin susceptibility was evaluated using two biofilm models. Firstly, the 96-well plate biofilm assay was used because it has several advantages (Coffey and Anderson, 2014). One of those is the applicability to perform screening for a large number of bacterial strains in a single assay (Merritt et al., 2005). Moreover, its protocol is simple to perform using common laboratory instruments. However, besides these benefits this assay does has some drawbacks such as using the crystal violet. The latter stains biomass, which is not equivalent to a viable count as it will stain both dead and alive cells as well as the extracellular polymeric matrix (Coffey and Anderson, 2014). Therefore, to address the limitations that could result in an overestimation mass of adherent bacteria, the microtiter plate assay was also combined with another biofilm model, the colony biofilm assay (Merritt et al., 2005). In the colony biofilm model, biofilms grow at the air surface-interface. This way of growing is probably a better reflection of how biofilms grow in the lungs. Additionally, the parameter that was used to assess the activity of tobramycin in colony biofilm assay was through counting the number of living bacterial cells instead of total biofilm biomass. This assay also has its disadvantages, such as the underestimation of the number of living cells that are counted. As this assay only measures the number of the living culturable cells, however, the biofilms have also populations that they are alive but non-culturable because of their very low metabolic rate (Azeredo et al., 2017). Our data from both biofilm assays indicated that using tobramycin at the clinically achievable concentrations was only able to reduce biofilm biomass/viable count by 40-60%, however, complete eradication was not observed in all of the tested strains. Such tolerance of these biofilms to the action of tobramycin could be explained by several mechanisms, however, we have not tested any of them. These mechanisms involved the slowed growth rate of cells inside

biofilms, the decreased penetration of tobramycin through biofilm matrix (Field et al., 2005; Ye et al., 2018), and recently there are reports suggested that *P. aeruginosa* cells inside the biofilm can resist antibiotics including tobramycin by a genetic changes, which resulted in producing cyclic glucose polymers termed as periplasmic glucans that can sequester tobramycin and decrease its activity (Rogan et al., 2004; Hill et al., 2005). Importantly these data could explain the current challenges for the treatment of these biofilms in the clinical setting. Our data were in accordance with previous study (Field et al., 2005), which showed that using tobramycin at a dose up to 128 mg/L both under aerobic and anaerobic conditions was unable to eradicate biofilms of *P. aeruginosa* clinical CF isolates and PAO1.

The implications of exposing *P. aeruginosa* biofilms to sub-lethal concentrations of tobramycin was investigated in our study. Our findings revealed that there was a trend of slight induction of biofilm formation, but it was statistically not significant. In contrast to our findings, other studies found a significant and clear induction of biofilm formation of tobramycin at sub-MICs (Hoffman et al., 2005; Tahrioui et al., 2019). It is, however, noteworthy to mention that different strains and growth media were used in those studies. For example, the study by Tahrioui et al (2019) used different strain of *P. aeruginosa* H103. Another study by Hoffman et al (2005) was performed using MHB growth medium. To reproduce their work, our experiments were re-performed using MHB. Surprisingly, our results did not change by using the MHB. This highlights an issue raised in a number of studies, in which there are concerns with the lack of standardisation in biofilm research, while there should be a requirement to follow guidelines and standards for describing experimental methods. These standards have been established for several biological studies including biofilms research to facilitate repeatability and reproducibility of the experiments (Taylor et al., 2008; Boudarel et al., 2018). However, due to the lack of standardization, there is a significant heterogenicity and variability in the results obtained and published in literature. Such variability is related to different biofilm protocols, designs with various growth conditions that are used in the experiments, such as growth media composition, pH, and temperature, as all of which can lead to variation in the results. Therefore, it is difficult to reproduce and compare results between the published studies (Taylor et al., 2008; Boudarel et al., 2018).

A previous study demonstrated that iron has a major role in *P. aeruginosa* infections (Banin et al., 2005). In this context, the influence of iron on growth rate and susceptibility of planktonic *P. aeruginosa* towards tobramycin in terms of MICs was measured. Regarding the planktonic growth rate, the data suggested that neither nil or low iron (0.01 µM), nor high iron (100 µM) concentrations had an effect on the growth rate of *P. aeruginosa.* Similarly, the MIC data indicated that there was no change in tobramycin activity in low and high iron levels, and we can therefore conclude that iron is not a limiting factor under the tested conditions. Our work was in agreement with Cai et al. (2009), where they found that MICs for tobramycin did not change under iron repletion (100 µM) and iron depletion conditions. Noteworthy to mention that in this study they used 2, 2-dipyridyl as a chelator to induce an iron restricted environment in the MHB medium.

The effect of iron on biofilm formation in *P. aeruginosa* was also assessed. Our results suggested a trend of increased tolerance to tobramycin in some of the tested *P. aeruginosa* strains under high iron (100 µm) conditions and a trend of decreased tolerance under low iron concentration (0.01 µm) with exception of *P. aeruginosa* NCTC 6750. However, the difference between the two iron concentrations was not statistically significant. One explanation for these data may be that our MOPS medium has another source of iron rather than the specified amounts, which could be as a contaminant in some of the salts, and this means the actual concentrations in MOPS medium are higher than the assumed concentrations. This was confirmed (data not shown) in our work, where three strains out of four were able to grow in MOPS without any addition of iron, which could suggest the presence of iron contamination in the medium. Such a problem has been discussed by Ezraty et al (2016), as one of the sources for the variable iron results obtained in the literature. Indeed, under low iron tested concentration, the bacterial cells enter into slow metabolism mode of growth, which could make them also less susceptible to tobramycin treatment (Williamson et al., 2012). Another possible reason is that under iron-restricted conditions, iron sequestration genes are upregulated in *P. aeruginosa*. These genes result in activation of an iron uptake system using siderophores such as pyoverdine and pyochelin (Gi et al., 2015). In contrast, in iron-load conditions siderophore production is downregulated. Our data were in agreement with what was found by Oglesby-Sherrouse et al (2014), where they observed that using iron 100 µM resulted in enhancing tobramycin resistance in PAO1 biofilm and this effect was removed when they added deferasirox as an iron chelator. In the contrary, our work was in conflict with what Musk

and colleagues found (Musk et al., 2005), as they determined that iron resulted in enhanced susceptibility to tobramycin. The most plausible explanation for this could be because differences in experimental design such as the use of a different *P. aeruginosa* strain (PA14), which was grown in a different medium (Tryptic soya agar, TSA). In addition, they used very high iron concentrations of up to 500 µM, which might be not clinically relevant. This high concentration could result in biofilm disruption and enhanced tobramycin susceptibility. Such an increase in the susceptibility is mainly attributed to the formation of reactive oxygen species, such as a hydroxyl species through the Fenton reaction. This reactive oxygen species can be dangerous and toxic to bacterial cells by attacking their cellular components and causing DNA breakage (Schaible and Kaufmann, 2004).

A more clinically relevant medium ASM was also used to evaluate the activity of tobramycin and colistin against planktonic *P. aeruginosa*. Our results showed that the MICs of tobramycin and colistin were increased in ASM medium by four and two-fold respectively as compared to the MOPS medium. However, even the MICs values were increased, they still considered susceptible to either tobramycin or colistin according to BSAC breakpoints (Andrews, 2007). It should be noted that those breakpoints are only determined in standard media such as Iso-Sensitest or Mueller-Hinton broth. One explanation would be because of the components that are present in ASM. These for instance include mucin and DNA, which might act as an inhibitor for tobramycin because of electrostatic interactions between poly-anionic mucins or DNA and cationic tobramycin or colistin. Such binding could result in less free available tobramycin or colistin and consequently reducing their bacterial killing potency. Our findings were in good agreement with what previously reported (Huang et al., 2015; Schneider-Futschik et al., 2018). For instance, Huang et al (2015) found an elevation in MICs for tobramycin and colistin against several Gram-negative bacteria including *P. aeruginosa* when these antibiotics were incubated with different concentrations of mucin, which is one of the main components of CF sputum. This suggest that the components of CF sputum decrease the bioavailability of antibiotics, which consequently results in decreased the efficacy. Similarly, the work that has been done by Schneider-Futschik et al (2018) suggested that the components of ASM medium resulted in the elevation of MICs for colistin and other polypeptides antibiotics against *P. aeruginosa*. Our data and other cited papers suggest that it is essential to consider using a more clinically relevant culture media for testing the susceptibility of antibiotics.

Surprisingly, under the biofilm conditions, ASM did not affect tobramycin potency and the activity was almost similar to that in the MOPS medium. Similar work has been done previously (Braun et al., 2018), but that study used natural human mucus, which revealed a significant decrease in tobramycin activity. This could be explained by different characteristics between ASM and human mucus. For instance, the elasticity and viscosity of human mucus might affect intermolecular forces interactions between mucus and drugs. Finally, the activity of colistin was also evaluated against biofilms of *P. aeruginosa*. The data showed that colistin resulted in a 50-60% reduction in the viable count, however, complete eradication was not achieved. It is possible that this is a reflection of the findings in another study (Pamp et al., 2008), which found that colistin was able to kill the *P. aeruginosa* bacterial subpopulation with low metabolic activity, but not the subpopulation of the biofilm with a high metabolic activity. However, we did not confirm here that it was only the cells with high metabolic activity that were tolerant to colistin.

3.4 Conclusion

In this chapter, the activity of one of the most clinically important antibiotics in the treatment of CF patients, tobramycin, was evaluated against *P. aeruginosa* biofilms using ASM. Tobramycin resulted only in a 40-60% reduction in biofilm biomass/viable count in most of the tested strains, however, complete eradication of *P. aeruginosa* biofilms was challenging. This could highlight for important clinical consequences of such infection. Similarly, such data was also observed with colistin, where only a 50-60% reduction in viable count was achieved. The presence of resistant *P. aeruginosa* biofilms simultaneously with the declining rate of the pipeline development of new antibiotics suggests that it is important to search for an alternative way to effectively use the currently available antibiotics to overcome biofilms resistance. Therefore, our aim in the next following chapters is to explore the possible mechanisms that could be used to improve the activity of tobramycin against *P. aeruginosa* biofilms. This will be achieved by examining two main possible strategies. Firstly, the activity of tobramycin as a dry powder inhaler will be investigated utilizing one of the most important physical properties of the powder, particle size, as a possible way to enhance tobramycin efficacy. Secondly, the activity of tobramycin will be evaluated by establishing an effective drug combination with tobramycin as another possible ways to promote its activity.

Chapter 4: Results Section II

Investigating the Effect of Tobramycin Dry Powder Inhaler on the Eradication of *Pseudomonas aeruginosa* Biofilms

4.1 Introduction

The most commonly identified pathogen in chronic CF lung infections is *P. aeruginosa,* which is settled and localized in a thick mucus layer in the trachea-bronchial region of the respiratory airways. Treating such infections using the systemic delivery of antibiotic agents is challenging because high doses are required to reach the lung tissue. Such doses are associated with severe adverse reactions. Therefore, the pulmonary delivery of antibiotics is an attractive approach for the treatment of lung infections (Worlitzsch et al., 2002; Geller et al., 2011). This is because delivering the drug directly to the site of infection achieves high therapeutic concentrations and rapid onset of action. Furthermore, minimum adverse reactions are achieved due to the limited systemic absorption (Yang et al., 2009; Mangal et al., 2018).

Pulmonary delivery of antibiotics is widely used in the treatment of *P. aeruginosa* lung infections in CF patients, and this is through using inhaled antibiotics. The inhaled antibacterial drugs are in two forms, being either nebulized solutions or dry powder formulations. Currently, the approved nebulized antibiotic solutions for the treatment of CF lung infections are colistin, aztreonam, and tobramycin (Geller et al., 2011; Ambrus et al., 2018). These nebulised solutions have a well-documented efficacy (Chuchalin et al., 2009), but they are also associated with some disadvantages. Among them, there is a prolonged administration time of 15-20 minutes. Moreover, these nebulized solutions are administered via bulky devices, which also requires the presence of a power source. Finally, the stability issues of nebulized solutions need that they are stored in a refrigerator (VanDevanter and Geller, 2011). All these together can reduce the adherence of patients to the treatment and can consequently result in the treatment failure.

Dry powder inhalers have addressed the limitations that are encountered with using nebulized solutions (Geller et al., 2011). For instance, dry powder inhalers are portable, easy to use by patients with a much shorter administration time (~ 5 minutes). Furthermore, the solid state is chemically more stable than the liquid state (Yang et al., 2014; Lee et al., 2016; Ambrus et al., 2018). Despite the advantages of dry powder inhalers, they still have some issues for delivering high doses, in which patients need to load and inhale multiple capsules to achieve the target dose, and as a result of this, patients could experience mild to moderate cough as an adverse drug reaction, although this gradually disappears with time (Parumasivam et al., 2017).

The currently approved inhaled dry powder antibiotics for treating *P. aeruginosa* CF lung infections are colistin and tobramycin. For instance, TOBI Podhaler® 28mg is an approved dry powder inhalation formulation of tobramycin, which is widely used in CF patients (McKeage, 2013). As a drug product, TOBI Podhaler® consists of the active ingredient, tobramycin sulfate (~85%) and excipient components. Among them, distearoylphosphatidylcholine (DSPC;14% (w/w)), which acts as a shell-forming agent that decreases interparticle attraction forces. Other excipients that are important during the process of dry powder production are sulfuric acid to adjust the pH, and calcium chloride as an emulsion stabilizer (VanDevanter and Geller, 2011; Weers and Miller, 2015).

Following inhalation of tobramycin powder, the inhaled particles deposit on the lung airway surface and once the deposition occurs, the physiological fate of these particles depends on a complex interaction between different factors. These involve the pathologic conditions in the lungs and the nature and physical properties of inhaled particles. In CF lung infections, inhaled drug particles are required to overcome several barriers, and these can significantly affect their pharmacological efficacy. Initially, deposited particles must dissolve in the mucus. This is then followed by diffusion to reach the target that is mostly localized and colonized inside this viscous dehydrated mucus. During this penetration process, the inhaled antibiotic might interact with the mucus components such as mucins and/or DNA, which in turn can influence the efficacy of the inhaled antibiotic by limiting its bioavailability at the target site. Beside this barrier, another obstacle to overcome, is the biofilm matrix around the bacteria that mainly consists of alginate polysaccharides and other molecules (Bos et al., 2017). Apart from pathological conditions in the lung, another factor can also play a role in the fate of inhaled particles, which is the physical state of inhaled powder. For instance, the process of dissolution is influenced by the physical properties of inhaled particles such as particle size (Timsina et al., 1994; Wenzler et al., 2016; Ciciliani et al., 2017).

Drug particle size is an important property that can influence both the deposition and fate of particles in the respiratory airways. Normally, inhaled drug particles are polydisperse in nature with a large particle size range (Deng et al., 2018). These include particles >10 µm, which are

mostly deposited in the oropharyngeal region and do not reach the lungs. Other particles are between 3-10 µm, which are mostly deposited in the trachea-bronchial region. Furthermore, particles at a range of 1-3 µm target the alveolar zone of the lungs. Particles that are smaller than <1 µm are known to be exhaled out of the lung due to the low inertia and gravitational powers which are insufficient to deposit them (Nafee et al., 2014). Therefore, inhaled powder particle size is an important characteristic of the powder, which can impact several processes from deposition to absorption and clinically efficacy (Pilcer et al., 2008; Taki et al., 2010).

Currently, *in vitro* antibiotic activity against biofilms is measured by using biofilm models such as 96-well plate assay. In these, the activity is tested on antibiotics that are completely dissolved in liquid, ready to be absorbed by biofilms that are also submerged in liquid. However, in CF lung infections, antibiotics are widely administered as an inhaled dry powder, where air-interface biofilms are exposed to the drug as dry particles with different particle sizes. These particle sizes could have an impact on antibiotic activity. Accordingly, such a critically important property of inhaled dry powder is missing from the currently used biofilm models. Therefore, this highlights the need for a model that is a better representative of the *in vivo* conditions. Such model should allow modelling of lung infections and studying the impact of particle size on the antibacterial activity of inhaled antibiotics. This can be performed by using a particle size pharmaceutical analysis assay combined with a biofilm model that is a more representative of the lung. One model that better reflects the *in vivo* lung environment is the *ex vivo* model that uses pig bronchial tissue (Harrison and Diggle, 2016). However, because of the time that might be required to establish and optimize such model to enable deposition of dry powder antibiotic, we therefore used a simpler *in vitro* model called colony biofilm (Merritt et al., 2005). This *in vitro* model for instance is unlike a 96-well plate assay (Coffey and Anderson, 2014), as the colony biofilm assay does provide an air interface and enables the deposition of dry powder antibiotics. This can help to further understand the role of particle size on antibiotic efficacy, which could be useful for improving the pharmacologic activity of inhaled antibiotics.

The *in vitro* particle size characterization of inhaled drug aerosols is mostly carried out using cascade impactors. The most commonly used impactor is a Next Generation Pharmaceutical Impactor (NGI) (Marple et al., 2003). The NGI is an instrument used to measure *in vitro*

behaviour of inhalable dry powder products (Rowland et al., 2018), in which NGI sequentially separates drug aerosols into various size categories from larger to smaller particles on the basis of the particles' aerodynamic diameter (Guo et al., 2008; Roberts and Mitchell, 2013; Wang et al., 2017). The aerodynamic diameter of a particle is the parameter that characterizes aerosol movements and depositions in the lungs (Pilcer et al., 2008; Wang et al., 2017). The deposition of the inhaled drugs on NGI compartments represents as closely as possible aerosol deposition in the respiratory system, thus, it is designed to operate in a range of flow rates from 30 to 100 L/min (Roberts and Mitchell, 2013). These are similar to flow rates that have been measured in most CF patients at age 6 years and older, however, some patients generated higher flow rates up to 170 L/min (Tiddens et al., 2014).

The NGI system consists of several parts (Figure 4.1), which includes an inhaler device, mouthpiece adaptor, induction port, pre-separator, seven impactor stages, and micro-orifice collector (MOC). Firstly, the inhaler device which contains the drug aerosol encased within a capsule is attached to the mouthpiece adaptor. The next part is the induction port, which is a pipe with a right-angle bend that operates possibly similar to the oropharyngeal region of patients, and it acts as an entrance of incoming aerosols from the inhaler device. The following part is the pre-separator, which is interposed between the induction port ending and the beginning of the fractionation stages. This pre-separator is considered as the initial size-separating stage comprising of a plate with 6 nozzles designed to collect the coarse or over-sized particles (50-100 µm), whilst the finer particles continue in the air stream for further size fractionation in the impactor stages (Mitchell et al., 2007; Roberts and Mitchell, 2019). Other NGI setup system in Figure 4.1 such as critical flow controller and air pump has been described before (See Materials and Methods Chapter, Section 2.8.5).

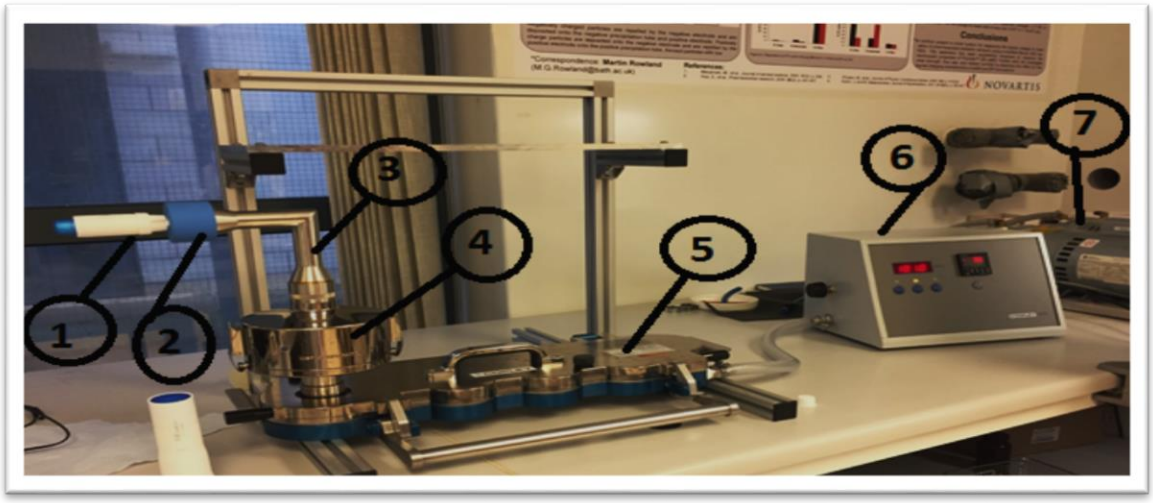

Figure 4.1. Complete NGI setup system. Inhaler device (1), mouthpiece adaptor (2), induction port (3), pre-separator (4), NGI (5), critical flow controller (6), Air pump (7). (unpublished image)

The other components of the NGI are the seven impactor stages (Figure 4.2), each of which parallels with a plate containing one or more circular nozzles with decreasing diameters as shown in Figure 4.2. Such a design allows each stage to act as a size separator of the incoming aerosols, where each stage captures particles larger than a specific aerodynamic diameter as shown in Table 4.1, which are previously determined by Marple et al (2003), in which these values were determined following calibration of the NGI with monodispersed aerosols. Finally, the last part of the NGI is the MOC, which is designed to collect the very fine particles (Mitchell et al., 2007; Roberts and Mitchell, 2013).

Figure 4.2. NGI in an open position. A nozzle plate with several nozzle diameters (1), a stage plate (2) with seven collection stages (S1-S7) and MOC: micro-orifice collector to collect the incoming powder from the above nozzles. (unpublished image)

Table 4.1. Cut-off aerodynamic diameter for each NGI stage at flow rates of 30 L/min and 60 L/min (Marple et al., 2003).

NGI stages	Cut-off diameter (µm) at 30 L/min	Cut-off diameter (µm) at 60 L/min
Stage 1	11.7	8.06
Stage 2	6.40	4.46
Stage 3	3.99	2.82
Stage 4	2.3	1.66
Stage 5	1.36	0.94
Stage 6	0.83	0.55
Stage 7	0.54	0.34
MOC	0.36	0.14

The deposition of particles from the standard NGI occurs directly on a solid impactor stage. This leads to high-speed deposition of particles in a small area resulting in the formation of strong agglomerates which then behave as larger particles (Price and Shur, 2018). Therefore, in addition to the standard NGI described above, for some experiments, an aerosol collection apparatus (Figure 4.3) was also introduced into the NGI. This collection system enables a slow and uniform deposition of aerosol particles over a single, large surface area of glass fibre filter instead of particle deposition directly on impactor stage. Particles therefore deposit slowly and subsequently behave as a single particle. Different types of aerosol collection apparatus were used in this study (See Material and Method Chapter, Section 2.8.6).

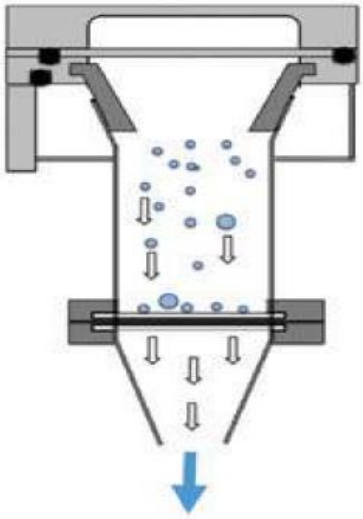

Figure 4.3 Schematic diagram of aerosol collection apparatus. Reproduced from (Price and Shur, 2018) with permission.

Using the NGI model for testing dry powder inhaler requires finding a quantification assay to determine the amount of drug that is deposited in every compartment of the NGI. Numerous analytical assays have been reported to quantify antibiotics including, microbiological (Kirby-Bauer disk diffusion) and chemical assays. (Dafale et al., 2016). Among the chemical assays, high-performance liquid chromatography (HPLC) is the most widely used and known to be an accurate and sensitive analysis of aminoglycoside antibiotics including tobramycin (El-Zaher and Mahrouse, 2013). However, tobramycin like all aminoglycoside antibiotics has a significant challenge in its determination and analysis using the traditional HPLC-UV (Blanchaert et al., 2017), because of the lack of a UV absorbing chromophore in its molecular structure. A chromophore is a chemical substance in a compound that responsible for absorbing UV light at a specific wavelength (Guo et al., 2006). Therefore, the detection of tobramycin using a UV-detector is unfeasible unless a derivatization process is used. However, this derivatization technique has some disadvantages including the stability of the derivatized analyte, its laborious nature with several sample preparations, and its low precision (Attema-de Jonge et al., 2008; Chen et al., 2014). Because of this, nowadays mass spectrometry MS used as an alternative, which does not require any complicated derivatization reactions. This HPLC-MS is known to have good sensitivity and selectivity for tobramycin determination.

This work described in this chapter aimed to provide a comprehensive investigation of the activity of tobramycin dry powder inhaler against *P. aeruginosa* biofilms. The investigations were in terms of studying the effect of differently sized tobramycin particles on its anti-biofilm activity. To achieve this, several preliminary experimental designs were needed. Therefore, the initial aims were to measure tobramycin powder particle size using the NGI and then to establish and validate an assay to quantify tobramycin powder from the NGI. This was followed by testing the activity of these differently sized particles against *P. aeruginosa* biofilms.

4.2 Results

4.2.1 Tobramycin particle size analysis

4.2.1.1 SEM analysis

SEM analysis was used to image tobramycin particles that had been extracted from the NGI stages using the method outlined in the Materials and Methods Chapter (Section 2.8.5). The size of particles deposited on the various stages of the NGI do not require routine measurement, as these are determined by the geometry of the NGI and as such are known in advance. However, deposition in the NGI is determined by aerodynamic diameter. So, our aim in this section was to determine particle size distributions in terms of geometric diameters for particles collected from various stages of the NGI. Representative SEM micrographs for tobramycin particles are shown in Figure 4.4. SEM micrographs show polydisperse, approximately spherical, and porous microparticles. These SEM images were further analysed for physical particle size measurements (See Section 4.2.2.1) using ImageJ software.

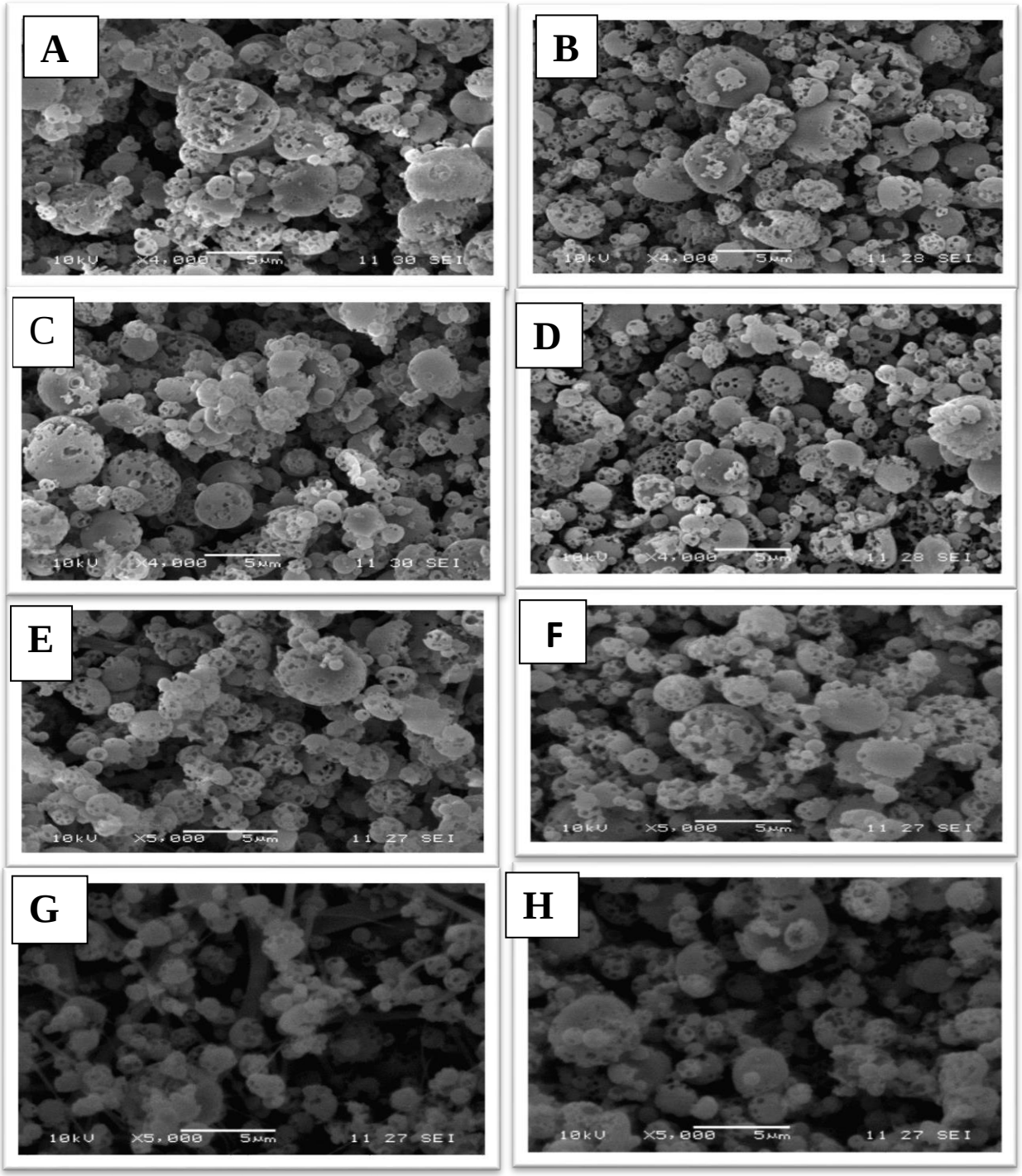

Figure 4.4. Representative SEM micrographs of tobramycin particles from NGI stages at different flow rates. Stage 2, at 30 L/min (A) and at 60 L/min (B). Stage 4, at 30 L/min (C) and at 60 L/min (D). Stage 5, at 30 L/min (E) and at 60 L/min (F). Stage 6, at 30 L/min (G) and at 60 L/min (H). All pictures were taken at x5,000 magnification (Scale bar = 5 µm).

4.2.2.1 Tobramycin particle size distribution in terms of physical diameter

In the section above, SEM images of tobramycin particles were captured, here these images were further analysed in order to obtain useful information about tobramycin particle size distribution and geometric diameters. To that aim, tobramycin particle size distributions plots were constructed as shown in Figure 4.5. Particle size distributions were produced by plotting the cumulative proportion of undersized particles (by number) against particle size (on a log - scale). Our data (Figure 4.5, A), showed that on stage 2 at 30 L/min, the particle size distribution included coarse particles with diameters between 1-10 µm, which were not seen on stages 4 to stage 6 (Figure 4.5, B to H), where the particle size distributions were in the finer size range.

Using the data from Figure 4.5, the geometric diameter characteristics for tobramycin particles were calculated and are summarized in Table 4.2. The particle size distribution of tobramycin is characterized by the D_{50} (geometric median diameter), which is the diameter at which 50% of the sample mass is smaller than this size and 50% is larger. Also, the D_{10} and D_{90} were measured, which represent the diameters of the particles at which 10% and 90% of the sample mass are less than this size. The D_{50} values were < 6 µm and decreased progressively from stage 2 to stage 6, as expected. In addition, the D_{50} values decreased from 30 L/min to 60 L/min, proving that finer particles are collected at a higher flow rate.

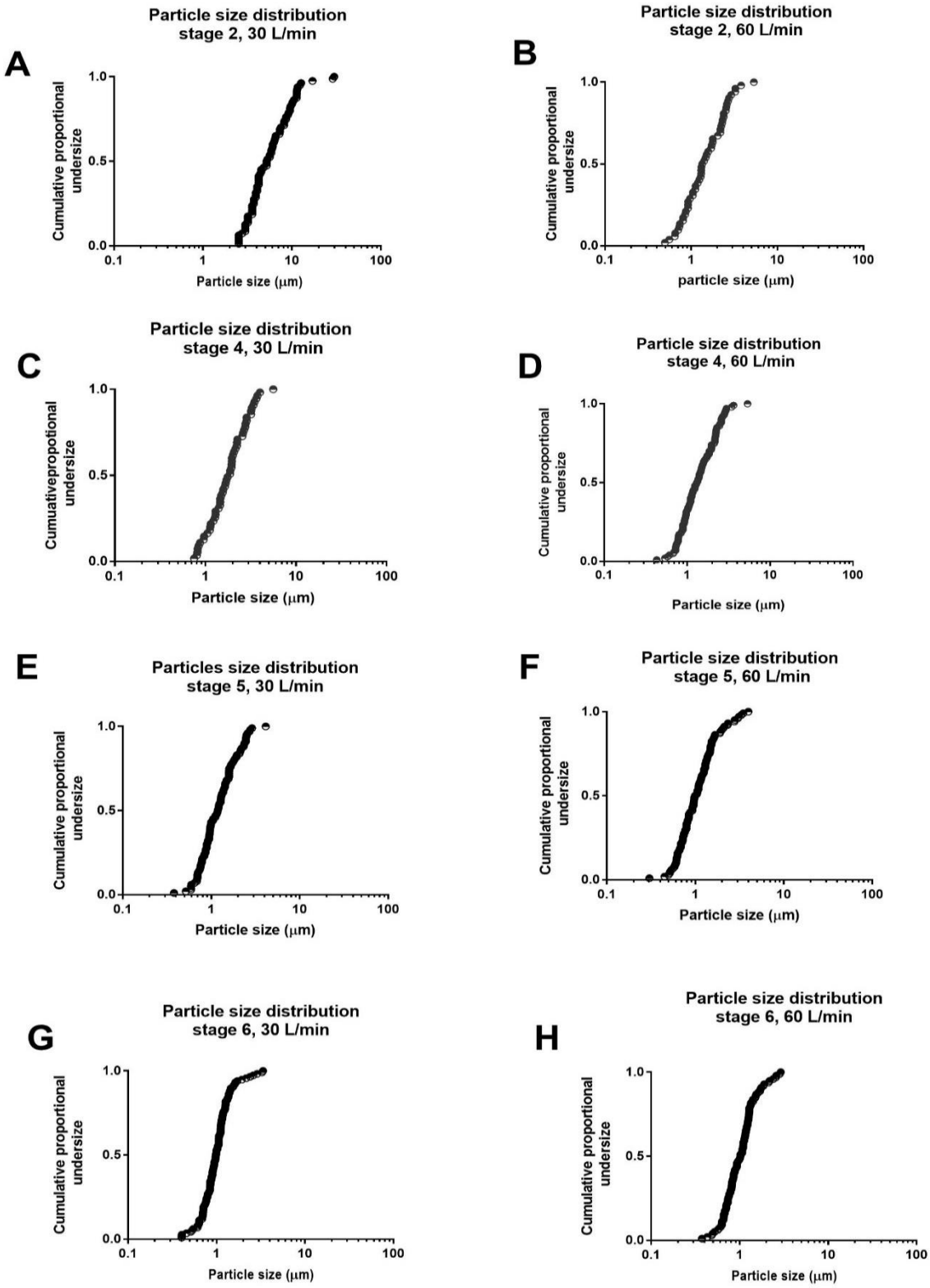

Figure 4.5 Comparison of the cumulative particle size distributions of tobramycin particles from TOBI Podhaler® measured from different stages of the NGI at 30 L/min and 60 L/min respectively. Stage 2 (A-B), stage 4 (C-D), stage 5 (E-F), stage 6 (G-H).

Table 4.2. Comparison of tobramycin particle size distribution from different NGI stages at different flow rates. Geometric diameters are defined as D_{10}, D_{50}, and D_{90}.

	30 L/min			**60 L/min**		
NGI stages	**D_{10} [µm]**	**D_{50} [µm]**	**D_{90} [µm]**	**D_{10} [µm]**	**D_{50} [µm]**	**D_{90} [µm]**
Stage 2	2.73	5.56	11.30	0.696	1.42	2.88
Stage 4	0.93	1.76	3.30	0.712	1.35	2.29
Stage 5	0.65	1.19	2.17	0.55	1.05	1.99
Stage 6	0.59	0.98	1.62	0.58	1.00	1.73

It should be noted that these geometric diameters are not directly comparable with the previously described aerodynamic diameters in Table 4.1, because the measurements are based on a different definition of the diameter of a particle and a different method of particle quantification (number vs mass).

4.2.2 Tobramycin quantification assay

Following the first group of preliminary work, the second set of preparational work was to develop an assay to quantify tobramycin from the NGI. To that purpose, tobramycin quantification was carried out using HPLC-MS. Initial results (Figure 4.6) revealed a poor linear relationship with the correlation coefficient of $r^2 = 0.8732$. Other non-linear regressions (data not shown) were also applied, however, these had not improved the correlation coefficient and internal standard was required to improve precision of our data.

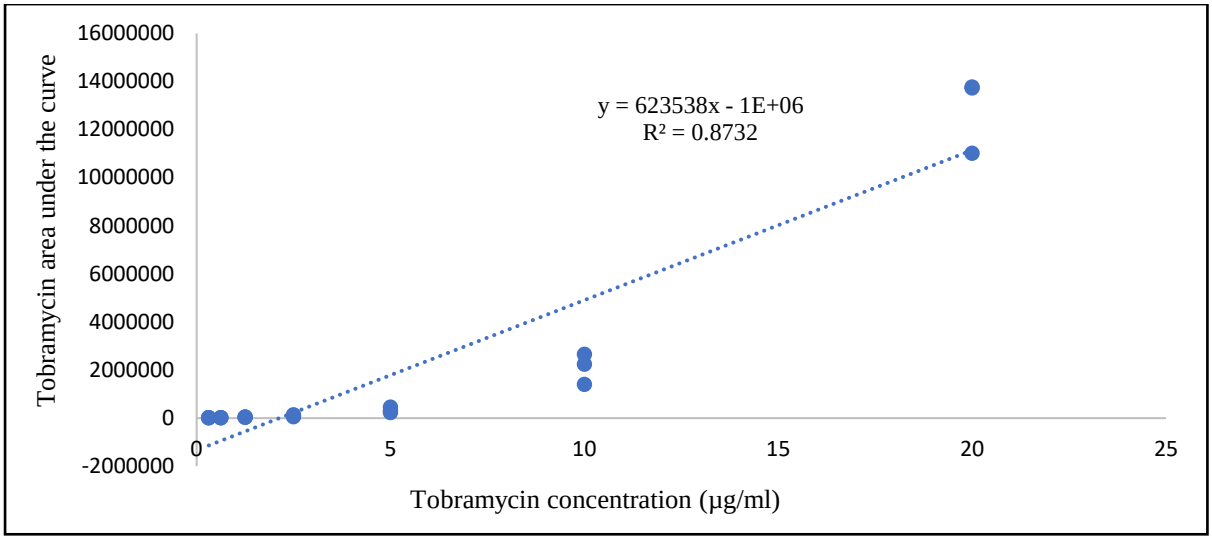

Figure 4.6 Tobramycin calibration curve. Area under the curve of tobramycin versus concentration of tobramycin.

The internal standard is a substance that should have the same signals as the analyte, but should be distinguishable from the analyte, which means the internal standard should have similar structural and chemical properties as the analyte (Blanchaert et al., 2017). Accordingly, the internal standard that was chosen to tobramycin (Figure 4.7, A) is kanamycin (Figure 4.7, B) because it has similar structure to tobramycin.

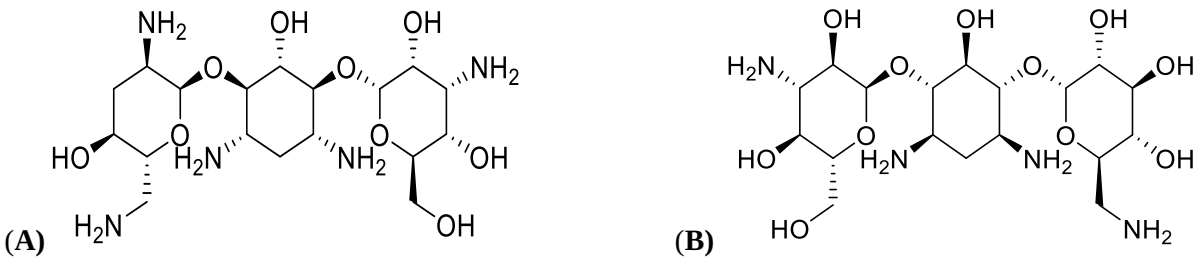

Figure 4.7 Chemical structure of tobramycin (A) and kanamycin, internal standard, (B).

Tobramycin calibration curve following the addition of kanamycin as an internal standard is depicted below (Figure 4.8). A good linear relationship between the area ratio of tobramycin-kanamycin and corresponding concentrations was determined. As can be seen from the curve, the correlation coefficient of $r^2 = 0.998$ improved significantly as compared to the previously obtained (Figure 4.6). Therefore, it was decided to keep adding the internal standard in all our

HPLC-MS quantification assays. For the next following sections, this assay was used to quantify tobramycin from the NGI.

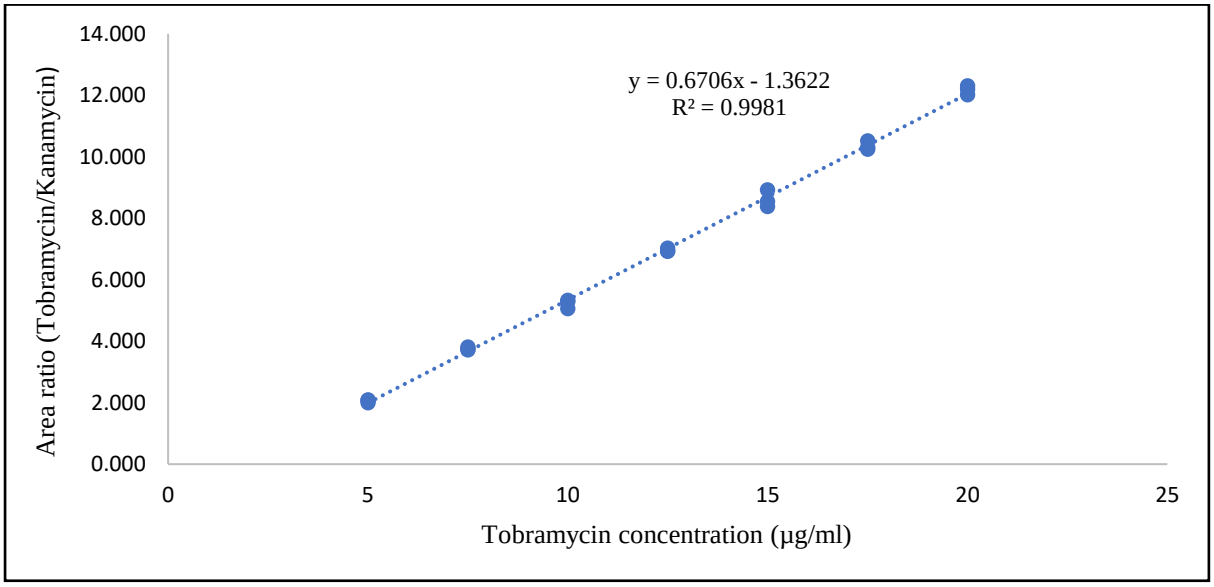

Figure 4.8 Tobramycin calibration curve. Area ratio between tobramycin to kanamycin (internal standard) vs concentration of tobramycin.

4.2.3 Tobramycin particle size distribution in terms of aerodynamic diameter

After establishing an HPLC-MS assay in the previously described section, our aim here was to use this assay to determine the particle size distribution of the aerosol emitted from the TOBI Podhaler® at 30 L/min and at 60 L/min flow rates. This was achieved using the NGI, and so was expressed in terms of aerodynamic diameter as a function of tobramycin mass (in contrast to the SEM analysis described above). In this regard, a tobramycin capsule for each experiment was aerosolised through the NGI for 10 seconds, which was chosen as it is sufficient for complete dispersion of the powder from the capsule. The results are displayed in Figure 4.9 A and B, which show tobramycin aerodynamic particle size distribution profiles from the NGI in terms of mass. These aerodynamic diameters are previously calculated by Marple et.al (2003) as outlined in Table 4.1. The data revealed that at 30 L/min (Figure 4.9, A), tobramycin particle size distribution was mostly between 6.4-0.83 µm with less mass deposited on the other stages. At 60 L/min (Figure 4.9, B), tobramycin particle size distribution was between 4.46-0.55 µm

with lower masses deposited on the other stages. These data were used to determine the tobramycin dose, collection stage at the tested flow rates in subsequent experiments.

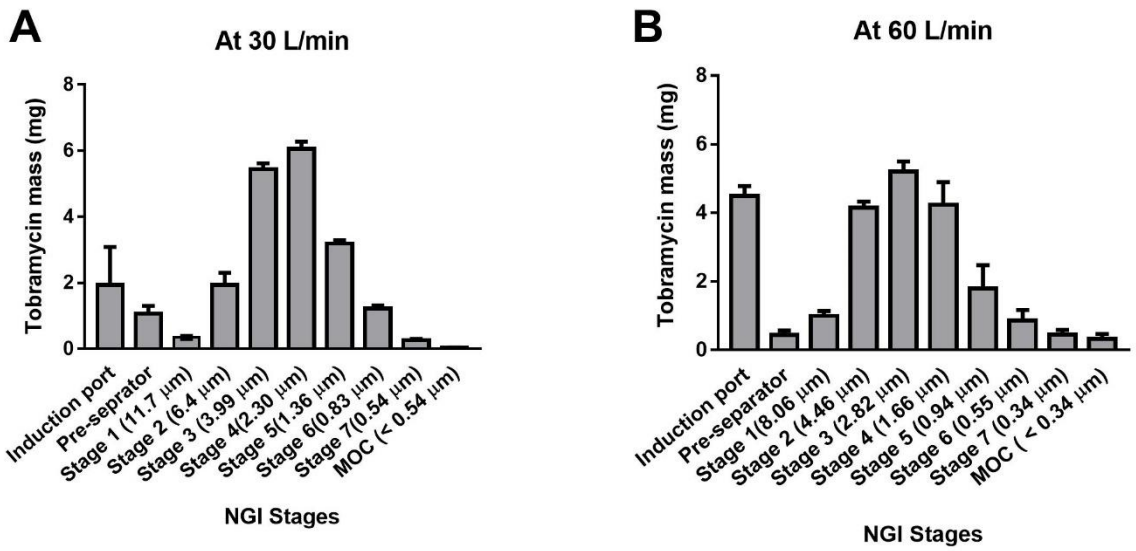

Figure 4.9 Aerosol particle size distribution of tobramycin powder from TOBI Podhaler® device following aerosolization into the NGI at different flow rates. At 30 L/min **(A)** and at 60 L/min **(B)**. The NGI was operated for 10 seconds, and one capsule of 28 mg/test was aerosolized for each flow rates. Error bars represent the standard error of the mean from five independent experiments for each flow rate. Stages 1-7 indicate the impactor stages, followed by their corresponding lower aerodynamic diameter in parentheses. MOC: micro-orifice collector.

4.2.4 Tobramycin collection and mass measurements from the NGI

In the same way as above, HPLC-MS assay was used also in this section to quantify tobramycin mass that was deposited in the NGI. Tobramycin mass measurements were performed to identify the masses of different sized tobramycin particles. To that purpose, the NGI was operated as previously outlined in the Materials and Methods chapter (Section 2.8.5 and 2.8.6) with minor modification, in which commercially available TOBI 28 mg tobramycin capsules were replaced with manually filled capsules with tobramycin powder extracted from TOBI Podhaler® capsules. This was because the high dose contained in the commercially available product resulted in a high mass collected on the filter. This was difficult to collect because it resulted in damage of the filters. Tobramycin was collected from the NGI using the aerosol

collection apparatus, because of the advantages that are offered by this system as described in section 4.1.

4.2.4.1 Tobramycin mass deposited in the single aerosol collection apparatus mounted on stage 2

In this section, our initial aim was to determine tobramycin capsule filling dose, which resulted in the collection of similar tobramycin masses on filter in single aerosol apparatus (Figure 4.10) at stage 2 of the NGI at different flow rates (i.e. with different particle sizes). To that purpose, the initial manually filled dose of tobramycin was 2.5 mg to be aerosolized at 60 L/min. This filling dose was chosen after testing several filling doses through a trial and error process. The second step was to find a new filling dose to be fired at a flow rate of 30 L/min, which resulted in the collection of the same mass as that was obtained from aerosolizing 2.5 mg tobramycin at 60 L/min at stage 2. The results (Figure 4.11) revealed that loaded tobramycin capsules with 4.4 mg at 30 L/min and 2.5 mg at 60 L/min, resulted respectively in collection a mean mass of 0.993 mg for particles < 11.7 µm and a mean mass of 0.96 mg for particles < 8.06 µm, the difference between the collected masses was about 3.4% ($p > 0.05$).

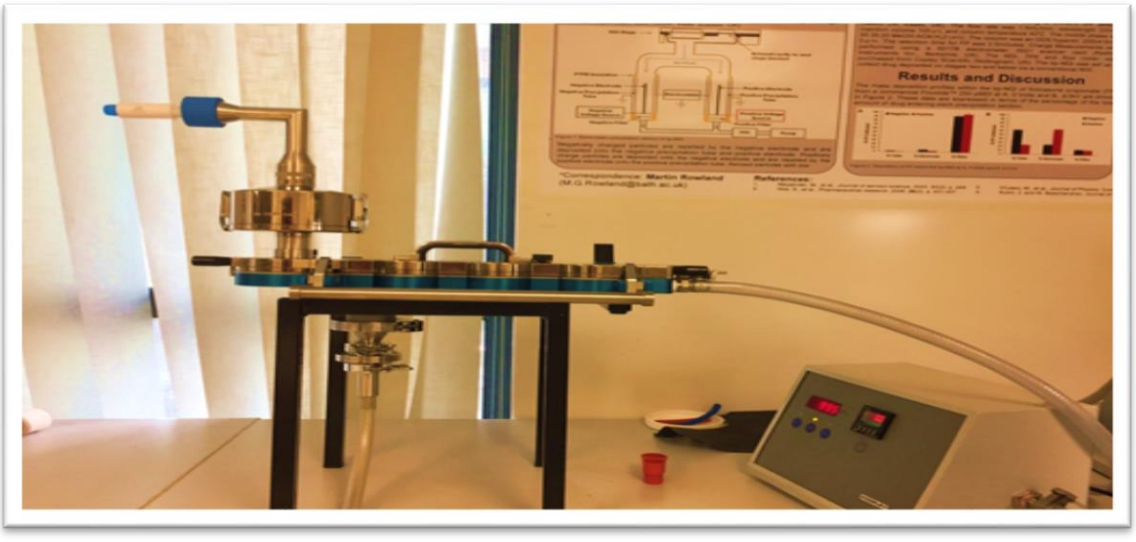

Figure 4.10. The whole NGI with the single aerosol collection apparatus connected down to the NGI. (unpublished image).

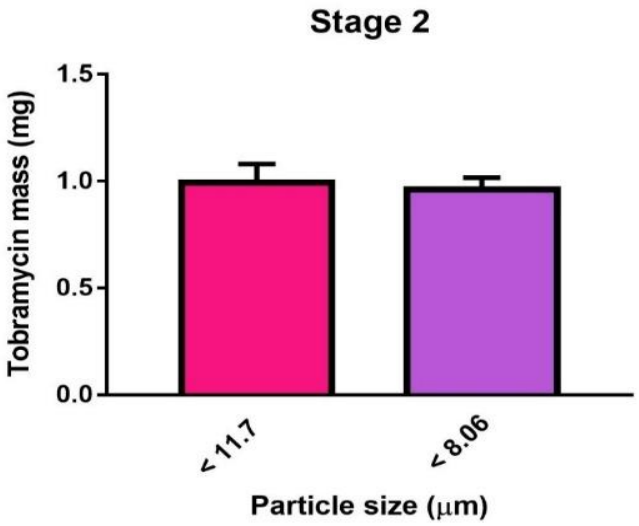

Figure 4.11 Comparison of tobramycin masses with different particle sizes deposited on the filter in the single aerosol collection apparatus mounted on stage 2 of the NGI. The NGI was operated for 10 seconds, and tobramycin capsules of 4.4 mg and 2.5 mg were fired at 30 and 60 L/min respectively. Error bars represent the standard error of the mean from ten independent experiment. Statistical significance was analysed using unpaired 2-tailed *t* test ($p > 0.05$). Full details of the statistical analysis are shown in appendix 1.

For the following sections, the double aerosol collection apparatus (Figure 4.12) replaced the single aerosol collection device. This is because the latter did not work properly at a high flow rate of 60 L/min, when filters from different manufacturers were used. Such filters were damaged and made the collection of tobramycin particles impossible. Accordingly, using the double aerosol apparatus resulted in the dividing the airflow and decreasing the pressure on the filters, because it consists of two filters for particles collection. These two filters within this apparatus collect two equal masses simultaneously, which meant that half the amount of tobramycin collected on the filter of the single aerosol collection apparatus (Figure 4.10) was collected on each of the two filters of the double aerosol collection apparatus.

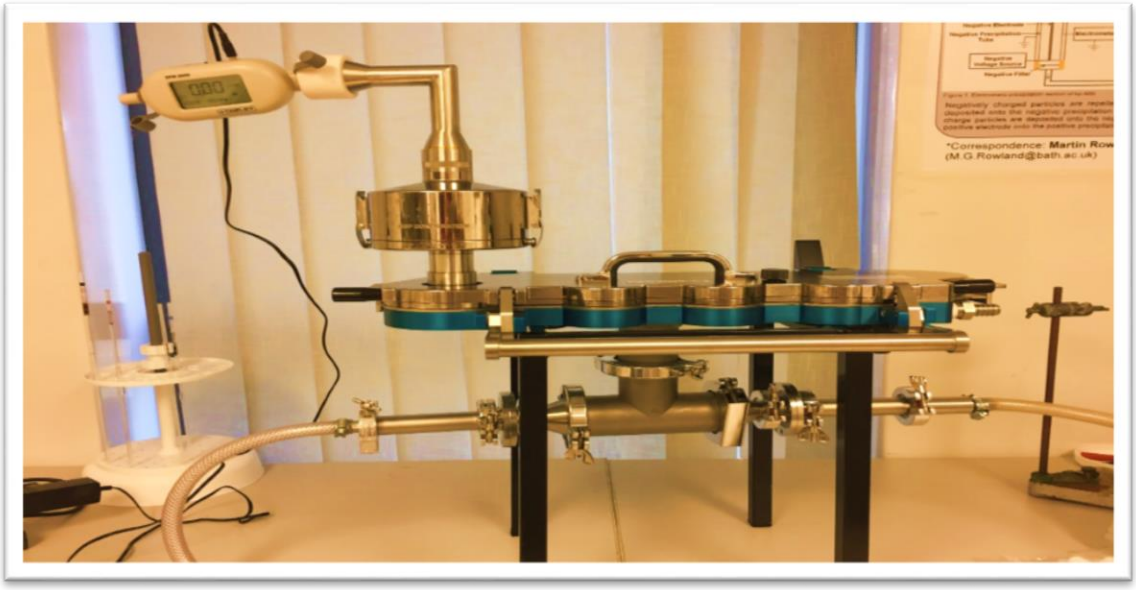

Figure 4.12. NGI incorporated with a double aerosol collection apparatus down to the NGI. (unpublished image)

4.2.4.2 Tobramycin masses deposited on double aerosol collection apparatus

In the previous section, the determined filling doses of tobramycin successfully resulted in the collection of approximately equal masses of tobramycin with different particle sizes on single aerosol collection apparatus mounted on stage 2. Next, our aim was to determine if these tobramycin filling doses are also applicable to the other NGI stages, and in particular when the double aerosol collection apparatus was used. Because this aerosol collection apparatus has two sites with filters (F1, F2) to collect particles, it was important to confirm that both sites collect the same mass. Therefore, this device was mounted individually from stage 2 to stage 6 of the NGI and the manually loaded 4.4 mg and 2.5 mg tobramycin capsules/experiment were aerosolised through the NGI at 30 L/min and at 60 L/min respectively. The data revealed (Figure 4.13, A-H) that at stages from 2 to 6, similar tobramycin masses were collected on both sites at the tested flow rates.

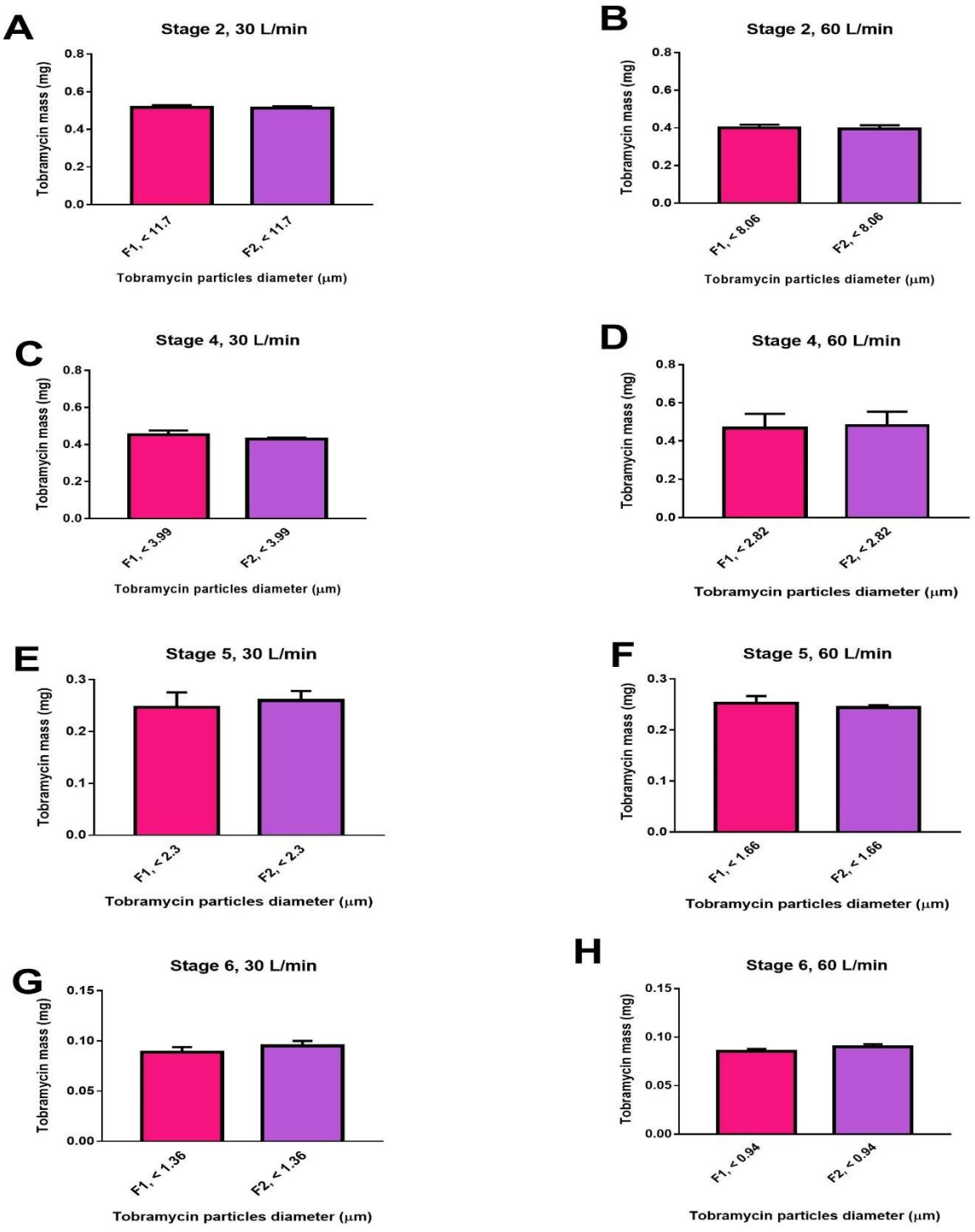

Figure 4.13. Comparison of tobramycin masses deposited on the filters in the double aerosol collection apparatus were housed on multiple stages of the NGI at (30 and 60) L/min respectively. Stage 2 (A-B), stage 4 (C-D), stage 5 (E-F), and stage 6 (G-H). NGI was operated for 10 seconds and tobramycin capsules of 4.4 mg and 2.5 mg were fired at 30 and 60 L/min respectively. F1, F2 are representing the filters that collect different sized tobramycin particles on double aerosol collection apparatus. Error bars represent standard error of the mean from four independent experiments for each stage and every filter. Statistical significance was analysed using unpaired 2-tailed *t* test ($p > 0.05$). Full details of the statistical analysis are shown in appendix1.

4.2.4.3 Tobramycin masses deposited on double aerosol collection apparatus mounted on stage 2 and stage 4

In the earlier work, tobramycin filling doses and approximately equal masses were measured on the double aerosol collection apparatus that was mounted on the same stages at different flow rates and particle sizes. In this section, our aim was to determine filling doses of tobramycin capsules that enable the collection of similar masses of differently sized particles, using double aerosol collection apparatus mounted on different stages and at different flow rates. In this context, numerous trials and errors were made to establish the filling doses for tobramycin capsule that allowed us to collect the same mass of tobramycin on the aerosol collection apparatus mounted firstly on stages 2 at 30 L/min and secondly on stage 4 at 60 L/min, in order to collect particles < 11.7 µm and < 2.82 µm respectively. The results suggested (Figure 4.14) that filling tobramycin capsules with 4.4 mg and 4.3 mg to be aerosolised at 30 L/min, stage 2 and at 60 L/min, stage 4, respectively, resulted in the collection a mean mass of 0.513 mg for particles < 11.7 µm and a mean mass of 0.476 mg for particles < 2.82 µm and the difference between masses was about 7.8% (p> 0.05).

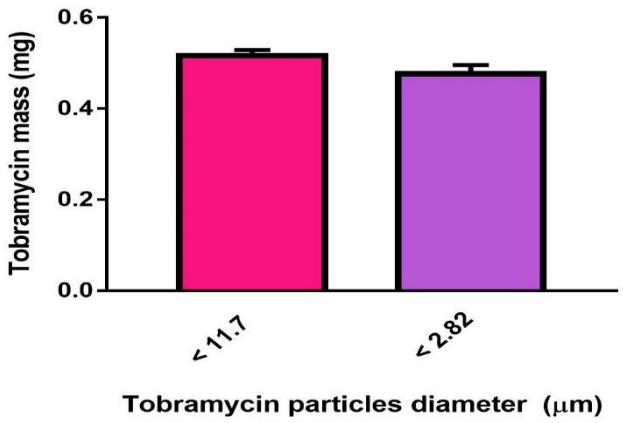

Figure 4.14. Comparison of tobramycin masses with different particle sizes deposited on the filters in the double aerosol collection apparatus. Pink bar: tobramycin particles < 11.7 µm that were collected from stage 2 at 30 L/min. Purple bar: tobramycin particles < 2.82 µm that were collected from stage 4 at 60 L/min. Error bars represent standard error of the mean from ten independent experiments. Statistical significance was analysed using unpaired 2-tailed *t* test (p> 0.05). Full details of the statistical analysis are shown in appendix 1.

4.2.5 The influence of differently sized tobramycin particles against *P. aeruginosa* biofilms

In the previous sections, equal masses of tobramycin with different particle sizes were collected from the NGI. The next step in this section was to investigate the effect of small and large micron-sized tobramycin particles against *P. aeruginosa* biofilms. This is because drug particle size influences the physical properties of a drug such as the dissolution rate (Shekunov et al., 2007; Wang et al., 2017). It is generally recognized that dissolution rate of small-sized particles can be significantly better than the large-sized particles, which is attributed to the larger surface area of the small particles (Watts and Williams, 2011; Riley et al., 2012; van der Wiel et al., 2017; Tay et al., 2018). Therefore, we aimed to test the influence of such different tobramycin particle sizes against bacterial biofilm. Notably, due to technical issues and the trial and error process described above, the influence of differently sized particles was initiated by studying tobramycin particles with a small difference in size range, which was then followed with the comparison of particles with a large difference in size.

4.2.5.1 The influence of tobramycin particles < 11.7 µm and < 8.06 µm against *P. aeruginosa* biofilms

In this section, our aim was to evaluate the activity of small and large micron-sized tobramycin particles against *P. aeruginosa* biofilms. To that end, the colony biofilm assay was used to grow biofilms of *P. aeruginosa* strains as outlined in the Material and Methods chapter (Section 2.6.2), in which these strains were grown for 48 h in ASM medium by inoculation of 100 µl of bacterial culture into polycarbonate membranes. Next, the biofilms were treated with 0.99 mg/filter tobramycin of different particle sizes (< 11.7 µm and < 8.06 µm), This was followed by incubation for 24 h at 37°C. Then the viable count was measured as described in the Materials and Methods chapter (Section 2.6.2). The results (Figure. 4.15, A to C) revealed that in all tested clinical isolates, there was a trend for smaller micron-sized tobramycin particles being more effective than larger micron-sized particles against *P. aeruginosa* biofilms, albeit the difference was statistically not significant (p= 0.36, 0.83, and 0.45 in Figure 4.15 A-C, respectively). Only for the lab strain PAO1 (Figure 4.15, D, p=.97), this trend was not observed.

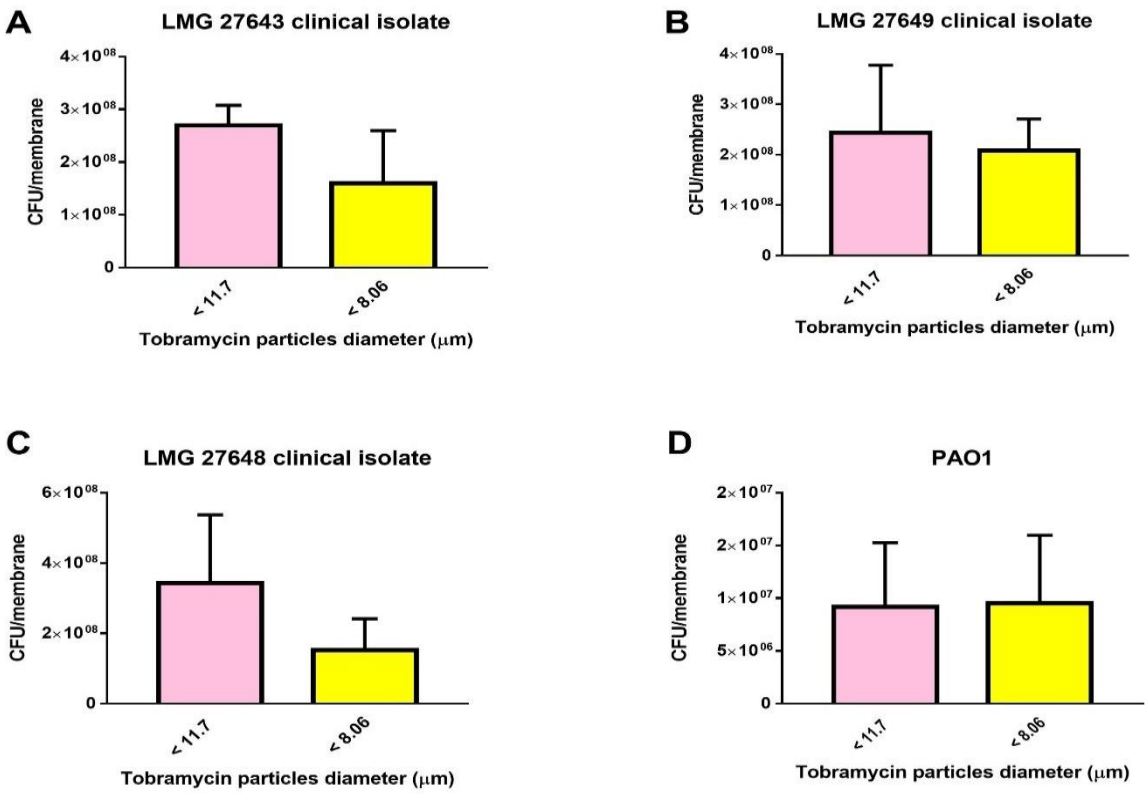

Figure 4.15. The influence of differently sized tobramycin particle on the eradication of *P. aeruginosa* biofilms. (A-C) show clinical isolates, (D) indicates a lab strain PAO1. Bacterial cells were grown in ASM as colony biofilms for 48 h at 37°C and then were treated with different tobramycin particle sizes (< 11.7 µm and < 8.06 µm) for 24 h. The data shown represent the standard error of the mean from three biological repeats and each biological repeat consisted of at least two technical repeats. Statistical significance was analysed using unpaired 2-tailed *t* test. Full details of the statistical analysis are shown in appendix 1.

4.2.5.2 The influence of tobramycin particles < 11.7 µm and < 2.82 µm against *P. aeruginosa* biofilms

In the section above, the influence of a small difference in particle size range was evaluated against *P. aeruginosa.* Here, the influence of a wide difference in particle size range was investigated. This was technically more challenging to achieve involving a lot of trial and error, as it was difficult to get an equal mass of particles with a significant different particle size. However, it was hoped that the difference observed would be more pronounced with a larger difference in particle sizes and with smaller doses than that were used in section 4.2.5.1. In this respect, *P. aeruginosa* biofilms were grown as mentioned earlier with the addition of the

controls, that were used as a baseline, but was not included in the statistical evaluations. The biofilms were challenged with a dose of 0.5 mg/filter tobramycin of different tobramycin particle size (< 11.7 µm and < 2.82 µm). In the same way, filters without tobramycin were placed on each control. Afterward, the biofilms were incubated for 24 h and the viable count was determined. The results revealed (Figure 4.16, A- D) that the trend of better activity with smaller particles, which was observed in section 4.2.5.1 disappeared and no distinct difference was noticed between small and large tobramycin particles. As mentioned earlier, the difference is with the previous experiments is, however, that in this case the total mass of tobramycin used was about half as compared to the experiments in section 4.2.5.1.

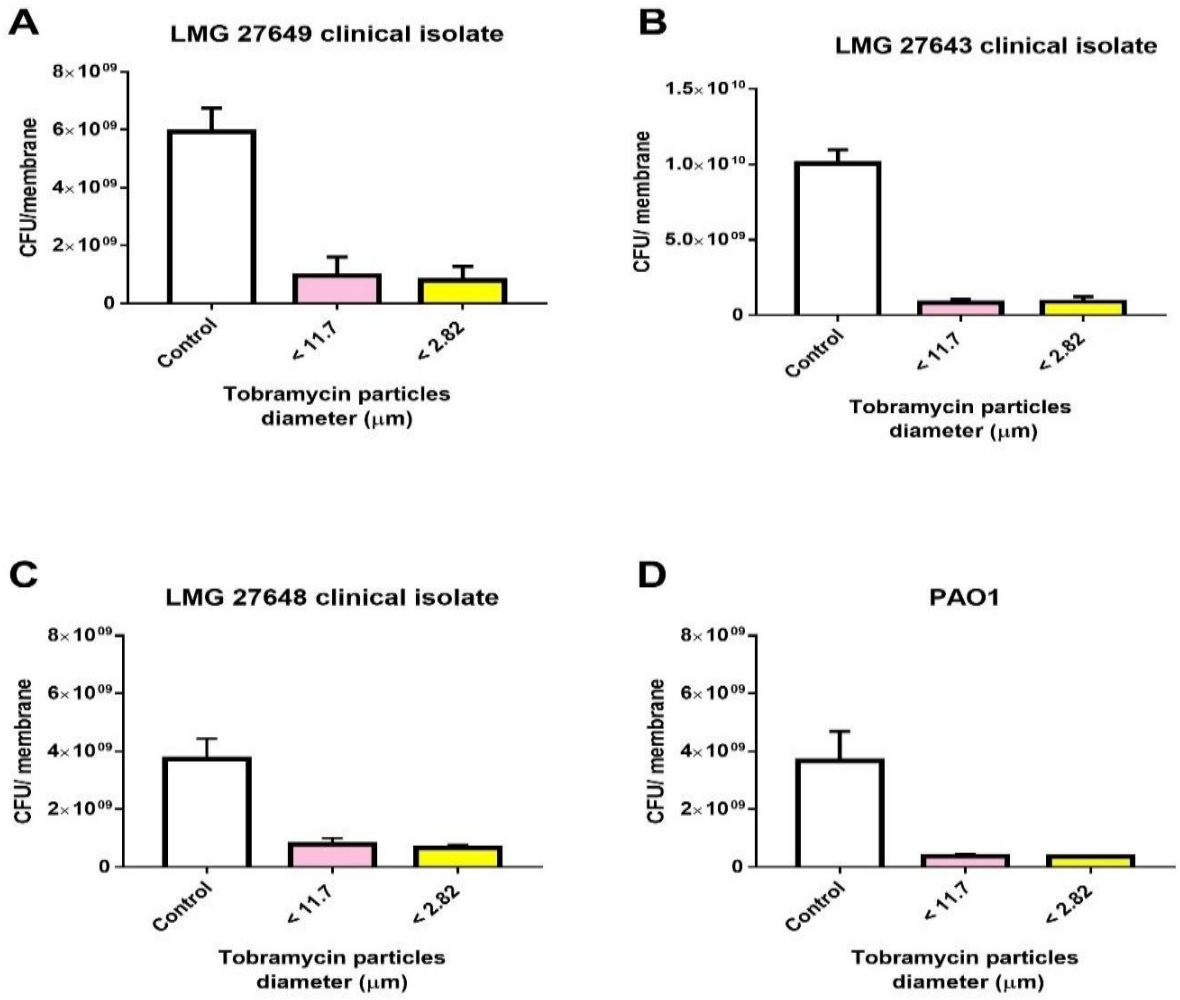

Figure 4.16. The influence of differently sized tobramycin particles on the eradication of *P. aeruginosa* biofilms. (A-C) show clinical isolates, (D) indicates a lab strain PAO1. Bacterial cells were grown in ASM as colony biofilms for 48 h at 37°C and then were treated with different tobramycin particle sizes (< 11.7 µm and < 2.82 µm) for 24 h. The data shown represent the standard error of the mean from three biological repeats and each biological repeat consisted of at least two technical repeats. Statistical significance was analysed using unpaired 2-tailed *t* test. Full details of the statistical analysis are shown in appendix 1.

The rate of dissolution for drug particles is a kinetic and time-dependent process (Watts and Williams, 2011). Therefore, these results directed us to investigate the effect of particle size at various incubation times. In the CF lung, it has been reported that almost 2-3 h following tobramycin inhalation treatment, about 90% of tobramycin concentration is cleared out lung (Schulz and Schmoldt, 2003; Garo et al., 2007) and others have reported that the elimination of tobramycin is variable ranging from 1.5 h to 13 h (Geller et al., 2002). Therefore, we selected to test the activity of tobramycin particles at different physiological relevant incubation times. The results suggested that at t = 3 h, smaller tobramycin particles < 2.82 µm resulted in better efficacy by 20% reduction in viable count with a statistically significant difference as compared to larger particles < 11.7 µm in the two clinical isolates (Figure 4.17, A and B). In comparison, for the other strains (Figure 4.19, C and D) the trend toward smaller sized particles being more effective than the larger counterparts was still present but it was statistically not significant.

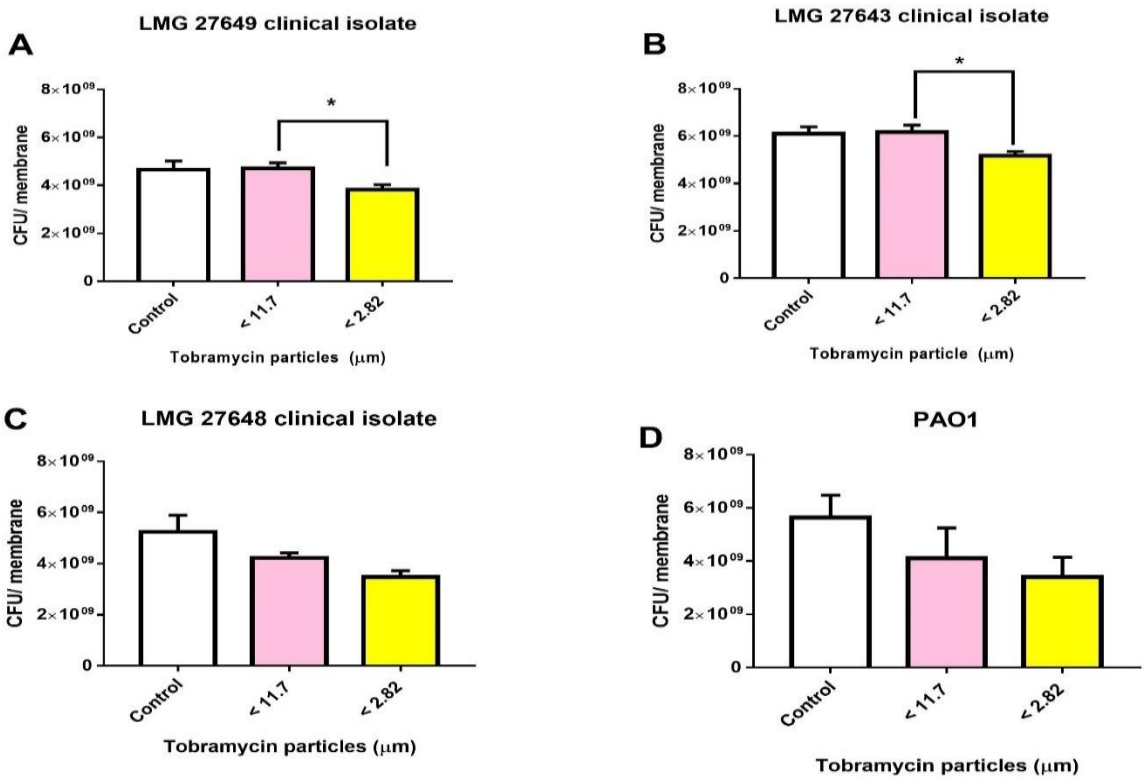

Figure 4.17. The influence of differently size tobramycin particle on the eradication of *P. aeruginosa* biofilms. (A-C) show clinical isolate, (D) indicates a lab strain PAO1. Bacterial cells were grown in ASM as colony biofilms for 48 h at 37°C and then were treated with different tobramycin particle sizes (< 11.7 µm and < 2.82 µm) for 3 h. The data shown represent the standard error of the mean from three biological repeats and each biological repeat consisted of at least two technical repeats. Statistics were analysed using unpaired 2-tailed *t* test. Statistically significant differences between large and small particles are indicated (*, p<0.05). Full details of the statistical analysis are shown in appendix 1.

As can be deduced from the results above, the effect of particle size seemed to be time and strain dependent. Therefore, these encouraging results were considered for further investigations, in which we had a closer look at the effect of particle size at different incubation times. We selected LMG 27649 clinical isolate for further investigation and as can be seen in Figure 4.18, the data showed that at a shorter incubation time of 1.5 h (Figure 4.18), smaller particles < 2.82 µm resulted in a ~35% reduction in viable count as compared to the larger particles < 11.7 µm. This was the larger difference between differently sized particles as compared to other longer incubation times of 3, 5, 8, and 24 h (Figure 4.18). For instance, the reduction in viable count for smaller particles as compared to larger particles was ~20%, 10%, 20%, at 3, 5, 8 h respectively, with almost no difference at 24 h. Although a statistically significant difference was not achieved at all tested incubation times, however, the trend was reproducible with every repeat.

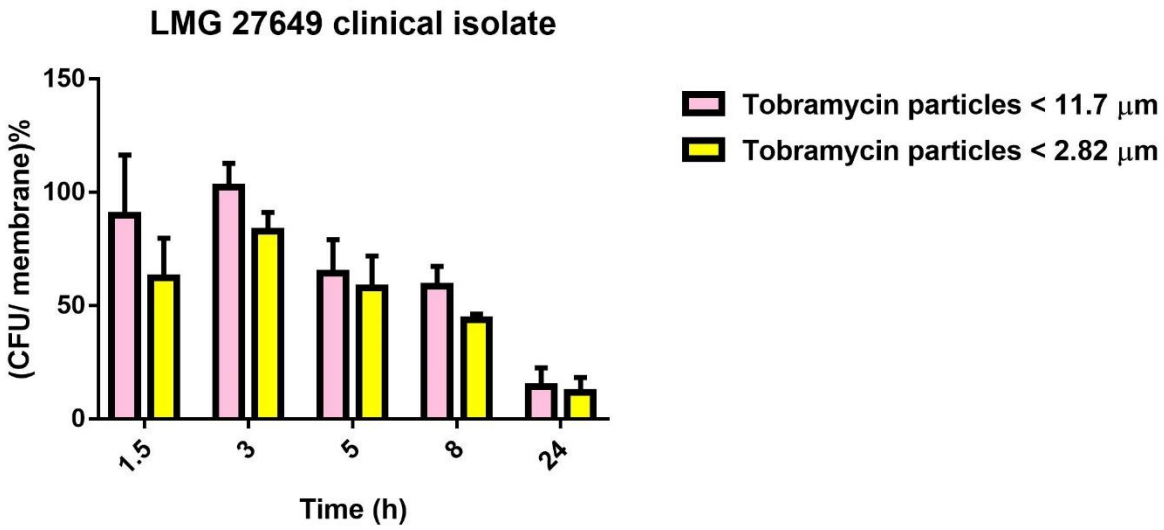

Figure 4.18. The influence of differently sized tobramycin particle on the eradication of LMG 27649 clinical isolate *P. aeruginosa* biofilms. Bacterial cells were grown in ASM as colony biofilms for 48 h at 37°C and then were treated with different tobramycin particle sizes (< 11.7 µm and < 2.82 µm) at several incubation time points (1.5, 3, 5, 8, 24) h. The data shown represent the standard error of the mean from three biological repeats and each biological repeat consisted of at least two technical repeats. The data were normalized relative to controls. Statistical significance was analysed using two-way ANOVA followed by multiple comparison Tukey test. Full details of the statistical analysis are shown in appendix 1.

4.3 Discussion

In this chapter, we studied tobramycin dry powder inhaler and investigated the influence of differently sized tobramycin particles against *P. aeruginosa* biofilms. This work was preceded by multiple preliminary experiments. Firstly, a quantification assay for tobramycin was established and validated. Secondly, the model to fractionate tobramycin into different sizes was developed and optimized. Finally, the influence of these differently sized tobramycin particles was assessed against CF clinical isolates of *P. aeruginosa* biofilms.

Particle size analysis of tobramycin dry powder was performed using two techniques, which were the SEM analysis and the NGI. To begin with SEM analysis, we were able to visualise tobramycin particles and to calculate the geometric diameters of particles. However, this assay is associated with limitations, which are not easy to control or minimize. For instance, the adjacent particles could be measured as one particle. Moreover, errors result from manual measurements, for example, the bias in the selection of particles and measuring of a very small proportion of all the particles in a sample (Shekunov et al., 2007). The other particle sizing techniques in our study was the NGI, which is the most up to date pharmaceutical impactor for aerosol particle size analysis. NGI overcomes the limitations of other impactors such as the Anderson Cascade Impactor (ACI) (Taki et al., 2011). For instance the ACI measurements are limited to a specific flow rate of 28 L/min and less applicable at higher flow rates (Yoshida et al., 2017) that were important in our work to get a variety of particle size ranges. Therefore, we used the NGI, however, it still has some restrictions. For instance, the re-entrainment of particles where particles bounce off the stage and re-enter the air stream and subsequently impact on the following stage (Wang et al., 2017). This limitation was minimized by coating the surface of impactor stages as described in Materials and Methods chapter (Section 2.8.5).

An important drawback for our purposes is that the NGI separates powder into different size fractions with different masses for each fraction. To compare between differently sized particles, it was essential to equalize the masses between each fraction. Using a trial and error process, differently sized but an equal mass of tobramycin particles was collected from the NGI. Consistency between experiments was important here, but initial results were not very

reproducible. This was due to the hygroscopic nature of tobramycin, which can negatively affect its aerosolization. To improve that, all the conditions that could affect tobramycin aerosolization such as humidity, temperature, and capsule types were standardized and adjusted as described in Materials and Methods chapter (Section 2.8.4).

The evaluation of different tobramycin particles was made depending on the NGI stages that were selected. These include stage 2 and stage 4. Stage 2 was chosen because it captures all the particles with a diameter of less than 11.7 µm at 30 L/min and lower than 8.06 µm at 60 L/min. Such a range is known to penetrate and deposit in the lung. Stage 4 was included in the comparison because it collects all the fine particles with a diameter of < 3.99 µm at 30 L/min and < 2.82 µm at 60 L/min. The particles within this range are considered optimal particles the can distribute and penetrate further peripherally to the smaller airways and deposit in the zone where the infection is found (Geller et al., 2011; Buttini et al., 2016). Comparisons were made between particles that were collected from stage 2 and stage 4. This was due to the difficulty in comparing stage 2 with the later stages as there was a large difference in masses. Because of such difference, it was challenging to collect similar amounts of tobramycin from these stages as compared to the mass that was collected from stage 2.

The influence of differently sized tobramycin particles was determined against *P. aeruginosa* biofilms. For *P. aeruginosa*, to be inhibited with tobramycin particles, these must firstly dissolve in order to exert their pharmacological activity and the dissolution process depends on particle size and time (Wang et al., 2016). Accordingly, the influence of tobramycin particles was investigated by testing differently sized particles combined with various incubation times from 1.5 h to 24 h. For instance, it was observed that at short incubation time, there was a trend for small particles of < 2.82 µm were being more effective by a 20% as compared to large particles < 11.7 µm, with a significant difference being found at t = 3 h in LMG 27649 and LMG 27643 clinical isolates. However, at longer incubation time of t = 24 h, the activity of small and large tobramycin particles in inhibition biofilms did not show any pronounced difference. One plausible explanation for the observed results could be related to the properties of tobramycin particles. For instance, small size particles are known to have a faster dissolution rate than the larger size counterparts because of a relatively larger surface area of the small particles. Indeed, the dissolution is a kinetic and time-associated process (Watts and Williams,

2011), accordingly, this could explain the difference in inhibitory activity between the tested particles at shorter versus longer incubation times. The effects were not seen in all *P. aeruginosa* strains, which might be because the tested strains are phenotypically and genetically different. That, in turn, could result in the formation of heterogeneous biofilms (e.g. compositions and thickness) (Wimpenny et al., 2000), which consequently could lead to different responses. For example, the studied clinical isolates but not PAO1 are known to be alginate producers. Another difference that was observed with the clinical isolate LMG 27649 (but not other strains), this strain was unable to grow unless casamino acids were added to the MOPS growth medium (data not shown), which suggests that the LMG 27649 is auxotrophic. The other strains were able to grow without casamino acids and this indicates that they are prototrophic strains. Whether this would influence the effects of tobramycin particles is not known, but it does clearly show that the strains differ from each other. Overall the observed influences of small tobramycin particles are most likely related to the faster dissolution rate of these particles as compared to the larger counterparts, in which the dissolution rate appeared to be a rate-limiting step at only short incubation time. Interestingly and similar to our work, the influence of differently sized particles of other drugs were evaluated, in which the results from these studies indicated better efficacy for smaller sized particles as compared to the larger counterparts (Shah et al., 1997; Jinno et al., 2006; Leach et al., 2009; Liu et al., 2015). One of these drugs is cilostazol, which is an oral vasodilator. Smaller cilostazol particles of 2.4 µm had shown better dissolution rate and efficacy than the larger particles of 13 µm (Jinno et al., 2006). Another drug is inhaled solution of dornase alfa, which is a mucolytic agent used in CF patients to decrease the viscosity of sputum. This drug was more effective, when it was administered as small particles of 3.42 µm as compared to particles 6.87 µm (Shah et al., 1997). In the same way, inhaled beclomethasone corticosteroid solution was more effective in particle size of 1.1 µm as compared to 4 µm (Vanden Burgt et al., 2000; Van Schayck and Donnell, 2004; Leach et al., 2009).

In our work, it was important to develop an assay to quantify tobramycin from the NGI. We initially used a conventional bioassay, which is a microbiological technique in which tobramycin was dissolved and deposited on a 6 mm paper disc, followed by a disc diffusion assay using a sensitive strain. However, it was difficult to achieve a reproducible relationship with an appropriate correlation coefficient even by applying a different type of regressions such as linear, polynomial, and exponential regression (data not shown). Moreover, this assay has

several restrictions. For example, it is sensitive to parameters such as the thickness of the agar plates, the concentration of inoculums, and the conditions of incubations (Dafale et al., 2016). Thereby, it was not feasible to continue with this assay. The HPLC-MS assay was developed and optimised for the determination of tobramycin. Due to the hydrophilic and polar properties of tobramycin, several columns and mobile phases were evaluated during HPLC-MS methodology development. The final chromatographic conditions were outlined in the Materials and Methods chapter (Section 2.8.3). We were able to establish a quantification assay, but this was required optimization. For instance, for tobramycin standard curve, multiple trials were made to improve the correlation coefficient of the curves. These were including trying several concentration ranges, in which we experienced difficulties with including small concentrations within the standard curve. Also, we tried to prepare these concentrations by serial dilutions to decrease errors. However, these steps were not able to improve the poor correlation coefficient. Therefore, the internal standard was included, which significantly improved the results. Finally, our HPLC-MS assay was successfully applied to quantify tobramycin content that was extracted from the NGI.

We should acknowledge that our study has a number of limitations. Firstly, the slight differences of <10% in the tobramycin masses that were collected for small and large sized particles from different stages/flow rates, however, such difference was statistically not significant (p> 0.05). In addition, in our work we know the maximum particle size that we collected on the filters, but we could not control the minimum particle size. So, although the average particle sizes were different, they could have been more different from each other if we had been able to control the minimum particle size as well. Our hypothesis was only tested for one dry powder inhaler antibiotic, tobramycin, and it will be of interest to test this with other antibiotics particularly those with less solubility than tobramycin, in which the dissolution rate could be a rate-limiting step and a more pronounced effect for small particles might be found. Furthermore, our system had used the *in vitro* colony biofilm model (Merritt et al., 2005) that possibly simulates lung *in vivo* conditions, in which such model allows biofilm to be grown at an air-interface and enables dry powder antibiotic to be deposited on those biofilm. However, in the future more advanced models should be used that better mimic the *in vivo* lung pathological conditions such as the *ex vivo* model (Harrison and Diggle, 2016) or the *in vivo* models (Kukavica-Ibrulj and Levesque, 2008). Finally, more molecular or genetic studies are required to better understand the difference in behavior between bacterial strains. This could

be due to levels of alginate production, but we have not demonstrated that directly and other factors may be involved.

4.4 Conclusion

Inhaled antibiotics are the fundamental treatment of care for CF patients with *P. aeruginosa* lung infections. Tobramycin dry powder inhaler is one of the most widely used inhaled antibiotics in the treatment of CF lung infections. In this chapter, the influence of tobramycin dry powder inhaler in terms of particle size was investigated against *P. aeruginosa* biofilm. Small micron-sized tobramycin particles (< 2.82 µm) showed better efficacy by a 20% reduction in the viable count as compared to larger particles (< 11.7 µm) at shorter incubation times (3 h) against *P. aeruginosa* biofilms of LMG 27649 and LMG 27643. This short incubation time is clinically important, in which tobramycin is cleared from the lung at a short time ~ 2-3 h. These initial findings highlight that particle size can affect tobramycin dry powder inhaler antibiofilm activity, however, more *in vitro* and *in vivo* research are still required. Finally, these findings could be more significant with less soluble antibiotics than tobramycin.

Chapter 5: Results section III

Evaluation Tobramycin Combinations with Non-antibiotic Drugs Against *P. aeruginosa* biofilms

5.1 Introduction

Nowadays, antimicrobial resistance is becoming a significant health hazard at the global level (Silver, 2016; Wright, 2016; Momin et al., 2018; Miró-Canturri et al., 2019). The British government and the Wellcome Trust have predicted that there will be many deaths by 2050 following the rapid dissemination of multi-drug resistant pathogens (Nikaido and Pagès, 2012; Miró-Canturri et al., 2019). For instance, a report from northern Europe has stated that almost 60% of *P. aeruginosa* isolates from cystic fibrosis patients were found to be multi-drug resistant (Tunney et al., 2018). Such resistance was found most commonly against penicillin, cephalosporins, and aminoglycosides (Tunney et al., 2018; Oliva et al., 2019). Aminoglycoside antibiotics such as tobramycin have been effectively used in the treatment of this pathogen (Hentzer et al., 2002; Ratjen et al., 2009; She et al., 2018; Oliva et al., 2019). However, the emergence of *P. aeruginosa* resistance towards tobramycin has been increasingly documented (Field et al., 2005; Herrmann et al., 2010; Roberts et al., 2015; Wright, 2016; Fong et al., 2018). This recalcitrance is attributed to several types of resistance mechanisms (Detailed explanation discussed in Chapter 1, Section 1.4), which are intrinsic, phenotypic, and acquired (Taylor et al., 2014; Wright, 2016).

P. aeruginosa is known to have several intrinsic resistance mechanisms such as low permeability across the outer membrane. This restricted permeability for instance could act as a major barrier that reduces the penetration of several antibiotic agents (Taylor et al., 2014). Such limited permeability is a significant resistance mechanism in *P. aeruginosa* toward aminoglycoside antibiotics (Whiteley et al., 2001). Another intrinsic mechanism is the abundance of efflux pump systems (Breidenstein et al., 2011). For example, twelve resistance nodulation division (RND) efflux pumps are described in *P. aeruginosa* (Diggle and Whiteley, 2019). Among them, it has been found that overexpression of multidrug efflux pump termed MexXY-OprM, results in *P. aeruginosa* resistance to aminoglycoside such as tobramycin (Hoiby et al., 2010a). Moreover, the resistance of *P. aeruginosa* to aminoglycosides results from aminoglycoside modifying-enzymes such as acetyltransferases and phosphoryl transferases (Beceiro et al., 2013).

In addition to the intrinsic mechanisms, another type is called phenotypic tolerance, which also has an important role in *P. aeruginosa* tolerance to antibiotic therapies (Fernández et al., 2011). The phenotypic tolerance is mainly stimulated by triggering factors and particular conditions such as antibiotics at sub-minimum inhibitory concentrations (Sub-MICs), nutrient and oxygen depletion, and importantly the biofilm mode of growth (Taylor et al., 2014). The phenotypic tolerance due to biofilm behaviour is clinically important (Hill et al., 2005; Wright, 2016) and it is attributed to several factors. These include the presence of dormant cells inside a biofilm (Zenga et al., 2012; Maiden et al., 2018). Such populations are known to be very tolerant to antibiotics, especially anti-microbial agents that mostly act on rapidly dividing cells (Fong et al., 2018). Another factor that also contributes to biofilm tolerance is the extracellular polymeric substance (EPS) matrix that surrounds cells in a biofilm (Haagensen et al., 2007; Rybtke et al., 2011; Liu et al., 2017). Such a matrix may act as a barrier that decreases the penetration of antibiotics such as aminoglycosides and polymyxins (Fong et al., 2018). This reduced penetration most probably results from the electrostatic interactions between the EPS and drug molecules (Al-Azemi et al., 2011; Liu et al., 2017; Maiden et al., 2018). As it is clear from the discussion above, *P. aeruginosa* is intrinsically and phenotypically tolerant to antibiotics. Therefore, with the restricted pharmacological options that are available for treating this pathogen, there is an urgent need to find alternative approaches that can improve the activity of the already available antibiotics (Doern, 2014; Wright, 2016; Umerska et al., 2018). Such an approach could involve using tobramycin in combination therapy (Balke et al., 2006; Imperi et al., 2013; Otto et al., 2019).

Combination antibiotic therapy is one of the promising strategies that currently being tested in the treatment of multi-drug resistant pathogens (Fischbach and Walsh, 2009; Domalaon et al., 2018). This strategy can be used to promote antimicrobial activity, to minimize the emergence of resistance, and to mitigate toxicity owing to the lower doses being used for the combined drugs (Sader et al., 2003; Wright, 2016). Normally, combination therapy takes place by combining two or more antibiotics from different classes, but recently considerable attention has been made towards using combination therapy of antibiotics with drugs referred to as "non-antibiotics" (Wright, 2016; Laudy et al., 2017; Liu et al., 2017; Otto et al., 2019). These drugs are already approved for different indications from treating bacterial infections, but they are found to have antibacterial and anti-virulence properties (Imperi et al., 2013; Nehme et al., 2018; Miró-Canturri et al., 2019). Using these non-antibiotic drugs that are clinically in use

can be beneficial, as their pharmacokinetics and safety profiles are well-documented, so their development would be much faster and quicker than developing new antibiotics (Rampioni et al., 2017b; Maiden et al., 2018; Miró-Canturri et al., 2019). Therefore, testing such drugs as adjuvants with the available antibiotics can be scientifically and economically advantageous (Kaatz et al., 2003).

Numerous numbers of FDA-approved non-antibiotic drugs have been described in the literature for their additional anti-bacterial and anti-virulence properties (Bohnert et al., 2011; Ayaz et al., 2015). Examples of those drugs are anti-depressants (Mandal et al., 2010; Bohnert et al., 2011; Ayaz et al., 2015), anti-helminthics (Imperi et al., 2013; Rajamuthiah et al., 2015; Domalaon et al., 2019), anti-hypertensives (Middleton et al., 2005; Treerat et al., 2008), anti-psychotics (Hendricks et al., 2003; Coutinho et al., 2008; Nehme et al., 2018), chelating agents (Finnegan and Percival, 2015; Liu et al., 2017; Umerska et al., 2018), and other naturally derived compounds such as quercetin and furanones (Kristiansen and Amaral, 1997; Ayaz et al., 2015; Singh and Bhatia, 2018; Otto et al., 2019). From these non-antibiotic drugs and based on the evidence (see below), we selected one antibiotic and several non-antibiotic drugs from different classes to be tested in combination with tobramycin. The chosen drugs with their chemical structures are displayed in Figure 5.1, and the scientific evidence about their anti-bacterial potentials will be discussed in the following paragraphs.

Colistin (COL) is an old antibiotic that, due to issues with multidrug resistance, has been revived in the current clinical management of *P. aeruginosa* infections (Cummins et al., 2009). COL has a good *in vitro* and *in vivo* activity against Gram-negative pathogens such as *P. aeruginosa* (Lee et al., 2016). In this study, colistin was selected specifically, because it has been used frequently with tobramycin for the management of *P. aeruginosa* lung infections in CF patients, and several studies have reported a synergistic interaction of colistin with tobramycin (Hill et al., 2005; Herrmann et al., 2010). However, such studies evaluated this using standard growth media and against the PAO1 lab strain, therefore, it is essential to investigate this combination using more clinically relevant media and against a large number of clinical CF isolates.

In addition to colistin, we selected non-antibiotic drugs. The first one was amitriptyline (AMT). AMT is a tricyclic antidepressant that is used to treat patients with depression and neuropathic pain (Seale et al., 2014). The antibacterial activity of amitriptyline has been investigated against several Gram-negative bacteria including *P. aeruginosa* (Kaatz et al., 2003; Mandal et al., 2010; Ayaz et al., 2015). There is conflicting data about the possible antibacterial mechanism of amitriptyline. For instance, one study suggested that this could be due to its ability to inhibit efflux pumps (Kristiansen et al., 2010), but another paper indicated that AMT is a substrate for efflux pumps (Laudy et al., 2017). Besides amitriptyline, sertraline is another anti-depressant termed a selective serotonin reuptake inhibitor, which has been also found to exert antibacterial actions, due to its role in the inhibition of efflux pumps (Munoz-Bellido et al., 2000; Bohnert et al., 2011).

Anti-virulence activity has also been reported with niclosamide (NIC), which is an anti-helminthic drug for the treatment of human tapeworm infections (Chen et al., 2018). Recently, a study found that NIC has antibacterial activity against *P. aeruginosa* PA14 (Imperi et al., 2013). Such activity was attributed to its ability to inhibit the quorum sensing system (Imperi et al., 2013; Rajamuthiah et al., 2015; Singh and Bhatia, 2018; Miró-Canturri et al., 2019). Furthermore, the anti-virulence activity of niclosamide was also observed against Gram-positive bacteria (Rajamuthiah et al., 2015; Domalaon et al., 2019).

As in the case with AMT and NIC, the anti-bacterial activity of amiloride (AML) has been also studied. AML is a sodium channel blocker for the treatment of hypertensive patients (Treerat et al., 2008). AML has been found to display antibacterial activity and to synergise tobramycin against *Burkholderia cepecia* in a pilot clinical trial study (Middleton et al., 2005). This antibacterial activity was attributed to its effect on sodium and potassium ions in bacterial cells (Giunta et al., 1985). It was found that these cations can antagonize the action of aminoglycosides by blocking their uptake through the outer membrane in Gram-negative bacteria, therefore, AML might has a role in enhance antibiotic activity (Treerat et al., 2008).

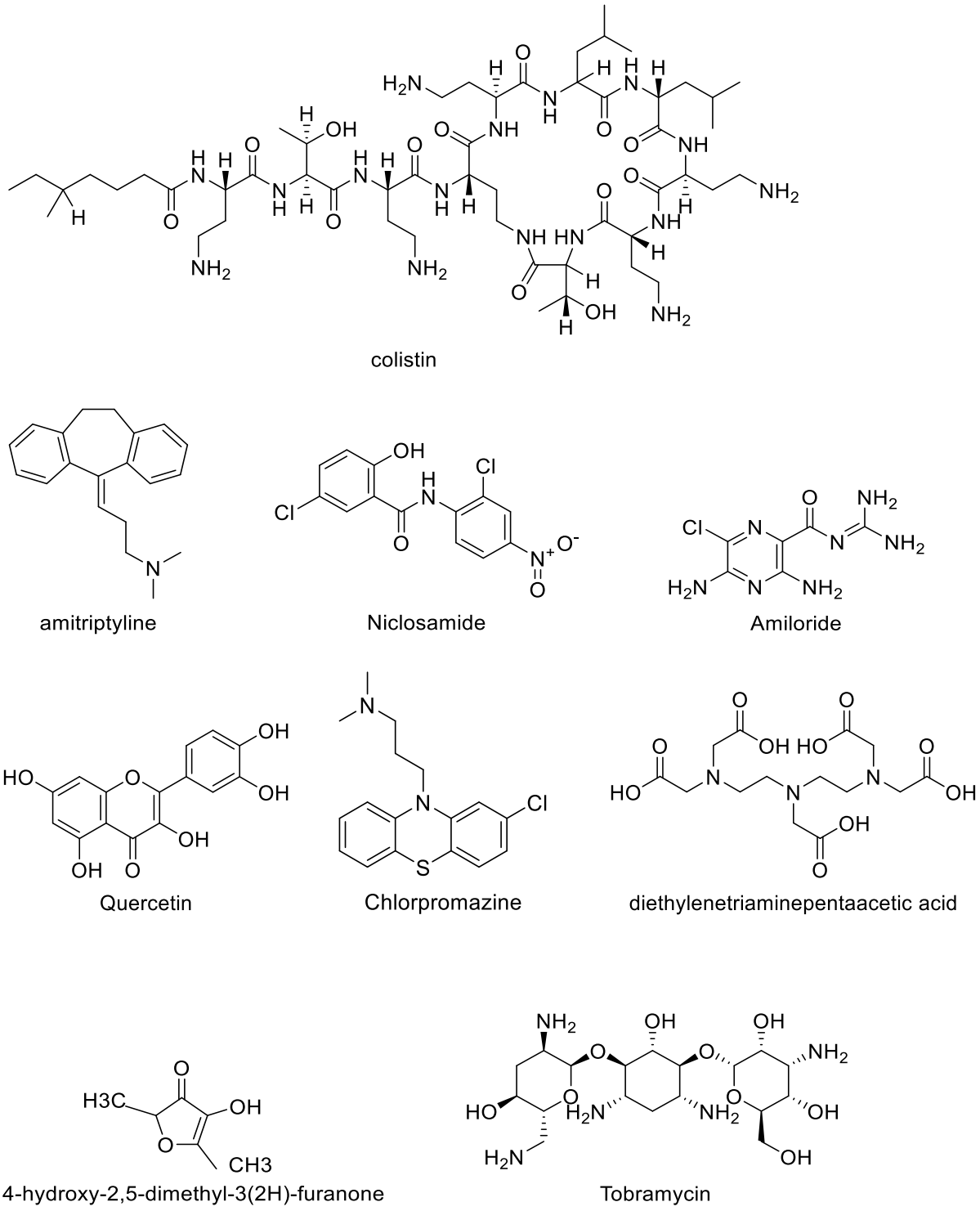

Figure 5.1. Chemical structures antibiotics and non-antibiotic drugs. colistin, amitriptyline, niclosmaide, amiloride, quercetin, chlorpromazine hydrochloride, diethylenetriaminepentaacetic acid, furanone, and tobramycin.

Quercetin (QUE) in turn is a flavonoid, which is naturally found in fruits and vegetables, and has also been found to have anti-virulence properties (Pawlikowska-Pawlęga et al., 2007; Siriwong et al., 2016; Roy et al., 2018). This antibacterial activity has been found against *P. aeruginosa,* in which this activity was related to either its role to inhibit the quorum sensing system or to its ability to disrupt the inner bacterial cytoplasmic membrane (Hirai et al., 2010; Gopu et al., 2015; Siriwong et al., 2016).

Like the above-mentioned drugs, the anti-psychotic phenothiazine chlorpromazine (CPH) has been studied *in vitro* for its antibacterial action (Dastidar et al., 2013). For instance, CPH showed antibacterial activity against Gram-negative bacteria such as *Salmonella* spp., *Klebsiella pneumonia,* and *P. aeruginosa* (Dastidar et al., 2013). This antibacterial activity was proposed to be due to its action on the bacterial cytoplasmic membrane (Dastidar et al., 2013).

Besides these drugs, another FDA-approved drug with a different mechanism of action and therapeutic indication has also been evaluated for antibacterial activity. This drug, diethylenetriaminepentaacetic acid (DTP), is a metal chelating agent for the treatment of patients with heavy metal ion poisoning such as with lead and mercury (Umerska et al., 2018). Currently, it has been found that DTP has anti-biofilm potency because of its ability to sequester the outer membrane-associated cations such as calcium and magnesium (Liu et al., 2017; Umerska et al., 2018). Additionally, a derivative of DTP is EDTA that has also been used as an anti-biofilm agent in treating wound infections alone and in combinations with anti-microbial agents (Finnegan and Percival, 2015).

Other drugs or compounds with anti-virulence properties against bacterial pathogens are natural compounds such as furanones (FUR), which are released from seaweed (Hentzer et al., 2002; Maeda et al., 2012; Rampioni et al., 2017b). FUR antibacterial properties have been reported against Gram-negative bacteria including *E. coli* and *P. aeruginosa*. Such activity was attributed to the disruption of quorum sensing systems and to the inhibition of biofilm formation in these bacteria (Hentzer et al., 2002; Kuehl et al., 2009). However, furanones were found to stimulate biofilm formation in some Gram-positive bacteria (Kuehl et al., 2009).

The current studies on tobramycin address its activity mostly in combination with other antibiotics, while its combination with non-antibiotic drugs is poorly studied. Therefore, this chapter aimed at the investigations of the potential *in vitro* combination of tobramycin and several FDA-approved non-antibiotic drugs belonging to different classes against *P. aeruginosa*. Such *in vitro* combinations were tested using a clinically relevant artificial sputum medium (ASM) and against both planktonic cultures and biofilms of *P. aeruginosa*.

5.2 Results

5.2.1 *In vitro* interactions between tobramycin and antibiotic/non-antibiotic drugs against planktonic PAO1

As outlined in the introduction section, tobramycin tolerance is growing, and several non-antibiotic drugs have been reported to have antimicrobial activity against Gram-negative bacteria. So, we aimed to assess the antibacterial activity of these drugs alone, and also in combination with tobramycin against *P. aeruginosa*. Therefore, we used the checkerboard assay (See Materials and Methods Chapter) to examine the potential interactions between tobramycin and antibiotic/non-antibiotic drugs against *P. aeruginosa* PAO1 using the standard Mueller Hinton Broth (MHB) medium. The results are summarized in Table 5.1.

Table 5.1. *In vitro* interactions between tobramycin and antibiotic/non-antibiotic drugs against *P. aeruginosa* PAO1 in MHB. MICs and FICs were determined in duplicate.

Antibiotics/non-antibiotic drugs	Drugs combination A[c]/B[d]	MICs [a] alone A/B	MICs combined A/B	FICs [b] Index	Activity
COL	TOB/COL	0.5/0.5	1/0.5	3	Indifferent
AMT	TOB/AMT	0.5/512	2/2	4	Antagonist
NIC	TOB/NIC	0.5/512	2/2	4	Antagonist
AML	TOB/AML	0.5/512	1/2	2	Indifferent
QUE	TOB/QUE	1/512	2/2	2	Indifferent
CHL	TOB/ CHL	1/512	2/2	2	Indifferent
DTP	TOB/DTP	1/512	2/2	2	Indifferent
HDF	TOB/HDF	0.5/256	1/4	2	Indifferent

TOB, tobramycin; COL, colistin; AMT, amitriptyline; NIC, niclosamide; AML, amiloride; QUE, quercetin; CHL, chlorpromazine; DTP, diethylenetriaminepentaacetic acid; HDF, 4-hydroxy-2,5-dimethyl-3(2H)-furanone. [a] the MIC: Minimum Inhibitory Concentrations (µg/ml) alone or combined, [b] the FIC: Fractional Inhibitory Concentration index. [c] tobramycin in all combinations, [d] the other drugs in the combination as sequenced in the table

The checkerboard data revealed that none of the tested antibiotics/non-antibiotic drugs displayed a synergistic interaction with tobramycin. For instance, the majority of drugs showed indifferent interaction as the measured FICs index was ≥ 2. The other drugs, AMT and NIC resulted in antagonistic interactions with FICs that were ≥ 4. As a monotherapy, it was observed that tobramycin or colistin demonstrated a good activity with MIC values of 0.5 µg/ml, while none of the other tested drugs displayed anti-bacterial activity against PAO1 with MICs ≥ 256 µg/ml.

Currently, tobramycin combination studies are mostly evaluated using the standard growth media e.g. MHB, which are not adequately representative of the *in vivo* conditions. Therefore, our aim was to test such tobramycin interactions using a more clinically relevant ASM medium, which could better reflect the influence of such combinations in a condition as similar as possible to the *in vivo* environment. In this regard, these tobramycin combinations were also re-evaluated using the ASM medium. The results are depicted in Table 5.2.

Table 5.2. *In vitro* interactions between tobramycin and antibiotic/non-antibiotic drugs against *P. aeruginosa* PAO1 in ASM medium. MICs and FICs were determined in triplicate.

Antibiotics/non-antibiotic drugs	**Drugs combination A/B**	**MICs alone A/B**	**MICs combined A/B**	**FIC Index**	**Activity**
COL	TOB/COL	0.5/4	1/4	3	Indifferent
AMT	TOB/AMT	0.5/512	4/512	9	Antagonism
NIC	TOB/NIC	0.5/512	2/2	4	Antagonism
AML	TOB/AML	0.5/ 256	1/2	2	Indifferent
QUE	TOB/QUE	0.5/256	2/2	4	Antagonism
CHL	TOB/ CHL	0.5/1024	2/2	4	Antagonism
DTP	TOB/DTP	0.5/1024	32/2	64	Antagonism
HDF	TOB/HDF	0.5/1024	4/16	8	Antagonism

The observed data suggested that using ASM medium resulted in some interactions, which were not observed using standard MHB. For instance, QUE, CHL, DTP, and HDF showed antagonistic interactions, with FIC reaching to 64 when DTP was used. Moreover, much higher MIC values up to 1024 µg/ml were documented as compared to 512 µg/ml in MHB. Such results indicate that testing the drug interactions using MHB could not simulate the *in vivo* conditions, and it is important to use more clinically relevant media to evaluate drug combination therapies. Accordingly, for the following studies, the ASM medium was used to test the influence of these tobramycin combinations against *P. aeruginosa* biofilms.

5.2.2 *In vitro* interactions between tobramycin and antibiotic/non-antibiotic drugs against PAO1 biofilm

In the previous section, tobramycin interactions were evaluated against planktonic PAO1. In the current section, our aim was to evaluate such interactions against PAO1 biofilms. This is because of the different lifestyles between planktonic and biofilm phenotypes (Das et al., 2016; Ghorbani et al., 2017), and also due to different infections that are caused by these phenotypes. For instance, acute infections are mostly caused by planktonic forms, while chronic infections are mainly associated with biofilms. Therefore, we further determined the influence of tobramycin interactions with antibiotic/non-antibiotic drugs against biofilms of *P. aeruginosa* PAO1.

To that purpose, the 96-well plate biofilm assay was used, in which PAO1 biofilms were grown in ASM medium and were challenged with either tobramycin/drugs alone or in combination for 24 h. The concentrations for antibiotic/non-antibiotic drugs were chosen because these have been shown to elicit antimicrobial activity against *P. aeruginosa* in the literature. The results (Figure 5.2 A-C) showed that COL, AMT, and NIC significantly ($p< 0.05$) potentiated activity of tobramycin with more than 50% reduction in biofilm biomass as compared to the controls and tobramycin alone against PAO1 biofilms.

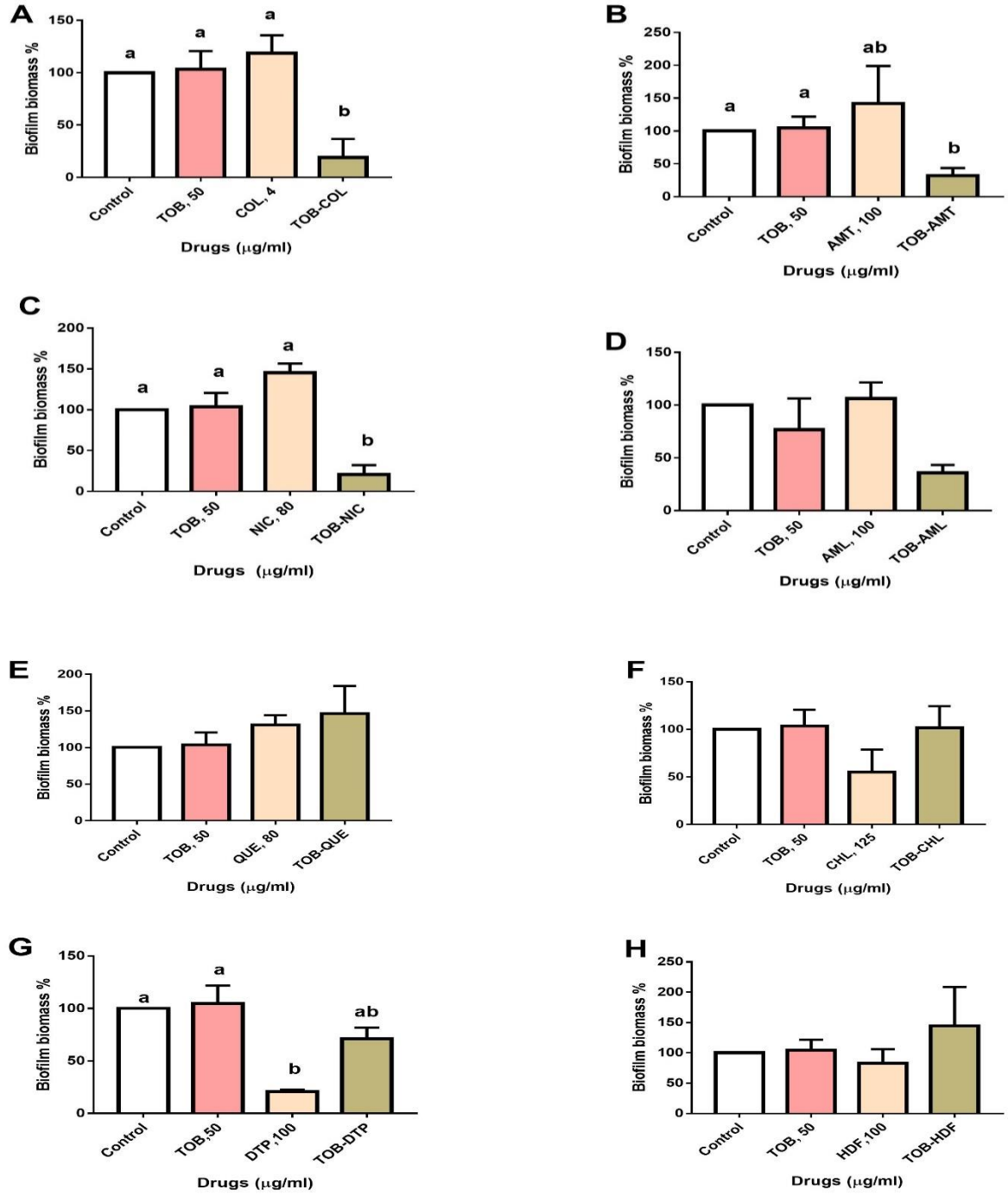

Figure 5.2 The effect of TOB, COL, AMT, NIC, AML, QUE, CHL, DTP, and HDF alone and in combination against *P. aeruginosa* PAO1 biofilms in ASM medium. Control (drug free); TOB 50 = 50 µg/ml tobramycin; Col 4 = 4 µg/ml colistin; AMT 100 **=** 100 µg/ml amitriptyline; NIC 50 = 50 µg/ml niclosamide; AML 100 = 100 µg/ml amiloride; QUE 80 = 80 µg/ml quercetin; CHL 125 = 125 µg/ml chlorpromazine hydrochloride; DTP 100 = 100 µg/ml diethylenetriaminepentaacetic acid**;** HDF 100 = 100 µg/ml 4-hydroxy-2,5-dimethyl-3(2H)-furanone. Error bars represent the standard error of the mean from three independent experiments with at least six technical replicate wells. Statistical significance was analysed using one-way analysis of variance (ANOVA) followed by Tukey multiple comparison test. The same letters indicate non-significant difference. Full details of the statistical analysis are shown in appendix 1.

Conversely, the other drugs showed no difference when combined with tobramycin (Figure 5.2 D-H). Notably, neither tobramycin nor any of these drugs alone displayed anti-biofilm activity. The only exception was observed in the biofilms that were challenged with DTP (Figure 5.2 G), in which significant ($p< 0.05$) reduction in biofilm biomass was observed. This could be because DTP acts as a chelating agent, which can chelate metal cations such as calcium, magnesium, and importantly iron (Lambert et al., 2004; Wright, 2016). Interestingly, when DTP was combined with tobramycin, it resulted in apparent antagonism ($p= 0.07$), which could confirm the antagonism that we observed against planktonic PAO1 in section 5.2.1.

5.2.3 *In vitro* interactions between tobramycin and antibiotic/non-antibiotic drugs against biofilms of clinical *P. aeruginosa* isolates

In the previously described section, tobramycin combinations were evaluated against biofilms of the lab strain PAO1. In this section, this was further expanded against clinical CF isolates *P. aeruginosa* of LMG 27643 and LMG 27648 biofilms. The results (Figure 5.3 A-H and I-P) for LMG 27643 and LMG 27648, respectively, suggested different responses between clinical CF isolates and PAO1(Section 5.2.2). For instance, in the previous section with PAO1 three of the tested drugs (COL, AMT, NIC) were able to synergize tobramycin against PAO1 biofilms. In contrast, for both clinical CF isolates we only found one synergistic interaction for a combination of tobramycin with AMT ($p< 0.05$) (Figure 5.3 B) against LMG 27643 biofilms, in which AMT-TOB combination caused 80% reduction in biofilm biomass as compared tobramycin alone (Figure 5.3 B). The other drugs either alone or in combination with tobramycin did not have anti-biofilm activity against either biofilm of LMG 27643 (Figure 5.3 A and C-H) or LMG 27648 (Figure 5.3 I-P). Such data indicate that every *P. aeruginosa* strain responds differently to the same drug combinations.

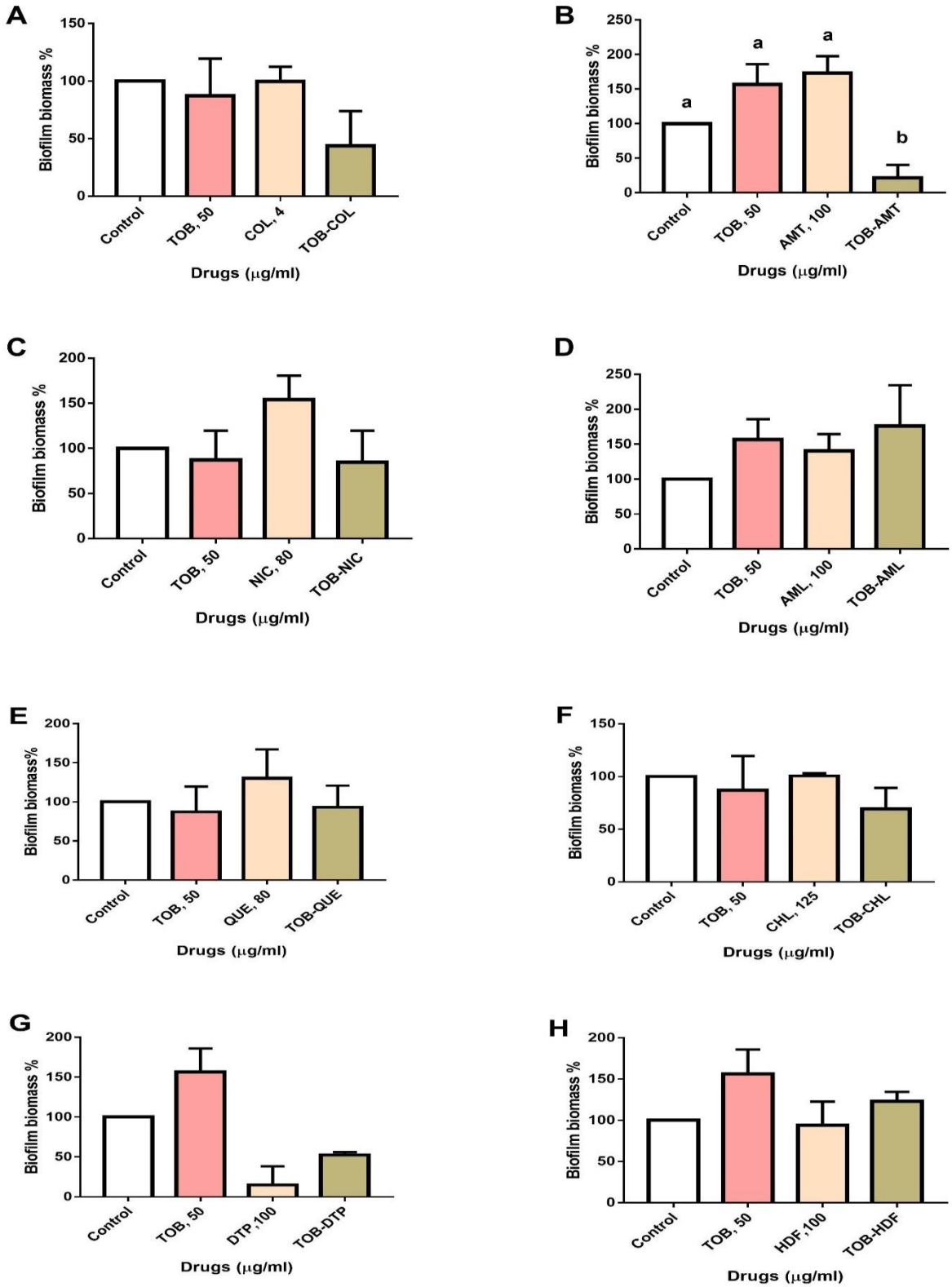
A
Biofilm biomass %
150
100
50
0
Control
TOB, 50
COL, 4
TOB-COL
Drugs (μg/ml)
B
Biofilm biomass %
250
200
150
100
50
0
a
a
a
b
Control
TOB, 50
AMT, 100
TOB-AMT
Drugs (μg/ml)
C
Biofilm biomass %
200
150
100
50
0
Control
TOB, 50
NIC, 80
TOB-NIC
Drugs (μg/ml)
D
Biofilm biomass %
250
200
150
100
50
0
Control
TOB, 50
AML, 100
TOB-AML
Drugs (μg/ml)
E
Biofilm biomass%
200
150
100
50
0
Control
TOB, 50
QUE, 80
TOB-QUE
Drugs (μg/ml)
F
Biofilm biomass %
150
100
50
0
Control
TOB, 50
CHL, 125
TOB-CHL
Drugs (μg/ml)
G
Biofilm biomass %
200
150
100
50
0
Control
TOB, 50
DTP ,100
TOB-DTP
Drugs (μg/ml)
H
Biofilm biomass %
200
150
100
50
0
Control
TOB, 50
HDF ,100
TOB-HDF
Drugs (μg/ml)

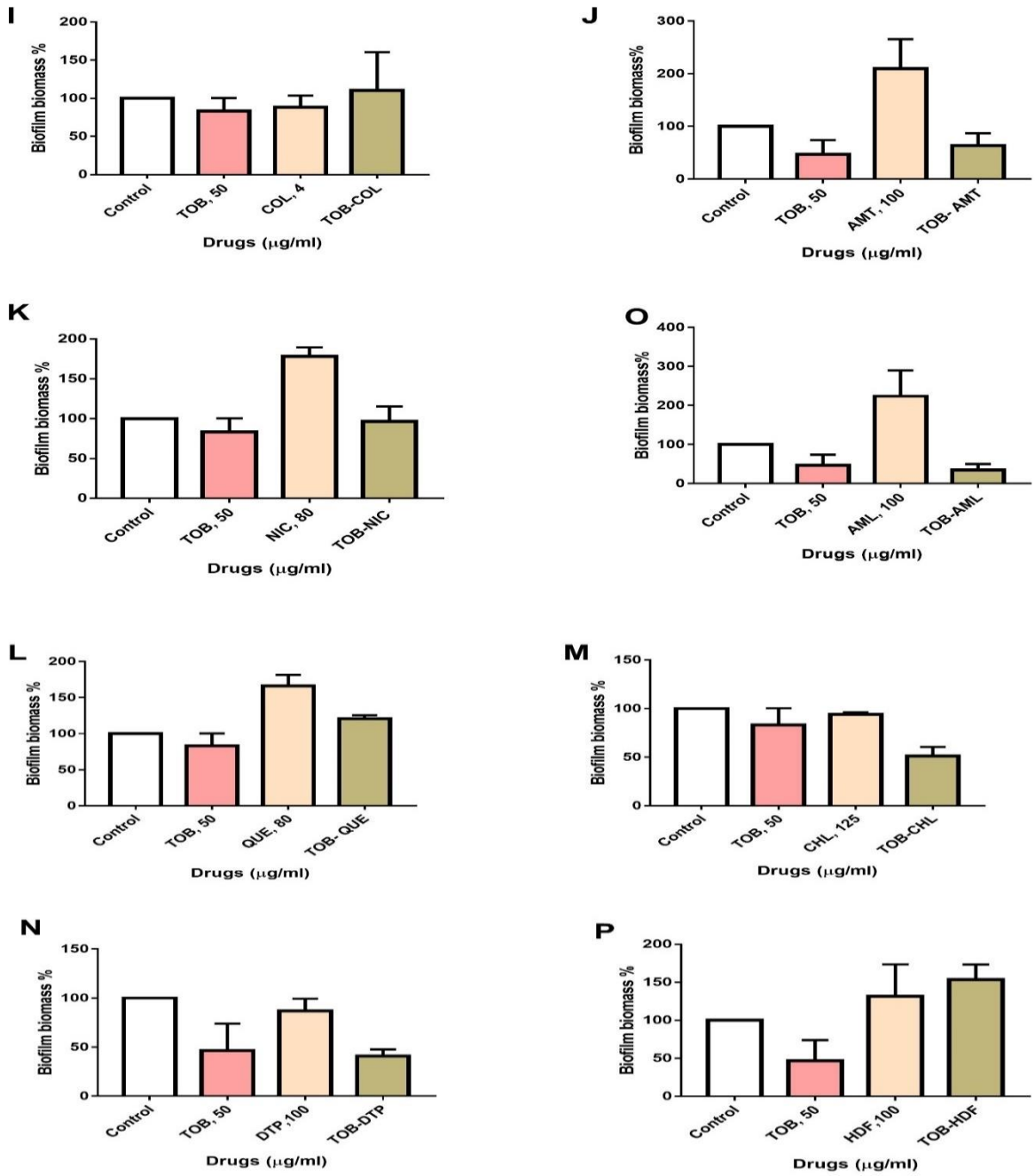

Figure 5.3 The effect of TOB, COL, AMT, NIC, AML, QUE, CHL, DTP, and HDF alone and in combination against biofilms of clinical *P. aeruginosa* isolate in ASM. LMG 27643 (A-H) and LMG 27648 (I-P). Control (drug free); TOB 50 = 50 µg/ml tobramycin; Col 4 = 4 µg/ml colistin; AMT 100 = 100 µg/ml amitriptyline; NIC 80 = 80 µg/ml niclosamide; AML 100 = 100 µg/ml amiloride; QUE 80 = 80 µg/ml quercetin; CHL 125 = 125 µg/ml chlorpromazine hydrochloride; DTP 100 =100 µg/ml diethylenetriaminepentaacetic acid**;** HDF 100 = 100 µg/ml 4-hydroxy-2,5-dimethyl-3(2H)-furanone. Error bars represent the standard error of the mean from three independent experiments with at least six technical replicate wells. Statistical significance was analysed using one-way analysis of variance (ANOVA). The same letters indicate non-significant difference. Full details of the statistical analysis are shown in appendix 1.

5.3 Discussion

In this chapter, we tested various tobramycin combinations with antibiotic/non-antibiotic drugs and other natural compounds using ASM medium against *P. aeruginosa*. These combinations were performed using the checkerboard assay, in which the antibacterial activity of each drug alone and in combination with tobramycin was assessed.

The detection of potential synergistic or antagonistic interactions between drug combinations is determined using several *in vitro* assays (Orhan et al., 2005). These include techniques of Epsilometer (E-test), time-kill curve, and checkerboard (Bonapace et al., 2000). Each of these methods measures synergy using different endpoint parameters (White et al., 1996; Balouiri et al., 2016; Brennan-Krohn and Kirby, 2019). For instance, the time-kill assay determines the rate of killing over several time points, while the E-test and the checkerboard assays measure the inhibitory activity at a fixed time point (Doern, 2014). For all these methods, there is no consensus on which assay is the most clinically relevant. However, the most established and widely used assay is the checkerboard assay (Cappelletty and Rybak, 1996; Doern, 2014). The checkerboard assay was therefore employed to test tobramycin combinations.

Using antibiotic agents in combination with non-antibiotic drugs is now becoming an interesting strategy to treat bacterial infections (Laudy et al., 2017; Otto et al., 2019). Therefore, in this work we evaluated tobramycin combinations with antibiotic/non-antibiotic drugs and natural compounds against *P. aeruginosa*. Our tobramycin combinations data indicated mixed results, in which these results were different according to the growth media, the bacterial lifestyles, and the strains that were used.

Firstly, using different growth media in the checkerboard assay indicated varying results. For example, testing tobramycin interactions using the standard MHB medium resulted mostly in indifferent interactions, while only amitriptyline and niclosamide showed antagonistic interaction. On the other hand, using a clinically relevant ASM medium more antagonistic interactions were observed with only two drugs, colistin and amiloride showed indifference. Such multiple antagonistic interactions that were noticed with ASM medium, suggest that the

cells responded differently to tobramycin combination under CF-like sputum conditions. This could be attributed for instance to the components of the ASM medium. These include for instance DNA and mucin glycoproteins, which might have a role in the adsorption of both tobramycin and also non-antibiotic drugs. For example, it is known that some of these non-antibiotic drugs are highly protein binding such as amitriptyline, niclosamide, and chlorpromazine (Brinkschulte et al., 1982; Silva et al., 2004; Domalaon et al., 2019). These data indicate that using a more clinically relevant ASM medium is essential in testing the influence of drug combinations. Importantly and after further *in vitro* and *in vivo* studies, such antagonistic interactions suggested that careful attention should be considered when these drugs are used in combination with tobramycin particularly in acute *P. aeruginosa* infections. Comparing our results with other studies might be difficult because most of tobramycin combination studies in literature are with antibiotic drugs, however, limited studies about tobramycin combination with non-antibiotic drugs are available. Indeed, if there are studies for tobramycin with non-antibiotic drugs, they were evaluated using different non-antibiotic drugs, growth media, and strains.

Secondly, testing tobramycin combinations against different bacterial lifestyles and strains showed variations in the observed results. For example, as discussed above, mostly antagonistic interactions were observed against planktonic PAO1 such as amitriptyline, niclosamide, quercetin, chlorpromazine, diethylenetriaminepentaacetic acid, and furanone. In contrast, for the biofilm phenotypes, some tobramycin combinations such as colistin, amitriptyline, and niclosamide showed synergistic interactions against PAO1 biofilms with 80% reduction in biofilm biomass. However, this was not observed with clinical isolate biofilms, with one exception being with LMG 26743, where the only synergistic interaction was observed with amitriptyline. One plausible explanation for such a difference could be attributed to the profoundly different gene expressions and behaviours between planktonic and biofilm counterparts (Haagensen et al., 2007; Das et al., 2016). Such behaviour was also observed by other investigators (Hill et al., 2005; Ghorbani et al., 2017), where they found different responses between planktonic/biofilm *P. aeruginosa* when the latter were challenged with the same combination of antibiotics. In the same way, other researchers observed different bacterial response to the combination therapies of tobramycin with non-antibiotic agents such as bicarbonate and triclosan (Kaushik et al., 2016; Maiden et al., 2018). For instance, Kaushik et al (2016) found a synergistic interaction for tobramycin-bicarbonate against planktonic cells

but not biofilms. Other investigators Maiden et al (2018) found that tobramycin-triclosan combination was synergistic against biofilm, while no difference was observed against planktonic cells. The findings from our study and other cited papers highlight the importance of considering the bacterial mode of growth when the drug combinations are evaluated. Additionally, our data indicate that the influence of tobramycin combinations vary according to bacterial isolates. Therefore, this suggests the importance of evaluating drug combinations with diverse strain collections.

The synergistic interactions that were discussed above with colistin, amitriptyline, and niclosamide could be explained by a different mechanism of action. However, the exact mechanism behind such synergy for these drugs is not known and, in this work, we have not carried out further studies to investigate this. These synergies could result from specific mechanisms for each drug. For example, the observed synergy between colistin and tobramycin could be explained by different molecular targets that were attacked by these drugs. Colistin mainly acts on the bacterial outer membrane (Stein et al., 2015), where this might enhance penetration of tobramycin into its cellular target site. Another explanation could be related to the different bacterial cell populations inside biofilms (Williamson et al., 2012), where there is a population at the top of the biofilm with high metabolic activity and another population at the bottom of the biofilm with low metabolic rate (Herrmann et al., 2010; Rybtke et al., 2011). These populations have different susceptibility towards antibiotics (Williamson et al., 2012). For instance, tobramycin inhibits the actively diving bacterial cells at the surface, while colistin is highly active against the cells with the low metabolic rate at the bottom of biofilms (Rybtke et al., 2011). Our data were in agreement with other studies (Hill et al., 2005; Herrmann et al., 2010). For instance, Hill et al (2005) found that combination of tobramycin and colistin was the best as compared to other tobramycin combinations with meropenem or ciprofloxacin antibiotics against biofilms *P. aeruginosa* CF isolates. Similarly, Herrmann et al (2010) showed superior efficacy of tobramycin-colistin combinations against biofilms of PAO1. Thus, this combination seemed to be more effective than the monotherapy of each drug against biofilms.

For the other combination synergies with amitriptyline and niclosamide, none of these drugs have been tested before in combination with tobramycin against *P. aeruginosa* biofilms. Firstly, the synergy that was obtained with amitriptyline could be explained by the ability of

amitriptyline to inhibit efflux pumps (Kristiansen et al., 2010), which in turn could enhance the accumulation of tobramycin inside the cell. Another synergy that was observed with niclosamide, could be explained by one of the possible mechanisms. For instance, tobramycin tolerance in *P. aeruginosa* is affected by the quorum sensing system (Roberts et al., 2015) and it is known that this system largely controls biofilm formation in *P. aeruginosa* (She et al., 2018). Therefore, combining these data with the current evidence about the role of niclosamide in inhibiting quorum sensing system in *P. aeruginosa* (Domalaon et al., 2019) might explain the enhanced activity of tobramycin with niclosamide.

Finally, for any of the tested non-antibiotic drugs and natural compounds as a monotherapy we did not see any antibacterial or anti-biofilm activity, which could be expected as some of these non-antibiotic drugs are presumed to act as inhibitors for efflux pumps or quorum sensing in bacterial cells. Our results for chlorpromazine, amitriptyline, and niclosamide were in line with studies that showed very poor activity of these drugs against Gram-negative *P. aeruginosa* (Hendricks et al., 2003; Nehme et al., 2018; Domalaon et al., 2019; Otto et al., 2019). For another compound, quercetin, there is conflicting evidence, with some studies (Hirai et al., 2010) showing no effect (similar to the results obtained here), and others showing a reduction in biofilm formation (Gopu et al., 2015). Such discrepancy can be explained by the different *P. aeruginosa* strain (PUFSTb04) and growth medium (Luria-Bertani) were used in that study. For amiloride, we did not find any activity either alone or in combination with tobramycin. This was in conflict with a paper that shown synergy with tobramycin (Treerat et al., 2008), however, as mentioned earlier the comparison is difficult as different strains, growth media, and method design were used.

Furanone has been shown to exert quorum sensing inhibitory activity, but in our study, we have not found an activity for furanone against *P. aeruginosa*. Some studies (Kuehl et al., 2009; Maeda et al., 2012) have shown similar results to that observed here, while another paper (Hentzer et al., 2003) suggested that furanone has antibiofilm activity and could enhance tobramycin susceptibility. Such discrepancy with our work could be explained firstly by using different furanone derivatives, as it has been demonstrated that minor modifications of the functional groups in the structure of furanone, can significantly affect its activity against the tested bacteria (Kuehl et al., 2009). Secondly, the biofilm model, strain, medium, and technique

of treatment were all different. Collectively, it is clear that there is a lack of standardization in biofilm testing which can make interpretation of data quite complicated when comparing data from different laboratories (Boudarel et al., 2018).

Our work with DTP was in accordance with studies that found using chelating agents such as EDTA at only very high concentrations (up to 16384 µg/ml) were able to inhibit the growth of *P. aeruginosa* (Lambert et al., 2004; Umerska et al., 2018). They found that using such high concentrations of EDTA can displace calcium, magnesium from the outer membrane, whereas at low concentrations no cell lysis was observed (Lambert et al., 2004). However, these high concentrations are not physiologically achievable. For DTP action in combination with tobramycin against PAO1 biofilms, we apparently found an antagonism. This might be related to tobramycin's cationic properties, which could result in interaction with DTP. Another possible explanation could be related to tobramycin bacterial cell killing mechanism. It has been found that part of aminoglycoside antibacterial activity is associated with stimulating the production of hydroxyl radicals through a Fenton reaction (Kohanski et al., 2007). This means using DTP, which is known to chelate iron could reduce the ability of tobramycin to kill cells by inhibition of the Fenton reaction.

5.4 Conclusion

P. aeruginosa biofilm tolerance to antibiotics is a serious health problem, which the medical community is now facing. This current situation also combines with decreasing production and development of new antibiotics. Therefore, finding alternative strategies to efficiently use the available antibiotics is highly desired. Accordingly, in this chapter, we evaluated tobramycin in combination with several non-antibiotic drugs and natural compounds using a clinically relevant ASM medium against planktonic and biofilm *P. aeruginosa*. We found only the combination of tobramycin with colistin, amitriptyline, and niclosamide resulted in enhanced tobramycin activity against *P. aeruginosa* PAO1 biofilms, where such synergy resulted in 80% reduction in biofilm biomass as compared to tobramycin alone. The safety profiles of these drugs are known and established. Therefore, further cytotoxicity studies are not required. However, further investigations are needed to clearly understand the antibiofilm mechanisms

of action for these drugs, the influences of different doses, and their role in the treatment of *P. aeruginosa* biofilm infections. Moreover, the ability of this *in vitro* synergy to predict *in vivo* correlation is unknown, therefore, further clinical studies are warranted especially as the effectiveness of drug combinations is strain dependent. Finally, these drugs could be appropriate candidates to be used as adjuvant therapy with tobramycin to improve its activity against chronic *P. aeruginosa* biofilm infections. However, caution should be taken using some of these non-antibiotics combinations against acute *P. aeruginosa* infections, as our results showed antagonistic interactions against planktonic phenotypes.

Chapter 6:

General Conclusion and Future Work

6.1 General overview

P. aeruginosa infections in CF patients are considered amongst the most challenging infections for treatment. One of the extreme difficulties in the treatment of these infections is attributed to the ability of *P. aeruginosa* to grow in sessile structured communities called biofilms, which have a major role in antibiotic tolerance to many antibacterial classes. Among these are aminoglycosides and particularly tobramycin, which is the most widely used antibiotic in the treatment of *P. aeruginosa* infections.

The general aim of the work presented in this thesis was to investigate the role of tobramycin and possible potential ways to improve its activity in the eradication of *P. aeruginosa* biofilms. Specifically, this work had three overarching aims. Firstly, to determine the activity of tobramycin using a clinically relevant artificial sputum medium (ASM) against *P. aeruginosa* clinical CF isolates. Secondly, to investigate the activity of tobramycin dry powder inhaler (TOBI Podhaler®) in terms of particle size. Thirdly, to evaluate tobramycin activity in combination therapy with non-antibiotic drugs. These experiments designed to address the aims that have been described in this thesis in chapters 3-5, and the following paragraphs will briefly summarise them.

6.2 The activity of tobramycin in eradication *P. aeruginosa* biofilms

To address aim one (chapter 3), the activity of tobramycin was evaluated against a number of clinical CF isolates and PAO1 lab strain. This was performed using two different *in vitro* biofilm models, which were the 96-well plate and the colony biofilm models. The latter could be a much better simulation than the microtiter plate assay for biofilms grow in the lung, as it provides an air-interface surface. Two different growth media minimal MOPS and artificial sputum medium (ASM) were used. The former is a standard minimal medium, whereas the latter is a clinically more relevant medium, as it has CF-sputum like properties. For instance, it contains DNA, mucin, and salts. Our key findings from using these media suggested different values for MICs of tobramycin. For example, we observed that the MIC values of tobramycin

for the tested strains were four-fold higher when ASM was used as compared with MOPS, which might be explained by the interactions between ASM components and tobramycin. Therefore, such data indicate that it is important to consider using the more clinically relevant ASM medium for determining antibiotic susceptibility. Other key findings from this work suggested that tobramycin was able to reduce biofilm biomass and viable count by 40-60% in most of the tested strains, but that complete eradication of *P. aeruginosa* biofilms was difficult to achieve. This is mainly attributed to the advantages that growing in a biofilm-like structure offers to bacterial cells. We have not investigated this specifically for tobramycin in our biofilm models, but it is likely to be a combination of several reasons. For instance, biofilms can act as a barrier that decreases the penetration of tobramycin because of the electrostatic binding between tobramycin and biofilm matrix components. Additionally, bacterial cells inside the biofilm grow at a low metabolic rate, which could also reduce the activity of tobramycin. Moreover, the microaerobic environment inside a biofilm could also affect the anti-biofilm activity of tobramycin. Therefore, these data have a critical clinical implication and strongly suggest that further research and studies are warranted to improve the activity of tobramycin against *P. aeruginosa* biofilms.

6.3 The activity of tobramycin dry powder inhaler in terms of particle size

Following the findings described in section 6.2, the work was continued by evaluating the activity of tobramycin dry powder (TOBI Podhaler®). This work addressed the second aim (chapter 4), where we determined the efficacy of tobramycin dry powder inhaler against *P. aeruginosa* with a specific aim to analyse the effect of particle size. In the first step, we optimized a model to fractionate tobramycin dry powder into different particle size categories, which was performed using the Next Generation Impactor (NGI). In the second step, we developed and optimised an HPLC-MS assay, allowing us to quantify the mass of differently sized tobramycin particles from the NGI. These were preliminary steps before testing the activity of different tobramycin particle sizes against *P. aeruginosa* biofilms. In the next step, we used ASM as a growth medium and also optimized an *in vitro* biofilm model that allows growing biofilms at an air-interface. This was performed by using the colony biofilm assay.

The main aim of using these models was to develop an *in vitro* model that might be a better reflection for the conditions in the CF lung by growing biofilms at an air-interface, and also allow us to apply tobramycin as a dry powder directly to the biofilms.

The key findings suggested that the particle size of tobramycin does influence the antibiofilm activity in a time-dependent fashion. Smaller tobramycin particles (< 2.82 µm) were more effective by about ~20% reduction in viable count as compared to the larger particles (< 11.7 µm) in the eradication of *P. aeruginosa* biofilms of LMG 27649 and LMG 27643 after a short incubation time (3 hours). This time of incubation is potentially important, as this is similar to the time taken for the clearance of tobramycin from the lung. Because of the effect that was observed at 3 hours, further experiments were conducted with LMG 27649 clinical isolate at different incubation time points which showed a reproducible trend of better efficacy of smaller particles when the incubation time was less than 24 hours, although statistical significance was not achieved. With respect to our *in vitro* results, it is not yet clear whether our data have a clinical significance, and further experiments both *in vitro* and *in vivo* are required to confirm this.

6.4 The activity of tobramycin in combination therapy

Following determination of the influence of tobramycin in terms of particle size, we further studied the potential improvement of tobramycin activity by evaluating the combinations of tobramycin with another antibiotic (colistin) or non-antibiotic drugs (amitriptyline, niclosamide, amiloride, quercetin, chlorpromazine, diethylenetriaminepentaacetic acid, and furanone). This work addressed the third aim (Chapter 5), where we determined the influence of these non-antibiotic drugs in combination with tobramycin against planktonic and biofilms of *P. aeruginosa*. The evaluation of tobramycin combined with non-antibiotic drugs was carried out using the checkerboard technique, which was analysed using the Fractional Inhibitory Concentrations (FICs). Mueller-Hinton Broth (MHB) and ASM growth media were used to evaluate these combinations. The data obtained from this work suggested vital information about tobramycin combinations using ASM as compared with MHB against planktonic cells. For instance, using ASM resulted mostly in antagonistic interactions with

tobramycin, whereas with MHB most of the combinations showed indifference. Therefore, such findings contained in this chapter are important as they highlight, similar to chapter 3, the importance of using a more clinically relevant medium in testing antibiotic activity. Despite we used in our study a more physiologically relevant medium, which is a better reflection to *in vivo* lung conditions than standard growth media. The *in vivo* implications of our findings remain to be investigated. Accordingly, our *in vitro* results cannot be expanded to clinical practice until further *in vivo* data are obtained.

Besides studying the activity of tobramycin combined with other drugs against planktonic cells, we also investigated the influence of these combinations against biofilms. Our data showed mixed results with some combinations showing no difference, while others showed synergistic interactions with tobramycin. It is noteworthy that there is a large variation in the results of such combinations in the literature, which may relate to the lack of standardization in biofilm research. In our study, we observed no difference when tobramycin was combined with amiloride, quercetin, chlorpromazine, diethylenetriaminepentaacetic acid, and furanones. For other drugs, we found synergistic combinations with colistin, niclosamide, and amitriptyline. These combinations resulted in about 80% reduction in biofilm biomass as compared to tobramycin alone. Such synergistic interactions were mostly observed against PAO1 but were not always obvious with all clinical isolates except LMG27643, in which amitriptyline synergized tobramycin. These data indicate that it is essential to test drug combinations against a wide range of clinical isolates. Finally, for these tobramycin combinations to be considered for therapeutic potential, further experiments both *in vitro* and *in vivo* are warranted.

Finally, as a general conclusion from this thesis, it is obvious that *P. aeruginosa* biofilm eradication is challenging and difficult. Therefore, considerable efforts and research are needed to preserve or further improve antibiotic activity to be able to eliminate these biofilms. Such improvement should be expanded and not only be focused on antibiotics themselves, as it is not the sole determinant. Other factors such as a pharmaceutical formulation, delivery to the target organ, and a combined antibiotic formulation can all play major roles and contribute to enhance the efficacy of the available antibiotics. Meanwhile, early aggressive antibiotic therapy can have a major role in the prevention establishment of chronic infections.

6.5 Future work

1- In future studies, it could be of interest to test the influence of using differently sized tobramycin particles against other species such as *Burkhoderia cepacia* and *Staphylococcus aureus* that are also part of polymicrobial lung infections in CF patients. Furthermore, it would be desirable to test the effect of particle size in more advanced models such as *ex-vivo* and *in vivo* lung models.

2- Here a successful model for testing the dry powder inhaler antibiotic has been developed. Our study needs to be expanded to test other antibiotics administered via a dry powder inhaler. This might be of particular importance for those antibiotics with a lower aqueous solubility than tobramycin. Examples of these drugs are ciprofloxacin and colistin. For instance, the octanol-water partition coefficient (log P_{oct}) of ciprofloxacin is 2.3, and for colistin is - 2.4 as compared to -7.3 for tobramycin. Particles of these drugs are therefore likely to dissolve more slowly than those of tobramycin, so there could be a more significant effect of the particle size on the rate of dissolution and thus biofilm activity. The potential results from testing these drugs could improve the activity of dry powder inhaler antibiotics by formulating dry powder inhaler with higher percentages of the most effective particle size range.

3- In future studies of tobramycin combined with other drugs, it would be interesting to test these synergistic tobramycin combinations against a large library of clinical isolates and strains to confirm their efficacy. Additionally, this work can be further expanded by evaluating a broader range of non-antibiotic drugs for their antibacterial activity and role as adjuvant therapy with tobramycin. This could offer further knowledge that could help to determine the possible synergistic as well as antagonistic interactions of tobramycin with non-antibiotic drugs. When the synergistic activity of drugs with tobramycin or other antibiotics is confirmed, these then need to be formulated and tested for their behaviour as a dry powder. This would initially involve studies using the NGI as outlined in chapter 4, as well as studies testing these formulations in *in vitro* and *in vivo* models.

Research output from this thesis

The 6th European Congress on Biofilms. Euro-biofilms 3-6 September 2019, Glasgow, Scotland-UK. Investigating the influence of dry powder inhaler antibiotics against *P. aeruginosa* biofilms (Poster presentation).

The 8th Congress of European Microbiologist FEMS 7-11 July 2019, Glasgow, Scotland-UK. Investigating the influence of dry powder inhaler antibiotics against *P. aeruginosa* biofilms (Poster presentation).

Outreach Public Engagement Activity (oral talk) at Soapbox Science, 13 July 2019, Bristol-UK. http://soapboxscience.org/soapbox-science-2019-bristol/.

Center Therapeutic Innovation Showcase CTI Showcase 25 June 2019 University of Bath-UK, Investigating the influence of dry powder inhaler antibiotics against *P. aeruginosa* biofilms (Poster presentation).

Annual Microbiology Society conference 8-11 April 2019 ICC Belfast-UK. Investigating the influence of dry powder inhaler antibiotics against *P. aeruginosa* biofilms (Poster presentation).

Meeting Abstract in Microbiology Journal investigating the effect of tobramycin dry powder inhaler on the eradication of *Pseudomonas aeruginosa* biofilms. First Published: 08 April 2019 **https://doi.org/10.1099/acmi.ac2019.po0039.**

BSAC Spring Conference 21 – 22 March 2019, Birmingham-UK, Investigating the influence of dry powder inhaler antibiotics against *P. aeruginosa* biofilms (Poster presentation).

References

Aeschlimann, J.R., 2003. The role of multidrug efflux pumps in the antibiotic resistance of Pseudomonas aeruginosa and other gram-negative bacteria. Insights from the Society of Infectious Diseases Pharmacists. *Pharmacotherapy*, 23(7), pp. 916-924.

Al-Azemi, A., Fielder, M.D., Abuknesha, R.A. and Price, R.G., 2011. Effects of chelating agent and environmental stresses on microbial biofilms: relevance to clinical microbiology. *J Appl Microbiol*, 110(5), pp. 1307-1313.

Amaral, L., Kristiansen, J.E., Viveiros, M. and Atouguia, J., 2001. Activity of phenothiazines against antibiotic-resistant Mycobacterium tuberculosis: a review supporting further studies that may elucidate the potential use of thioridazine as anti-tuberculosis therapy. *J Antimicrob Chemother*, 47(5), pp. 505-511.

Ambrus, R., Benke, E., Farkas, A., Balashazy, I. and Szabo-Revesz, P., 2018. Novel dry powder inhaler formulation containing antibiotic using combined technology to improve aerodynamic properties. *Eur J Pharm Sci*, 123, pp. 20-27.

Andersson, D.I. and Hughes, D., 2014. Microbiological effects of sublethal levels of antibiotics. *Nat Rev Microbiol*, 12, pp. 465-478.

Andrews, J.M., 2001. Determination of minimum inhibitory concentrations. *J Antimicrob Chemother*, 48 Suppl 1, pp. 5-16.

Andrews, J.M., 2007. BSAC standardized disc susceptibility testing method (version 6). *J Antimicrob Chemother*, 60(1), pp. 20-41.

Aristoteli, L.P. and Willcox, M.D.P., 2003. Mucin degradation mechanisms by distinct Pseudomonas aeruginosa isolates in vitro. *Infect Immun*, 71(10), pp. 5565-5575.

Ashish, A., Shaw, M., Winstanley, C., Ledson, M.J. and Walshaw, M.J., 2012. Increasing resistance of the Liverpool Epidemic Strain (LES) of Pseudomonas aeruginosa (Psa) to antibiotics in cystic fibrosis (CF)--a cause for concern? *J Cyst Fibros*, 11(3), pp. 173-179.

Askoura, M., Mottawea, W., Abujamel, T. and Taher, I., 2011. Efflux pump inhibitors (EPIs) as new antimicrobial agents against Pseudomonas aeruginosa. *Libyan J Med*, 6. https://doi.org/10.3402/ljm.v6i0.5870.

Attema-de Jonge, M.E., Bekkers, J.M., Oudemans-van Straaten, H.M., Sparidans, R.W. and Franssen, E.J., 2008. Simple and sensitive method for quantification of low tobramycin concentrations in human plasma using HPLC-MS/MS. *J Chromatogr B Analyt Technol Biomed Life Sci*, 862(1-2), pp. 257-262.

Avent, M.L., Rogers, B.A., Cheng, A.C. and Paterson, D.L., 2011. Current use of aminoglycosides: indications, pharmacokinetics and monitoring for toxicity. *Intern Med J*, 41(6), pp. 441-449.

Ayaz, M., Subhan, F., Ahmed, J., Khan, A.-U., Ullah, F., Ullah, I., Ali, G., Syed, N.-I.H. and Hussain, S., 2015. Sertraline enhances the activity of antimicrobial agents against pathogens

of clinical relevance. *J Biol Res (Thessalon)*, 22(1). https://doi.org/10.1186/s40709-015-0028-1.

Azeredo, J., Azevedo, N.F., Briandet, R., Cerca, N., Coenye, T., Costa, A.R., Desvaux, M., Di Bonaventura, G., Hébraud, M., Jaglic, Z., Kačániová, M., Knøchel, S., Lourenço, A., Mergulhão, F., Meyer, R.L., Nychas, G., Simões, M., Tresse, O. and Sternberg, C., 2017. Critical review on biofilm methods. *Crit Rev Microbiol,* 43, pp. 313-351.

Babić, F., Venturi, V. and Maravić-Vlahoviček, G., 2010. Tobramycin at subinhibitory concentration inhibits the RhlI/R quorum sensing system in a Pseudomonas aeruginosaenvironmental isolate. *BMC Infect Dis*, 10(1). https://doi.org/10.1186/1471-2334-10-148.

Bahamondez-Canas, T.F., Zhang, H., Tewes, F., Leal, J. and Smyth, H.D.C., 2018. PEGylation of Tobramycin Improves Mucus Penetration and Antimicrobial Activity against Pseudomonas aeruginosa Biofilms in Vitro. *Mol Pharm,* 15(4), pp. 1643-1652.

Balke, B., Hogardt, M., Schmoldt, S., Hoy, L., Weissbrodt, H. and Häussler, S., 2006. Evaluation of the E test for the assessment of synergy of antibiotic combinations against multiresistant Pseudomonas aeruginosa isolates from cystic fibrosis patients. *Eur J Clin Microbiol Infect Dis,* 25(1), pp. 25-30.

Balouiri, M., Sadiki, M. and Ibnsouda, S.K., 2016. Methods for in vitro evaluating antimicrobial activity: A review. *J Pharm Anal*, 6(2), pp. 71-79.

Banerjee, S.K., Jagannath, C., Hunter, R.L. and Dasgupta, A., 2000. Bioavailability of tobramycin after oral delivery in FVB mice using CRL-1605 copolymer, an inhibitor of P-glycoprotein. *Life Sci,* 67(16), pp. 2011-2016.

Banin, E., Brady, K.M. and Greenberg, E.P., 2006. Chelator-Induced Dispersal and Killing of Pseudomonas aeruginosa Cells in a Biofilm. *Appl Environ Microbiol,* 72(3), pp. 2064-2069.

Banin, E., Vasil, M.L. and Greenberg, E.P., 2005. Iron and Pseudomonas aeruginosa biofilm formation. *Proc Natl Acad Sci U S A,* 102(31), pp. 11076-11081.

Barth, A.L. and Pitt, T.L., 1996. The high amino-acid content of sputum from cystic fibrosis patients promotes growth of auxotrophic Pseudomonas aeruginosa. *J Med Microbiol,* 45(2), pp. 110-119.

Bassetti, M., Vena, A., Croxatto, A., Righi, E. and Guery, B., 2018. How to manage Pseudomonas aeruginosa infections. *Drugs Context*, 7. https://doi.org/10.7573/dic.212527.

Beceiro, A., Tomas, M. and Bou, G., 2013. Antimicrobial resistance and virulence: a successful or deleterious association in the bacterial world? *Clin Microbiol Rev,* 26(2), pp. 185-230.

Becker, D.E., 2013. Antimicrobial drugs. *Anesth Prog,* 60(3), pp. 111-123.

Bergan, T. and Hoiby, N., 1975. Epidemiological markers for Pseudomonas aeruginosa. *Acta Pathol Microbiol Scand Suppl,* 83(6), pp. 553-560.

Berlutti, F., Morea, C., Battistoni, A., Sarli, S., Cipriani, P., Superti, F., Ammendolia, M.G. and Valenti, P., 2005. Iron Availability Influences Aggregation, Biofilm, Adhesion and Invasion of Pseudomonas Aeruginosa and Burkholderia Cenocepacia. *Int J Immunopathol Pharmacol*, 18(4), pp. 661-670.

Bjarnsholt, T., Buhlin, K., Dufrene, Y.F., Gomelsky, M., Moroni, A., Ramstedt, M., Rumbaugh, K.P., Schulte, T., Sun, L., Akerlund, B. and Romling, U., 2018. Biofilm formation - what we can learn from recent developments. *J Intern Med*, 284(4), pp. 332-345.

Bjarnsholt, T., Jensen, P.O., Burmolle, M., Hentzer, M., Haagensen, J.A.J., Hougen, H.P., Calum, H., Madsen, K.G., Moser, C., Molin, S., Hoiby, N. and Givskov, M., 2005. Pseudomonas aeruginosa tolerance to tobramycin, hydrogen peroxide and polymorphonuclear leukocytes is quorum-sensing dependent. *Microbiology*, 151(2), pp. 373-383.

Bjarnsholt, T., Jensen, P.O., Fiandaca, M.J., Pedersen, J., Hansen, C.R., Andersen, C.B., Pressler, T., Givskov, M. and Hoiby, N., 2009. Pseudomonas aeruginosa biofilms in the respiratory tract of cystic fibrosis patients. *Pediatr Pulmonol*, 44(6), pp. 547-558.

Blanchaert, B., Huang, S., Wach, K., Adams, E. and Van Schepdael, A., 2017. Assay Development for Aminoglycosides by HPLC with Direct UV Detection. *J Chromatogr Sci*, 55(3), pp. 197-204.

Bohnert, J.A., Szymaniak-Vits, M., Schuster, S. and Kern, W.V., 2011. Efflux inhibition by selective serotonin reuptake inhibitors in Escherichia coli. *J Antimicrob Chemother*, 66(9), pp. 2057-2060.

Bonapace, C.R., White, R.L., Friedrich, L.V. and Bosso, J.A., 2000. Evaluation of antibiotic synergy against Acinetobacter baumannii: a comparison with Etest, time-kill, and checkerboard methods. *Diagn Microbiol Infect Dis*, 38(1), pp. 43-50.

Bos, A.C., Passé, K.M., Mouton, J.W., Janssens, H.M. and Tiddens, H.A.W.M., 2017. The fate of inhaled antibiotics after deposition in cystic fibrosis: How to get drug to the bug? *J Cyst Fibros*, 16(1), pp. 13-23.

Bos, A.C., van Holsbeke, C., de Backer, J.W., van Westreenen, M., Janssens, H.M., Vos, W.G. and Tiddens, H.A.W.M., 2015. Patient-Specific Modeling of Regional Antibiotic Concentration Levels in Airways of Patients with Cystic Fibrosis: Are We Dosing High Enough? *PLoS One*, 10(3). https://doi.org/10.1371/journal.pone.0118454.

Boudarel, H., Mathias, J.D., Blaysat, B. and Grediac, M., 2018. Towards standardized mechanical characterization of microbial biofilms: analysis and critical review. *NPJ Biofilms Microbiomes*, 4. https://doi.org/10.1038/s41522-018-0062-5.

Braun, A., Sewald, K., Müller, L., Wronski, S., Murgia, X., Lehr, C.-M., Börger, C., Siebenbürger, L., Hittinger, M., Schwarzkopf, K. and Häussler, S., 2018. Human airway mucus alters susceptibility of Pseudomonas aeruginosa biofilms to tobramycin, but not colistin. *J Antimicrob Chemother*, 73(10), pp. 2762-2769.

Breidenstein, E.B., de la Fuente-Nunez, C. and Hancock, R.E., 2011. Pseudomonas aeruginosa: all roads lead to resistance. *Trends Microbiol*, 19(8), pp. 419-426.

Brennan-Krohn, T. and Kirby, J.E., 2019. Antimicrobial Synergy Testing by the Inkjet Printer-assisted Automated Checkerboard Array and the Manual Time-kill Method. *JoVE*, (146). https://doi.org/doi:10.3791/58636.

Brinkschulte, M., Gaertner, H.J., Schied, H.W. and Breyer-Pfaff, U., 1982. Plasma protein binding of perazine and amitriptyline in psychiatric patients. *Eur J Clin Pharmacol*, 22(4), pp. 367-373.

Buttini, F., Brambilla, G., Copelli, D., Sisti, V., Balducci, A.G., Bettini, R. and Pasquali, I., 2016. Effect of Flow Rate on In Vitro Aerodynamic Performance of NEXThaler((R)) in Comparison with Diskus((R)) and Turbohaler((R)) Dry Powder Inhalers. *J Aerosol Med Pulm Drug Deliv*, 29(2), pp. 167-178.

Cai, Y., Yu, X.H., Wang, R., An, M.M. and Liang, B.B., 2009. Effects of iron depletion on antimicrobial activities against planktonic and biofilm Pseudomonas aeruginosa. *J Pharm Pharmacol*, 61(9), pp. 1257-1262.

Campódonico, V.L., Gadjeva, M., Paradis-Bleau, C., Uluer, A. and Pier, G.B., 2008. Airway epithelial control of Pseudomonas aeruginosa infection in cystic fibrosis. *Trends Mol Med*, 14(3), pp. 120-133.

Cappelletty, D.M. and Rybak, M.J., 1996. Comparison of methodologies for synergism testing of drug combinations against resistant strains of Pseudomonas aeruginosa. *Antimicrob Agents Chemother*, 40(3), pp. 677-683.

CDC, 2017. *Pseudomonas aeruginosa in Health Care Settings* [Online]. The Centers for Disease Control and Prevention. Available from: *https://www.cdc.gov/hai/organisms/pseudomonas.html* [Accessed 12-01-2020].

Charrier, C., Rodger, C., Robertson, J., Kowalczuk, A., Shand, N., Fraser-Pitt, D., Mercer, D. and O'Neil, D., 2014. Cysteamine (Lynovex®), a novel mucoactive antimicrobial & antibiofilm agent for the treatment of cystic fibrosis. *Orphanet J Rare Dis*, 9. https://doi.org/10.1186/s13023-014-0189-2.

Chen, L., Chen, H. and Shen, M., 2014. Hydrophilic interaction chromatography combined with tandem mass spectrometry method for the quantification of tobramycin in human plasma and its application in a pharmacokinetic study. *J Chromatogr B Analyt Technol Biomed Life Sci*, 973, pp. 39-44.

Chen, L., Zou, Y., She, P. and Wu, Y., 2015. Composition, function, and regulation of T6SS in Pseudomonas aeruginosa. *Microbiol Res*, 172, pp. 19-25.

Chen, W., Mook, R.A., Jr., Premont, R.T. and Wang, J., 2018. Niclosamide: Beyond an antihelminthic drug. *Cell Signal*, 41, pp. 89-96.

Chiang, W.C., Pamp, S.J., Nilsson, M., Givskov, M. and Tolker-Nielsen, T., 2012. The metabolically active subpopulation in Pseudomonas aeruginosa biofilms survives exposure to membrane-targeting antimicrobials via distinct molecular mechanisms. *FEMS Immunol Med Microbiol*, 65(2), pp. 245-256.

Chuchalin, A., Amelina, E. and Bianco, F., 2009. Tobramycin for inhalation in cystic fibrosis: Beyond respiratory improvements. *Pulm Pharmacol Ther*, 22(6), pp. 526-532.

Ciciliani, A.-M., Langguth, P. and Wachtel, H., 2017. In vitro dose comparison of Respimat(®) inhaler with dry powder inhalers for COPD maintenance therapy. *Int J Chron Obstruct Pulmon Dis,* 12, pp. 1565-1577.

Ciofu, O., Mandsberg, L.F., Wang, H. and Hoiby, N., 2012. Phenotypes selected during chronic lung infection in cystic fibrosis patients: implications for the treatment of Pseudomonas aeruginosa biofilm infections. *FEMS Immunol Med Microbiol,* 65(2), pp. 215-225.

Ciofu, O. and Tolker-Nielsen, T., 2019. Tolerance and Resistance of Pseudomonas aeruginosa Biofilms to Antimicrobial Agents—How P. aeruginosa Can Escape Antibiotics. *Front Microbiol,* 10(913). https://doi.org/10.3389/fmicb.2019.00913.

Ciofu, O., Tolker-Nielsen, T., Jensen, P.O., Wang, H. and Hoiby, N., 2015. Antimicrobial resistance, respiratory tract infections and role of biofilms in lung infections in cystic fibrosis patients. *Adv Drug Deliv Rev,* 85, pp. 7-23.

Coffey, B.M. and Anderson, G.G., 2014. Biofilm formation in the 96-well microtiter plate. *Methods Mol Biol,* 1149, pp. 631-641.

Coutinho, H.D., Costa, J.G., Lima, E.O., Falcao-Silva, V.S. and Siqueira-Junior, J.P., 2008. Enhancement of the antibiotic activity against a multiresistant Escherichia coli by Mentha arvensis L. and chlorpromazine. *Chemotherapy,* 54(4), pp. 328-330.

Cummins, J., Reen, F.J., Baysse, C., Mooij, M.J. and O'Gara, F., 2009. Subinhibitory concentrations of the cationic antimicrobial peptide colistin induce the pseudomonas quinolone signal in Pseudomonas aeruginosa. *Microbiology,* 155(9), pp. 2826-2837.

Dafale, N.A., Semwal, U.P., Rajput, R.K. and Singh, G.N., 2016. Selection of appropriate analytical tools to determine the potency and bioactivity of antibiotics and antibiotic resistance. *J Pharm Anal,* 6(4), pp. 207-213.

Damron, F.H. and Goldberg, J.B., 2012. Proteolytic regulation of alginate overproduction in Pseudomonas aeruginosa. *Mol Microbiol,* 84(4), pp. 595-607.

Das, M.C., Sandhu, P., Gupta, P., Rudrapaul, P., De, U.C., Tribedi, P., Akhter, Y. and Bhattacharjee, S., 2016. Attenuation of Pseudomonas aeruginosa biofilm formation by Vitexin: A combinatorial study with azithromycin and gentamicin. *Sci Rep,* 6. https://doi.org/10.1038/srep23347.

Dastidar, S.G., Kristiansen, J.E., Molnar, J. and Amaral, L., 2013. Role of Phenothiazines and Structurally Similar Compounds of Plant Origin in the Fight against Infections by Drug Resistant Bacteria. *Antibiotics (Basel),* 2(1), pp. 58-72.

de Bentzmann, S. and Plesiat, P., 2011. The Pseudomonas aeruginosa opportunistic pathogen and human infections. *Environ Microbiol,* 13(7), pp. 1655-1665.

Delcour, A.H., 2009. Outer membrane permeability and antibiotic resistance. *Biochim Biophys Acta,* 1794(5), pp. 808-816.

Deng, Q., Ou, C., Chen, J. and Xiang, Y., 2018. Particle deposition in tracheobronchial airways of an infant, child and adult. *Sci Total Environ,* 612, pp. 339-346.

Diggle, S.P. and Whiteley, M., 2019. Microbe Profile: Pseudomonas aeruginosa: opportunistic pathogen and lab rat. *Microbiology*. https://doi.org/https://doi.org/10.1099/mic.0.000860.

Doern, C.D., 2014. When does 2 plus 2 equal 5? A review of antimicrobial synergy testing. *J Clin Microbiol*, 52(12), pp. 4124-4128.

Domalaon, R., De Silva, P.M., Kumar, A., Zhanel, G.G. and Schweizer, F., 2019. The Anthelmintic Drug Niclosamide Synergizes with Colistin and Reverses Colistin Resistance in Gram-Negative Bacilli. *Antimicrob Agents Chemother*, 63(4). https://doi.org/10.1128/AAC.02574-18.

Domalaon, R., Idowu, T., Zhanel, G.G. and Schweizer, F., 2018. Antibiotic Hybrids: the Next Generation of Agents and Adjuvants against Gram-Negative Pathogens? *Clin Microbiol Rev*, 31(2). https://doi.org/10.1128/CMR.00077-17.

Doring, G., Conway, S.P., Heijerman, H.G., Hodson, M.E., Hoiby, N., Smyth, A. and Touw, D.J., 2000. Antibiotic therapy against Pseudomonas aeruginosa in cystic fibrosis: a European consensus. *Eur Respir J*, 16(4), pp. 749-767.

Dozzo, P. and Moser, H.E., 2010. New aminoglycoside antibiotics. *Expert Opin Ther Pat*, 20(10), pp. 1321-1341.

Dreier, J. and Ruggerone, P., 2015. Interaction of antibacterial compounds with RND efflux pumps in Pseudomonas aeruginosa. *Front Microbiol*, 6(660). https://doi.org/10.3389/fmicb.2015.00660.

Driscoll, J.A., Brody, S.L. and Kollef, M.H., 2007. The epidemiology, pathogenesis and treatment of Pseudomonas aeruginosa infections. *Drugs*, 67(3), pp. 351-368.

EARS-NET, 2010. *Distribution of aminoglycoside resistance in P. aeruginosa in EARS-Net countries* [Online]. European Antimicrobial Resistance Surveillance Network. Available from: *https://atlas.ecdc.europa.eu/public/index.aspx?Dataset=27&HealthTopic=4* [Accessed 8-2-2020].

EARS-NET, 2018. *Distribution of aminoglycosides resistance P. aeruginosa in EARS-Net countries* [Online]. European Antimicrobial Resistance Surveillance Network. Available from: *https://atlas.ecdc.europa.eu/public/index.aspx?Dataset=27&HealthTopic=4* [Accessed 8-2-2020].

El-Zaher, A.A. and Mahrouse, M.A., 2013. Utility of Experimental Design in Pre-Column Derivatization for the Analysis of Tobramycin by HPLC-Fluorescence Detection: Application to Ophthalmic Solution and Human Plasma. *Anal Chem Insights*, 8, pp. 9-20.

Ernst, R.K., Moskowitz, S.M., Emerson, J.C., Kraig, G.M., Adams, K.N., Harvey, M.D., Ramsey, B., Speert, D.P., Burns, J.L. and Miller, S.I., 2007. Unique lipid a modifications in Pseudomonas aeruginosa isolated from the airways of patients with cystic fibrosis. *J Infect Dis*, 196(7), pp. 1088-1092.

Evans, L.R. and Linker, A., 1973. Production and characterization of the slime polysaccharide of Pseudomonas aeruginosa. *J Bacteriol*, 116(2), pp. 915-924.

Ezraty, B. and Barras, F., 2016. The 'liaisons dangereuses' between iron and antibiotics. *FEMS Microbiol Rev*, 40(3), pp. 418-435.

Fernández, L., Breidenstein, E.B.M. and Hancock, R.E.W., 2011. Creeping baselines and adaptive resistance to antibiotics. *Drug Resist Updat*, 14(1), pp. 1-21.

Field, T.R., White, A., Elborn, J.S. and Tunney, M.M., 2005. Effect of oxygen limitation on the in vitro antimicrobial susceptibility of clinical isolates of Pseudomonas aeruginosa grown planktonically and as biofilms. *Eur J Clin Microbiol Infect Dis*, 24(10), pp. 677-687.

Filloux, A., Hachani, A. and Bleves, S., 2008. The bacterial type VI secretion machine: yet another player for protein transport across membranes. *Microbiology*, 154(6), pp. 1570-1583.

Finnegan, S. and Percival, S.L., 2015. EDTA: An Antimicrobial and Antibiofilm Agent for Use in Wound Care. *Adv Wound Care*, 4(7), pp. 415-421.

Fischbach, M.A. and Walsh, C.T., 2009. Antibiotics for emerging pathogens. *Science*, 325(5944), pp. 1089-1093.

Fong, J., Mortensen, K.T., Norskov, A., Qvortrup, K., Yang, L., Tan, C.H., Nielsen, T.E. and Givskov, M., 2018. Itaconimides as Novel Quorum Sensing Inhibitors of Pseudomonas aeruginosa. *Front Cell Infect Microbiol*, 8. https://doi.org/10.3389/fcimb.2018.00443.

Furiga, A., Lajoie, B., El Hage, S., Baziard, G. and Roques, C., 2015. Impairment of Pseudomonas aeruginosa Biofilm Resistance to Antibiotics by Combining the Drugs with a New Quorum-Sensing Inhibitor. *Antimicrob Agents Chemother*, 60(3), pp. 1676-1686.

Garo, E., Eldridge, G.R., Goering, M.G., DeLancey Pulcini, E., Hamilton, M.A., Costerton, J.W. and James, G.A., 2007. Asiatic acid and corosolic acid enhance the susceptibility of Pseudomonas aeruginosa biofilms to tobramycin. *Antimicrob Agents Chemother*, 51(5), pp. 1813-1817.

Gaspar, M.C., Couet, W., Olivier, J.C., Pais, A.A. and Sousa, J.J., 2013. Pseudomonas aeruginosa infection in cystic fibrosis lung disease and new perspectives of treatment: a review. *Eur J Clin Microbiol Infect Dis*, 32(10), pp. 1231-1252.

Gellatly, S.L. and Hancock, R.E., 2013. Pseudomonas aeruginosa: new insights into pathogenesis and host defenses. *Pathog Dis*, 67(3), pp. 159-173.

Geller, D.E., Pitlick, W.H., Nardella, P.A., Tracewell, W.G. and Ramsey, B.W., 2002. Pharmacokinetics and bioavailability of aerosolized tobramycin in cystic fibrosis. *Chest*, 122(1), pp. 219-226.

Geller, D.E., Weers, J. and Heuerding, S., 2011. Development of an inhaled dry-powder formulation of tobramycin using PulmoSphere technology. *J Aerosol Med Pulm Drug Deliv*, 24(4), pp. 175-182.

Germoni, L.A., Bremer, P.J. and Lamont, I.L., 2016. The effect of alginate lyase on the gentamicin resistance of Pseudomonas aeruginosa in mucoid biofilms. *J Appl Microbiol*, 121(1), pp. 126-135.

Ghani, M. and Soothill, J.S., 1997. Ceftazidime, gentamicin, and rifampicin, in combination, kill biofilms of mucoid Pseudomonas aeruginosa. *Can J Microbiol*, 43(11), pp. 999-1004.

Ghorbani, H., Memar, M.Y., Sefidan, F.Y., Yekani, M. and Ghotaslou, R., 2017. In vitro synergy of antibiotic combinations against planktonic and biofilm Pseudomonas aeruginosa. *GMS Hyg Infect Control*, 12. https://doi.org/10.3205/dgkh000302.

Gi, M., Lee, K.-M., Kim, S.C., Yoon, J.-H., Yoon, S.S. and Choi, J.Y., 2015. A novel siderophore system is essential for the growth of Pseudomonas aeruginosa in airway mucus. *Sci Rep*, 5. https://doi.org/10.1038/srep14644.

Giunta, S., Galeazzi, L., Turchetti, G., Sampaoli, G. and Groppa, G., 1985. In vitro antistreptococcal activity of the potassium-sparing diuretics amiloride and triamterene. *Antimicrob Agents Chemother*, 28(3), pp. 419-420.

Giunta, S., Pieri, C. and Groppa, G., 1984. Amiloride, a diuretic with in vitro antimicrobial activity. *Pharmacol Res Commun*, 16(8), pp. 821-829.

Goldberg, J.B. and Pier, G.B., 2000. The role of the CFTR in susceptibility to Pseudomonas aeruginosa infections in cystic fibrosis. *Trends Microbiol*, 8(11), pp. 514-520.

Gopu, V., Meena, C.K. and Shetty, P.H., 2015. Quercetin Influences Quorum Sensing in Food Borne Bacteria: In-Vitro and In-Silico Evidence. *PLoS One*, 10(8). https://doi.org/10.1371/journal.pone.0134684.

Greally, P., Whitaker, P. and Peckham, D., 2012. Challenges with current inhaled treatments for chronic Pseudomonas aeruginosa infection in patients with cystic fibrosis. *Curr Med Res Opin*, 28(6), pp. 1059-1067.

Guo, C., Gillespie, S.R., Kauffman, J. and Doub, W.H., 2008. Comparison of delivery characteristics from a combination metered-dose inhaler using the Andersen cascade impactor and the next generation pharmaceutical impactor. *J Pharm Sci*, 97(8), pp. 3321-3334.

Guo, M.X., Wrisley, L. and Maygoo, E., 2006. Measurement of tobramycin by reversed-phase high-performance liquid chromatography with mass spectrometry detection. *Anal Chim Acta*, 571(1), pp. 12-16.

Gutu, A.D., Sgambati, N., Strasbourger, P., Brannon, M.K., Jacobs, M.A., Haugen, E., Kaul, R.K., Johansen, H.K., Hoiby, N. and Moskowitz, S.M., 2013. Polymyxin resistance of Pseudomonas aeruginosa phoQ mutants is dependent on additional two-component regulatory systems. *Antimicrob Agents Chemother*, 57(5), pp. 2204-2215.

Haagensen, J.A., Klausen, M., Ernst, R.K., Miller, S.I., Folkesson, A., Tolker-Nielsen, T. and Molin, S., 2007. Differentiation and distribution of colistin- and sodium dodecyl sulfate-tolerant cells in Pseudomonas aeruginosa biofilms. *J Bacteriol*, 189(1), pp. 28-37.

Halfon, Y., Jimenez-Fernandez, A., La Rosa, R., Espinosa Portero, R., Krogh Johansen, H., Matzov, D., Eyal, Z., Bashan, A., Zimmerman, E., Belousoff, M., Molin, S. and Yonath, A., 2019. Structure of ribosomes from an aminoglycoside-resistant clinical isolate. *Proc Natl Acad Sci U S A*, 116(44), pp. 22275-22281.

Hamad, M.A., Di Lorenzo, F., Molinaro, A. and Valvano, M.A., 2012. Aminoarabinose is essential for lipopolysaccharide export and intrinsic antimicrobial peptide resistance in Burkholderia cenocepacia. *Mol Microbiol*, 85(5), pp. 962-974.

Hamed, K., Conti, V., Tian, H. and Loefroth, E., 2017. Adherence to tobramycin inhaled powder vs inhaled solution in patients with cystic fibrosis: analysis of US insurance claims data. *Patient Prefer Adherence*, 11, pp. 831-838.

Haney, E.F., Trimble, M.J., Cheng, J.T., Vallé, Q. and Hancock, R.E.W., 2018. Critical Assessment of Methods to Quantify Biofilm Growth and Evaluate Antibiofilm Activity of Host Defence Peptides. *Biomolecules*, 8(2). https://doi.org/10.3390/biom8020029.

Harrison, F. and Diggle, S.P., 2016. An ex vivo lung model to study bronchioles infected with Pseudomonas aeruginosa biofilms. *Microbiology*, 162(10), pp. 1755-1760.

Haussler, S., Ziegler, I., Lottel, A., von Gotz, F., Rohde, M., Wehmhohner, D., Saravanamuthu, S., Tummler, B. and Steinmetz, I., 2003. Highly adherent small-colony variants of Pseudomonas aeruginosa in cystic fibrosis lung infection. *J Med Microbiol*, 52(4), pp. 295-301.

Heijerman, H., Westerman, E., Conway, S. and Touw, D., 2009. Inhaled medication and inhalation devices for lung disease in patients with cystic fibrosis: A European consensus. *J Cyst Fibros*, 8(5), pp. 295-315.

Hendricks, O., Butterworth, T.S. and Kristiansen, J.E., 2003. The in-vitro antimicrobial effect of non-antibiotics and putative inhibitors of efflux pumps on Pseudomonas aeruginosa and Staphylococcus aureus. *Int J Antimicrob Agents*, 22(3), pp. 262-264.

Hentzer, M., Riedel, K., Rasmussen, T.B., Heydorn, A., Andersen, J.B., Parsek, M.R., Rice, S.A., Eberl, L., Molin, S., Hoiby, N., Kjelleberg, S. and Givskov, M., 2002. Inhibition of quorum sensing in Pseudomonas aeruginosa biofilm bacteria by a halogenated furanone compound. *Microbiology*, 148(1), pp. 87-102.

Hentzer, M., Teitzel, G.M., Balzer, G.J., Heydorn, A., Molin, S., Givskov, M. and Parsek, M.R., 2001. Alginate overproduction affects Pseudomonas aeruginosa biofilm structure and function. *J Bacteriol*, 183(18), pp. 5395-5401.

Hentzer, M., Wu, H., Andersen, J.B., Riedel, K., Rasmussen, T.B., Bagge, N., Kumar, N., Schembri, M.A., Song, Z., Kristoffersen, P., Manefield, M., Costerton, J.W., Molin, S., Eberl, L., Steinberg, P., Kjelleberg, S., Hoiby, N. and Givskov, M., 2003. Attenuation of Pseudomonas aeruginosa virulence by quorum sensing inhibitors. *EMBO J*, 22(15), pp. 3803-3815.

Herrmann, G., Yang, L., Wu, H., Song, Z., Wang, H., Hoiby, N., Ulrich, M., Molin, S., Riethmuller, J. and Doring, G., 2010. Colistin-tobramycin combinations are superior to monotherapy concerning the killing of biofilm Pseudomonas aeruginosa. *J Infect Dis*, 202(10), pp. 1585-1592.

Hill, D., Rose, B., Pajkos, A., Robinson, M., Bye, P., Bell, S., Elkins, M., Thompson, B., MacLeod, C., Aaron, S.D. and Harbour, C., 2005. Antibiotic Susceptibilities of Pseudomonas aeruginosa Isolates Derived from Patients with Cystic Fibrosis under Aerobic, Anaerobic, and Biofilm Conditions. *J Clin Microbiol*, 43(10), pp. 5085-5090.

Hirai, I., Okuno, M., Katsuma, R., Arita, N., Tachibana, M. and Yamamoto, Y., 2010. Characterisation of anti-Staphylococcus aureus activity of quercetin. *Int J Food Sci Tech*, 45(6), pp. 1250-1254.

Hocquet, D., Vogne, C., El Garch, F., Vejux, A., Gotoh, N., Lee, A., Lomovskaya, O. and Plesiat, P., 2003. MexXY-OprM efflux pump is necessary for a adaptive resistance of Pseudomonas aeruginosa to aminoglycosides. *Antimicrob Agents Chemother*, 47(4), pp. 1371-1375.

Hoffman, L.R., D'Argenio, D.A., MacCoss, M.J., Zhang, Z., Jones, R.A. and Miller, S.I., 2005. Aminoglycoside antibiotics induce bacterial biofilm formation. *Nature*, 436(7054), pp. 1171-1175.

Hoffmann, N., Rasmussen, T.B., Jensen, P.O., Stub, C., Hentzer, M., Molin, S., Ciofu, O., Givskov, M., Johansen, H.K. and Hoiby, N., 2005. Novel mouse model of chronic Pseudomonas aeruginosa lung infection mimicking cystic fibrosis. *Infect Immun*, 73(4), pp. 2504-2514.

Hogardt, M. and Heesemann, J., 2010. Adaptation of Pseudomonas aeruginosa during persistence in the cystic fibrosis lung. *Int J Med Microbiol*, 300(8), pp. 557-562.

Hoiby, N., 2011. Recent advances in the treatment of Pseudomonas aeruginosa infections in cystic fibrosis. *BMC Med*, 9. https://doi.org/10.1186/1741-7015-9-32.

Hoiby, N., Bjarnsholt, T., Givskov, M., Molin, S. and Ciofu, O., 2010a. Antibiotic resistance of bacterial biofilms. *Int J Antimicrob Agents*, 35(4), pp. 322-332.

Hoiby, N., Ciofu, O. and Bjarnsholt, T., 2010b. Pseudomonas aeruginosa biofilms in cystic fibrosis. *Future Microbiol*, 5(11), pp. 1663-1674.

Housseini B Issa, K., Phan, G. and Broutin, I., 2018. Functional Mechanism of the Efflux Pumps Transcription Regulators From Pseudomonas aeruginosa Based on 3D Structures. *Front Mol Biosci*, 5. https://doi.org/10.3389/fmolb.2018.00057.

Huang, J.X., Blaskovich, M.A., Pelingon, R., Ramu, S., Kavanagh, A., Elliott, A.G., Butler, M.S., Montgomery, A.B. and Cooper, M.A., 2015. Mucin Binding Reduces Colistin Antimicrobial Activity. *Antimicrob Agents Chemother*, 59(10), pp. 5925-5931.

Imperi, F., Massai, F., Ramachandran Pillai, C., Longo, F., Zennaro, E., Rampioni, G., Visca, P. and Leoni, L., 2013. New life for an old drug: the anthelmintic drug niclosamide inhibits Pseudomonas aeruginosa quorum sensing. *Antimicrob Agents Chemother*, 57(2), pp. 996-1005.

Jan, A.T., 2017. Outer Membrane Vesicles (OMVs) of Gram-negative Bacteria: A Perspective Update. *Front Microbiol*, 8(1053). https://doi.org/10.3389/fmicb.2017.01053.

Jinno, J.-i., Kamada, N., Miyake, M., Yamada, K., Mukai, T., Odomi, M., Toguchi, H., Liversidge, G.G., Higaki, K. and Kimura, T., 2006. Effect of particle size reduction on dissolution and oral absorption of a poorly water-soluble drug, cilostazol, in beagle dogs. *J Control Release*, 111(1), pp. 56-64.

Jung, I.Y., Jeong, S.J., Lee, K.M., Ahn, J.Y., Ku, N.S., Han, S.H., Choi, J.Y., Yong, D., Yoon, S.S., Song, Y.G., Jeong, S.H., Kim, J.M. and Lee, K., 2018. Risk factors for mortality in patients with Pseudomonas aeruginosa pneumonia: Clinical impact of mucA gene mutation. *Respir Med,* 140, pp. 27-31.

Kaatz, G.W., Moudgal, V.V., Seo, S.M., Hansen, J.B. and Kristiansen, J.E., 2003. Phenylpiperidine selective serotonin reuptake inhibitors interfere with multidrug efflux pump activity in Staphylococcus aureus. *Int J Antimicrob Agents,* 22(3), pp. 254-261.

Kang, D. and Kirienko, N.V., 2018. Interdependence between iron acquisition and biofilm formation in Pseudomonas aeruginosa. *J Microbiol,* 56(7), pp. 449-457.

Kaushik, K.S., Stolhandske, J., Shindell, O., Smyth, H.D. and Gordon, V.D., 2016. Tobramycin and bicarbonate synergise to kill planktonic Pseudomonas aeruginosa, but antagonise to promote biofilm survival. *NPJ Biofilms Microbiomes*, 2. https://doi.org/10.1038/npjbiofilms.2016.6.

Khalil, H., Chen, T., Riffon, R., Wang, R. and Wang, Z., 2008. Synergy between polyethylenimine and different families of antibiotics against a resistant clinical isolate of Pseudomonas aeruginosa. *Antimicrob Agents Chemother,* 52(5), pp. 1635-1641.

Kipnis, E., Sawa, T. and Wiener-Kronish, J., 2006. Targeting mechanisms of Pseudomonas aeruginosa pathogenesis. *Med Mal Infect,* 36(2), pp. 78-91.

Kirchner, S., Fothergill, J.L., Wright, E.A., James, C.E., Mowat, E. and Winstanley, C., 2012. Use of artificial sputum medium to test antibiotic efficacy against Pseudomonas aeruginosa in conditions more relevant to the cystic fibrosis lung. *J Vis Exp*, (64). https://doi.org/10.3791/3857.

Kiser, T.H., Obritsch, M.D., Jung, R., MacLaren, R. and Fish, D.N., 2010. Efflux pump contribution to multidrug resistance in clinical isolates of Pseudomonas aeruginosa. *Pharmacotherapy,* 30(7), pp. 632-638.

Kohanski, M.A., Dwyer, D.J., Hayete, B., Lawrence, C.A. and Collins, J.J., 2007. A common mechanism of cellular death induced by bactericidal antibiotics. *Cell,* 130(5), pp. 797-810.

Konstan, M.W., Geller, D.E., Minic, P., Brockhaus, F., Zhang, J. and Angyalosi, G., 2011. Tobramycin inhalation powder for P. aeruginosa infection in cystic fibrosis: the EVOLVE trial. *Pediatr Pulmonol*, 46(3), pp. 230-238.

Krause, K.M., Serio, A.W., Kane, T.R. and Connolly, L.E., 2016. Aminoglycosides: An Overview. *Cold Spring Harb Perspect Med*, 6(6). https://doi.org/10.1101/cshperspect.a027029.

Kreamer, N.N., Costa, F. and Newman, D.K., 2015. The ferrous iron-responsive BqsRS two-component system activates genes that promote cationic stress tolerance. *MBio*, 6(2). https://doi.org/10.1128/mBio.02549-14.

Kristiansen, J.E. and Amaral, L., 1997. The potential management of resistant infections with non-antibiotics. *J Antimicrob Chemother,* 40(3), pp. 319-327.

Kristiansen, J.E., Thomsen, V.F., Martins, A., Viveiros, M. and Amaral, L., 2010. Non-antibiotics reverse resistance of bacteria to antibiotics. *In Vivo,* 24(5), pp. 751-754.

Kuehl, R., Al-Bataineh, S., Gordon, O., Luginbuehl, R., Otto, M., Textor, M. and Landmann, R., 2009. Furanone at Subinhibitory Concentrations Enhances Staphylococcal Biofilm Formation by *Lux S* Repression. *Antimicrob Agents Chemother,* 53(10), pp. 4159-4166.

Kukavica-Ibrulj, I. and Levesque, R.C., 2008. Animal models of chronic lung infection with Pseudomonas aeruginosa: useful tools for cystic fibrosis studies. *Lab Anim,* 42(4), pp. 389-412.

Kung, V.L., Ozer, E.A. and Hauser, A.R., 2010. The accessory genome of Pseudomonas aeruginosa. *Microbiol Mol Biol Rev,* 74(4), pp. 621-641.

LaBauve, A.E. and Wargo, M.J., 2012. Growth and laboratory maintenance of Pseudomonas aeruginosa. *Curr Protoc Microbiol,* 25(1), pp. 6E.1.1-6E.1.8.

Labiris, N.R. and Dolovich, M.B., 2003. Pulmonary drug delivery. Part II: The role of inhalant delivery devices and drug formulations in therapeutic effectiveness of aerosolized medications. *Br J Clin Pharmacol,* 56(6), pp. 600-612.

Lai, S.K., Wang, Y.Y. and Hanes, J., 2009. Mucus-penetrating nanoparticles for drug and gene delivery to mucosal tissues. *Adv Drug Deliv Rev,* 61(2), pp. 158-171.

Lambert, R.J., Hanlon, G.W. and Denyer, S.P., 2004. The synergistic effect of EDTA/antimicrobial combinations on Pseudomonas aeruginosa. *J Appl Microbiol,* 96(2), pp. 244-253.

Lamppa, J.W. and Griswold, K.E., 2013. Alginate Lyase Exhibits Catalysis-Independent Biofilm Dispersion and Antibiotic Synergy. *Antimicrob Agents Chemother,* 57(1), pp. 137-145.

Laudy, A.E., Kulińska, E. and Tyski, S., 2017. The Impact of Efflux Pump Inhibitors on the Activity of Selected Non-Antibiotic Medicinal Products against Gram-Negative Bacteria. *Molecules,* 22(1). https://doi.org/10.3390/molecules22010114.

Leach, C., Colice, G.L. and Luskin, A., 2009. Particle size of inhaled corticosteroids: Does it matter? *J Allergy Clin Immunol,* 124(6), pp. S88-S93.

Lee, S.H., Teo, J., Heng, D., Ng, W.K., Zhao, Y. and Tan, R.B., 2016. Tailored Antibiotic Combination Powders for Inhaled Rotational Antibiotic Therapy. *J Pharm Sci,* 105(4), pp. 1501-1512.

Leitão, J.H., Alvim, T. and Sá-Correia, I., 1996. Ribotyping of Pseudomonas aeruginosa isolates from patients and water springs and genome fingerprinting of variants concerning mucoidy. *FEMS Immunol Med Microbiol,* 13(4), pp. 287-292.

Lenoir, G., Antypkin, Y.G., Miano, A., Moretti, P., Zanda, M., Varoli, G., Monici Preti, P.A. and Aryayev, N.L., 2007. Efficacy, safety, and local pharmacokinetics of highly concentrated nebulized tobramycin in patients with cystic fibrosis colonized with Pseudomonas aeruginosa. *Paediatr Drugs,* 9 Suppl 1, pp. 11-20.

Li, X., Plésiat, P. and Nikaido, H., 2015. The challenge of efflux-mediated antibiotic resistance in Gram-negative bacteria. *Clin Microbiol Rev*, 28(2), pp. 337-418.

Li, X., Vogt, F.G., Hayes, D., Jr. and Mansour, H.M., 2014. Design, characterization, and aerosol dispersion performance modeling of advanced co-spray dried antibiotics with mannitol as respirable microparticles/nanoparticles for targeted pulmonary delivery as dry powder inhalers. *J Pharm Sci*, 103(9), pp. 2937-2949.

Linares, J.F., Gustafsson, I., Baquero, F. and Martinez, J.L., 2006. Antibiotics as intermicrobial signaling agents instead of weapons. *Proc Natl Acad Sci U S A*, 103(51), pp. 19484-19489.

Lister, P.D., Wolter, D.J. and Hanson, N.D., 2009. Antibacterial-resistant Pseudomonas aeruginosa: clinical impact and complex regulation of chromosomally encoded resistance mechanisms. *Clin Microbiol Rev*, 22(4), pp. 582-610.

Liu, D., Pan, H., He, F., Wang, X., Li, J., Yang, X. and Pan, W., 2015. Effect of particle size on oral absorption of carvedilol nanosuspensions: in vitro and in vivo evaluation. *Int J Nanomedicine*, 10, pp. 6425-6434.

Liu, Z., Lin, Y., Lu, Q., Li, F., Yu, J., Wang, Z., He, Y. and Song, C., 2017. In vitro and in vivo activity of EDTA and antibacterial agents against the biofilm of mucoid Pseudomonas aeruginosa. *Infection*, 45(1), pp. 23-31.

Lutz, L., Leão, R.S., Ferreira, A.G., Pereira, D.C., Raupp, C., Pitt, T., Marques, E.A. and Barth, A.L., 2013. Hypermutable Pseudomonas aeruginosa in Cystic fibrosis patients from two Brazilian cities. *J Clin Microbiol*, 51(3), pp. 927-930.

Lyczak, J.B., Cannon, C.L. and Pier, G.B., 2000. Establishment of Pseudomonas aeruginosa infection: lessons from a versatile opportunist. *Microbes Infect*, 2(9), pp. 1051-1060.

Maeda, T., Garcia-Contreras, R., Pu, M., Sheng, L., Garcia, L.R., Tomas, M. and Wood, T.K., 2012. Quorum quenching quandary: resistance to antivirulence compounds. *Isme j*, 6(3), pp. 493-501.

Magiorakos, A.P., Srinivasan, A., Carey, R.B., Carmeli, Y., Falagas, M.E., Giske, C.G., Harbarth, S., Hindler, J.F., Kahlmeter, G., Olsson-Liljequist, B., Paterson, D.L., Rice, L.B., Stelling, J., Struelens, M.J., Vatopoulos, A., Weber, J.T. and Monnet, D.L., 2012. Multidrug-resistant, extensively drug-resistant and pandrug-resistant bacteria: an international expert proposal for interim standard definitions for acquired resistance. *Clin Microbiol Infect*, 18(3), pp. 268-281.

Maiden, M.M., Hunt, A.M.A., Zachos, M.P., Gibson, J.A., Hurwitz, M.E., Mulks, M.H. and Waters, C.M., 2018. Triclosan Is an Aminoglycoside Adjuvant for Eradication of Pseudomonas aeruginosa Biofilms. *Antimicrob Agents Chemother*, 62(6). https://doi.org/10.1128/aac.00146-18.

Malone, J.G., 2015. Role of small colony variants in persistence of Pseudomonas aeruginosa infections in cystic fibrosis lungs. *Infect Drug Resist*, 8, pp. 237-247.

Mandal, A., Sinha, C., Kumar Jena, A., Ghosh, S. and Samanta, A., 2010. An Investigation on in vitro and in vivo Antimicrobial Properties of the Antidepressant: Amitriptyline Hydrochloride. *Braz J Microbiol*, 41(3), pp. 635-645.

Mangal, S., Nie, H., Xu, R., Guo, R., Cavallaro, A., Zemlyanov, D. and Zhou, Q.T., 2018. Physico-Chemical Properties, Aerosolization and Dissolution of Co-Spray Dried Azithromycin Particles with L-Leucine for Inhalation. *Pharm Res*, 35(2). https://doi.org/10.1007/s11095-017-2334-9.

Marple, V., Roberts, D., Romay, F., C Miller, N., G Truman, K., Van Oort, M., Olsson, B., J Holroyd, M., Mitchell, J. and Hochrainer, D., 2003. Next Generation Pharmaceutical Impactor (A New Impactor for Pharmaceutical Inhaler Testing). Part I: Design. *J Aerosol Med Pulm Drug Deliv*, 16, pp. 283-299.

Marshall, L.J., Oguejiofor, W., Price, R. and Shur, J., 2016. Investigation of the enhanced antimicrobial activity of combination dry powder inhaler formulations of lactoferrin. *Int J Pharm*, 514(2), pp. 399-406.

Masák, J., Čejková, A., Schreiberová, O. and Řezanka, T., 2014. Pseudomonas biofilms: possibilities of their control. *FEMS Microbiol Ecol*, 89(1), pp. 1-14.

Mathee, K., Narasimhan, G., Valdes, C., Qiu, X., Matewish, J.M., Koehrsen, M., Rokas, A., Yandava, C.N., Engels, R., Zeng, E., Olavarietta, R., Doud, M., Smith, R.S., Montgomery, P., White, J.R., Godfrey, P.A., Kodira, C., Birren, B., Galagan, J.E. and Lory, S., 2008. Dynamics of Pseudomonas aeruginosa genome evolution. *Proc Natl Acad Sci U S A*, 105(8), pp. 3100-3105.

McKeage, K., 2013. Tobramycin Inhalation Powder: A Review of Its Use in the Treatment of Chronic Pseudomonas aeruginosa Infection in Patients with Cystic Fibrosis. *Drugs*, 73(16), pp. 1815-1827.

Meletiadis, J., Pournaras, S., Roilides, E. and Walsh, T.J., 2010. Defining Fractional Inhibitory Concentration Index Cutoffs for Additive Interactions Based on Self-Drug Additive Combinations, Monte Carlo Simulation Analysis, and *In vitro-In Vivo* Correlation Data for Antifungal Drug Combinations against Aspergillus fumigatus. *Antimicrob Agents Chemother*, 54(2), pp. 602-609.

Merritt, J.H., Kadouri, D.E. and O'Toole, G.A., 2005. Growing and analyzing static biofilms. *Curr Protoc Microbiol*, Chapter 1. https://doi.org/10.1002/9780471729259.mc01b01s00.

Meylan, S., Porter, C.B.M., Yang, J.H., Belenky, P., Gutierrez, A., Lobritz, M.A., Park, J., Kim, S.H., Moskowitz, S.M. and Collins, J.J., 2017. Carbon Sources Tune Antibiotic Susceptibility in Pseudomonas aeruginosa via Tricarboxylic Acid Cycle Control. *Cell chemical biology*, 24(2), pp. 195-206.

Middleton, P.G., Kidd, T.J. and Williams, B., 2005. Combination aerosol therapy to treat Burkholderia cepacia complex. *Eur Respir J*, 26(2), pp. 305-308.

Miller, D.P., Tan, T., Nakamura, J., Malcolmson, R.J., Tarara, T.E. and Weers, J.G., 2017. Physical Characterization of Tobramycin Inhalation Powder: II. State Diagram of an Amorphous Engineered Particle Formulation. *Mol Pharm*, 14(6), pp. 1950-1960.

Miró-Canturri, A., Ayerbe-Algaba, R. and Smani, Y., 2019. Drug Repurposing for the Treatment of Bacterial and Fungal Infections. *Front Microbiol*, 10(41). https://doi.org/10.3389/fmicb.2019.00041.

Mishra, S.K., Basukala, P., Basukala, O., Parajuli, K., Pokhrel, B.M. and Rijal, B.P., 2015. Detection of Biofilm Production and Antibiotic Resistance Pattern in Clinical Isolates from Indwelling Medical Devices. *Curr Microbiol*, 70(1), pp. 128-134.

Mitchell, J., Newman, S. and Chan, H.K., 2007. In vitro and in vivo aspects of cascade impactor tests and inhaler performance: a review. *AAPS PharmSciTech*, 8(4). https://doi.org/10.1208/pt0804110.

Moller, S.A., Jensen, P.O., Hoiby, N., Ciofu, O., Kragh, K.N., Bjarnsholt, T. and Kolpen, M., 2019. Hyperbaric oxygen treatment increases killing of aggregating Pseudomonas aeruginosa isolates from cystic fibrosis patients. *J Cyst Fibros*, 18(5), pp. 657-664.

Momin, M.A.M., Tucker, I.G., Doyle, C.S., Denman, J.A., Sinha, S. and Das, S.C., 2018. Co-spray drying of hygroscopic kanamycin with the hydrophobic drug rifampicin to improve the aerosolization of kanamycin powder for treating respiratory infections. *Int J Pharm*, 541(1), pp. 26-36.

Moore, J.E. and Mastoridis, P., 2017. Clinical implications of Pseudomonas aeruginosa location in the lungs of patients with cystic fibrosis. *J Clin Pharm Ther*, 42(3), pp. 259-267.

Moreau-Marquis, S., Coutermarsh, B. and Stanton, B.A., 2015. Combination of hypothiocyanite and lactoferrin (ALX-109) enhances the ability of tobramycin and aztreonam to eliminate Pseudomonas aeruginosa biofilms growing on cystic fibrosis airway epithelial cells. *J Antimicrob Chemother*, 70(1), pp. 160-166.

Moreau-Marquis, S., O'Toole, G.A. and Stanton, B.A., 2009. Tobramycin and FDA-approved iron chelators eliminate Pseudomonas aeruginosa biofilms on cystic fibrosis cells. *Am J Respir Cell Mol Biol*, 41(3), pp. 305-313.

Morita, Y., Tomida, J. and Kawamura, Y., 2014. Responses of Pseudomonas aeruginosa to antimicrobials. *Front Microbiol*, 4. https://doi.org/10.3389/fmicb.2013.00422.

Muheim, C., Gotzke, H., Eriksson, A.U., Lindberg, S., Lauritsen, I., Norholm, M.H.H. and Daley, D.O., 2017. Increasing the permeability of Escherichia coli using MAC13243. *Sci Rep*, 7(1). https://doi.org/10.1038/s41598-017-17772-6.

Munoz-Bellido, J.L., Munoz-Criado, S. and Garcia-Rodriguez, J.A., 2000. Antimicrobial activity of psychotropic drugs: selective serotonin reuptake inhibitors. *Int J Antimicrob Agents*, 14(3), pp. 177-180.

Musk, D.J., Banko, D.A. and Hergenrother, P.J., 2005. Iron salts perturb biofilm formation and disrupt existing biofilms of Pseudomonas aeruginosa. *Chem Biol*, 12(7), pp. 789-796.

Nafee, N., Husari, A., Maurer, C.K., Lu, C., de Rossi, C., Steinbach, A., Hartmann, R.W., Lehr, C.M. and Schneider, M., 2014. Antibiotic-free nanotherapeutics: ultra-small, mucus-penetrating solid lipid nanoparticles enhance the pulmonary delivery and anti-virulence efficacy of novel quorum sensing inhibitors. *J Control Release*, 192, pp. 131-140.

Nehme, H., Saulnier, P., Ramadan, A.A., Cassisa, V., Guillet, C., Eveillard, M. and Umerska, A., 2018. Antibacterial activity of antipsychotic agents, their association with lipid nanocapsules and its impact on the properties of the nanocarriers and on antibacterial activity. *PLoS One*, 13(1). https://doi.org/10.1371/journal.pone.0189950.

Nikaido, H., 1996. Multidrug efflux pumps of gram-negative bacteria. *J Bacteriol*, 178(20), pp. 5853-5859.

Nikaido, H., 2003. Molecular Basis of Bacterial Outer Membrane Permeability Revisited. *Microbiol Mol Biol Rev*, 67(4), pp. 593-656.

Nikaido, H., 2011. Structure and mechanism of RND-type multidrug efflux pumps. *Adv Enzymol Relat Areas Mol Biol*, 77, pp. 1-60.

Nikaido, H. and Pagès, J.-M., 2012. Broad-specificity efflux pumps and their role in multidrug resistance of Gram-negative bacteria. *FEMS Microbiol Rev*, 36(2), pp. 340-363.

Nikaido, H. and Vaara, M., 1985. Molecular basis of bacterial outer membrane permeability. *Microbiol Rev*, 49(1), pp. 1-32.

Oglesby-Sherrouse, A.G., Djapgne, L., Nguyen, A.T., Vasil, A.I. and Vasil, M.L., 2014. The complex interplay of iron, biofilm formation, and mucoidy affecting antimicrobial resistance of Pseudomonas aeruginosa. *Pathog Dis*, 70(3), pp. 307-320.

Oliva, A., Garzoli, S., De Angelis, M., Marzuillo, C., Vullo, V., Mastroianni, C.M. and Ragno, R., 2019. In-Vitro Evaluation of Different Antimicrobial Combinations with and without Colistin Against Carbapenem-Resistant Acinetobacter Baumannii. *Molecules*, 24(5). https://doi.org/10.3390/molecules24050886.

Olivares, E., Badel-Berchoux, S., Provot, C., Jaulhac, B., Prevost, G., Bernardi, T. and Jehl, F., 2017. Tobramycin and Amikacin Delay Adhesion and Microcolony Formation in Pseudomonas aeruginosa Cystic Fibrosis Isolates. *Front Microbiol*, 8. https://doi.org/10.3389/fmicb.2017.01289.

Orhan, G., Bayram, A., Zer, Y. and Balci, I., 2005. Synergy tests by E test and checkerboard methods of antimicrobial combinations against Brucella melitensis. *J Clin Microbiol*, 43(1), pp. 140-143.

Otto, R.G., van Gorp, E., Kloezen, W., Meletiadis, J., van den Berg, S. and Mouton, J.W., 2019. An alternative strategy for combination therapy: Interactions between polymyxin B and non-antibiotics. *Int J Antimicrob Agents*, 53(1), pp. 34-39.

Ozer, E.A., Allen, J.P. and Hauser, A.R., 2014. Characterization of the core and accessory genomes of Pseudomonas aeruginosa using bioinformatic tools Spine and AGEnt. *BMC Genomics*, 15(1). https://doi.org/10.1186/1471-2164-15-737.

Pamp, S.J., Gjermansen, M., Johansen, H.K. and Tolker-Nielsen, T., 2008. Tolerance to the antimicrobial peptide colistin in Pseudomonas aeruginosa biofilms is linked to metabolically active cells, and depends on the pmr and mexAB-oprM genes. *Mol Microbiol*, 68(1), pp. 223-240.

Parumasivam, T., Leung, S.S.Y., Tang, P., Mauro, C., Britton, W. and Chan, H.-K., 2017. The Delivery of High-Dose Dry Powder Antibiotics by a Low-Cost Generic Inhaler. *AAPS J*, 19(1), pp. 191-202.

Patton, J.S., Brain, J.D., Davies, L.A., Fiegel, J., Gumbleton, M., Kim, K.J., Sakagami, M., Vanbever, R. and Ehrhardt, C., 2010. The particle has landed--characterizing the fate of inhaled pharmaceuticals. *J Aerosol Med Pulm Drug Deliv*, 23 Suppl 2, pp. S71-87.

Pawlikowska-Pawlęga, B., Ignacy Gruszecki, W., Misiak, L., Paduch, R., Piersiak, T., Zarzyka, B., Pawelec, J. and Gawron, A., 2007. Modification of membranes by quercetin, a naturally occurring flavonoid, via its incorporation in the polar head group. *Biochim Biophys Acta*, 1768(9), pp. 2195-2204.

Pilcer, G., Rosiere, R., Traina, K., Sebti, T., Vanderbist, F. and Amighi, K., 2013. New co-spray-dried tobramycin nanoparticles-clarithromycin inhaled powder systems for lung infection therapy in cystic fibrosis patients. *J Pharm Sci*, 102(6), pp. 1836-1846.

Pilcer, G., Vanderbist, F. and Amighi, K., 2008. Correlations between cascade impactor analysis and laser diffraction techniques for the determination of the particle size of aerosolised powder formulations. *Int J Pharm*, 358(1), pp. 75-81.

Price, R. and Shur, J., 2018. *Apparatus and method for determination of the fine particle dose of a powder inhalation formulation*. United States Patent and Trademark Office *US 2018/0275022 A1*. Mar. 19,2018.

Pritt, B., O'Brien, L. and Winn, W., 2007. Mucoid Pseudomonas in cystic fibrosis. *Am J Clin Pathol*, 128(1), pp. 32-34.

Rajamuthiah, R., Fuchs, B.B., Conery, A.L., Kim, W., Jayamani, E., Kwon, B., Ausubel, F.M. and Mylonakis, E., 2015. Repurposing salicylanilide anthelmintic drugs to combat drug resistant Staphylococcus aureus. *PLoS One*, 10(4). https://doi.org/10.1371/journal.pone.0124595.

Ramirez, M.S. and Tolmasky, M.E., 2010. Aminoglycoside modifying enzymes. *Drug Resist Updat*, 13(6), pp. 151-171.

Rampioni, G., Pillai, C.R., Longo, F., Bondi, R., Baldelli, V., Messina, M., Imperi, F., Visca, P. and Leoni, L., 2017a. Effect of efflux pump inhibition on Pseudomonas aeruginosa transcriptome and virulence. *Sci Rep*, 7(1). https://doi.org/10.1038/s41598-017-11892-9.

Rampioni, G., Visca, P., Leoni, L. and Imperi, F., 2017b. Drug repurposing for antivirulence therapy against opportunistic bacterial pathogens. *Emerg Top Life Sci*, 1(1), pp. 13-22.

Ratjen, F., Brockhaus, F. and Angyalosi, G., 2009. Aminoglycoside therapy against Pseudomonas aeruginosa in cystic fibrosis: A review. *J Cyst Fibros*, 8(6), pp. 361-369.

Reza, A., Sutton, M.J. and Rahman, M.K., 2019. Effectiveness of Efflux Pump Inhibitors as Biofilm Disruptors and Resistance Breakers in Gram-Negative (ESKAPEE) Bacteria. *Antibiotics*, 8(4). https://doi.org/10.3390/antibiotics8040229.

Riley, T., Christopher, D., Arp, J., Casazza, A., Colombani, A., Cooper, A., Dey, M., Maas, J., Mitchell, J., Reiners, M., Sigari, N., Tougas, T. and Lyapustina, S., 2012. Challenges with

developing in vitro dissolution tests for orally inhaled products (OIPs). *AAPS PharmSciTech*, 13(3), pp. 978-989.

Roberts, A.E., Kragh, K.N., Bjarnsholt, T. and Diggle, S.P., 2015. The Limitations of In Vitro Experimentation in Understanding Biofilms and Chronic Infection. *J Mol Biol*, 427(23), pp. 3646-3661.

Roberts, D.L. and Mitchell, J.P., 2013. The effect of nonideal cascade impactor stage collection efficiency curves on the interpretation of the size of inhaler-generated aerosols. *AAPS PharmSciTech*, 14(2), pp. 497-510.

Roberts, D.L. and Mitchell, J.P., 2019. Measurement of Aerodynamic Particle Size Distribution of Orally Inhaled Products by Cascade Impactor: How to Let the Product Specification Drive the Quality Requirements of the Cascade Impactor. *AAPS PharmSciTech*, 20(2). https://doi.org/10.1208/s12249-018-1276-9.

Rogan, M.P., Taggart, C.C., Greene, C.M., Murphy, P.G., O'Neill, S.J. and McElvaney, N.G., 2004. Loss of microbicidal activity and increased formation of biofilm due to decreased lactoferrin activity in patients with cystic fibrosis. *J Infect Dis*, 190(7), pp. 1245-1253.

Rowland, M., Cavecchi, A., Thielmann, F., Kulon, J., Shur, J. and Price, R., 2018. Measuring The Bipolar Charge Distributions of Fine Particle Aerosol Clouds of Commercial PMDI Suspensions Using a Bipolar Next Generation Impactor (bp-NGI). *Pharm Res*, 36(1). https://doi.org/10.1007/s11095-018-2544-9.

Roy, R., Tiwari, M., Donelli, G. and Tiwari, V., 2018. Strategies for combating bacterial biofilms: A focus on anti-biofilm agents and their mechanisms of action. *Virulence*, 9(1), pp. 522-554.

Rybtke, M.T., Jensen, P.O., Hoiby, N., Givskov, M., Tolker-Nielsen, T. and Bjarnsholt, T., 2011. The implication of Pseudomonas aeruginosa biofilms in infections. *Inflamm Allergy Drug Targets*, 10(2), pp. 141-157.

Sader, H.S., Huynh, H.K. and Jones, R.N., 2003. Contemporary in vitro synergy rates for aztreonam combined with newer fluoroquinolones and beta-lactams tested against gram-negative bacilli. *Diagn Microbiol Infect Dis*, 47(3), pp. 547-550.

Sato, Y., Unno, Y., Ubagai, T. and Ono, Y., 2018. Sub-minimum inhibitory concentrations of colistin and polymyxin B promote Acinetobacter baumannii biofilm formation. *PLoS One*, 13(3). https://doi.org/10.1371/journal.pone.0194556.

Schaible, U.E. and Kaufmann, S.H., 2004. Iron and microbial infection. *Nat Rev Microbiol*, 2(12), pp. 946-953.

Schneider-Futschik, E.K., Paulin, O.K.A., Hoyer, D., Roberts, K.D., Ziogas, J., Baker, M.A., Karas, J., Li, J. and Velkov, T., 2018. Sputum Active Polymyxin Lipopeptides: Activity against Cystic Fibrosis Pseudomonas aeruginosa Isolates and Their Interactions with Sputum Biomolecules. *ACS Infect Dis*, 4(5), pp. 646-655.

Schroeder, M., Brooks, B.D. and Brooks, A.E., 2017. The Complex Relationship between Virulence and Antibiotic Resistance. *Genes*, 8(1). https://doi.org/10.3390/genes8010039.

Schulz, M. and Schmoldt, A., 2003. Therapeutic and toxic blood concentrations of more than 800 drugs and other xenobiotics. *Die Pharmazie*, 58, pp. 447-474.

Seale, J.P., Dittmer, T., Sigman, E.J., Clemons, H. and Johnson, J.A., 2014. Combined abuse of clonidine and amitriptyline in a patient on buprenorphine maintenance treatment. *J Addict Med*, 8(6), pp. 476-478.

Shah, P.L., Scott, S.F., Geddes, D.M., Conway, S., Watson, A., Nazir, T., Carr, S.B., Wallis, C., Marriott, C. and Hodson, M.E., 1997. An evaluation of two aerosol delivery systems for rhDNase. *Eur Respir J*, 10(6), pp. 1261-1266.

She, P., Wang, Y., Luo, Z., Chen, L., Tan, R., Wang, Y. and Wu, Y., 2018. Meloxicam inhibits biofilm formation and enhances antimicrobial agents efficacy by Pseudomonas aeruginosa. *Microbiologyopen*, 7(1). https://doi.org/10.1002/mbo3.545.

Shekunov, B.Y., Chattopadhyay, P., Tong, H.H.Y. and Chow, A.H.L., 2007. Particle Size Analysis in Pharmaceutics: Principles, Methods and Applications. *Pharm Res*, 24(2), pp. 203-227.

Sherrard, L.J., Tunney, M.M. and Elborn, J.S., 2014. Antimicrobial resistance in the respiratory microbiota of people with cystic fibrosis. *The Lancet*, 384(9944), pp. 703-713.

Silva, D., Cortez, C.M. and Louro, S.R.W., 2004. Chlorpromazine interactions to sera albumins: A study by the quenching of fluorescence. *Spectrochim Acta A Mol Biomol Spectrosc*, 60(5), pp. 1215-1223.

Silver, L.L., 2016. A Gestalt approach to Gram-negative entry. *Bioorg Med Chem*, 24(24), pp. 6379-6389.

Singh, S. and Bhatia, S., 2018. In silico identification of albendazole as a quorum sensing inhibitor and its in vitro verification using CviR and LasB receptors based assay systems. *Bioimpacts*, 8(3), pp. 201-209.

Siriwong, S., Teethaisong, Y., Thumanu, K., Dunkhunthod, B. and Eumkeb, G., 2016. The synergy and mode of action of quercetin plus amoxicillin against amoxicillin-resistant Staphylococcus epidermidis. *BMC Pharmacol Toxicol*, 17(1). https://doi.org/10.1186/s40360-016-0083-8.

Soberón-Chávez, G., Lépine, F. and Déziel, E., 2005. Production of rhamnolipids by Pseudomonas aeruginosa. *Appl Microbiol Biotechnol*, 68(6), pp. 718-725.

Song, T., Duperthuy, M. and Wai, N.S., 2016. Sub-Optimal Treatment of Bacterial Biofilms. *Antibiotics*, 5(2). https://doi.org/10.3390/antibiotics5020023.

Sopirala, M.M., Mangino, J.E., Gebreyes, W.A., Biller, B., Bannerman, T., Balada-Llasat, J.-M. and Pancholi, P., 2010. Synergy Testing by Etest, Microdilution Checkerboard, and Time-Kill Methods for Pan-Drug-Resistant Acinetobacter baumannii. *Antimicrob Agents Chemother*, 54(11), pp. 4678-4683.

Stein, C., Makarewicz, O., Bohnert, J.A., Pfeifer, Y., Kesselmeier, M., Hagel, S. and Pletz, M.W., 2015. Three Dimensional Checkerboard Synergy Analysis of Colistin, Meropenem,

Tigecycline against Multidrug-Resistant Clinical Klebsiella pneumonia Isolates. *PLoS One*, 10(6). https://doi.org/10.1371/journal.pone.0126479.

Stover, C.K., Pham, X.Q., Erwin, A.L., Mizoguchi, S.D., Warrener, P., Hickey, M.J., Brinkman, F.S., Hufnagle, W.O., Kowalik, D.J., Lagrou, M., Garber, R.L., Goltry, L., Tolentino, E., Westbrock-Wadman, S., Yuan, Y., Brody, L.L., Coulter, S.N., Folger, K.R., Kas, A., Larbig, K., Lim, R., Smith, K., Spencer, D., Wong, G.K., Wu, Z., Paulsen, I.T., Reizer, J., Saier, M.H., Hancock, R.E., Lory, S. and Olson, M.V., 2000. Complete genome sequence of Pseudomonas aeruginosa PAO1, an opportunistic pathogen. *Nature*, 406(6799), pp. 959-964.

Tahrioui, A., Duchesne, R., Bouffartigues, E., Rodrigues, S., Maillot, O., Tortuel, D., Hardouin, J., Taupin, L., Groleau, M.-C., Dufour, A., Déziel, E., Brenner-Weiss, G., Feuilloley, M., Orange, N., Lesouhaitier, O., Cornelis, P. and Chevalier, S., 2019. Extracellular DNA release, quorum sensing, and PrrF1/F2 small RNAs are key players in Pseudomonas aeruginosa tobramycin-enhanced biofilm formation. *NPJ biofilms and microbiomes*, 5. https://doi.org/10.1038/s41522-019-0088-3.

Taki, M., Marriott, C., Zeng, X.M. and Martin, G.P., 2010. Aerodynamic deposition of combination dry powder inhaler formulations in vitro: a comparison of three impactors. *Int J Pharm*, 388(1-2), pp. 40-51.

Taki, M., Marriott, C., Zeng, X.M. and Martin, G.P., 2011. The production of 'aerodynamically equivalent' drug and excipient inhalable powders using a novel fractionation technique. *Eur J Pharm Biopharm*, 77(2), pp. 283-296.

Tay, J.Y.S., Liew, C.V. and Heng, P.W.S., 2018. Dissolution of Fine Particle Fraction from Truncated Anderson Cascade Impactor with an Enhancer Cell. *Int J Pharm*, 545(1-2), pp. 45-50.

Taylor, C.F., Field, D., Sansone, S.A., Aerts, J., Apweiler, R., Ashburner, M., Ball, C.A., Binz, P.A., Bogue, M., Booth, T., Brazma, A., Brinkman, R.R., Michael Clark, A., Deutsch, E.W., Fiehn, O., Fostel, J., Ghazal, P., Gibson, F., Gray, T., Grimes, G., Hancock, J.M., Hardy, N.W., Hermjakob, H., Julian, R.K., Jr., Kane, M., Kettner, C., Kinsinger, C., Kolker, E., Kuiper, M., Le Novere, N., Leebens-Mack, J., Lewis, S.E., Lord, P., Mallon, A.M., Marthandan, N., Masuya, H., McNally, R., Mehrle, A., Morrison, N., Orchard, S., Quackenbush, J., Reecy, J.M., Robertson, D.G., Rocca-Serra, P., Rodriguez, H., Rosenfelder, H., Santoyo-Lopez, J., Scheuermann, R.H., Schober, D., Smith, B., Snape, J., Stoeckert, C.J., Jr., Tipton, K., Sterk, P., Untergasser, A., Vandesompele, J. and Wiemann, S., 2008. Promoting coherent minimum reporting guidelines for biological and biomedical investigations: the MIBBI project. *Nat Biotechnol*, 26(8), pp. 889-896.

Taylor, P.K., Yeung, A.T. and Hancock, R.E., 2014. Antibiotic resistance in Pseudomonas aeruginosa biofilms: towards the development of novel anti-biofilm therapies. *J Biotechnol*, 191, pp. 121-130.

Thomas, S.R., Ray, A., Hodson, M.E. and Pitt, T.L., 2000. Increased sputum amino acid concentrations and auxotrophy of Pseudomonas aeruginosa in severe cystic fibrosis lung disease. *Thorax*, 55(9), pp. 795-797.

Tiddens, H., 2004. Inhaled antibiotics. *Pediatr Pulmonol Suppl*, 26, pp. 92-94.

Tiddens, H.A., Bos, A.C., Mouton, J.W., Devadason, S. and Janssens, H.M., 2014. Inhaled antibiotics: dry or wet? *Eur Respir J,* 44(5), pp. 1308-1318.

Timsina, M.P., Martin, G.P., Marriott, C., Ganderton, D. and Yianneskis, M., 1994. Drug delivery to the respiratory tract using dry powder inhalers. *Int J Pharm,* 101(1), pp. 1-13.

Tre-Hardy, M., Nagant, C., El Manssouri, N., Vanderbist, F., Traore, H., Vaneechoutte, M. and Dehaye, J.P., 2010. Efficacy of the combination of tobramycin and a macrolide in an in vitro Pseudomonas aeruginosa mature biofilm model. *Antimicrob Agents Chemother,* 54(10), pp. 4409-4415.

Treerat, P., Widmer, F., Middleton, P.G., Iredell, J. and George, A.M., 2008. In vitro interactions of tobramycin with various nonantibiotics against Pseudomonas aeruginosa and Burkholderia cenocepacia. *FEMS Microbiol Lett,* 285(1), pp. 40-50.

Tunney, M.M., Payne, J.E., McGrath, S.J., Einarsson, G.G., Ingram, R.J., Gilpin, D.F., Juarez-Perez, V. and Elborn, J.S., 2018. Activity of hypothiocyanite and lactoferrin (ALX-009) against respiratory cystic fibrosis pathogens in sputum. *J Antimicrob Chemother,* 73(12), pp. 3391-3397.

UK CF Registry, National Report,, 2018. *UK Cystic Fibrosis Registry National Data Report.* UK. Available from: *https://www.cysticfibrosis.org.uk* [Accessed 24 December 2019].

Umerska, A., Strandh, M., Cassisa, V., Matougui, N., Eveillard, M. and Saulnier, P., 2018. Synergistic Effect of Combinations Containing EDTA and the Antimicrobial Peptide AA230, an Arenicin-3 Derivative, on Gram-Negative Bacteria. *Biomolecules,* 8(4). https://doi.org/10.3390/biom8040122.

van der Wiel, E., Lexmond, A.J., van den Berge, M., Postma, D.S., Hagedoorn, P., Frijlink, H.W., Farenhorst, M.P., de Boer, A.H. and Ten Hacken, N.H.T., 2017. Targeting the small airways with dry powder adenosine: a challenging concept. *Eur Clin Respir J,* 4(1). https://doi.org/10.1080/20018525.2017.1369328.

Van Schayck, C.P. and Donnell, D., 2004. The efficacy and safety of QVAR (hydrofluoroalkane-beclometasone diproprionate extrafine aerosol) in asthma (Part 2): Clinical experience in children. *Int J Clin Pract,* 58(8), pp. 786-794.

Vanden Burgt, J.A., Busse, W.W., Martin, R.J., Szefler, S.J. and Donnell, D., 2000. Efficacy and safety overview of a new inhaled corticosteroid, QVAR (hydrofluoroalkane-beclomethasone extrafine inhalation aerosol), in asthma. *J Allergy Clin Immunol,* 106(6), pp. 1209-1226.

VanDevanter, D.R. and Geller, D.E., 2011. Tobramycin administered by the TOBI(®) Podhaler(®) for persons with cystic fibrosis: a review. *Med Devices (Auckl),* 4, pp. 179-188.

Verbanck, S., Schuermans, D., Paiva, M. and Vincken, W., 2006. The functional benefit of anti-inflammatory aerosols in the lung periphery. *J Allergy Clin Immunol,* 118(2), pp. 340-346.

Vestby, L.K., Lönn-Stensrud, J., Møretrø, T., Langsrud, S., Aamdal-Scheie, A., Benneche, T. and Nesse, L.L., 2010. A synthetic furanone potentiates the effect of disinfectants on Salmonella in biofilm. *J Appl Microbiol,* 108(3), pp. 771-778.

Wang, H., Bhambri, P., Ivey, J. and Vehring, R., 2017. Design and pharmaceutical applications of a low-flow-rate single-nozzle impactor. *Int J Pharm,* 533(1), pp. 14-25.

Wang, W., Yu, J., He, Y., Wang, Z. and Li, F., 2016. Ambroxol inhibits mucoid conversion of Pseudomonas aeruginosa and contributes to the bactericidal activity of ciprofloxacin against mucoid P. aeruginosa biofilms. *APMIS,* 124(7), pp. 611-618.

Wassermann, T., Meinike Jorgensen, K., Ivanyshyn, K., Bjarnsholt, T., Khademi, S.M., Jelsbak, L., Hoiby, N. and Ciofu, O., 2016. The phenotypic evolution of Pseudomonas aeruginosa populations changes in the presence of subinhibitory concentrations of ciprofloxacin. *Microbiology,* 162(5), pp. 865-875.

Watts, A.B. and Williams, R.O., 2011. Nanoparticles for Pulmonary Delivery. In: H.D.C. Smyth and A.J. Hickey, eds. *Controlled Pulmonary Drug Delivery.* New York, NY: Springer, pp. 335-366.

Weers, J.G. and Miller, D.P., 2015. Formulation Design of Dry Powders for Inhalation. *J Pharm Sci,* 104(10), pp. 3259-3288.

Wenzler, E., Fraidenburg, D.R., Scardina, T. and Danziger, L.H., 2016. Inhaled Antibiotics for Gram-Negative Respiratory Infections. *Clin Microbiol Rev,* 29(3), pp. 581-632.

White, R.L., Burgess, D.S., Manduru, M. and Bosso, J.A., 1996. Comparison of three different in vitro methods of detecting synergy: time-kill, checkerboard, and E test. *Antimicrob Agents Chemother,* 40(8), pp. 1914-1918.

Whiteley, M., Bangera, M.G., Bumgarner, R.E., Parsek, M.R., Teitzel, G.M., Lory, S. and Greenberg, E.P., 2001. Gene expression in Pseudomonas aeruginosa biofilms. *Nature,* 413(6858), pp. 860-864.

Whiteley, M., Diggle, S.P. and Greenberg, E.P., 2017. Progress in and promise of bacterial quorum sensing research. *Nature,* 551(7680), pp. 313-320.

WHO, 2017. *Global priority list of antibiotic-resistant bacteria to guide research, discovery, and development of new antibiotics* [Online]. The World Health Organization. Available from: *https://www.who.int/medicines/publications/global-priority-list-antibiotic-resistant-bacteria/en/* [Accessed 21 December 2019].

Williamson, K.S., Richards, L.A., Perez-Osorio, A.C., Pitts, B., McInnerney, K., Stewart, P.S. and Franklin, M.J., 2012. Heterogeneity in Pseudomonas aeruginosa biofilms includes expression of ribosome hibernation factors in the antibiotic-tolerant subpopulation and hypoxia-induced stress response in the metabolically active population. *J Bacteriol,* 194(8), pp. 2062-2073.

Wimpenny, J., Manz, W. and Szewzyk, U., 2000. Heterogeneity in biofilms. *FEMS Microbiol Rev,* 24(5), pp. 661-671.

Woods, A. and Rahman, K.M., 2018. Antimicrobial molecules in the lung: formulation challenges and future directions for innovation. *Future Med Chem,* 10(5), pp. 575-604.

Worlitzsch, D., Tarran, R., Ulrich, M., Schwab, U., Cekici, A., Meyer, K.C., Birrer, P., Bellon, G., Berger, J., Weiss, T., Botzenhart, K., Yankaskas, J.R., Randell, S., Boucher, R.C.

and Doring, G., 2002. Effects of reduced mucus oxygen concentration in airway Pseudomonas infections of cystic fibrosis patients. *J Clin Invest,* 109(3), pp. 317-325.

Wright, G.D., 2016. Antibiotic Adjuvants: Rescuing Antibiotics from Resistance. *Trends Microbiol,* 24(11), pp. 862-871.

Yang, M.Y., Chan, J.G. and Chan, H.K., 2014. Pulmonary drug delivery by powder aerosols. *J Control Release,* 193, pp. 228-240.

Yang, Y., Bajaj, N., Xu, P., Ohn, K., Tsifansky, M.D. and Yeo, Y., 2009. Development of highly porous large PLGA microparticles for pulmonary drug delivery. *Biomaterials,* 30(10), pp. 1947-1953.

Yang, Y., Tsifansky, M.D., Wu, C.J., Yang, H.I., Schmidt, G. and Yeo, Y., 2010. Inhalable antibiotic delivery using a dry powder co-delivering recombinant deoxyribonuclease and ciprofloxacin for treatment of cystic fibrosis. *Pharm Res,* 27(1), pp. 151-160.

Ye, T., Sun, S., Sugianto, T.D., Tang, P., Parumasivam, T., Chang, Y.K., Astudillo, A., Wang, S. and Chan, H.K., 2018. Novel combination proliposomes containing tobramycin and clarithromycin effective against Pseudomonas aeruginosa biofilms. *Int J Pharm,* 552(1-2), pp. 130-138.

Yoshida, H., Kuwana, A., Shibata, H., Izutsu, K.I. and Goda, Y., 2017. Comparison of Aerodynamic Particle Size Distribution Between a Next Generation Impactor and a Cascade Impactor at a Range of Flow Rates. *AAPS PharmSciTech,* 18(3), pp. 646-653.

Zenga, J., Gagnon, P.M., Vogel, J. and Chole, R.A., 2012. Biofilm formation by otopathogenic strains of Pseudomonas aeruginosa is not consistently inhibited by ethylenediaminetetraacetic acid. *Otol Neurotol,* 33(6), pp. 1007-1012.

Zgurskaya, H.I., Löpez, C.A. and Gnanakaran, S., 2015. Permeability Barrier of Gram-Negative Cell Envelopes and Approaches To Bypass It. *ACS Infect Dis,* 1(11), pp. 512-522.

Appendix 1: full details of the statistical analysis

Table A1: overall details of the statistical analysis

Figures	Statistical tests	Overall statistical analysis
3.1 A	ANOVA	F= 9.55, df= 23, p= 0.0001
3.1 B	ANOVA	F= 1.23, df= 29, p= 0.32
3.1 C	ANOVA	F= 47.97, df= 29, p= < 0.0001
3.1 D	ANOVA	F= 13.95, df= 17, p= 0.0001
3.1 E	ANOVA	F= 144.1, df= 17, p <0.0001
3.2 A	t-test	t= 9.87, df= 10, p<0.0001
3.2 B	t-test	t= 7.95, df= 10, p<0.0001
3.2 C	t-test	t=9.7, df= 10, p<0.0001
3.2 D	t-test	t=7.42, df= 10, p<0.0001
3.2 E	t-test	t=5.18, df=10, p<0.0001
3.3 A	ANOVA	F= 2.08, df= 12, p= 0.17
3.3 B	ANOVA	F= 1.7, df= 23, p= 0.17
3.3 C	ANOVA	F= 0.33, df= 23, p= 0.92
3.3 D	ANOVA	F= 3.01, df=25, p= 0.28
3.4 A	ANOVA	F= 0.46, df= 14, p= 0.75
3.4 B	ANOVA	F= 0.85, df= 23, p= 0.36
3.4 C	ANOVA	F= 0.24, df= 23, p= 0.96
3.4 D	ANOVA	F= 0.12, df= 26, p= 0.99
3.6 A	ANOVA	F= 0.3, df= 8, p= 0.75
3.6 B	ANOVA	F= 1.76, df= 8, p= 0.24
3.6 C	ANOVA	F= 2.6, df= 8, p= 0.153
3.6 D	ANOVA	F= 2.5, df= 8, p= 0.158
3.7 A	ANOVA	F= 0.71, df= 5, p= 0.629
3.7 B	ANOVA	F= 1.98, df= 5, p= 0.117
3.7 C	ANOVA	F= 2.93, df= 5, p= 0.034
3.7 D	ANOVA	F= 1.83, df= 5, p= 0.146
3.8 A	t-test	t= 5.64, df= 8, p= 0.0005
3.8 B	t-test	t= 4.79, df= 10, p= 0.0007
3.8 C	t-test	t= 3.69, df= 8, p= 0.006
3.8 D	t-test	t= 5.17, df= 10, p= 0.0004
3.9 A	t-test	t= 2.35, df= 8, p= 0.046
3.9 B	t-test	t= 2.08, df= 10, p= 0.064
3.9 C	t-test	t= 3.12, df= 10, p= 0.011
3.9 D	t-test	t= 4.45, df= 10, p= 0.001
4.11	t-test	t= 0.31, df= 8, p= 0.76
4.13 A	t-test	t= 0.22, df= 4, p= 0.834
4.13 B	t-test	t= 0.24, df= 4, p= 0.82
4.13 C	t-test	t= 0.95, df= 4, p= 0.39
4.13 D	t-test	t= 0.13, df= 6, p= 0.89
4.13 E	t-test	t= 0.39, df= 4, p= 0.72
4.13 F	t-test	t= 0.61, df= 4, p= 0.58
4.13 G	t-test	t= 0.87, df= 6, p= 0.42
4.13 H	t-test	t= 1.23, df= 4, p= 0.29

4.14	t-test	t= 1.76, df= 4, p= 0.15
4.15 A	t-test	t= 1.02, df= 4, p= 0.36
4.15 B	t-test	t= 0.24, df= 4, p= 0.83
4.15 C	t-test	t= 0.85, df= 4, p= 0.45
4.15 D	t-test	t= 0.038, df= 4, p= 0.97
4.16 A	t-test	t= 0.19, df= 4, p= 0.85
4.16 B	t-test	t= 0.32, df= 4, p= 0.76
4.16 C	t-test	t= 0.16, df= 4, p= 0.88
4.16 D	t-test	t= 0.55, df= 4, p= 0.61
4.17 A	t-test	t= 2.77, df= 4, p= 0.04
4.17 B	t-test	t= 2.96, df= 6, p= 0.02
4.17 C	t-test	t= 1.5, df= 4, p= 0.26
4.17 D	t-test	t= 0.52, df= 4, p= 0.63
4.18	ANOVA	F= 0.43, df= 2, p= 0.66
5.2 A	ANOVA	F= 8.91, df= 11, p= 0.006
5.2 B	ANOVA	F= 11.56, df= 11, p= 0.03
5.2 C	ANOVA	F= 19.58, df= 11, p= 0.0005
5.2 D	ANOVA	F= 3.97, df= 11, p= 0.156
5.2 E	ANOVA	F= 1.02, df= 11, p= 0.43
5.2 F	ANOVA	F= 1.58, df= 11, p= 0.27
5.2 G	ANOVA	F= 14.5, df= 7, p= 0.012
5.2 H	ANOVA	F= 2.45, df= 11, p= 0.52
5.3 A	ANOVA	F= 1.3, df= 11, p= 0.32
5.3 B	ANOVA	F= 10.5, df= 7, p= 0.02
5.3 C	ANOVA	F= 1.4, df= 11, p= 0.31
5.3 D	ANOVA	F= 2.56, df= 11, p= 0.125
5.3 E	ANOVA	F= 0.46, df= 11, p= 0.71
5.3 F	ANOVA	F= 0.59, df= 11, p= 0.637
5.3 G	ANOVA	F= 10.5, df= 7, p=0.02
5.3 H	ANOVA	F= 5.28, df= 11, p= 0.026
5.3 I	ANOVA	F= 0.192, df= 11, p= 0.89
5.3 J	ANOVA	F= 4.87, df= 11, p= 0.03
5.3 K	ANOVA	F= 9.4, df= 11, p= 0.005
5.3 O	ANOVA	F= 5.61, df= 11, p= 0.02
5.3 L	ANOVA	F= 9.5, df= 11, p= 0.005
5.3 M	ANOVA	F= 4.89, df= 11, p= 0.032
5.3 N	ANOVA	F= 3.61, df= 11, p= 0.06
5.3 P	ANOVA	F= 2.91, df= 11, p= 0.1

Appendix 2: Anova analysis with considering tobramycin concentrations as continuous variables

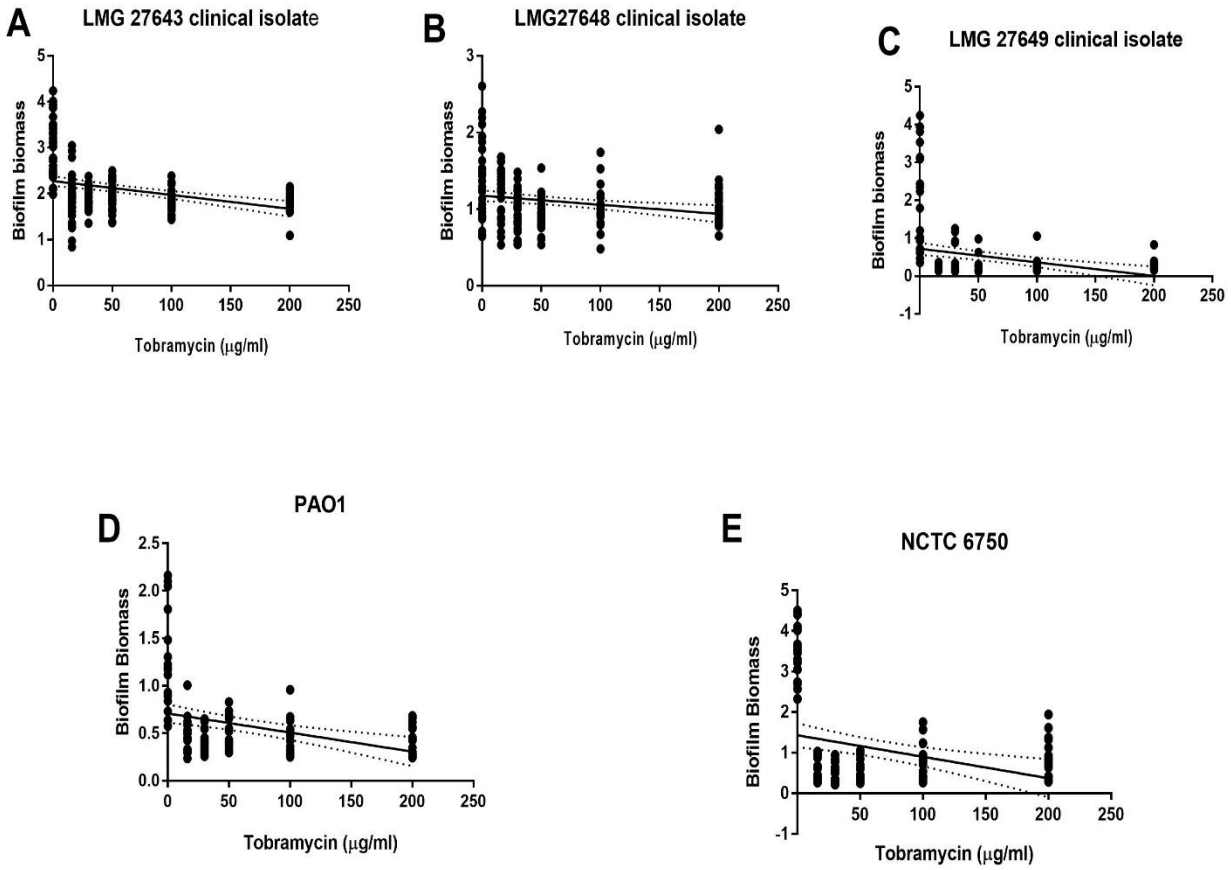

Table A2: overall Anova analysis

Figure 3.1 A	F= 28.15, df= 188, p= <0.0001
Figure 3.1 B	F= 9.76, df= 188, p= 0.002
Figure 3.1 C	F= 17.83, df= 174, p= <0.0001
Figure 3.1 D	F= 15.31, df= 105, p= 0.0002
Figure 3.1 E	F= 11.29, df= 107, p=0.001

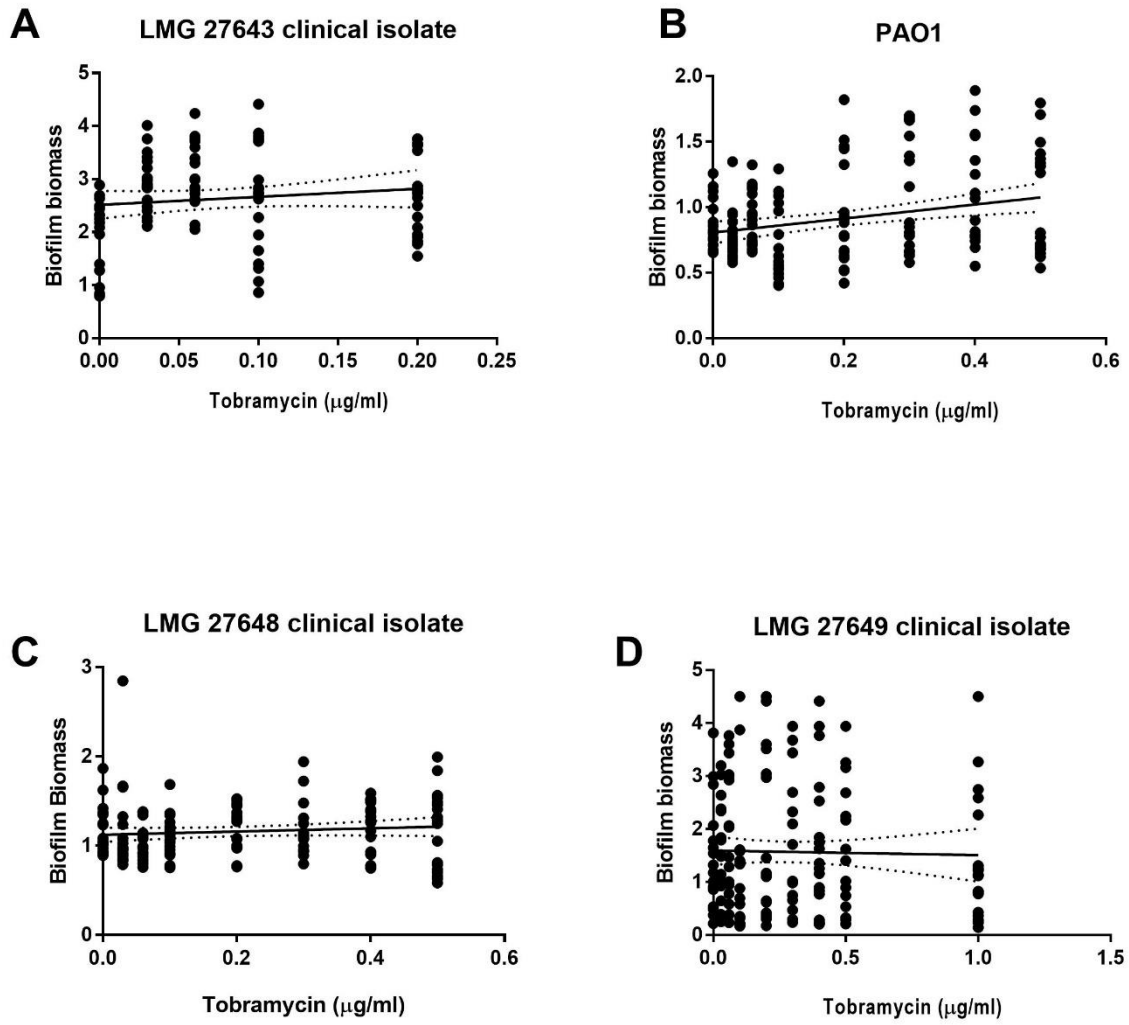

Table A3: overall ANOVA analysis

Figure 3.3 A	F= 1.4, df= 88, p= 0.23
Figure 3.3 B	F= 11, df= 142, p=0.001
Figure 3.3 C	F= 1.4, df= 143, p= 0.24
Figure 3.3 D	F= 0.069, df= 161, p= 0.79

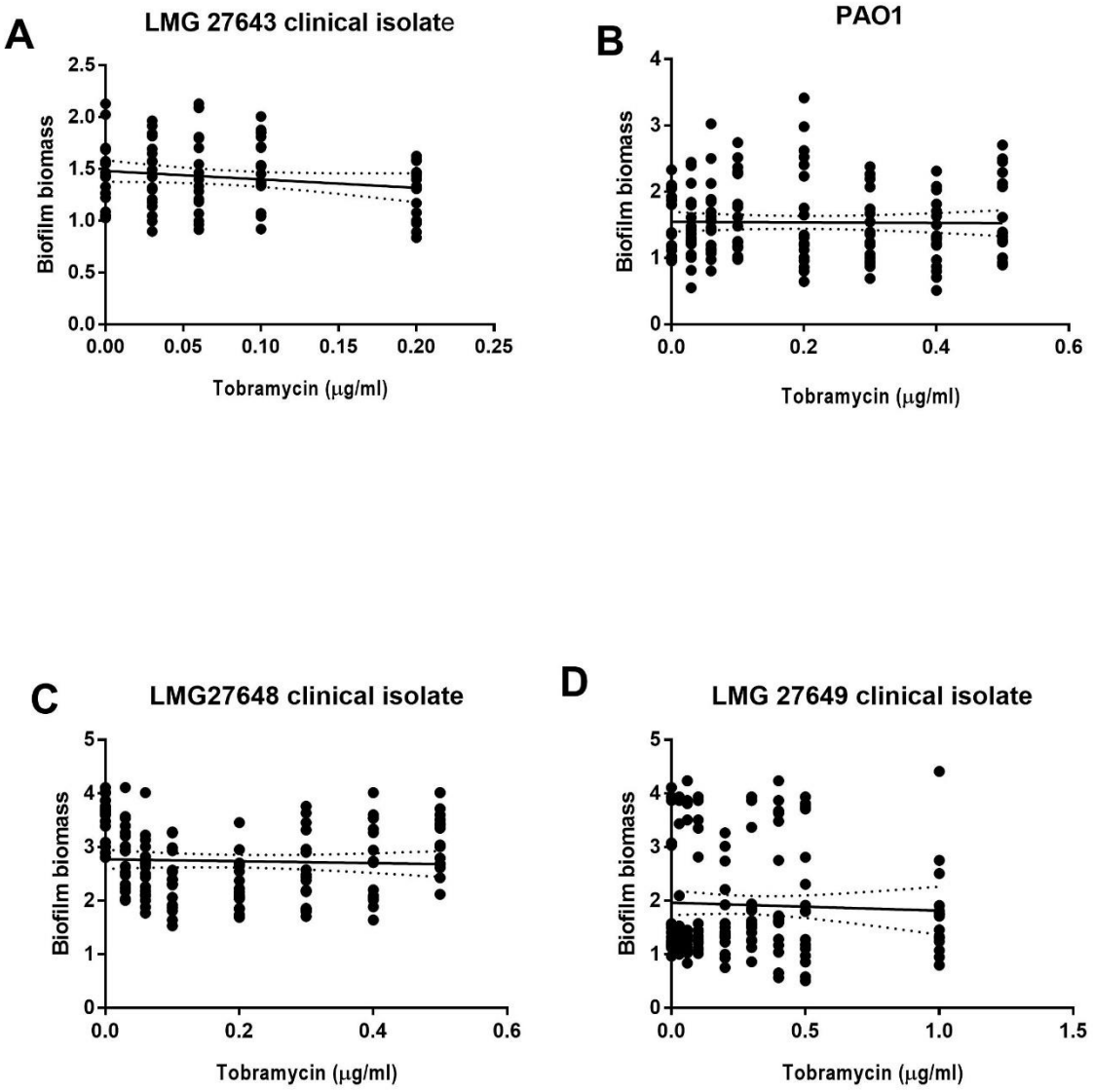

Table A4: overall ANOVA analysis

Figure 3.4 A	F= 2.62, df= 89, p= 0.11
Figure 3.4 B	F= 0.02, df= 142, p= 0.88
Figure 3.4 C	F= 0.26, df= 141, p= 0.61
Figure 3.4 D	F= 0.26, df= 153, p= 0.61